INTRACELLULAR AND EXTRACELLULAR BIOMARKERS OF DRUG-INDUCED LIVER INJURY

Thesis submitted in accordance with the requirements of the University of Liverpool for the degree of Doctor in Philosophy

By

Robert James Hornby

September 2015

DECLARATION

This thesis is the result of my own work. The material contained within this thesis has not been presented, nor is currently being presented wholly, or partially, for any other degree of qualification.

Robert James Hornby

This research was undertaken at the Department of Molecular & Clinical Pharmacology, at the Medical Research Council Centre for Drug Safety Science, Liverpool UK.

TABLE OF CONTENTS

CHAPTER 3

ABSTRACT

Intracellular and Extracellular biomarkers of drug-induced liver injury

Drug-induced liver injury (DILI) is a common form of adverse drug reaction (ADR) seen within the clinic. Sensitive and specific circulating biomarkers would aid in the prediction of DILI early in its course. However, the current biomarkers of DILI, such as alanine transaminase (ALT) suffer from a lack of specificity and sensitivity. Because of this, we have examined both intracellular and extracellular biomarkers of DILI in order to validate and identify novel biomarkers of DILI.

Protein tyrosine nitration (PTN), an intracellular marker of oxidative stress, has been shown to be present in paracetamol-DILI, and it is thought that the causative factor for its occurrence is mitochondrial damage. In order to test this, we used Furosemide (FS), a hepatotoxin not thought to cause mitochondrial injury or glutathione (GSH) depletion with the hypothesis that this compound would not generate PTN. First, we tested the role of GSH in protecting from PTN through depleting GSH in a mouse hepatoma cell line, followed by incubation with peroxynitrite. We found that GSH depletion was required in order to elicit PTN. Following this, we compared the ability of toxic doses of FS and paracetamol to cause PTN in mice. Interestingly, we found both compounds lead to PTN, suggesting that there is a pathway independent of GSH-depletion and mitochondrial injury which may lead to PTN.

MicroRNA-122 (miR-122) a potential novel extracellular biomarker of DILI, has been demonstrated to be elevated in the circulation earlier in the course of injury than current DILI biomarkers. We examined the potential for miR-122 to be released actively in exosomes during paracetamol-DILI in rats and multiple forms of DILI in humans. Our findings suggested that in both human and rodent's, miR-122 is released in a similar profile throughout the course of DILI in exosomes, and in an exosome-free (protein-rich fraction) form. We also examined whether miR-122 is selectively released in exosomes during hepatocellular, mixed and cholestatic DILI in humans which had been prescribed a number of hepatotoxic compounds. Our study suggested that, similar to our rodent model, there is no specific pattern of exosomal release of miR-122 in any of these forms of injury.

We then looked at new and relatively unexplored aspects of microRNAs, in order to evaluate how they may be used to look at damage to different zones of the liver, and damage to cells other than hepatocytes.

Hepatocytes are heterogeneous, with their phenotype depending on their localisation along the porto-central axis, which has resulted in certain drugs causing zone-specific hepatotoxicity. None of the current biomarkers is able to identify zone-specific injury. We examined zonal profiles of microRNA expression within the liver of rats under basal conditions and following paracetamol. Our analysis demonstrated that 45 miRNAs are significantly differentially expressed between zone I and zone III, with three species being expressed in only one zone. Of these differentially expressed miRNAs we found that 9 species were involved in regulating 109 members Wnt/β-Catenin pathway, the molecular driver of liver zonation. We also examined changes in zonal miRNA expression following a toxic dose of paracetamol in rats. Our study was able to demonstrate that paracetamol was able to cause significant changes in the profiles of 42 and 43 miRNAs in zone I and zone III respectively. Importantly, miRNAs were both up and down regulated in both zones, suggesting that not only a loss of miRNAs is occurring during liver injury in each zone.

Biliary epithelial cells (BEC) can be damaged by a plethora of different compounds, leading to vanishing bile duct syndrome, or bile duct hyperplasia. Current biomarkers for the diagnosis of BEC-injury lack in specificity, and are prone to false-positives. We developed a method to isolate BEC from the mouse liver and performed a global miRNA profile comparison of hepatocytes and BEC. As in previous studies we found miR-122-5p to be the most enriched miRNA in hepatocytes and miR-1224-5p in BEC. On comparison of the profiles we found that 83 miRNAs were detectable in BEC but not in Hepatocytes, however further work will be required to validate any of these as markers of BEC injury.

ACKNOWLEDGEMENTS

First, I would like to thank my primary supervisor, Professor Chris Goldring for his continued patience, support and advice throughout the PhD, in both success, and the many failures. In addition, I would also like to thank Dr Dan Antoine, Professor Kevin Park and Dr Neil Kitteringham for their input and advice on my projects.

I would like to acknowledge my many colleagues within the MRC CDSS for offering their help and advice throughout the four years. And, more specifically, I would like to thank Philip Starkey Lewis, my mentor throughout the course of my PhD, for his guidance on new projects and techniques; Joanne Walsh, for teaching me my first skills in the lab, and for always offering help, no matter how busy she was; James Heslop for offering his seemingly endless pool of knowledge on Ingenuity; Chris Pridgeon for his skills with a computer, and Richard Greensmith for his friendship, and our shared constant need for trips for food. I would also like to thank my family for their constant offerings of help and support throughout the course of the PhD.

Finally, and most importantly, I would like to thank Kelly Ward, whose care and support, has provided me with a constant escape from the stresses of the PhD throughout. I can honestly say that I do not believe that I would have made it to this point without her.

PUBLICATIONS

RESEARCH ARTICLES

Thulin P*, **Hornby RJ***, Auli M, Starkey Lewis P, Nordahl G, Antoine DJ, Goldring CEP, Prats N, Glinghammar B, Park BK, Schuppe-Koistinen I* (2016) A Longitudinal Assessment of miR-122 and GLDH as Novel Biomarkers of Drug-Induced Liver Injury in the Rat. Biomarkers (Accepted)

*joint first author

Hornby RJ, Mosedale M, N De Bois Brilliant, Holman N, Parks B, Eaddy S, Church R, Edgerton N, Williams D, Antoine DJ, Goldring CEP, Watkins PB and Park BK. Beyond miR-122: Expression Analysis of Liver MicroRNAs basally, and in Paracetamol-induced liver injury. (Manuscript in preparation).

REVIEW ARTICLES

Hornby RJ, Starkey Lewis P, Dear J, Goldring C, Park BK (2014) MicroRNAs as potential biomarkers of drug-induced liver injury: key current and future issues for translation to humans. Expert Reviews in Clinical Pharmacology **7**(3): 349-362

ABSTRACTS

Hornby RJ, Mosedale M, De Bois Brilliant N, Holman N, Jones C, Parks B, Eaddy S, Church R, Edgerton N, Williams D, Antoine D, Starkey Lewis P, Bushall M, Goldring C, Watkins P B and Park BK. Beyond miR-122: Expression Analysis of Liver MicroRNAs basally, and in Paracetamol-induced liver injury. Cellular and Molecular Mechanisms of Toxicity 2015, Gordon Research Conferences (Proctor Academy, NH, USA).

ABBREVIATIONS

3-NT	3-nitrotyrosine
ADR	adverse drug reaction
ALB	albumin
ALF	acute liver failure
ALT	alanine transaminase
ALP	alkaline phosphatase
APC	adenomatous polyposis coli
AST	aspartate transaminase
BEC	biliary epithelial cell/cholangiocyte
Cps1	carbamoylphosphate synthetase 1
CYP450	cytochrome-P450
Cyp2e1	CYP450 2E1
CK18	cytokeratin-18
DILI	drug-induced liver injury
FC	fold-change
FS	furosemide
GGT	γ-glutamyltransferase
GLDH	glutamate dehydrogenase
GS	glutamine synthetase
GSH	reduced glutathione
GSSG	glutathione di-sulphide (oxidised glutathione)
Hep	hepatocyte
K-19	keratin-19
LSEC	liver sinusoidal endothelial cell
miRNA	microRNA

miR-122	microRNA-122
mRNA	messenger RNA
NAPQI	*N*-acetyl-*p*-benzoquinoneimine
PCR	polymerase chain reaction
PP	Zone 1/periportal
PTN	protein tyrosine nitration
PV	Zone III/pericentral/centrilobular
qPCR	quantitative reverse transcription PCR

CHAPTER 1

GENERAL INTRODUCTION

1.1 ADVERSE DRUG REACTIONS AND DRUG-INDUCED LIVER INJURY

Adverse drug reactions (ADR) account for between 2.4-12% of hospital admissions cases in the western world, and are defined as any undesirable effect cause by a xenobiotic or therapeutic. ADRs can be separated into two sub-categories, Type A and Type B. Type A reactions are common and occur as part of a dose-dependent relationship usually involving an exaggeration of the on-target pharmacology of a drug. Type B, 'idiosyncratic' reactions are less common, but are often more severe and are a product of unanticipated off-target pharmacological effects of a drug, and are therefore much less predictable (Hussaini and Farrington 2007). ADRs are a major impediment to both the National Health Service (NHS) and also to the drug development industry. Four in one hundred hospital bed days in the UK are dedicated to treating ADRs, costing near to £400m per annum. Similarly, in the pharmaceutical industry, 99% of lead compounds will have their development halted due to an ADR or undesirable pharmacological properties, which represents a significant cost when it is considered that it costs $1bn to take a drug from development through to market. Drug-induced liver injury (DILI) is the most prominent form of ADR seen within the clinic in the UK and US, and is a major reason for the failure of new drugs in clinical trials (Ostapowicz et al. 2002). In the US, 50% of the cases of acute liver failure (ALF) are attributed to DILI when both cases of deliberate overdose and idiosyncratic reaction are considered, and therefore it is of no surprise that hepatotoxicity is the most cited reason for the withdrawal of a drug from the market during the post-marketing phase.

1.2 THE LIVER

The liver is the main organ responsible for the metabolism of endogenous and exogenous chemical entities, including drugs. Under normal conditions the liver is responsible for the detoxification of the systematic and portal blood supplies, as well as the production of blood and bile components (Adams et al. 2003; Rodes et al. 2007). The liver also has a role in protein, fat and steroid metabolism, and macronutrient storage (Bioulac-Sage et al. 1999). Structurally, the liver is made up of hexagonal groups of cells called liver lobules, which are each centred around a central vein. Each corner of the hexagonal lobule is formed by a portal triad, a grouping of vessels, which include the hepatic portal vein, the hepatic artery and a bile duct. The space between the central vein and portal triad is then filled by plates of non-parenchymal and parenchymal cells, making up a functional liver lobule. Plates of parenchymal cells are usually organised in cord like structures, which are separated from each other by the hepatic sinusoids, the capillaries of the liver, or intrahepatic bile ducts (Bioulac-Sage et al. 1999). The lobule can be separated into three distinct zones, I, II and III. The blood enters the liver from zone I, the region containing the portal triad, and exits the liver through the central vein in zone III, moving along the porto-central axis through zone II in between (Gebhardt 1992; Ito et al. 2007; Rappaport 1977; Smith and Wills 1981; Ugele et al. 1991).

At a cellular level, the liver is made up of parenchymal (hepatocytes) and non-parenchymal cells (liver sinusoidal endothelial cells; LSEC, biliary epithelial cells; BEC, kupffer cells; KC, hepatic stellate cells; HSC and natural killer t-cells) (Reviewed in (LeCluyse et al. 2012) (see table 1.1 for a description of cell types). Hepatocytes represent almost 80% of the liver mass, and 60% of the individual cells within the liver (Bioulac-Sage et al. 1999; Kmiec 2001). The non-parenchymal cells make up the remainder, encompassing 40% of the individual cells, but only 6.5% of the liver volume. While the hepatocytes play a major function in the liver, the often overlooked non-parenchymal cells have an important role in supporting and regulating hepatic growth, and function (Kmiec 2001).

Table 1.1 Summary of hepatic cell types. Adapted from LeCluyse et al. (2012)

	Hepatocyte	Cholangiocyte	Sinusoidal endothelial cell	Hepatic stellate cell	Kupffer cell	Pit Cell
Function	Metabolism of xenobiotics, lipid and cholesterol metabolism	Bile transport, bicarbonate secretion	Blood filtration, pinocytosis, cytokine secretion	Vitamin A storage, cytokine secretion, Inflammatory fibrotic response	Phagocytic activity in liver	Cytokine and chemokine production
% of total liver cells	60-70	2-3	2.5	1.4	2	<1
Diameter (µm)	20-25	12-15	8-10	10-12	10-12	8-10
Identification markers	Cytokeratin-18, albumin, cytochrome P450s	Keratin-19, human epithelial antigen-125/epithelial adhesion marker	CD31, vimentin, desmin, CD32b	Vimentin, desmin, autofluorescence of vitamin A, α smooth muscle actin, β tumor growth factor	CD68, CD56	CD8, CD56
Density (g/cm^3)	1.12-1.14	1.08-1.10	1.05-1.06	1.04-1.05	1.06-1.08	1.05-1.06
Method for isolation	• Collagenase perfusion • Centrifugation to remove non-parencymal cells	• Mince liver and perform density gradient separation to remove hepatocytes • MACS or Dynabead affinity purification	• Collagenase perfusion • Density gradient enrichment of NP cells • MACS or dynabead affinity purification	• Collagenase perfusion • Mince liver and perform density gradient	• Collagenase perfusion • Removal of parenchymal fraction by centrifugation • Density gradient enrichment • Adhesion to culture plates (30min, 37 degrees, 5% CO2) followed by washing	-

1.2.1 Hepatocytes

Hepatocytes are responsible for the majority of the physiological functions associated with the liver. Their main function within the body is protein, fat and steroid metabolism, the production of serum albumin, and the storage of vital nutrients. Hepatocytes are also responsible for the detoxification of endogenous and exogenous compounds, including drugs and environmental toxins (Boyer et al. 2003). Hepatocytes are specified for this function through their expression of specific metabolism enzymes, which can be classified into Phase I and II (Berry and Edwards. 2001). Phase I enzymes, which mainly fall into the sub-class, Cytochrome P450 enzymes, are responsible for the bio-activation of compounds, either into their active form, or into a possibly toxic reactive metabolite. Phase II enzymes are responsible for the detoxification of either parent compounds or metabolites through altering their chemical nature to become more hydrophilic. This usually occurs through the conjugation of the drug to another chemical structure (Rautou et al. 2010; Singh 2010). Morphologically, hepatocytes are cuboidal in shape, and are polarised in their expression of transporters, depending on their proximity to a bile canaliculi or hepatic sinusoid, which is critical for their function in bile synthesis and secretion (Fu et al. 2011). In addition, hepatocytes are not a homogenous species, with their function and overall expression profile depending on their location within the liver lobule (Reviewed by (Jungermann and Keitzmann 1996).

1.2.2 Liver sinusoidal endothelial cells

Liver sinusoidal endothelial cells (LSEC) are vascular cells that line the walls of the hepatic sinusoid, the capillaries of the liver. Compared to other vascular endothelial cells they possess a relatively large number of pinocytotic vesicles, hinting at their role in endocytotic activity (Wisse 1970). The adhesions between LSEC are much less prominent than those found between vascular endothelial cells, and their cell membranes are characterised by small pores or fenestrations (50-200nm diameter) which allow the passive movement of many substances between the blood and hepatocyte basolateral membrane (Cogger et al. 2010). This enables the hepatocyte to have a higher level of exposure to the bloods contents when compared to

cells within other organs, allowing for the efficient clearance of endogenous/exogenous substances. LSEC are part of the reticuloendothelial system and have three important roles in maintaining homeostasis within the liver. They are able to act as antigen presenting cells and are also to secrete a number of active substances, such as cytokines, eicosanoids, nitric oxide, endothelin-1, and extracellular matrix components (DeLeve 2007). This enables the liver to develop selective immunity to possible neo-antigens formed during hepatic metabolism. They also act as scavengers and act to clear the blood of macromolecular waste products using their high capacity for endocytosis (DeLeve 2007). Finally, they are able to act as a sieve for the bloods contents in order to control which substances are allowed to enter the hepatocytes (Wisse et al. 1985). Interestingly, they also contain a number of Cytochrome P450 (CYP450) enzymes, which have been demonstrated to produce reactive metabolites, demonstrating their role in hepatic metabolism and the clearance of xenobiotics. It was also demonstrated that paracetamol is able to cause toxicity in LSEC in the absence of hepatocytes, suggesting their capacity to produce *N*-acetyl-P-benzoquinoneimine (NAPQI), the reactive metabolite of paracetamol (Ito et al. 2003; Xie et al. 2010). LSEC have also been demonstrated to contain Phase II metabolism enzymes, however, it has been shown that their overall metabolism capacity is about 10% of that of a hepatocyte (Sacerdoti et al. 2003; Schrenk et al. 1991; Wu et al. 2008)

1.2.3 Biliary epithelial cells

Biliary epithelial cells or cholangiocytes (BEC) are the cells which line the biliary tract network. The biliary tract is made up of two separate components, the extrahepatic and intrahepatic biliary tract. The intrahepatic tract contains the canals of Hering, bile canaliculi, interlobular bile ducts, intrahepatic bile ducts, and the right and left hepatic bile ducts. The extrahepatic biliary tract contains the common hepatic duct, common bile duct, the cystic duct, and the gallbladder (Bogert and LaRusso 2007). Although BEC only account for 3-5% of the total liver cells, they are essential for the formation and effective transport of the bile components within the liver. Hepatocytes are able to secrete bile into the canalicular spaces

surround themselves, which is in turn transported through this network to the smallest of the bile duct structures, the cholangioles. The bile then passes through a series of increasingly large BEC-lined vessels, a process which allows the bile to become more alkaline and dilute through a series of absorptive and secretory processes. Morphologically BEC are cuboidal, but become progressively more columnar and mucus-secreting as they approach the portal triad and the extrahepatic ducts, as the vessels become larger. BEC which line the small branching ducts are around 3µm in diameter, whereas the larger bile ducts in the portal regions can be up to 80µm in diameter (Alpini et al. 1996). BEC which line the large bile ducts participate in mucin secretion and hormone-regulated bile secretion, whereas BEC which line the smaller bile ducts play a role in proliferation and possess a plasticity which is thought to play a role in reparative activity in disease conditions (Bogert and LaRusso 2007; Glaser et al. 2006; Marzioni et al. 2002).

BEC have been shown to be implicated in liver injury caused by a number of liver toxins, including erythromycin, chlorpromazine, flucloxacillin, phenytoin, carbamazepine, and trimethoprim/sulfamethoxazole, to name only a few examples (Reviewed by Padda et al. 2011; Read et al. 1961; Turner et al. 1988; Rodriguez et al. 1996; Zimmerman et al. 1999). However, small and large BEC are differentially susceptible to toxicity. Small BEC are most commonly affected by drug toxicities, which leads to vanishing bile duct syndrome. This aetiology often involves the permanent loss of the small branching intrahepatic bile ducts, which can ultimately lead to hepatic failure, requiring a liver transplant (Davies et al. 1994). In contrast the larger bile ducts are more commonly affected by bile duct hyperplasia, leading to a swelling of the large ducts and temporary, reversible jaundice. Unpublished data now suggests that patients suffering DILI involving bile duct damage have a much worse prognosis than those without, demonstrating the important of these cells in DILI (Fontana et al. 2015). Interestingly, large BEC express cyp2e1, the enzyme which forms NAPQI, the reactive metabolite of paracetamol, whereas small BEC do not (Lakehal et al. 1999).

1.2.4 Other non-parenchymal cells

HSC (Ito cells, fat-storing cells, perisinusoidal cells) reside in the space between the sinusoidal endothelial cells and the basolateral surface of the hepatocytes, called the space of Disse (Asahina et al. 2009). Under normal conditions HSC are involved in the storage of vitamin A, the turnover and production of the ECM, and the contractility of the sinusoid (Parola and Pinzani 2009; Wang et al. 2010). Under disease conditions, HSC take on a myofibroblastic phenotype, causing them to secrete growth factors and cytokines which cause an inflammatory fibrotic response within the liver (Ramadori et al. 2008). KC are the resident macrophages of the liver which have endocytic and phagocytic functions. Under normal conditions they modulate the turnover of other hepatic cells through initiation of apoptosis, followed by the removal of cellular waste by phagocytosis. Under pathological conditions, KCs play an important role in modulating the inflammatory response, as well as scavenging foreign particles (Kolios et al. 2006). Pit cells are liver-specific natural killer cells located in the sinusoid, which proliferate locally when stimulated by interleukin-2 and possess a high level of cytotoxicity against a number of tumor cell lines (Wisse et al. 1996).

1.2.5. Hepatocyte zonation

In order to maximise the efficiency of the liver, hepatocytes are both homologous, and also specialised. All hepatocytes similarly hold the ability to produce a range of serum proteins, including the transferrin and transthyretin transporters, and albumin. Hepatocytes are also highly specialised for their function depending on their location along the porto-central axis of the liver lobule, causing the hepatocyte to either be defined as periportal (PP; zone I), mid-zonal (Zone II), or pericentral (PV; Zone III) (Braeuning et al. 2006; Jungermann and Keitzmann 1996). Examples of well-defined specialised functions are, glucose metabolism which is largely based in zone I, and lipid metabolism, which is a zone III process (Berkowitz et al. 1995; Braeuning et al. 2006; Gebhardt 1992; Häussinger et al. 1991). Importantly, there is a large amount of evidence to suggest that the metabolism of xenobiotics and drugs is a zonated process. The cytochrome P450 system, responsible for the Phase I activation of many drugs is preferentially expressed within the zone III; whereas Phase II processes, such as sulfation occur within the Zone I region (Further examples of zonated processes can be seen in Figure 1.2). The zonated expression of CYP2E1 in the zone III, and GSH in the zone I causes the zone III region to be preferentially susceptible to paracetamol toxicity, due to increased bioactivation of the compound in this region, and decreased GSH conjugation (Anundi et al. 1993). In contrast, other compounds such as methapyrilene preferentially cause toxicity in the zone I region due to zonal expression profiles of detoxification proteins. Important also is the consideration of species differences in zonation, as much of the work investigating this area has been performed in rodents, with less information being available on zonation of the human liver. Studies to date have demonstrated that similar to rodent liver, human liver expresses gluconeogenic and glycolytic enzymes (Sokal et al. 1989; Morrison et al. 1965) in a zonal pattern whereas pyruvate kinase was found to be homogenously expressed throughout the liver in humans, dissimilarly to that of rodent liver (Wimmer et al. 1990).

Several explanations have been developed for the source of the zonated phenotype. The ‘developmental hypothesis’ suggests that zone III and zone I hepatocytes develop from

distinct origins, however there is limited evidence to support this, and the fact that the perinatal liver is not zonal in mice brings this into question (Häussinger et al. 1991; Notenboom et al. 1997). The 'streaming liver theory' suggests that hepatocyte proliferation mainly occurs in the zone I region of the liver, where putative stem cells reside. Newly formed hepatocytes then move along the porto-central axis throughout their lifetime, changing phenotype depending on their environment/location. Similarly to the first hypothesis, the evidence to support this is limited. In fact, it has been demonstrated using cell-tracing that hepatocytes proliferate in both the zone III and zone I zones (Bralet et al. 1994). The 'blood hypothesis' suggests that zonation is based on the composition of the blood arriving at hepatocytes in the different regions of the liver. The blood arriving in the zone I region of the liver is highly oxygenated, whereas the oxygen content in the zone III region is much lower. This hypothesis suggests that the differing microenvironment surrounding these hepatocytes drives the zonal phenotype and zonal functionality. Studies in which the hormone and oxygen content of afferent vessels was altered demonstrated that some zonal functions are reversible, such as glycolysis and gluconeogenesis. However, processes such as zonal ammonia detoxification were not altered, which suggests there is another layer of zonal regulation involved (Tygstrup et al. 1962). Studies examining mRNA profiles from zone I and zone III hepatocytes were able to demonstrate that zonal processes were under the control of mRNA expression (Drug metabolism, glucose and ammonia metabolism), suggesting that there is a level of transcriptional control over zonation (Braeuning et al. 2007). Studies examining the effector pathways of these genes identified the Wnt/β-catenin pathway as a critical regulator of hepatic zonation (Cadoret et al. 2002). This pathway is negatively regulated in the zone I regions of the liver by adenomatous polyposis coli (APC), a tumour suppressor gene product, whereas APC is not present in the zone III regions of the liver (Benhamouche et al. 2006a; Benhamouche et al. 2006b).

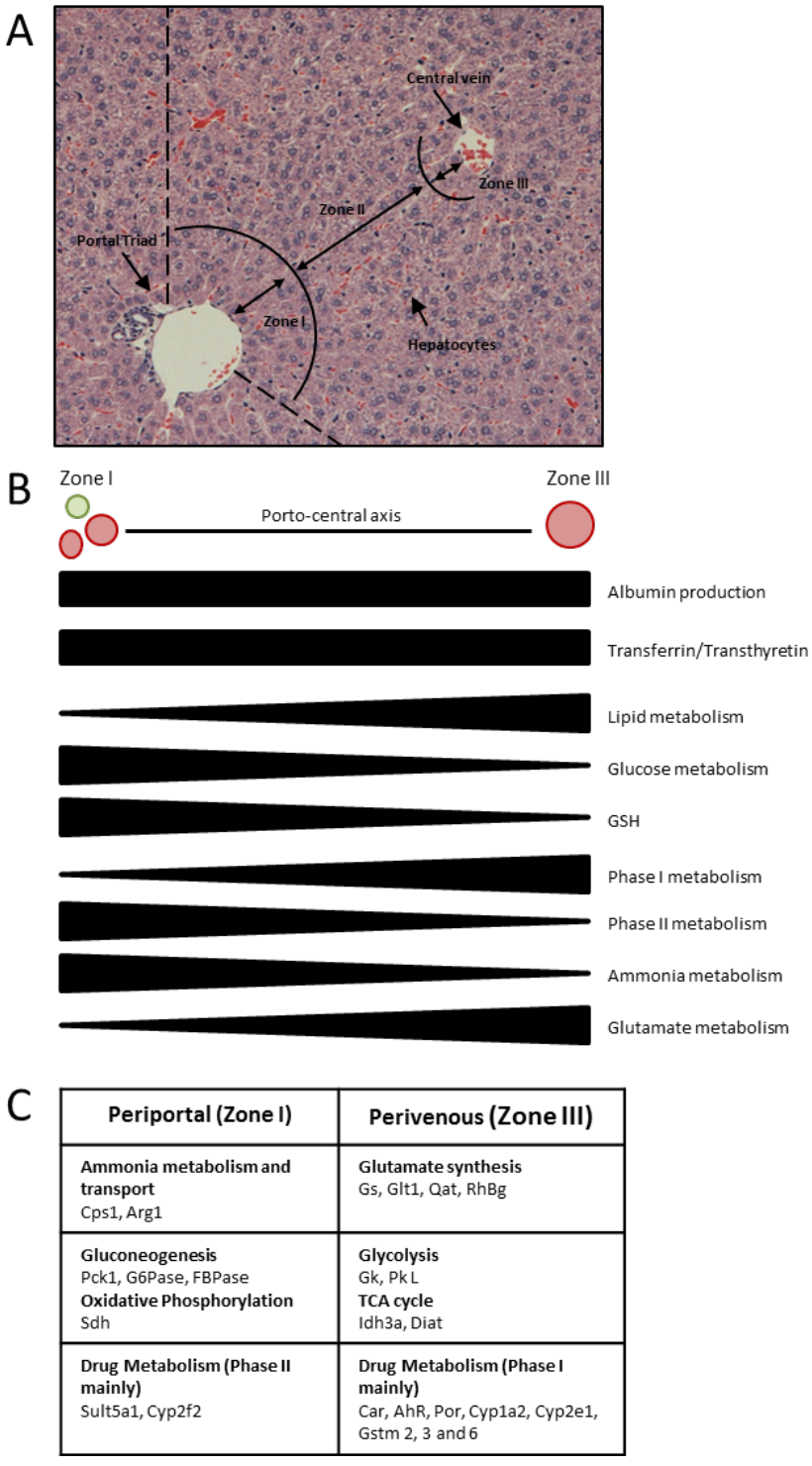

C

Periportal (Zone I)	Perivenous (Zone III)
Ammonia metabolism and transport Cps1, Arg1	**Glutamate synthesis** Gs, Glt1, Qat, RhBg
Gluconeogenesis Pck1, G6Pase, FBPase **Oxidative Phosphorylation** Sdh	**Glycolysis** Gk, Pk L **TCA cycle** Idh3a, Diat
Drug Metabolism (Phase II mainly) Sult5a1, Cyp2f2	**Drug Metabolism (Phase I mainly)** Car, AhR, Por, Cyp1a2, Cyp2e1, Gstm 2, 3 and 6

Figure 1.2 Hepatocyte zonation in mice (Adapted from Jungermann and Kietzman 1996)**. A,** hepatocytes are zonated and can be classified on their location along the porto-central axis (space between portal vein and central vein). Zone I hepatocytes reside in the portal triad region (within 6-cells radius), zone II hepatocytes reside between the two regions, and zone III hepatocytes reside within a 3 cell radius of the central vein. **B**, cellular processes which are expressed in a zonal manner (rectangles are expressed equally between regions). **C**, cellular proteins which are expressed in a zonal pattern.

1.3 DRUG-INDUCED LIVER INJURY

The liver is highly susceptible to DILI as it is the main organ responsible for the detoxification/metabolism of xenobiotics and natural toxins (Park et al. 2011). To date, over 1000 different drugs have been associated with hepatotoxicity, independent of class or indication (Hoofnagle et al. 2013). DILI, similarly to other ADR's can be can be divided into Type A, predictable and Type B, idiosyncratic reactions. Type A DILI is commonly caused by overdoses of compounds such as paracetamol, in which there is a clear dose-dependent link the drug and the onset of toxicity (Watkins et al. 2006), which will be discussed in further detail in a later section.

Type B reactions are less common, often severe and have been associated with a plethora of different drugs, including troglitazone (Murphy et al. 2000), flucloxacillin (Koek et al. 1994; Daly et al. 2009), diclofenac (Boelsterli et al. 2003) and amiodarone (Simon et al. 1984) to name only a few examples. The mechanisms behind type B DILI are complex and there is not one unifying mechanism between toxicities caused by different compounds (Watkins et al. 2006). In addition, these mechanisms are difficult to investigate due to the lack of test systems available to detect this type of DILI, which is further compounded by the low overall incidence of these reactions (1 in 10,000 to 1 in 100,000 patient-years) making it difficult to detect these reactions in clinical trials (Watkins et al. 2005). Several mechanisms have been suggested to play a role in the development of idiosyncratic DILI including mitochondrial heteroplasmy (Boelsterli et al. 2007), bile-salt export pump (BSEP) inhibition (Funk et al. 2011) and human leukocyte antigen (HLA) genotypes (Daly et al. 2009), however, no one overriding mechanism common to all type II reactions has been discovered.

A notable example of a type II toxin is troglitazone, a first-in-class PPAR-γ agonist used for the treatment of type II diabetes, which was initially enthusiastically received by doctors and patients. However, within 1 year of product launch, reports of acute liver failure associated

with this drug were being reported (Watkins et al. 1998). Troglitazone DILI was characterised by a relatively acute onset of hepatocellular-injury generally occurring after 1-7 months of treatment, with delayed jaundice and serum bilirubin elevations, which would lead to severe liver failure if treatment was not stopped in time (Graham et al. 2003a; Graham et al. 2003b). The mechanisms behind troglitazone DILI are now well investigated and yet still disputed, with some groups suggesting that mitochondrial dysfunction was an underlying mechanism (Ong et al. 2007), and other suggesting that troglitazone has bile salt export pump (BSEP) inhibitor activity, leading to a gradual build up of bile salts and eventually hepatocellular damage through cholestasis (Funk et al. 2001), highlighting the complexity of these types of reaction.

DILI can also be classified as hepatocellular, cholestatic or mixed (hepatocellular-cholestatic) depending on the histological features of the injury. Hepatocellur injury most commonly resembles acute viral hepatitis, typified by a large level of hepatocyte necrosis and inflammation with only minimal cholestasis (Zimmerman et al. 1976i). Compounds such as isoniazid (Bernstein et al. 1980), green tea (Molinari et al. 2006) and methyldopa (Seggie et al. 1979) most commonly lead to hepatocellular injury. Conversely, cholestatic injury usually resembles bile duct obstruction or choledocolithiasis, and involves bile stasis, portal inflammation and proliferation or injury of the biliary epithelium (Padda et al. 2011). Clinically this pathology usually presents as jaundice, with right upper quadrant pain and itching. Examples of compound which lead to cholestatic injury include amoxicillin/clavulanate (Stricker et al. 1989), ciprofloxacin (Labowitz et al. 1997) and the sulfonylureas (Frier et al. 1977). Mixed injury involves a mixture of the symptoms and features of both hepatocellular and cholestatic injury, and is the typical clinical presentation of DILI caused by the majority of drugs (Bjornsson and Jonasson. 2013). Drugs which cause a mixed pattern of injury include the sulphonamides (Westphal et al. 1994), phenytoin (Parker et al. 1979; Taylor et al. 1984) and enalapril (De La Puente et al. 2001). Clinically, the type of DILI is distinguished using the R value, which is derived from the ratio of serum ALT to

serum alkaline phosphatase, a marker of biliary function. Values of 5 or more are classed as hepatocellular, 2-5 as mixed and <2 as cholestatic (Aithal et al. 2011).

1.4 DRUG METABOLISM

1.4.1 Phase I Metabolism

Phase I metabolism is the unmasking of reactive functional groups (-OH, -CO_2H, -NH_2, -SH) via hydrolysis, hydration, reduction or oxidation, which in turn facilitates the process of conjugation and excretion (Phase II). These reactions are catalysed by enzymes, such as the cytochrome P450s (CYP450), alcohol dehydrogenases, flavin monooxygenases (FMO), and monoamine oxidases (MAO). CYP450 and FMOs are mixed-function oxidases which require both oxygen and NADPH as substrates in order to function. CYP450 are critical in phase I metabolism and reflect the enormous variety in endogenous and exogenous substances, in their broad and overlapping substrate specificities (Gibson and Skett 2001; Rang et al. 2014). CYP450 are located in both the endoplasmic reticulum and in the mitochondria, as the terminal component of the electron transport system. CYP450 are sub-divided into 42 subfamilies located across 60 distinct genes, in the human genome. The CYP450 families 1 to 3 are mainly implicated in drug metabolism, whilst other families are involved in the metabolism and production of endogenous substances, such as steroid metabolism. CYP450s can be classed as haem-containing enzymes which catalyse the basic reaction, monooxygenation. CYP450 are the family of enzymes responsible for the bioactivation of paracetamol into NAPQI, a hepatotoxic reactive metabolite (Lee et al. 1996).

There is a level of interspecies variation in the variety of CYP450s and their function, notably between rodents and humans (Lewis et al. 1998), which is of particular importance when it is considered that most pre-clinical studies are performed in rodents. Because of this it is important to be cautious when extrapolating results from animal models in which the translational similarity of the CYP450 isoforms involved is not understood. To address this a study has been carried out examining the interspecies differences in CYP450 expression and

function (Bogaards et al. 2000) with the aim of providing a tool to select the most relevant species model for use in pre-clinical testing. An example of the poor extrapolation model can be seen in that of coumarin-induced hepatotoxicity, which was highly prevalent in rats, due to the formation of an epoxide intermediate metabolite, which was not seen in other species (Vassallo et al. 2004). In addition, some CYP450s are highly polymorphic within species, an example of which is CYP2D6 in humans, a drug which is responsible for the metabolism of around 40 clinically relevant drugs (Aiklillu et al. 1996). In certain populations, such as the Ethiopian population a polymorphism causing an ultra-rapid metabolism phenotype is highly common (Aiklillu et al. 1996), whereas a polymorphism causing a slower metaboliser phenotype is more common in the African-American population (Bradford et al. 1998).

FMOs share many similarities to CYP450s, however their major difference is their inability to oxidise carbon atoms, and their lack of induction by exposure to drugs, or pollutants (Woolf. 1999). They are mainly located within the microsomal fraction of the liver and are able to oxidise nitrogen, phosphorous and sulphur containing compounds (Tynes and Philpot 1987). Alcohol dehydrogenases facilitate the conversion of alcohols to aldehydes and ketones, and MAOs are oxidases which are able to remove the amine group of a compound using an oxygen molecule. Phase I metabolism is somewhat important in several forms of DILI, as it is a method by which drugs can be transformed into toxic metabolites. The ability of these enzymes to reveal free-radical function groups presents the risk of covalent binding to cellular proteins, and a shift in the redox-balance of the cell, all of which could lead to DILI (Yu et al. 2014).

1.4.2 Phase II Metabolism

Phase II metabolism is the process of adding endogenous co-factors in order to increase the polarity of the molecule, causing it to become more hydrophilic, aiding excretion. Phase II reactions include glucoronidation, sulfation, acetylation, methylation, amino acid conjugation and GSH conjugation (Gibson and Skett 2001; Rang et al. 2014; Timbrell 1999). These all

involve the conjugation of a molecule to a reactive metabolite in order to produce a more hydrophilic unreactive compound.

Glucuronidation, the major phase II conjugation pathway involves a glucuronide acting as a conjugation molecule which binds to a substrate via the catalysis of glucuronosyltransferases. First, the co-substrate uridine diphosphate glucuronic acid (UDPGA) is formed through a series of reactions. Glucuronosyltransferases (UGTs) then catalyse the transfer of glucuronic acid from UDPGA to a substrate resulting in a glucuronidated substrate. UGTs play an important role in xenobiotic metabolism, because glucuronic acid can be coupled to a diverse range of functional groups (Testa and Krämer. 2008).

GSH is another method of conjugation and cellular protection following phase I activation of compounds. Conjugation of GSH to electrophilic species is facilitated by the phase II metabolism enzymes glutathione S-transferases (GSTs). GSTs are either cytosolic (alpha, mu, pi, theta and zeta) or microsomal, with the former accounting for 95% of GSTs (Raha and Tew. 1996). GSH conjugation involves the formation of a thio-ether bond between the cysteine residue of the GSH molecule, and the electrophile. GSH-conjugates are then excreted in bile and converted cysteine/mercapturic acid conjugates in the intestines/kidneys (DeLeve. 1997). Similarly to Phase I metabolism, species variation in GSH conjugation should be considered due to the increased activity of this pathway in some species (Hengstler et al. 1999).

1.5 CELLULAR DEFENCE MECHANISMS

The liver is the most adaptive and regenerative of the organs within the body, in order to allow it to be an effective first line of defence in the body against exogenous toxins, and endogenous waste. During chemical stress the liver is able to activate endogenous ‘stress response’ pathways through detection of reactive metabolites or reactive oxygen species. This response is able to initiate *de novo* synthesis of antioxidant/stress proteins which are expressed at low levels under normal homeostasis, in an attempt to reverse the oncoming toxic insult. This

response can result in the return to homeostasis, proliferation of cells, differentiation, or if the damage is too severe for recovery, the initiation of cell death pathways.

1.5.1 Glutathione

Glutathione (GSH) is an intracellular tripeptide made up of a glutamate, cysteine and glycine residues, which is contained at high levels (0.5-10mM) within the cytoplasm of the hepatocyte (Meister and Anderson 1983). GSH plays an important role in the maintenance of the redox-state of the cell through performing antioxidant and free-radical scavenging functions (Hayes and McLellan 1999). Its presence during toxic stress is critical to avoid the loss of function of important cellular proteins. GSH is able to perform this function as a result of containing a sulphydryl group within its cysteine residue, which is able to act as a nucleophilic scavenger, and electron donor. And because of its high cellular content, reactive metabolites favourably react with GSH over cellular proteins, allowing these proteins to remain in their reduced state, which is critical to their function.

GSH is present within the cell in both reduced and oxidised (GSSG) forms, with the former accounting for the majority, due to the presence of GSSG-reductase, an enzyme which catalyses the reduction of GSSG. GSH is the first line of defence against electrophilic reactive metabolites; it is able to detoxify these through the donation of a proton through a nucleophilic attack, resulting in an inactive metabolite and GSSG, or it is able to directly bind to the reactive metabolite to increase its excretion (DeLeve. 1997). GSH is able to react with aliphatic-, aromatic- (halo- and nitro-), alkene- and epoxide-containing compounds (Gibson and Skett 2001). GSH-conjugation can either occur spontaneously, or it can be catalysed by GST enzymes, as discussed previously. Upon depletion of GSH, or when the ability of GSSG-reductase to reduce GSSG is surpassed, *de novo* GSH synthesis is induced. GSH synthesis occurs through a two-step reaction process which involves the synthesis of γ-glutamylcysteine from L-glutamate, facilitated by γ-glutamylcysteine synthetase, followed by the addition of a

glycine residue by GSH synthetase, to form γ-glutamyl-cysteine-glycine (Raha and Tew. 1996).

1.5.2 The Nrf2 pathway

Nuclear factor (erythroid-derived 2)-like 2 (Nrf2), a basic leucine zipper transcription factor is the master regulator of the cells antioxidant response. Under homeostasis, Nrf2 is present at low levels in the cell due to it undergoing rapid degradation. In normal conditions Nrf2 is located in the cytoplasm, and is bound to Kelch-like ECH-associated protein-1 (Keap1), which directs it for degradation via the proteasome (Dinkova-Kostova et al. 2002; Reviewed by Copple et al. 2010). Under oxidative stress conditions, Keap1 is able to sense the presence of oxidants through highly reactive cysteine residues. Under these conditions, Keap1 then releases Nrf2 which allows its translocation to the nucleus of the cell, where it is able to bind to and activate the ARE (antioxidant response element) promoter which leads to an up regulation of ARE-driven genes, including GSTs, GCL, heam oxygenase 1 (HO-1) and NAD(P)H:quinine oxidoreductase (NQO1) (Alam et al. 1999; Nguyen et al. 2003; Rushmore and Kong. 2002). HO1 is a member of the heat shock protein family (Hsp32) and plays a role in stabilising protein formation within the cell, and NQO1 catalyses the 2-electron reduction of quinones into a less toxic hydroquinone. The function of GCL and GSTs has previously been discussed in other sections. Induction of these genes increases the defences of the cell with the aim of reducing the toxic burden and returning the cell to homeostasis.

1.6 MECHANISMS OF DRUG-INDUCED HEPATOTOXICITY

Drug-induced liver injury is used as an umbrella to describe all forms of hepatic damage caused by an exogenous drug or chemical, however, the route and outcome of the injury can be highly varied. Toxicity can involve the parent compound, or the metabolism of parent compounds to reactive metabolites, which may lead to covalent binding of macromolecules, oxidative stress and GSH depletion. These can all contribute to the damage of cellular organelles, such as the mitochondria or endoplasmic reticulum which can in turn lead to cell death, either through apoptosis or necrosis, or a combination of these processes.

1.6.1 Covalent binding

Covalent binding in DILI usually occurs through the activation of a compound by CYP450 mediated metabolism to a reactive metabolite (usually an electrophile), which can then in turn react with residues of proteins and macromolecules to form stable drug adducts. Covalent binding to cellular proteins may cause an alteration of the proteins function, which if deemed as a critical protein for cellular function, may cause the initiation of cell death. It has also been suggested that if sufficient levels of protein function are altered through covalent binding, the cells ability to maintain homeostasis may be reduced, which will cause an altered redox balance, eventually leading to cell death. Covalent binding has been proposed as one mechanism for the toxicity of paracetamol (Minamide et al. 1998). Additionally, covalent binding of hepatotoxic drugs is thought to be involved in the triggering of the immune system which often results in a worsening pathology, which is what has been demonstrated to be the mechanism in halothane-induced hepatitis (Kenna et al. 1987).

1.6.2 Oxidative Stress

Oxidative stress is the imbalance redox state of the cell, due to an increase in the level of ROS above the cells capacity to reduce these molecules to H_2O. Examples of ROS include

superoxide, hydroxyl radicals, peroxynitrite and hydrogen peroxide. The immediate result of the build-up of these molecules is lipid peroxidation, reduced membrane functionality, and in turn, the loss of the cells ability to generate its own energy, and maintain ionic homeostasis (Buege and Aust. 1978; Radi et al. 1991). ROS are formed under normal homeostasis in the mitochondria, through a 1-electron transfer in the electron transport chain. However, under pathological conditions, this chain can become uncoupled, leading to the accumulation of ROS within the cell. Oxidative stress in clofibrate-induced hepatocyte cell death has been demonstrated to cause damage to mtDNA, leading to mitochondrial dysfunction and cell death (Qu et al. 2001).

1.6.3 Glutathione depletion

It has been suggested that depletion of cellular GSH is a prerequisite for the onset of toxic events for certain hepatotoxins (Jollow et al. 1973; Mitchell et al. 1973; Reed and Fariss 1984). Depletion of GSH in paracetamol-DILI is a well characterised event, occurring as early as 1H after administration of a toxic dose of paracetamol by I.P. injection in rodents. NAPQI, the reactive metabolite of paracetamol is able to bind covalently to the cysteine residue of GSH, by which it is detoxified and excreted, along with the GSH molecule. It has been demonstrated that GSH needs to be depleted by at least 80% or more in order for toxicity to ensue in paracetamol-injury (Jollow et al. 1973).

1.6.4 Mitochondrial damage

Mitochondria are the organelle responsible for the production of cellular energy, mainly in the form of ATP. Other roles of the mitochondria are maintenance of redox homeostasis, proliferation, and steroid synthesis. Mitochondria are also the target of hepatotoxins and have the ability to initiate cell death. Many drugs have been shown to cause mitochondrial dysfunction in hepatocytes through a myriad of different mechanisms, reviewed in Labbe et al. (2008). Drug-induced mitochondrial dysfunction can cause adverse events such as steatosis, hepatitis and steatohepatitis, leading to cirrhosis, fibrosis and liver failure. The

failure to detect mitochondrial hazards during drug development has led to patient morbidity and mortality during clinical trials plus the termination of numerous drug projects.

Mitochondrial dysfunction can lead to the uncoupling of the electron transport chain, producing a build-up of ROS within the mitochondrial membrane. ROS are then able to bind to critical mitochondrial proteins to disrupt cellular energy production, which in-turn leads to release of pro-apoptotic proteins. The mitochondria are able to initiate apoptosis through the opening of the mitochondrial permeability transition (MPT) pore, which leads to an increase in the permeability of the mitochondrial membrane to proteins under 1.5KDa. This results in a loss of membrane potential and the release of cytochrome C into the cytoplasm. Activation of the MPT is also able to lead to necrosis, as well as apoptosis. Apoptosis is an energetic process that requires the function of a Na^{+}/Ca^{2+} exchanger to rid the cell of excess calcium, however if the toxicity is such that the mitochondria are no longer able to produce ATP, cell death will proceed to necrosis. If cellular ATP is depleted during apoptosis, cell death will then proceed to necrosis, causing so called necro-apoptosis (Kanduc et al. 2002). It has also been suggested that mitochondrial injury is able to silently accumulate over time, seemingly without effect, eventually reaching a critical threshold, abruptly triggering idiosyncratic DILI (Boelsterli and Lim 2007).

1.6.5 Endoplasmic reticulum stress and the unfolded protein response

The endoplasmic reticulum (ER) has two main functions within the cell, the translation of protein, and the metabolism of xenobiotics (Reviewed extensively in (Cribb et al. 2005; Malhotra and Kaufman 2007). In times of translational stress, due to a heavy burden on the translational machinery, or through ER protein damage by toxicants, the ER can elicit a stress response, the unfolded protein response (UPR) (figure 1.3). The UPR's function is to reduce translational stress; however, in severe cases the UPR can activate destructive cell death pathways. A number of studies have demonstrated that drugs are able to elicit an ER stress response *in vitro*, and *in vivo,* including carbamazepine (CBZ) (Fredriksson et al. 2014),

paracetamol (Uzi et al. 2013), non-nucleoside reverse transcriptase inhibitors (Apostolova et al. 2013), HIV protease inhibitors (Zhou et al. 2006), and methapyrilene (Auman et al. 2007). Arylating quinones are particularly susceptible to inducing the UPR (Wang et al. 2006).

Under low levels of ER stress, the UPR acts to down-regulate global protein synthesis, through phospho-activation of Eukaryotic Initiation Factor 2α (EIF2α) by Protein Kinase ds-RNA-Dependent-Like ER Kinase (PERK) (DuRose et al. 2009), and also through up regulation of the Endoplasmic reticulum to nucleus signalling 1 (IRE1) pathway. The UPR also increases expression of protein chaperones, such as Glucose Regulated Protein 78 (GRP78) and GRP94 (Bedard et al. 2004), through nuclear translocation of Activating Transcription Factor 6 (ATF6), as part of a negative feedback-loop, and also decreases cellular oxidative stress, through activation of the Nrf2 pathway by PERK (Cullinan and Diehl 2004; Cullinan et al. 2004; Cullinan et al. 2003).

Under conditions where stress exceeds the capacity of the cells defences, the UPR initiates a pro-apoptotic cascade which leads to the death of the cell (Rao et al. 2004). This can be initiated by xenobiotics or reactive metabolites which covalently bind to, or damage proteins involved in the endogenous function of the ER, such as GRP78/94. This in turn activates the C/EBP homologous protein (CHOP), through the PERK and ATF6 pathways, which converge leading to BAX/BAC mediated apoptosis (Marciniak et al. 2004). Severe ER stress is also able to lead to calpain mediated apoptosis (Sanges and Marigo 2006), through the release of intraluminal calcium stores through Inositol Triphosphate -3 receptor (IP-3R) activation, and also activation of the IRE1 pathway, which both lead to mitochondrial membrane depolarisation.

Fredriksson et al (2014) was able to demonstrate, using siRNA to knock-down elements of the UPR in a HepG2 CBZ/diclofenac (DCN) model of DILI that the protective, and destructive elements of the UPR are divergent pathways, which can act independently of each other. Another study examining the mechanisms of efavirenz-induced liver injury in Hep3B, and

primary human hepatocytes, was able to demonstrate increased expression of pathways related to UPR-induced apoptosis. Importantly however, this study was able to demonstrate, using Rho^0 cells without functional mitochondria, that the mitochondria are required for full activation of the UPR, suggesting the importance of cross-talk between the mitochondria and ER (Apostolova et al. 2013).

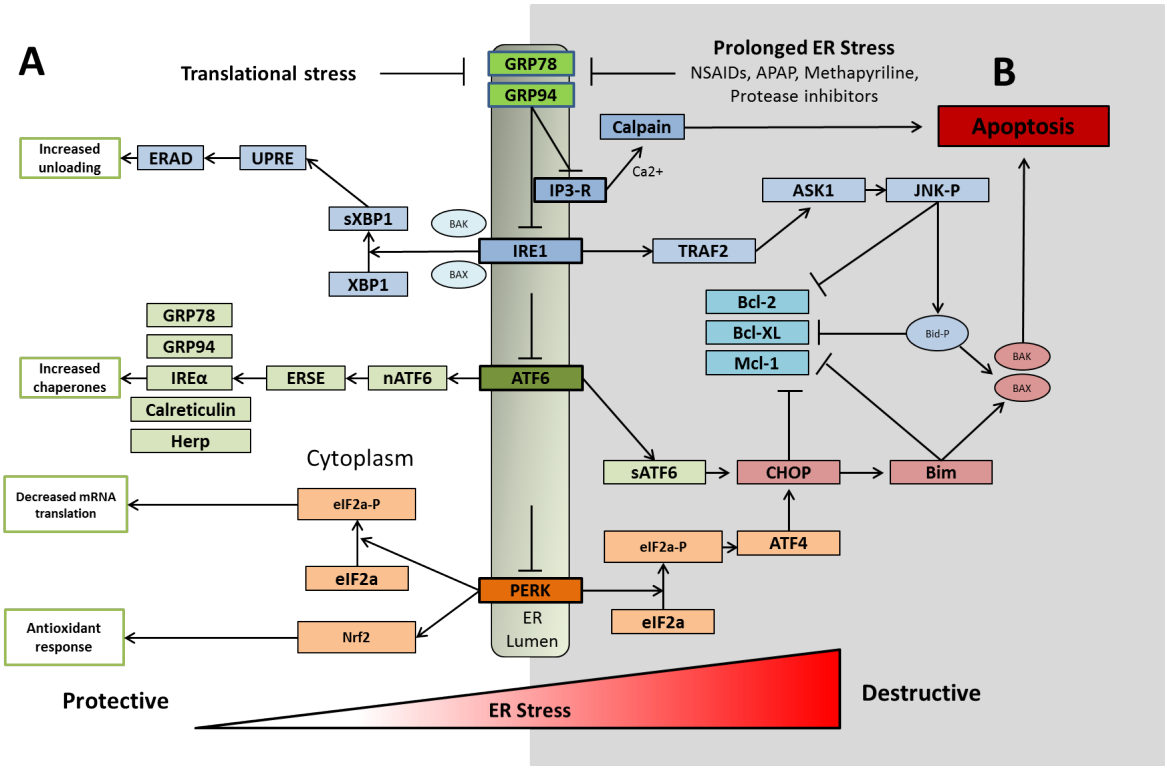

Figure 1.3 The protective and destructive functions of the UPR response. (Adapted from Chen et al. 2014 and Schonthal et al. 2012). **(A).** Under low levels of transcriptional/ER stress, the chaperones GRP78/94 release IRE-1, PERK and ATF6 to initiate downstream signalling events which result in reduced mRNA translation, increased antioxidant response through the Nrf2 pathway, and an increase in chaperone expression, as a negative feedback pathway. This is all with the goal of reducing the translational load on the ER in times of stress. **(B).** After prolonged or severe ER stress, or damage due to covalent binding of reactive metabolites/drugs to ER proteins, the UPR pathway can become destructive. Briefly, damage to, or down-regulation of chaperones (GRP78/94) during severe ER stress leads to activation of the CHOP and TRAF2 pathways, which lead to the down-regulation of anti-apoptotic signalling mechanisms and the activation of the pro-apoptotic Bid, and Bax. Prolonged stress can also cause release of intraluminal calcium stores from the ER, through the IP3 receptor, which can initiate caspase mediated apoptosis through a mitochondrial signalling route. This leads to increased oxidative stress, through release of ROS through the MTP, and an increase in inflammation through activation of NF-κB.

1.6.6 Apoptosis

Apoptosis is the programmed death of the cell, in order to prevent the transfer of damaged DNA to future lineages of cells. Cellular apoptosis is identifiable by characteristic nuclear condensation, DNA fragmentation and 'blebbing' of the plasma membrane. The blebbing plasma membrane then forms apoptotic bodies, small vesicles made up of the plasma membrane and the contents of the cytosol. These go on to be phagocytosed by scavenger cells such as macrophages, which recognise the externalised phosphatidylserine groups on the surface of the apoptotic bodies. This occurs in an efficient and ordered manner in order to not illicit an immune response (Savill et al. 1993).

Apoptosis can be initiated through two separate pathways, the intrinsic mitochondrial pathway, and the external death receptor pathway (Green and Reed 1998). The latter can be activated through the binding of a death receptor ligand (Fas-ligand, TRAIL, TNFα) to their receptor on the surface of the affected cell. Upon activation these receptors induce a signalling cascade which results in the formation of the death-induced signalling complex (DISC), which acts via adaptor proteins, FAD or TRADD to induce the caspase activation cascade. Caspases are a group of cysteine-aspartic-acid proteases which are able to cleave critical proteins containing aspartate residues, resulting the ceasing of cellular function and cell death (Cohen 1997; Earnshaw et al. 1999). The intrinsic pathway is mediated by the mitochondria as a result of cellular DNA damage by external factors, such as UV damage or chemical stress (Green and Reed 1998; Zamzami and Kroemer 2001), resulting in the MPT. This can also be activated by a shift in the balance of pro-apoptotic (BAX, BID) and anti-apoptotic (Bcl-$_x$1, Bcl-1) proteins within the cell. Once activated, the MPT causes a shift the permeability of the mitochondria, allowing the release of cytochrome C. Cytochrome c is a small heme protein associated with the mitochondrial membrane, its release from the mitochondria is able to activate the apoptosome, through binding of Apaf-1 and ATP, and the recruitment of pro-caspase 9. The apoptosome is able to cleave pro-caspase 9 to form caspase-9, which is then able to activate the effector caspases 3 and 7. Activation of these effectors leads to the cleavage

of other protein substrates which results in the apoptotic process. Cleavage of ICAD/DFF45 leads to DNA fragmentation carried out by Caspase Activated DNase (CAD), causing the characteristic DNA ladder formation. Apoptosis is not limited to pathological situations, it a key regulator in the development of organisms and is also involved in regulating the number of cells within an organ (Williams and Smith 1993).

1.6.7 Necrosis

Unlike apoptosis, Necrosis is a process of cell death which is not ordered and does not require the function of cellular energy production mechanisms (Kanduc et al. 2002). It is a process that is caused by acute cellular injury and results in the release of cellular contents into the surround area, due to plasma membrane damage. Characteristics of necrosis are mitochondrial swelling and loss of plasma membrane integrity, without any morphological changes to the nuclei. Necrosis is the pathway by which hepatocytes undergo cell death in paracetamol-DILI. However, in this form of injury there is also evidence for activation of apoptosis pathways, but no morphological sign of this, suggesting that neither form of cell death is mutually exclusive (Shen and Vandenabeele. 2014).

1.7 MODEL COMPOUNDS FOR THE ASSESSMENT OF DILI

1.7.1 Paracetamol

Paracetamol is one of the most commonly used over-the-counter analgesic and antipyretic drugs in the world, largely due to its wide availability and the contraindication of aspirin-containing products for paediatric use (Ward et al. 2001). Although paracetamol has an excellent safety profile, it is one of the most commonly associated compounds with intentional and unintentional overdoses (Penna et al. 2001), being the most common cause of acute liver failure, replacing viral hepatitis and the second most common cause of liver failure requiring liver transplant (Fontant et al. 2008). The US National Poison Data System reports of over 50,000 exposures (per annum.) related to paracetamol alone and 20,000 related to paracetamol in combination with another drug, which led to 65 and 42 deaths respectively (Mowry et al. 2015). Clinical symptoms often feature nausea and vomiting in the early stages of toxicity, followed by abdominal pain, tachycardia and hypotension at around 18h following ingestion. This is then followed by the hepatic phase, in which wide-spread hepatic necrosis and dysfunction is apparent, associated with jaundice, coagulopathy, hypoglycaemia and hepatic encephalopathy. After this secondary organ failure leading to death may occur if an appropriate therapeutic intervention is not put in place (Fontana et al. 2008). The standard approach to treatment often involves the use of activated charcoal, if presentation is <1h after ingestion, or an intravenous course of *N*-acetylcysteine, which is almost 100% hepatoprotective if administered within 8h of ingestion (Woodhead et al. 2012).

Paracetamol is an important model hepatotoxin. It produces predictable, dose-dependent liver injury in man and a strikingly similar hepatotoxicity in rodent models. An enormous amount of work to elucidate the molecular mechanisms that underpin paracetamol-induced ALI has been conducted in order to better understand the basis of DILI in a wider context. This work has been reviewed previously (Jaeschke and Bajt. 2006; James et al. 2003). At therapeutic

doses, the majority of paracetamol is directly conjugated by phase II metabolising systems. Approximately 50% of the dose is glucuronidated by several members of UGTs to form a stable glucuronide whilst a smaller proportion, approximately 30%, is sulphated by members of the SULT enzymes (Schenker et al. 2001). These non-toxic metabolites can be detected in serum and are excreted in the urine alongside a small proportion of parent drug and other minor metabolites. A small but significant proportion of the therapeutic dose (5-15%) undergoes oxidative metabolism via cytochrome P450-2E1 (CYP2E1) (and to a lesser extent by CYP1A2 and CYP3A4) (Chen et al. 1998; Patten et al. 1993; Thummel et al. 1993) (Figure 1.4). This oxidative metabolism yields a reactive electrophilic intermediate, n-acetyl-p-benzoquinone imine (NAPQI), which has the propensity to bind macromolecular components of the cell and elicit toxicity. The excellent safety profile of paracetamol is afforded by the vast levels of glutathione (GSH) in the hepatocyte which quench and detoxify the relatively small levels of NAPQI at therapeutic doses.

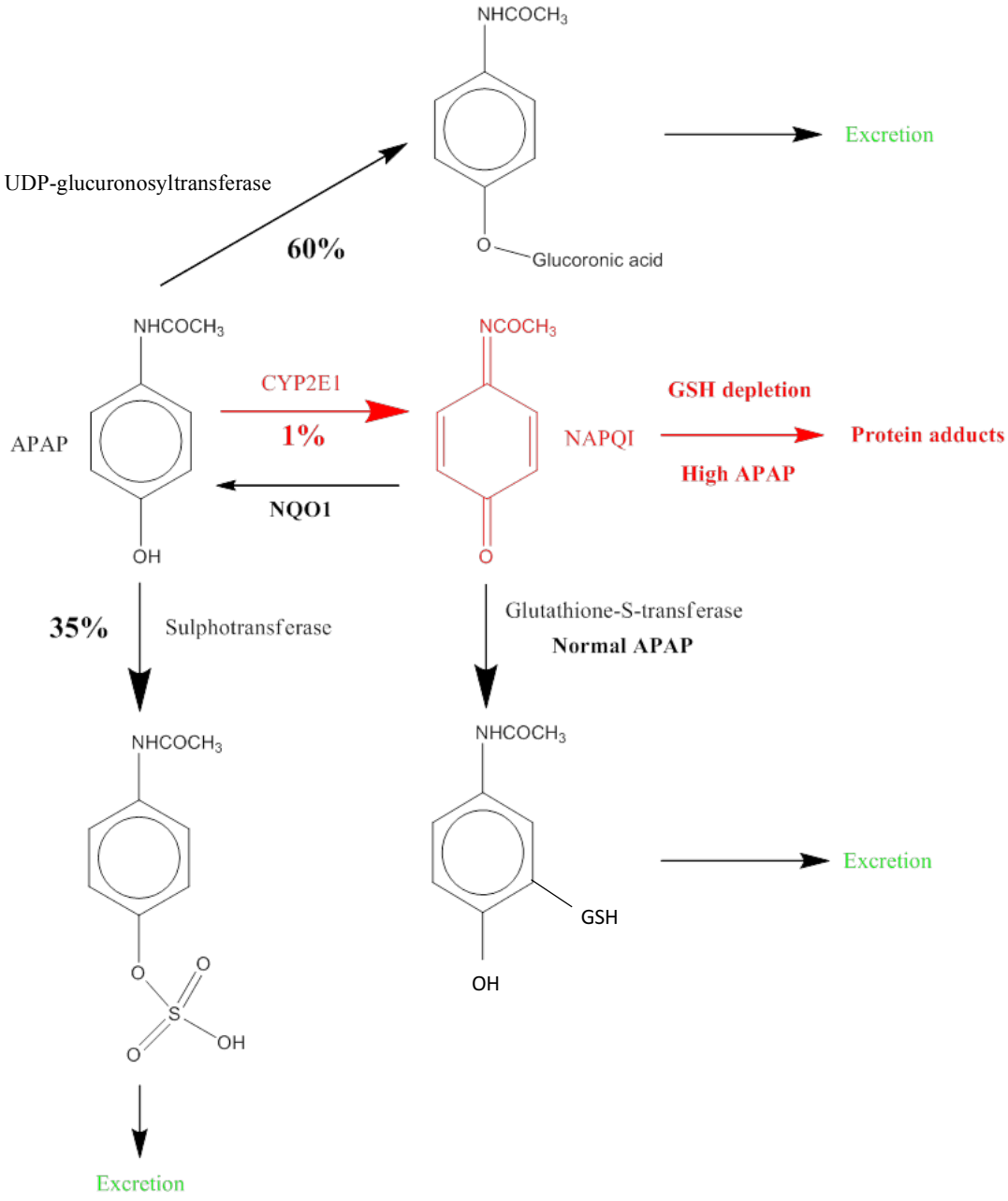

Figure 1.4 Metabolism of paracetamol. Paracetamol is conjugated, in the liver, to glucuronides (60%) and sulphates (35%), which are inert. 5-15% is converted by CYP2E1 to the reactive metabolite N-acetyl-P-benzoquinone (NAPQI). At normal doses NAPQI is conjugated to glutathione (GSH), at high doses the cell is GSH deficient and NAPQI accumulates. NAPQI can also be converted back to paracetamol by NADPH dehydrogenase quinone 1 (NQO1).

1.7.2 Furosemide

Furosemide (FS) is a carboxylic acid based loop diuretic used routinely for the treatment of oedematous states and hypertension (Ponto and Schoenwald 1990). FS has been shown to possess a hepatotoxic risk in rodent models, through a mechanism independent from its pharmacological action, whereas it is not generally recognised as being hepatotoxic in humans (Mitchell et al. 1976). FS displays a varied hepatotoxic potential between rodent species. Initial studies in mice found that FS causes severe hepatic centrilobular necrosis at high doses through the generation of a chemically-reactive metabolite (Mitchell et al. 1976; Mitchell et al. 1974). Later studies showed that rats could develop mild diffuse necrosis which could be exacerbated by pre-treatment with phenobarbital whereas hamsters appeared highly resistant to FS-induced hepatotoxicity (Lagarriga et al. 1976). A recent study found that the ability to form FS-glutathione conjugates *in vivo* may explain the species differences in toxicity between rats and mice (Williams et al. 2007).

FS contains several well-defined toxicophores including a furan ring, carboxylic acid and a primary amine group. Several studies have shown that the toxic metabolite is mediated by cytochrome P450s (Mitchell et al. 1976). Hepatotoxicity in mice appears to be associated with oxidation of the furan ring through an epoxide intermediate (Mitchell et al. 1976; Williams et al. 2007). Inhibition of epoxide hydrolase and subsequent covalent binding data support the theory that epoxide formation is the primary step in FS metabolism mediated hepatotoxicity (Wirth et al. 1976) (Figure 1.5). The extent of FS covalent binding also appears to correlate with the severity of liver injury (Mitchell et al. 1976) suggesting that the reactive intermediate can bind to macromolecules in the cell and exert toxicity. To date, no protein adducts have been reported with FS, however inhibition of mitochondrial enzymes has been found following FS treatment suggesting that the toxic intermediate can bind to and perturb endogenous protein function (Thorgeirsson et al. 1976). Disaggregation of polyribosomes, vesiculation of the rough endoplasmic reticulum, and dilation of the smooth endoplasmic reticulum have been reported as early histopathological findings during FS-induced liver

injury (Walker and McElligott 1981). The finding that FS does not deplete glutathione (GSH), an important thiol-containing antioxidant, distinguishes FS from other typical hepatotoxins like paracetamol and carbon tetrachloride (Mitchell et al. 1974). Wong and colleagues reported that both cytosolic and mitochondrial GSH levels were unaffected by FS treatment (Wong et al. 2000) suggesting that the mitochondria may not play a major role in FS-mediated liver injury. Furthermore, recent studies have shown that FS causes serum ALT activity rises (a signal of hepatocellular necrosis) but only modest concomitant glutamate dehydrogenase (GLDH) rises (a signal of mitochondrial dysfunction) in mice (McGill et al. 2012). These findings suggest that FS may initiate toxicity through a mechanism independent of the mitochondria, possibly through endoplasmic reticulum stress.

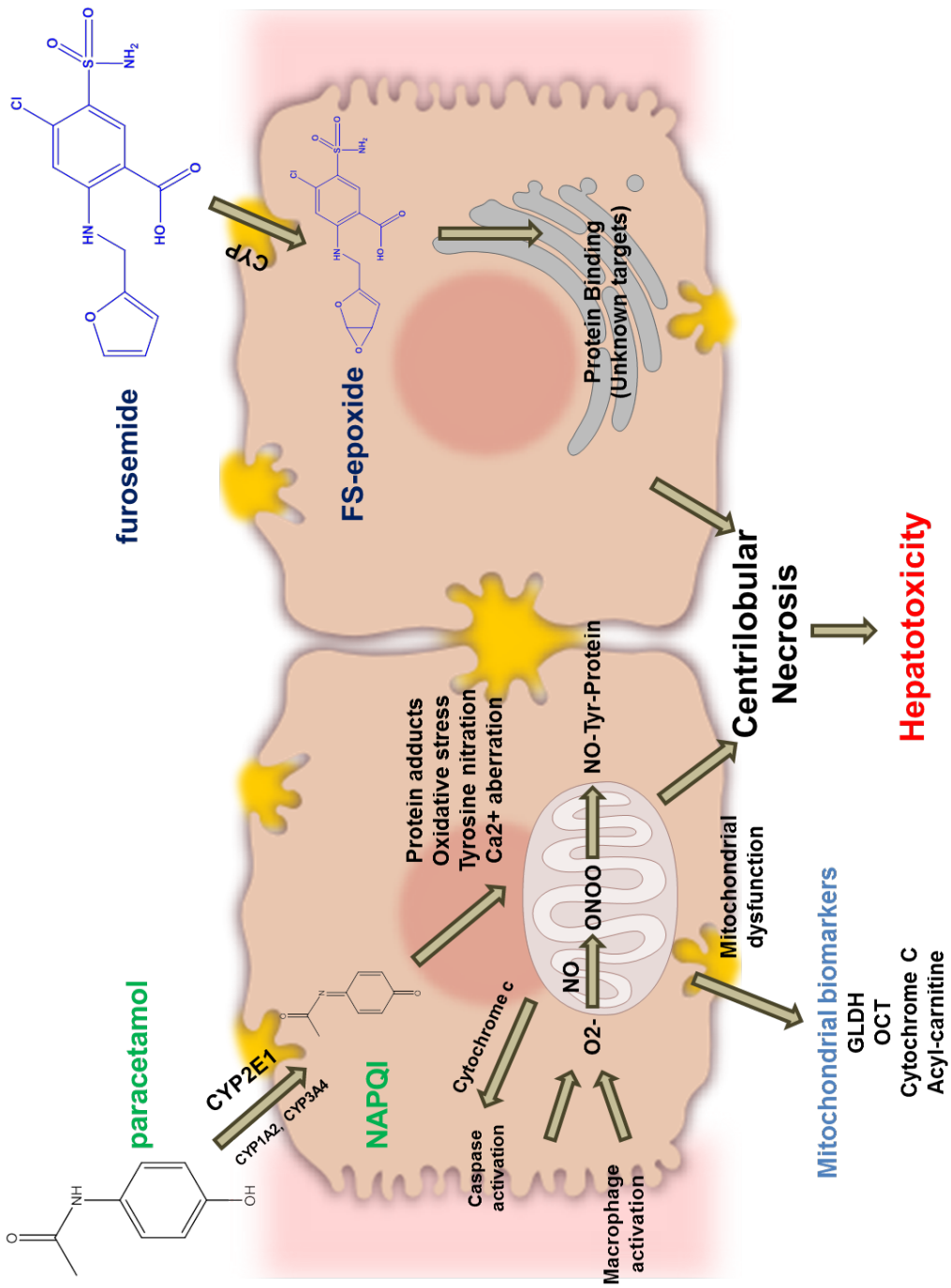

Figure 1.5 The diverging and re-converging pathways of paracetamol and FS toxicity. PARACETAMOL undergoes metabolism by the CYP450, CYP2E1 and forms the reactive metabolite NAPQI. NAPQI initiates a cascade of protein binding, oxidative stress and redox imbalance, leading to mitochondrial dysfunction and pericentral necrosis. Furosemide undergoes CYP450 metabolism, but then causes pericentral necrosis through a different route, thought to involve endoplasmic reticulum stress.

1.8 3-NITROTYROSINE AND HEPATIC PROTEIN TYROSINE NITRATION

The role of nitric oxide (NO) as an important signal transducer in the vasculature and nervous system has been well established. However, NO is also implicated in the development of a range of pathologies due to the propensity to form highly potent reactive nitrogen species (RNS). RNS can chemically modify specific amino acids on proteins by nitrating tyrosine residues (or nitrosylating cysteine residues) leading to a possible loss of protein function. Protein tyrosine nitration (PTN) is a covalent post-translational modification of a tyrosine residue at the ortho-carbon position of the phenolic ring, in which a nitro- group is substituted in place of a hydrogen molecule (figure 1.6). For this reaction to occur, a nitro- group must be produced, with nitric oxide providing the source (Radi et al. 2004). PTN can occur through several mechanisms and can be caused by more than one nitrating agent, the most common of which is peroxynitrite anion (ONOO-), formed through the reaction of endogenous nitric oxide and superoxide. ONOO- is a potent nitrating and oxidising agent, able to react with proteins (at tyrosine and cysteine residues), lipids and DNA (Figure 1.6). Under normal physiological conditions, peroxynitrite forms a carboxylate radical through homolysis and reaction with carbon dioxide, which is in turn able to nitrate oxidised tyrosine residues on proteins (Radi et al. 2004). Recently, other nitrating agents have been identified such as the formation of nitrogen dioxide by hemeperoxidases/transition metal complexes during nitrite metabolism (Pfeiffer et al. 2001; Pfeiffer et al. 2000; Thomas et al. 2002).

PTN has been shown to be present and in some cases implicated in a diverse set of disease states, including, neurodegenerative disorders (Lee et al. 2009) cardiovascular disease (Turko and Murad 2002) and diabetes. PTN has also been shown to be involved in the development of a range of liver diseases. PTN was evidenced in 54 patients with chronic viral hepatitis (HBV and HCV) (García-Monzón et al. 2000). Importantly, the levels of PTN correlated with the severity of hepatocellular injury in these patients, as determined by the histological activity index. This study also showed that PTN could distinguish between chronic viral hepatitis and

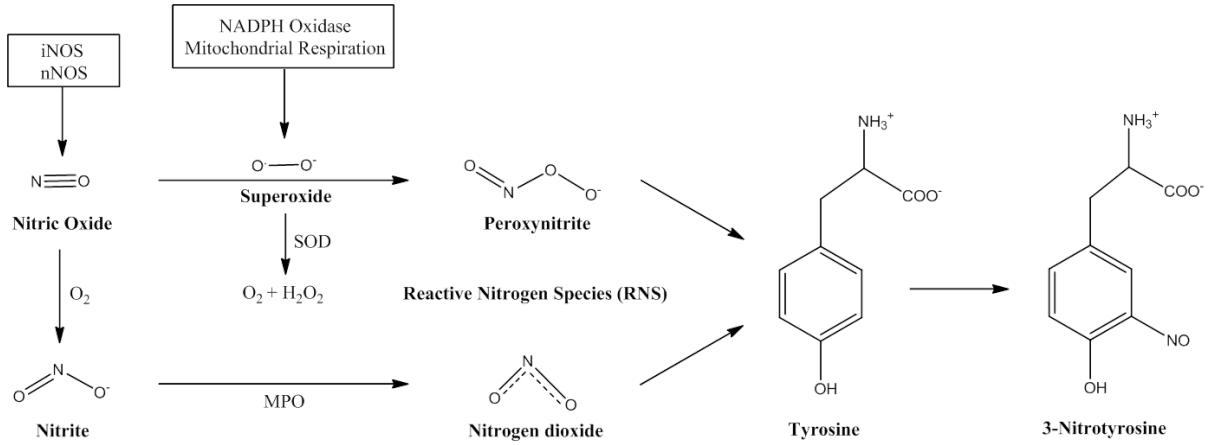

Figure 1.6 Mechanisms of reactive nitrogen species production and formation of 3-nitrotyrosine. Nitric oxide is endogenously produced by iNOS/nNOS and under pathological conditions can react with oxygen containing compounds to form highly reactive nitrogen species. Under oxidative stress conditions high levels of superoxide are produced by mitochondrial respiration or NADPH oxidase. Superoxide is able to react with nitric oxide in a spontaneous reaction to form peroxynitrite, a highly reactive nitrogen species. In conditions in which low levels of superoxide are produced, superoxide dismutase (SOD), an enzyme present in the cytosol and mitochondria, is able to metabolise superoxide to oxygen and hydrogen peroxide, thus reducing levels of nitrosative stress. Nitrogen dioxide, another reactive nitrogen species can also be produced through the formation of nitrite from a reaction between nitric oxide and oxygen, which can be enzymatically transformed, by myeloperoxidase (MPO) into the reactive species, nitrogen dioxide. Reactive nitrogen species are able to react spontaneously with certain tyrosine residues of proteins and form 3-nitrotyrosine residues.

alcohol steatosis suggesting that PTN is involved in specific mechanisms of liver injury. In a separate study, PTN levels were raised in patients with primary biliary cirrhosis and patients with autoimmune hepatitis (Sanz-Cameno et al. 2002). Visual scoring of both PTN and iNOS levels correlated with the histological grade of liver injury. These studies show that PTN is a clinically-relevant phenomenon that can contribute to the severity and development of liver disease in patients. Similar findings have been reported in experimental models of liver disease. In a diabetic rat model, PTN was found to be elevated in the mitochondria of hepatocytes which were associated with ultrastructural damage to the mitochondria (Ren et al. 2008). Another study showed that in mice fed on a high-fat diet that develop non-alcoholic steatohepatitis (NASH), mitochondrial function was diminished (Mantena et al. 2009). Importantly, PTN levels were increased in mitochondrial proteins and closely reflected the hypoxia gradient. Mitochondrial proteins are particularly susceptible to PTN due to these

organelles being the major intracellular source of superoxide, other ROS and neuronal NOS (nNOS). It was recently shown that in a mouse model of acute alcohol liver dysfunction, tyrosine residues in complex V proteins of the mitochondrial respiratory chain were nitrated causing loss of function (Larosche et al. 2010). These effects were prevented in mice with induced expression of manganese superoxide dismutase (MnSOD), an enzyme implicated in the detoxification of reactive oxygen species. Clearly, whilst an unequivocal role in disease pathogenesis remains to be shown, PTN may contribute to the development of liver injury in specific liver diseases.

PTN is a selective process, in which specific tyrosine residues are nitrated, e.g. residue Y_{115} is preferentially nitrated on ribonuclease A and residue Y_{102} is nitrated on phospholipase A_2 (Souza et al. 1999). Unlike phosphorylation, the primary protein sequence does not affect this, but factors such as the proximity to reactive cysteine residues or negatively charged amino acids, steric hindrance, tyrosine surface exposure and the location of tyrosine residues within the tertiary structure of the protein can influence the pattern of PTN. Additionally, the nature of the nitrating agent also affects the pattern of PTN, an example of which is ribonuclease A which is preferentially nitrated by nitrogen dioxide, whereas phospholipase A_2 is preferentially nitrated by peroxynitrite (Souza et al. 1999). PTN can cause loss of protein function; however some proteins retain function after nitration has occurred. The site of nitration appears to be an important factor on protein function. MnSOD, an important mitochondrial enzyme is nitrated at Y_{34}, which is located directly in the catalytic side of the protein and leads to a loss of enzymatic function (MacMillan-Crow et al. 1998). However, mitochondrial aconitase is nitrated at residues Y_{151} and Y_{452} (Tórtora et al. 2007). These residues are located far from the catalytic site of the protein and cause no functional change. PTN may also cause a change of protein function; nitration of cytochrome C abolishes its function in the apoptosome, however cytochrome C gains peroxidise activity (Figure 1.7).

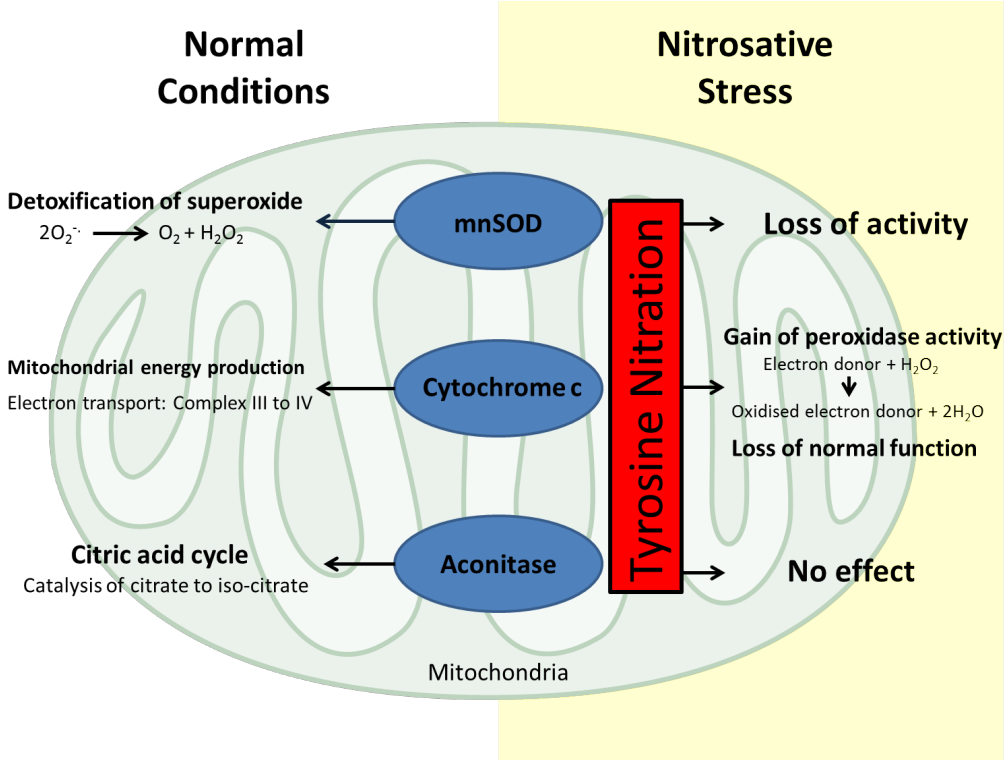

Figure 1.7 Nitration of tyrosine residues within cellular proteins can have mixed consequences. Manganese superoxide dismutase (mnSOD) is nitrated within its active catalytic site and loses its function. Cytochrome C gains peroxidase activity after nitration, and nitration of aconitase has no effect on the proteins function.

1.9 BIOMARKERS OF DILI

1.9.1 Current biomarkers of DILI

The current gold-standard biomarkers of liver injury are ALT and aspartate transaminase (AST) (Ozer et al. 2008). These enzymes are involved in amino acid biosynthesis and are released into the circulation following hepatocyte cell membrane breakdown during necrosis. Despite these markers being the gold standard, they suffer from a lack of liver specificity. ALT exists in two isoforms (ALT1 and ALT2), which are expressed in heart, kidney and muscle tissue to different degrees, therefore, these enzymes may not only report on liver injury. ALT1 has been demonstrated to be expressed in high levels in human liver tissue, as well as being the most abundant isoform detectable in human serum. Importantly however, ALT1 is also detectable in high levels in kidney and muscle tissue, hampering the use of an isoform- specific assay (Lindblom et al. 2007). As a product of this, ALT has previously been demonstrated to be elevated in cases of muscle injury (Zhang et al. 2010). A variety of studies have also demonstrated that ALT levels may become raised in humans undertaking extreme endurance sports events (Koutedakis et al. 1993). Additionally, ALT can be raised by hyperalimentation (Kubo et al. 2007) and basal expression can be induced by drugs (Lee and Kenney 1970). ALT2 does not offer use as a biomarker of liver injury, as it is expressed at negligible levels in the liver (Lindblom et al. 2007).

Due to the clear lack of an appropriate clinical biomarker to detect DILI, the usual method of practice in clinics in the UK is to establish a causal relationship between the drug in question and the possible diagnosis of liver damage. To establish this relationship, several qualitative scoring systems have been developed, a commonly used example of which is the Roussel Uclaf Causality Assessment Method/Council for International Organizations of Medical Sciences scale (RUCAM/CIOMS) (Benichou et al. 1993; Lewis et al. 2008; Rochon et al. 2008). The RUCAM/CIOMS scale takes the type of liver injury into account (hepatocellular, cholestatic or mixed) and is a qualitative system that scores on seven criteria: temporal

relationship, clinical course, risk factors, concomitant drugs, non-drug aetiologies, likelihood of reaction based on published research and response to re-challenge (Benichou et al. 1993). The score developed from this scale then allows clinicians to categorise patients based on their risk of developing DILI. The limitations of this system have now been highlighted in several studies which suggest that the lack of a clear scoring method and non-intuitive output have limited the reliability of this system (Tajiri et al. 2008; Rochon et al. 2008). In the UK, the standard method of practice is to assess the risk of poor outcome (i.e., development of liver failure) in cases of liver injury using the King's College Criteria, developed at the Liver Unit, King's College Hospital (London, UK) (O'Grady et al. 1989). The King's College Criteria is also qualitative system, which takes into account blood pH, serum creatinine, grade of encephalopathy and prothrombin time to assess patient's prognosis of outcome (Anand et al. 1997; O'Grady et al. 1989).

Outside of the clinic in drug development, the current FDA- and EMA-endorsed approach is the combined use of four markers, ALT, AST, alkaline phosphatase and total bilirubin, providing an integrated assessment of liver function. This approach is based on Hy's law, which states that if a drug causes ALT/AST levels to increase to >3x upper limit of normal (ULN) and total bilirubin levels to increase above 2x ULN and there is not an obvious indication of viral hepatitis or other obvious cause, a drug is likely to cause hepatotoxicity. Despite this approach, each of these markers is limited by the possibility that they may also rise in other indications, aside from liver injury (Shi et al. 2010). AST, similar to ALT, is liable to rise in muscle injury (Ozer et al. 2008); bilirubin detection can also be a by-product of erythrocyte haemolysis through macrophage-mediated recycling of the released haemoglobin into unconjugated bilirubin and also several other non-DILI-related conditions (Fabris et al. 2009; Ohmori et al. 2003). Serum alkaline phosphatase, a marker of cholestasis, is also not liver-enriched and may rise in bone diseases and in pregnancy

1.9.2 Serum GLDH

Glutamate dehydrogenase (GLDH) is an enzyme that is enriched in the mitochondria of hepatocytes, with smaller amounts contained within the mitochondria of kidney and muscle tissue. GLDH plays an endogenous role in the detoxification of urea, as well as supporting amino acid metabolism (Mühlberger and Kraft 1994). A spectrophotometric assay exists that allows GLDH activity to be measured in serum, analogous to serum ALT activity measurement (Passonneau et al. 1993). Due to the large size of GLDH (330 KDa), it is restricted within the cell after release from a damaged mitochondrion. GLDH elevations can only be detected in the circulation after cell necrosis. In humans, GLDH was demonstrated to be a sensitive marker of DILI when tested with a range of different hepatotoxic compounds, including paracetamol (Schomaker et al. 2013). The same study demonstrated that serum GLDH levels return to baseline before that of ALT, suggesting that GLDH has a shorter circulatory half-life. GLDH may therefore reflect more closely the true morphology of the liver compared to ALT. However, in a previous study in both humans and mice, it was suggested that GLDH was a mechanistic marker of mitochondrial injury (McGill et al. 2012). An *in vivo* mouse study demonstrated that after administration of paracetamol (McGill et al. 2012), serum GLDH levels were vastly increased alongside mitochondrial DNA (mtDNA) levels. Interestingly when FS was administered at a toxic dose, serum GLDH and circulating mtDNA levels remained in the normal range, even at peak toxicity when ALT levels were high. In a clinical setting, GLDH offers much promise as a sensitive marker of liver injury. However, a recent letter highlighted that a meticulous methodology for the preparation of serum samples is essential to measure GLDH activity appropriately (Jaeschke et al. 2013). It was suggested that GLDH levels may become falsely elevated in serum if intact circulating mitochondria released from cells are not extracted first before freezing. Nevertheless, GLDH is a potentially valuable biomarker of hepatic mitochondrial dysfunction due to hepatic enrichment and the ability to provide mechanistic insight into the basis of liver injury.

1.9.3 MicroRNAs

MicroRNAs (miRNA) are short, non-coding sections of RNA, usually 18-22 nucleotides in length (Arasu et al. 1991; Wightman et al. 1991), which have been suggested to play a role in the pathology of a wide range of diseases. miRNAs are also present and highly stable in bio-fluids, such as blood and urine, so can be easily accessed in a non-invasive manner. The stability of miRNAs has been attributed to the various forms in which they are released from cells, including in vesicle-encapsulated forms (Arroyo et al. 2011) and protein-bound complexes (Arroyo et al. 2011; Turchinovich et al. 2011). Additionally, some miRNAs demonstrate remarkable tissue enrichment, such as miR-1 in the heart (Ai et al. 2010) and miR-122 in the liver, representing approximately 70% of the total liver miRNA content (Lagos-Quintana et al. 2002). All of which together suggests that miRNAs hold many of the properties required of successful circulating biomarkers of disease and injury.

1.9.4 MicroRNA Biogenesis (Figure 1.8)

miRNAs are usually encoded by intron sections of DNA and are initially formed as pri-miRNAs (~thousands of nucleotides in length). These are cleaved within the nucleus by Drosha, a class 2 RNase III enzyme (Lee et al. 2003), to form pre-miRNAs (~70 nucleotides). Pre-miRNAs are actively exported from the nucleus to the cytosol through transporters such as exportin 5 (Bohnsack et al. 2004). Within the cytosol, pre-miRNAs form a RNA-induced silencing complex (RISC) with proteins such as argonaute 2 (Ago2) (Chendrimada et al. 2005), which leads to their cleavage by Dicer, an endoribonuclease, to liberate mature single-stranded miRNAs (microRNA biogenesis is reviewed extensively in (Cullen 2004)). Mature miRNA/RISC complexes target specific mRNAs through antisense recognition via the

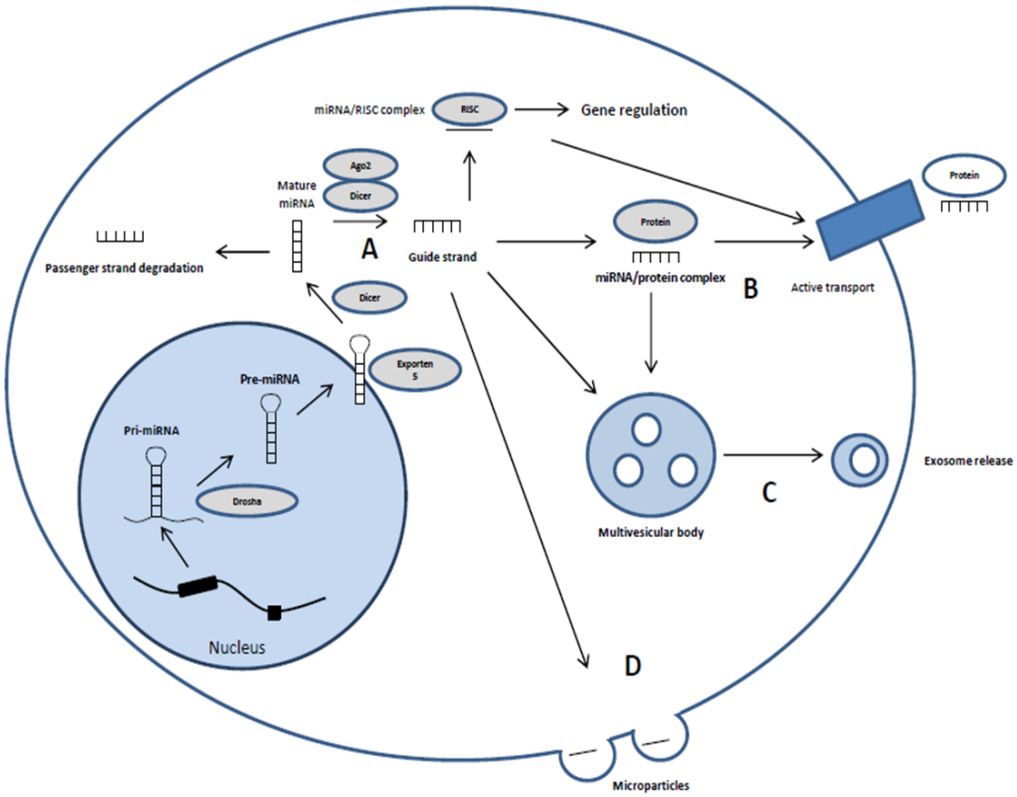

Figure 1.8 MicroRNA biogenesis and release into the circulation. A, microRNAs are transcribed within the nucleus as pri-microRNAs, which are then cleaved to form pre-microRNAs. Pre-microRNAs are then exported from the nucleus and further cleaved to form a mature microRNA. Mature microRNAs then form a functional RISC (RNA-induced silencing complex) with proteins such as Ago2. **B-D,** microRNAs can be released into the circulation in several forms, protein complexes, exosomes and microparticles (microvesicles).

miRNA sequence and thereby regulate RNA translation through a variety of mechanisms (Ørom et al. 2008; Xu et al. 2010). miRNAs play an important role in embryogenesis (Pauli et al. 2011), cell differentiation (Tay et al. 2008), tissue homeostasis (Miyaki et al. 2010), carcinogenesis (Datta et al. 2008), cardiotoxicity (Horie et al. 2010) and viral infections (Stern-Ginossar et al. 2007). Importantly, miRNAs can be also highly conserved between species (Pasquinelli et al. 2000). Because of this, they have great potential as translational biomarkers in pre-clinical models, as well as in the clinic.

1.9.5 MiR-122: a liver enriched microRNA

Several liver-enriched microRNAs have previously been identified which provided the first suggestion that microRNAs may be specific markers of the liver. miR-122 (mature strand of miR-122-5p) was first identified to be highly enriched in mouse liver tissue by (Lagos-Quintana et al. 2002), and is has since been suggested that it makes up almost 70% of the microRNAs contained within the liver of humans. Its sequence has since been shown to be highly conserved between 18 species, as well as between adult and foetal liver (Kozomara et al. 2011).

A growing body of evidence shows that miR-122 plays an important role in the physiology of the hepatocyte. Several web-based algorithms predict that miR-122 may target several thousand genes but most of these are yet to be experimentally verified. Studies utilizing anti-sense oligonucleotides in mice to inhibit miR-122 have established its role in the regulation of lipid and cholesterol metabolism. It was observed that when miR-122 function is abolished, the translation of important enzymes in these processes becomes deregulated, such as cholesterol 7α-hydroxylase (CYP7A1) (Esau et al. 2006). However, in pathological states it has been also shown that miR-122 may play a role in the development of cancerous tumours and in Hepatitis C infection (Girard et al. 2008; Jopling et al. 2005). In a study examining the replication of hepatitis C (HCV), it was observed that HCV was unable to replicate in cell-lines which did not express miR-122 (HepG2) when compared with lines that were miR-122

positive (Huh 7). This was further explored utilising antisense strategies to knock-down miR-122 expression, which consistently noted impaired HCV replication (Jopling et al. 2005). Interestingly, miR-122 is now being investigated as a drug target for HCV in phase II studies (Horie et al. 2010). In HCC, miR-122 is specifically down regulated in both humans and rodents (Kutay et al. 2006), and interestingly, has been demonstrated to modulate *cyclin* G1in HCC derived cell lines. Further studies in primary tumour cells lines have demonstrated an inverse expression relationship between miR-122 and *cyclin* G1, suggesting that down regulation of miR-122 in HCC may affect the cell cycle (Gramantieri et al. 2007). Mice that are genetically deficient of miR-122 are viable but develop spontaneous liver lesions and hepatocellular carcinomas early in life (Kutay et al. 2006). Therefore, it is clear that miR-122 plays an important role in liver biology and defines the phenotype of the mature hepatocyte.

1.9.6 MicroRNAs as novel biomarkers of liver injury

Initially, many of the studies examining the potential of miRNAs to serve as biomarkers focussed on the use of these molecules to detect cancer (Mitchell et al. 2008). However, recent studies have demonstrated the utility of some liver-enriched miRNAs, in particular miR-122, as possible markers of DILI and other forms of liver injury. Due to the large abundance and remarkable liver-enrichment of miR-122, several studies examined the use of this miRNA to serve as a circulating biomarker of liver injury. In a study examining paracetamol-induced liver injury in mice, the authors were able to demonstrate that miR-122 as well as another liver-enriched miRNA, miR-192, detected liver injury earlier and at lower toxic doses, than serum ALT activity when measured in serum (Wang et al. 2009). To test the translational potential of miR-122 and miR-192 as biomarkers of DILI, a study examining these markers in 53 patients admitted to hospital after taking an paracetamol overdose was performed. We demonstrated that both miR-122 and -192 were raised in serum when compared with healthy controls. Another observation in this study was that miR-122 levels returned to baseline between 3 and 7 days after initial hospitalisation, whereas serum ALT levels remained elevated (Starkey Lewis et al. 2011). This suggests that miR-122 has a shorter circulatory half-

life, which may allow miR-122 to closely reflect the actual state of the liver more than a biomarker which remains in the circulation for a long period of time without degradation. More recently, a study examining the utility of several mechanistic biomarkers of DILI in patients which had ingested a single toxic dose of paracetamol demonstrated that initial miR-122 levels at hospital presentation provided a significant correlation with both the maximum ALT activity and peak international normalised ratio (INR) score during the hospital stay of the patient. This highlighted for the first time that miR-122 is raised very early during liver injury in man, and may provide prognostic value to identify at patients who develop liver injury (Antoine et al. 2013a). Moreover, miR-122 was raised as early as 4 hrs after a toxic paracetamol dose, almost 8 hrs before ALT levels usually detected in serum, Since those initial studies, miR-122 has been found to report on a number of different drugs associated with liver injury, including heparin (Harrill et al. 2012), galactosamine and alcohol (Zhang et al. 2010). This data collectively suggests that miR-122 could be a liver-specific, early and sensitive marker of DILI within the clinic, which may be able to predict the severity of the pathology.

Additionally, to the utility of miR-122 as a biomarker of DILI, it has also been demonstrated to have use as a marker of hepatitis. Zhang *et al* was able to show that plasma miR-122 levels change in a disease-severity relationship in patients infected with hepatitis B (HVB), showing a strong correlation with plasma ALT activity (Zhang et al. 2009). Additionally, to this, miR-122 levels were raised earlier in the plasma and correlated strongly with histological grading. The strength of miR-122 as a biomarker (versus ALT) was tested using a ROC analysis and a multivariate logistic regression analysis, which suggested that miR-122, is a more sensitive biomarker of HVB-associated liver injury, than ALT (Zhang et al. 2009). In a different study examining patients with chronic hepatitis C (CHC), serum miR-122 levels were shown to strongly correlate with serum ALT levels in patients undergoing necro-inflammation associated with CHC (Bihrer et al. 2011). However, miR-122 did not correlate with changes in liver function and also the fibrosis stage of hepatitis, suggesting in CHC, miR-122 is a marker of cellular damage and not overall liver function (Bihrer et al. 2011). An additional

study testing the value of miRNAs as biomarkers to distinguish between hepatocellular carcinoma (HCC) and chronic hepatitis using a ROC analysis was able to support the use of miR-122 as a suitable biomarker of cellular damage. However, miR-122 was only able to distinguish patients with chronic hepatitis from healthy controls and not from patients with HCC, once again suggesting that miR-122 is a marker of hepatocyte damage (Xu et al. 2011).

1.9.7 miRNA stability in circulation and forms of release

Despite the RNA-based structure of miRNAs, which can be degraded quickly by cellular RNases, miRNAs are extremely stable in blood-based biofluids (Mitchell et al. 2008). Good stability is an ideal quality for a biomarker, as clinical samples in their very nature are unlikely to be collected, processed, and stored in exactly the same way, especially without an accepted universal protocol. Previous work has attributed this stability to the various forms in which miRNAs exist in the circulation (Arroyo et al. 2011). Previously miRNAs have been detected in the circulation within various biofluids, such as serum, plasma and urine, enveloped within small vesicles (Cortez and Calin 2009; Nilsson et al. 2009). More recently however, miRNAs have been detected circulating in a vesicle-free form, in which miRNAs are in complex with a protein or lipoprotein complex (Arroyo et al. 2011; Turchinovich et al. 2011; Vickers et al. 2011).

1.9.8 Vesicle-based miRNAs

1.9.8.1 Exosomes

Exosomes are a class of phospholipid nanovesicle, around 30-150nm in diameter which are formed within endocytic compartments called multivesicular bodies (MVB) and are then released into the circulation through exocytosis (Conde-Vancells et al. 2010). Exosomes were initially thought to be cellular debris and harbour no function. However, now it is understood that exosomes play a distinct role in cellular signalling, which allows them to play a role in the development of malignancies (Taylor and Gercel-Taylor 2005) and in the spread of viral infections (Ramakrishnaiah et al. 2013). Their full endogenous role still requires study due to

their relatively recent discovery (Pan and Johnstone 1983). Exosomes are released from a myriad of cell types, including hepatocytes (Conde-Vancells et al. 2010) and inflammatory cells (Brooks 1986), and have been demonstrated to contain cellular proteins, DNA, mitochondrial DNA (Sharma et al. 2013) RNA, lipids, as well as miRNAs (Exocarta provides an encyclopaedia of recorded exosome contents; www.exocarta.org). MiRNAs can associate with MVBs at the pre-miRNA stage, controlled by the presence of specific sequence motifs in the miRNAs (Villarroya-Beltri et al. 2013) and are then packaged into exosomes before release into the circulation, which is controlled by a ceramide-secretory system (Cocucci et al. 2009). Exosomes can be extracted from circulating biofluids through a variety of methods including ultracentrifugation (Pisitkun et al. 2004), immunoprecipitation (Taylor et al. 2011) and through use of specific exosome isolation solutions (Exoquick, SBI, Cambridge bioscience/Total exosome extraction solution, Life Technologies). The presence of exosomes in solution can be accessed through monitoring the presence of specific exosome markers such as CD63 (Valadi et al. 2007) or TSG101 (Conde-Vancells et al. 2008), using molecular biology techniques such as western blotting or through visualisation and measurement using electron microscopy or nanoparticle tracking analysis (Conde-Vancells et al. 2008; Oosthuyzen et al. 2013; Pisitkun et al. 2004).

A recent *in vivo* study examining drug-induced, alcoholic and inflammatory liver injury, demonstrated that miR-122 was detected in different fractions of blood during the different forms of injury. In paracetamol-DILI, miR-122 was largely detected in the 'protein-rich' fraction (remainder of serum, minus exosomes). They hypothesised that this was due to the necrotic injury phenotype of paracetamol, which allowed this marker to leak into the circulation in complex with the RISC, the functional unit of microRNA translation silencing, upon breakdown of the hepatocytes plasma membrane. In contrast, miR-122 was largely detected in the exosome-bound fraction in alcoholic liver injury, which was suggested to be due to the slower injury phenotype, involving activation of the cells adaptive processes, and recruitment of the immune system. This is also supported by the presence of miR-155, a

miRNA implicated in inflammation and immune regulation, in the exosomal-fraction, suggesting a possible role for exosomes in activating the inflammatory process (Bala et al. 2012). This together suggests that exosomes may offer a novel method for the cell to promote adaptation to liver injury, through both selective loss of cellular contents, and through cell-cell signalling.

1.9.8.2 Microparticles

Microparticles are a class of secretary vesicle, above 100 nm in diameter which are formed through 'blebbing' of the plasma membrane and are distinctly different from exosomes in their qualitative/quantitative content (Jy et al. 2004). This process is regulated by intracellular calcium levels, cytoskeleton protein reorganisation and changes in membrane lipid asymmetry (Yano et al. 1994). Microparticle release has been documented to take place during cellular apoptosis and is thought to be a cellular response to attempt to reverse apoptosis (Boulanger et al. 2006). Changes in the levels of plasma microparticles have been associated with many disease states, including cardiovascular disease (Boulanger et al. 2006), metabolic syndrome (Agouni et al. 2008) and diabetes (type 1 and 2) (Sabatier et al. 2002). Similarly to exosomes, microparticles have been shown to be implicated in cell-cell signalling, showing function in recipient cells (Mesri and Altieri 1999). Witek *et al*, demonstrated that liver-derived microparticles can alter gene expression in recipient liver endothelial cells through hedgehog signalling (Witek et al. 2009). Microparticles, like exosomes, have been demonstrated to contain protein, DNA, RNA and lipids. In a study examining the content of microparticles secreted from mesenchymal stem cells, the RNA content of microparticles was almost exclusively consisted of miRNAs, demonstrating that packing of these vesicles is a selective process which does not necessarily reflect the donor cell content (Chen et al. 2010). Interestingly, this study found hsa-let-7b and hsa-let-7g are secreted in their immature pre-miRNA forms, which would allow them to form a mature-miRNA/RISC complex in effecter cells and elicit an effect on RNA translation (Chen et al. 2010). This role is still yet to be understood fully and much work is still required before the role of microparticle packaged

miRNA is understood. Previous studies examining microparticles have focussed on the use of ultracentrifugation techniques to separate these vesicles from other vesicles such as exosomes and also from the microparticle depleted supernatant of biofluids. The success of this extraction is usually then assessed through measuring the expression of microparticle markers, such as phosphatidyl serine and annexin V in both the extracted microparticle solution and the supernatant (Théry et al. 2001).

1.9.9 Protein and lipid complexes

miRNAs have also been detected in the circulation in protein complexes usually formed with associated Ago2 proteins, a member of the RISC complex that mediates miRNAs function (Arroyo et al. 2011). Turchinovich *et al* (2011) demonstrated for the first time that miRNAs are almost exclusively present within the serum, under normal conditions in protein complexes associated with Ago2. This suggests that circulating miRNAs on the most part are a by-product of dead cells that remain in the extracellular space. However, recent work demonstrated that this association does not seem to be a random occurrence and that some miRNAs associate either with protein-complexes or with extracellular vesicles. Arroyo *et al* (2011) demonstrated through differential-centrifugation and size-exclusion chromatography of human serum, that different miRNAs exist within vesicles or associated with protein-bound complexes (Arroyo et al. 2011). In the serum of healthy volunteers, miR-122 was found predominantly in a protein-bound form, whereas let-7a was found almost exclusively within exosomes/microparticles supporting the initial study by Turchinovich *et al* that miRNAs are present within the circulation in vesicle-free form. However, the mechanism through which these protein complexes are released remains poorly understood (Arroyo et al. 2011; Turchinovich et al. 2011).

High density lipoproteins (HDL), have also been demonstrated to transport miRNAs, through a neutral sphingomyelinase dependent mechanism (Vickers et al. 2011). MiRNA/HDL complexes travel to recipient cells and undergo endocytosis through a Scavenger receptor type

class 1 dependent mechanism. Notably in this study, the delivered complexes were able to modify RNA translation in hepatocyte model of atherosclerosis, suggesting that these complexes are a form of cell-cell signalling pathway (Vickers et al. 2011). However, work still needs to be done to assess the relevance of these complexes in biomarker release and function in DILI.

Project Aims

DILI is a leading form of ADR seen within the clinic and the number one cause of clinical drug trial failure, costing both the NHS, and the pharmaceutical industry hundreds of millions of pounds per year. Because of this, better biomarkers to aid in the early diagnosis of liver injury, and in pre-screening hepatotoxic compounds in drug-development. miR-122 has been shown to be a potentially useful biomarker of liver injury (Starkey Lewis et al. 2011; Antione et al. 2013), however little is understood about how it is released into the circulation, and how it is able to become elevated above baseline, earlier than conventional liver injury biomarkers. Additionally, although miR-122 is well characterised in the circulation, little is known about changes in hepatic miR-122 and other miRNAs under basal and injury conditions. Therefore, this thesis aims to:

- Establish whether exosomal transport plays a role in the release of microRNAs in drug-induced liver injury
- Examine the role of hepatic zonation in microRNA expression, including whether microRNAs are expressed zonally, and whether this can be linked to liver phenotype.
- Establish whether microRNAs have the potential to be used as biomarkers of injury in hepatic non-parenchymal cells.

It is now understood that formation of 3-NT protein adducts occurs in paracetamol-DILI (Hinson et al. 2000), however little is known about the route by which these occur and their overall function within the pathology. Therefore, this thesis aims to build on previous work examining 3-NT in paracetamol-injury, by comparing and contrasting this type of injury to FS-injury, in order to gain a greater understanding of the role of these adducts. Both paracetamol and FS are well-known pericentral hepatotoxins in rodents; however, they both cause injury through divergent pathways. paracetamol is known to target the mitochondria, whereas it is thought that FS targets the endoplasmic reticulum. 3-nitrotyrosine adduct formation has now been demonstrated to play a role in paracetamol-DILI; however, it remains unclear as to whether this cellular process plays a role in FS-DILI. Therefore, we aim to

investigate whether 3-NT is present in FS-DILI in order to further understand where the two pathways of toxicity diverge.

Hypothesis 1

Paracetamol and FS both produce necrosis in zone III of the liver, but both compounds cause this toxicity through distinct routes. We hypothesise that formation of 3-nitrotyrosine adducts, a marker of oxidative stress, will occur during paracetamol injury, but will not occur during FS injury, due to lack of mitochondrial damage in FS injury.

Hypothesis 2

miR-122 is detectable earlier in the course of DILI than conventional DILI markers due to its mechanism of release. We hypothesise that miR-122 is released actively from the liver in exosomes upon receiving a toxic insult in order to adapt to circumvent DILI.

Hypothesis 3

Liver microRNAs are expressed zonally depending on their proximity to a portal or ventral vein, and these expression changes will be related to hepatocyte phenotype and function in these regions. Upon liver injury by paracetamol, we expect to observe changes in microRNA expression in the region surrounding the central vein, however we also hypothesise that expression changes may occur away from this region in order to adapt to the oncoming toxicity.

Hypothesis 4

Intrahepatic biliary epithelial cells, which undergo damage during cholestatic injury, will contain a unique microRNA profile, differing from the surrounding hepatocytes. This profile will allow the selection of specific markers of ihBEC which will provide use as biomarkers of damage to this cell type in cell models, pre-clinical animal models, and possibly within the clinic.

CHAPTER 2

3-NITROTYROSINE FORMATION IS PRESENT IN BOTH PARACETAMOL- AND FUROSEMIDE-DILI IN THE MOUSE

2.1 INTRODUCTION

Protein tyrosine nitration (PTN) is the formation of 3-nitrotyrosine (3-NT) adducts in cellular proteins mediated by peroxynitrite, a reactive species formed by the rapid reaction of nitric oxide (NO) with superoxide (Ohshima et al. 1990). PTN has mixed functional effects on the target protein, depending on the site of nitration. Effects of PTN can include changing the proteins cellular function or abolishing their function altogether. PTN has previously been shown to be present early in paracetamol-DILI in mice (Hinson et al. 1998). It has since been demonstrated that PTN-adducts form in a number of critical mitochondrial and cytosolic proteins, including manganese superoxide dismutase, GSH peroxidase and mitochondrial alcohol dehydrogenase during paracetamol-injury *in vivo* (Abdelmegeed et al. 2013). *In vitro* studies in primary mouse hepatocytes aiming to examine the mechanisms behind PTN in paracetamol-DILI, have suggested a role for mitochondrial toxicity and the mitochondrial permeability transition (MPT), in the formation of PTN in paracetamol-DILI (Burke et al. 2010). Administration of cyclosporine A, an MPT inhibitor was able to abolish PTN and eliminate toxicity in a model examining the role of reactive oxygen/nitrogen species in paracetamol-toxicity. Whereas inhibitors of iNOS had little or no effect on the levels of PTN or toxicity, suggesting that the causative factor in PTN could be superoxide generated by the failing mitochondria. In order to examine this further, and confirm the role of the mitochondria in PTN formation, we chose to compare paracetamol, to furosemide (FS), a zone III hepatotoxin, which has previously been suggested not to target the mitochondria (Antoine et al. 2008; McGill et al. 2012), in contrast to paracetamol, which is known to cause mitochondrial injury, in order to assess whether mitochondrial perturbation is necessary for PTN formation. We hypothesise that FS-DILI in mice will not lead to PTN formation, as it is thought that this process is dependent on mitochondrial perturbation, which is not thought to occur in this type of toxicity.

2.2 METHODS

2.2.1 Experimental Animals

The protocols described within this chapter were performed by personal licence holders according to the regulations defined within the project licence granted under the Animals (Scientific Procedures) Act 1986 and approved by the University of Liverpool ethics committee. CD-1 mice were purchased from Charles River (Manston, UK) and housed at a constant temperature and humidity with free access to food and water. Animals were allowed to acclimatise for at least 7 days before any experimental procedure and were kept in a 12-hour light/dark cycle (Lights on: 08:00/Lights off: 20:00). Animals were humanely culled using a rising concentration of carbon dioxide before exsanguinations according to the Killing of Animals Under Schedule 1 to the Animals (Scientific Procedures) 1 Act 1986.

2.2.2 Serum ALT Activity Determination

Blood was taken from mice through cardiac puncture using a 25-gauge needle and was then allowed to clot at 4 ºC overnight. Serum was then extracted by centrifugation to initially remove the clot (1500 g, 5 min, 4 ºC), followed by another centrifugation step to purify the serum (10,000 g, 5 min, 4 ºC). Serum ALT levels were determined immediately using a Thermo Infinity ALT Liquid Stable Reagent-based (Thermo, Waltham, MA, USA) kinetic assay, at 37 ºC, according to the manufacturers protocol.

2.2.3 FFPE Tissue Preparation

NB: FFPE tissue blocks were kindly prepared by Julie Haigh and Valerie Tilston in a collaborative effort between the CDSS and the University of Liverpool Veterinary Pathology Department.

In brief, liver obtained during *in vivo* experiments was dissected into individual lobes and a section of the large lobe was preserved in 4% paraformaldehyde (PFA) for 24-96 h. The liver tissue was then removed from PFA and dehydrated using increasing concentrations of ethanol.

The dehydrated liver was then washed using xylene and infiltrated with molten paraffin wax (Ultraplast Polyisobutylene Histological Wax, Solmedia).

2.2.4 Haematoxylin and Eosin Staining (H&E

NB: H&E staining was performed by Julie Haigh in collaboration with the University of Liverpool Veterinary Pathology Department

Briefly, tissue sections were dewaxed in xylene and gradually rehydrated using descending concentrations of ethanol down to distilled water. Tissue sections were then stained in Mayer's haematoxylin (TCS Biosciences Ltd) for 5 minutes and were then washed under running water for 6 minutes. Sections were then stained with Eosin Y (CellPath) for 2 minutes and were then washed 3 times in 96% ethanol for 1 minute each. This washing process was then repeated with 100% ethanol (3x) and xylene (2x). The sections were then mounted in DPX mounting medium and a coverslip was placed on top. Sections were then imaged on a light microscope and the severity of injury was graded by a trained pathologist. Sections were given a grading between 1 and 6, with 1 being assessed as normal liver and 6 being massive hepatocellular necrosis involving entire lobules, and numbers in between being intermediary grades of necrosis.

2.2.5 Immunohistochemistry

NB: Immunohistochemistry work was solely done by Julie Haigh in a collaborative effort between the CDSS and the University of Liverpool Veterinary Pathology Department.

Immunohistochemical analyses were performed as described previously (Cowan et al. 1998) with the following modifications: slides were heated at 60°C for 1 h before de-parafinisation, rehydration, and quenching of endogenous peroxidase activity (3% hydrogen peroxide in methanol). The hydration process was completed by rinsing for 5 min in DAKO Tris buffered saline buffer (DAKO Corporation, Carpinteria, CA) containing 0.05% Tween 20 (DAKO Corporation). During heat-induced epitope recovery, sections were steam-heated in a standard

steamer (Black and Decker) while submerged in antigen-retrieval Citra buffer (BioGenex, San Ramon, CA) for 30 min. Sections were blocked in normal horse serum (Vectastatin Elite kit; Vector Laboratories, Burlingame, CA) for 15 min and then incubated with anti-3-nitrotyrosine monoclonal antibody (1:250; Merck Millipore) overnight at 4 °C in a humidity chamber. Sections were washed in DAKO Tris buffered saline buffer containing 0.05% Tween 20 and then loaded into the DAKO Autostainer (DAKO Corporation) for application and incubation of the biotinylated horse anti-rabbit IgG (Vectastatin Elite kit, Vector Laboratories) for 30 min at room temperature followed by avidin-biotin complex (Vectastatin Elite kit) for 30 min at room temperature. The chromogenic reaction was performed with SG (Vector Laboratories) for 10 min at room temperature. Slides were removed from the autostainer and counterstained with Nuclear Fast Red (Vector Laboratories) for 10 min and coverslipped with Permount (Richard-Allan Scientific, Kalamazoo, MI). Positive and negative controls were included with each run.

2.2.6 Determination of Total Hepatic GSH

The kinetic 5,5'dithiobis(2-nitrobenzoic acid)-GSH disulphide recycling assay was used to determine hepatic GSH abundance from livers obtained during *in vivo* studies. This method is described in detail by Vandeputte *et al* (1994).

2.2.7 Immunoblotting for 3-nitrotyrosine

Snap frozen livers were removed from storage in a -80 °C freezer and 50 mg of the left liver lobe was excised. The excised liver tissue was then suspended in 500 μL 1x PBS and subject to homogenisation using a Retsch Homogeniser (Retsch GmbH, Haan, Germany). Alternatively, cells were incubated with 200 μL (per well of a 6-well flat bottomed cell culture plate) of RIPA buffer (Sigma Aldrich) and placed on a rocker for 2 minutes before snap freezing on liquid nitrogen. Total protein concentration was determined using either method described by Lowry *et al* (1951), BCA assay or Bradford assay (Bradford et al. 1976), depending on the lysis buffer of choice. It is important to note that when using lysis buffers

containing SDS, the Lowry assay should be avoided due to the possibility of SDS interference with the reaction leading to inaccurate results (Dulley et al. 1975). Samples were diluted in double distilled water to a concentration of 100 µg protein/5 µL and then mixed with 4x LDS sample buffer and 10x reducing agent (Life Technologies, Foster City, CA). Samples were then denatured at 80 ºC for ten minutes and then separated on NuPage LDS polyacrylamide gels, according to the manufacturers protocol (Life Technologies). Separated proteins were then transferred to nitrocellulose membrane (GE Healthcare) using a Bio-Rad transfer module (Bio-Rad). The success of the transfer was then tested using Ponceau S to stain the total protein content of the membrane and then membranes were blocked in either 10% fat-free milk powder or bovine serum albumin in Tri-buffered Saline 0.1% Tween buffer (TBS-T). A primary antibody raised against 3-nitrotyrosine (06-284 Merck Millipore) was incubated at a dilution of 1:400 in 2% fat-free milk TBS-T buffer for 48 hours, followed by incubation with a secondary antibody targeted against rabbit proteins (A0545 Sigma Aldrich; 1:3000) for one hour. Blots were developed either in a dark room using an enhanced chemiluminescence method (Fisher Scientific) or using a Licor Odyssey with specific luminescent secondary antibodies (Licor Bioscience, Cambridge, UK). Densitometry was then performed using Licor software or Bio-Rad 1D software. The density of the entire well was used for the assessment of 3-nitrotyrosine presence.

2.2.8 Culture of hepa1c1c cells, GSH depletion using buthionine sulfoximine (BSO) and incubation with peroxynitrite

Mouse hepatoma cells (Hepa1c1c) were seeded at a density of 30,000 cells/cm^2 in DMEM containing 10% Foetal Bovine Serum and 5% penicillin-streptomycin and were split using 0.25% trypsin every 3 days or whenever confluent. Buthionine sulfoximine (BSO) was used to deplete cellular GSH levels, with the ideal dose being calculated using a standard curve of BSO with concentrations ranging from 0 to 500 µM for 24 h prior to dosing. 300 µM was found to cause a 70% depletion in the level of GSH and so was chosen for further use. Before cells were incubated with peroxynitrite, the serum was removed from the media immediately

prior to dosing, followed by administration of peroxynitrite (0-1 mM) for 30 minutes before harvesting.

2.2.9 Determination of Serum Glutamate Dehydrogenase (GLDH) Activity

GLDH activity levels were measured spectrophotometrically using the DGKC kit (Randox Laboratories, Kearneysville, WV, USA) as previously described in Harrill *et al* (2012). A decrease in absorbance was measured in each sample caused by the oxidation of nicotinamide adenine dinucleotide at 340 nm, as per the manufacturer's protocol.

2.2.10 Statistical analysis

Each data group was tested for normality using the Shapiro-Wilk normality test. Descriptive statistical analysis was performed on each data group. For normal data sets, the mean and standard deviation was determined and for non-normal data sets, the median and inter-quartile range was determined for each group. To determine statistical significance, comparisons were made using the Student's t-test (for two parametric groups), the Mann-Whitney U test (for two nonparametric groups), the ANOVA (for more than two parametric groups) and the Kruskall-Wallis test (for more than two nonparametric groups) (GraphPad Software, La Jolla, CA). For graphical interpretation GraphPad Prism 5 software was used (GraphPad Software, La Jolla, CA). Statistical significance was set at $P < 0.05$.

2.3 RESULTS

2.3.1 530mg/kg paracetamol and 400mg/kg FS cause necrosis in pericentral regions of the liver in a time-dependent manner in CD-1 mice

Groups of CD-1 mice were administered (i.p.) either 530 mg/kg paracetamol (n = 4), 400 mg/kg FS (n = 5) or vehicle for up to 8 h and 24 h respectively. Liver tissue slice preparation and H&E staining of liver was then performed for histological grading and analysis (figure 2.1). Paracetamol was found to cause a time-dependent increase in necrosis in the PC region, with peak necrosis occurring at 4 h post-dose (Grade 5). The columnar pattern of necrosis caused by paracetamol affected cells differentially within the PC region, with some succumbing to necrosis and others not. After 4 h the injury appeared to resolve, suggesting the occurrence of regeneration and recovery. FS similarly caused a time-dependent increase in PC necrosis, with the peak level arriving at 24 h post-dose (Grade 6) with no-resolve within this time-course, suggesting the peak of toxicity may yet be anticipated. The pattern of necrosis caused by FS-injury presented as a wave radiating outwards from the PC region as time-progressed, affecting all cells within this region similarly.

Figure 2.1 Histology staining and reading of mouse liver sections taken from a paracetamol toxicity time course with a final time point of 8 hours, and a furosemide toxicity time course with a final time point of 24 hours. A, Severity grading of paracetamol- and FS-DILI in CD-1 mice, scored by a trained pathologist. **B,** H&E staining of liver sections taken from mice administered either paracetamol or FS, for up to 24 h.

2.3.2 Toxic doses of paracetamol and FS cause elevations in serum transaminase levels in a time-dependent manner

To examine the utility of ALT, the gold-standard biomarker of DILI in both FS- and paracetamol- DILI, we measured the serum ALT activity in our CD-1 mouse models of DILI (figure 2.2). Paracetamol caused a time-dependent increase in serum ALT activity to 8 h post-dose, peaking at 2334.3 U/L, compared to 22.7 U/L for saline treated controls at 8 h (8 h paracetamol vs 8 h Saline $P<0.01$). Serum ALT activity in FS-DILI was marginally elevated from 8 h post-dose (8 h FS: 384 U/L vs 8 h PBS: 17.250 U/L), however by 24 h it had risen to 6836.3 U/L (average), compared to 21.8 U/L for the PBS-dosed control group ($p<0.0001$).

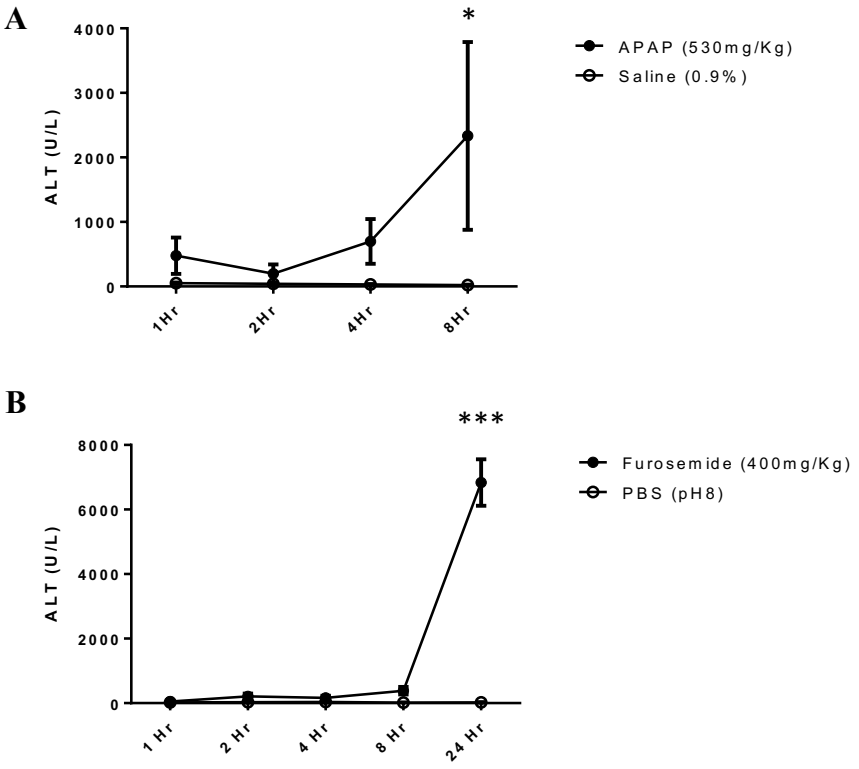

Figure 2.2 A, Serum ALT activity in CD-1 mice following 530 mg/kg paracetamol or 0.9% saline for up to 8 h. Serum ALT is significantly elevated at 8 h following paracetamol (*$p<0.01$) **B,** Serum ALT activity in mice following 400 mg/kg FS or 0.9% saline for up to 24 h. ALT is significantly elevated in the serum of mice administered 400 mg/kg FS for 24 h (***$p<0.0001$).

2.3.4 Hepatic GSH is depleted early in paracetamol-DILI, but is not depleted significantly in FS-DILI in CD-1 mice

To determine whether depletion of GSH is necessary to elicit necrosis within the liver, we aimed to determine whether hepatic GSH was significantly depleted during both paracetamol- and FS-DILI (figure 2.3). Baseline hepatic GSH levels were found to vary in both studies with peak GSH falling at 0 h and the lowest level of GSH being found at 8h in both studies which was due to the previously studied circadian expression of GSH in the liver (Beaver et al. 2012). After 1 h paracetamol mean hepatic GSH levels were significantly depleted (1 h paracetamol: 5.3 nmol/mg vs 1 h saline: 40.4 nmol/mg; $p<0.0001$, n=4). Mean hepatic GSH levels continued to remain low (2 h: 3.9nmol/mg, $p<0.001$; 4 h 5.0 nmol/mg, $p<0.0001$, n=4) until 8 h post-dose, at which point hepatic GSH levels rebound to match GSH levels in saline-treated controls (8 h paracetamol: 26.2 nmol/mg vs 8 h Saline: 24.5 nmol/mg). In FS-DILI, hepatic GSH did not differ significantly at any time-point from hepatic GSH levels in PBS-treated controls. In this study, the baseline level of hepatic GSH in both PBS-treated controls and FS-treated animals varied throughout the time-course, with the trough occurring at 8 h (FS: 123.6 nmol/mg; PBS: 134.2 nmol/mg) and the peak occurring at 4 h (FS: 209.3 nmol/mg; PBS: 211.0 nmol/mg; n = 5). This can be explained by the circadian expression cycle of GSH, in which GSH expression is at its highest in the morning and at its lowest in the evening (Matsunaga et al. 2004).

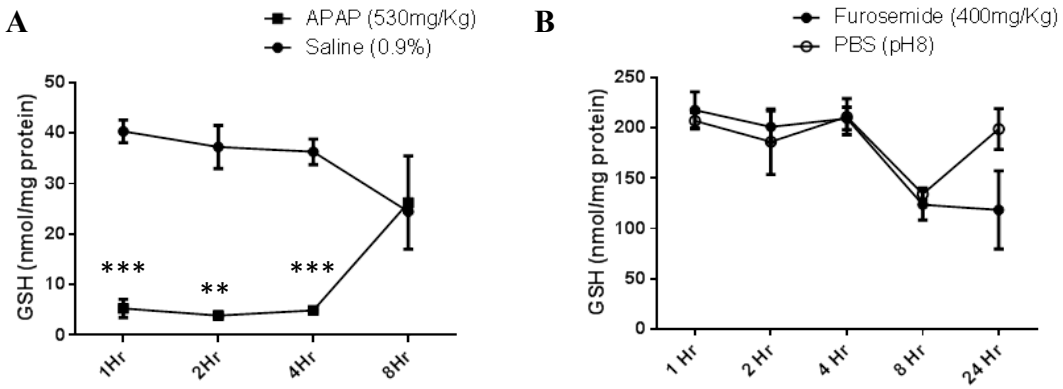

Figure 2.3 A, Total hepatic GSH levels in CD-1 mice following 530 mg/kg paracetamol or 0.9% saline for up to 8H. Paracetamol caused a significant GSH depletion at 1 h (***p<0.0001), 2 h (**P<0.001) and 4 h (***p<0.0001). GSH levels had rebounded by 8 h and matched those of the vehicle group. **B,** Total hepatic GSH following 400 mg/kg FS or 0.9% saline for up to 24 h. FS did not lead to a significant level of GSH depletion at any time during the time-course suggesting that FS causes toxicity independent of GSH-depletion.

2.3.5 Serum GLDH is significantly elevated following a toxic dose of paracetamol, but not after a toxic dose of FS

In order to determine the ability of serum GLDH to predict different forms of DILI, we aimed to determine whether this marker could predict injury in both paracetamol- and FS-DILI (figure 2.4). Paracetamol administration caused a time-dependent increase in serum GLDH levels from 2 h to 8 h (2 h: 46.5U/L; 4 h: 332.5 U/L; 8 h: 1707.5 U/L, $p<0.01$), when compared to saline dosed animals, which remained at baseline (22.75-51.75 U/L). At 1h after paracetamol, there was a small non-statistically significant difference between paracetamol-dose and Saline-dosed animals (Saline: 51.75 U/L vs paracetamol: 146.5 U/L). In FS-DILI, serum GLDH levels remained at baseline until 24h, at which point a highly-variable non-significant elevation was witnessed in FS-treated animals compared to PBS-treated (FS: 282.75 U/L vs PBS: 3.67 U/L). Comparison of peak serum GLDH levels between paracetamol- and FS-injury, demonstrates that paracetamol leads to a ~6-fold greater elevation in serum GLDH levels than FS at their peak. Correlation analysis of GLDH and ALT in both paracetamol- and FS-injury, demonstrates that GLDH and ALT have a strong positive correlation in paracetamol-injury (Pearson $R = 0.9359$; $p<0.0001$), whereas the two markers correlate weakly in FS-injury (Pearson $R = 0.039$; $p<0.01$).

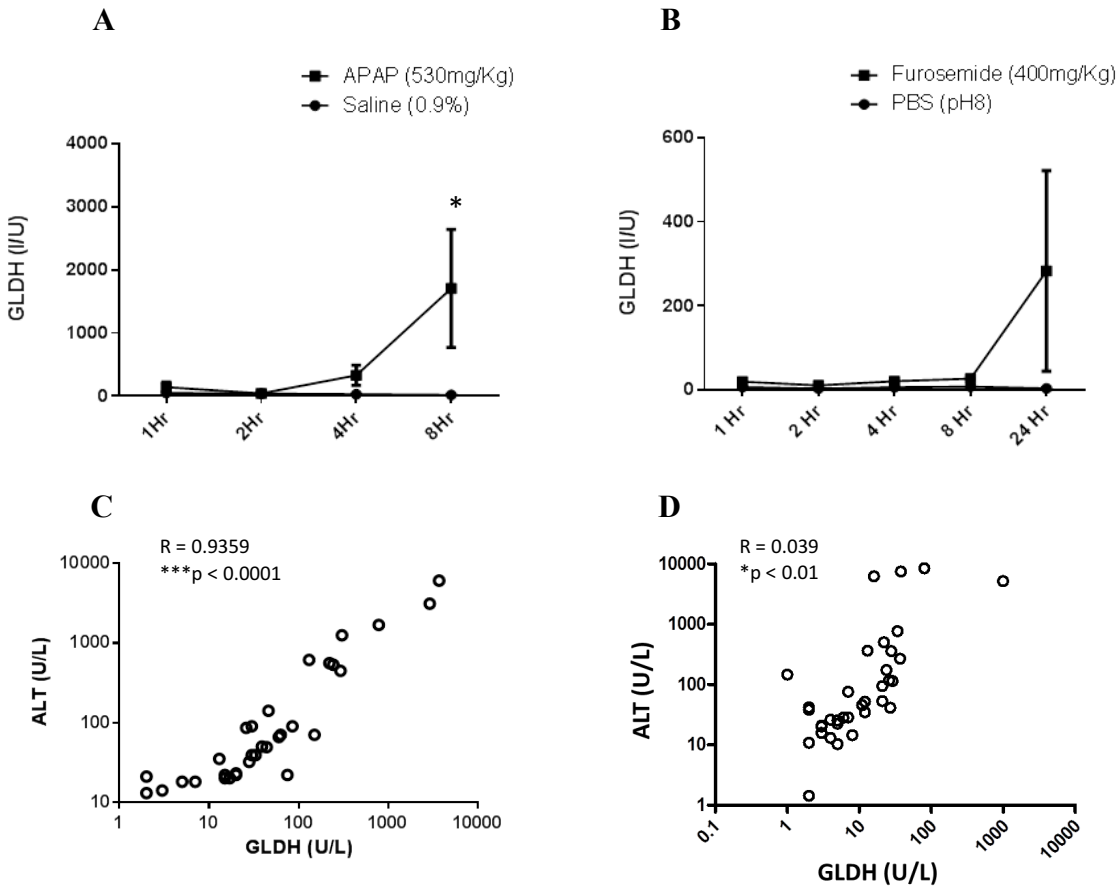

Figure 2.4 A, Serum GLDH activity in CD-1 mice following 530 mg/kg paracetamol or 0.9% saline for up to 8 h. **B,** Serum GLDH activity following 400 mg/kg FS or PBS for up to 24 h. **C,** Correlation analysis of serum ALT and serum GLDH in CD-1 mice following 530 mg/kg paracetamol or 0.9% saline for up to 8 h. **D,** Correlation analysis of serum ALT and serum GLDH in CD-1 mice following 400 mg/kg FS or PBS for up to 24 h. (*p <0.01, ***p < 0.0001).

2.3.6 Peroxynitrite mediated PTN of bovine serum albumin is reduced by the addition of a physiological concentration of GSH

In order to develop a western blot assay to detect PTN a positive control was developed through incubating a range of peroxynitrite concentrations (10 mM-1 pM) with bovine serum albumin (BSA; 1 mg/ml) to create nitro-BSA (figure 2.5). Using an anti-nitrotyrosine antibody (1:400 overnight incubations; Merck Millipore), we were able to detect 3-nitrotyrosine adducts in a peroxynitrite-concentration dependent manner, down to 1 µM peroxynitrite using a western blot. To examine the role of GSH in PTN-formation, we co-incubated peroxynitrite and BSA, with a physiological concentration of GSH (5 mM). The addition of GSH to the reaction abolished PTN formation up to 1mM peroxynitrite.

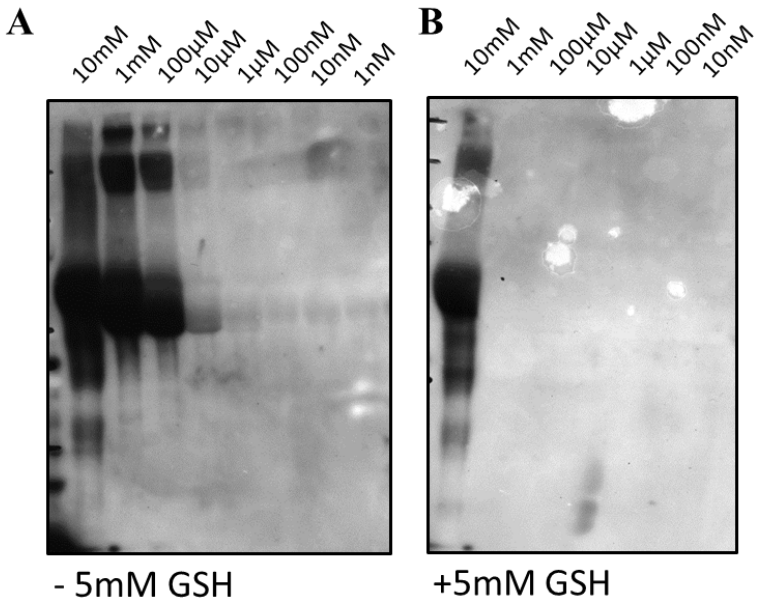

Figure 2.5 PTN western blot assay method development. A, 3-nitrotyrosine is detectable in a peroxynitrite concentration dependent manner in BSA. **B,** A physiological concentration of GSH (5 mM) is able to abolish nitration in a BSA up to a concentration of 10 mM peroxynitrite.

2.3.7 Cellular GSH is protective against PTN in a mouse hepatoma cell-line

To examine the role of cellular GSH in protection against PTN, we incubated hepa1c1c cells (mouse hepatoma cells) with 500 μM BSO (optimal dose calculated using standard curve and GSH micro titre assay – figure 2.6) for 24 h to deplete cellular GSH levels, before incubation with peroxynitrite to induce PTN (figure 2.7C). 24 h of 500 μM BSO led to a 70% reduction in cellular GSH levels (figure 2.6, $p<0.005$), but did not increase the susceptibility of cells to peroxynitrite mediated PTN formation over non-GSG depleted cells with or without serum-containing media (figure 2.7A+B). PTN was only detectable at 1 mM peroxynitrite in the – BSO group (serum-free, figure 2.7B and serum-containing, figure 2.7A), and 100 μM in the +BSO group (figure 2.7C). This experiment was then repeated, but instead using serum-free culture medium (serum removed immediately prior to peroxynitrite administration) and BSO depletion of GSH. BSO depletion in the absence of serum led to the detectability of PTN adducts down to 1nM peroxynitrite (compared to 1 mM without BSO, figure 2.7D).

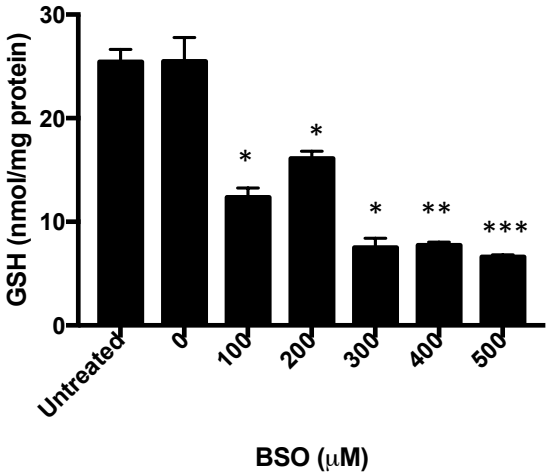

Figure 2.6. Depletion of glutathione in hepa1c1c cells using BSO. Cells were incubated with up to 500μM of BSO for 24 h and were then harvested for GSH quantification using the GSH recycling assay. Concentrations of greater than 100μM BSO led to significant levels of depletion of GSH (*100μM, 200μM, 300μM: $p<0.05$, **400μM: $p<0.01$, ***500μM: $p<0.005$).

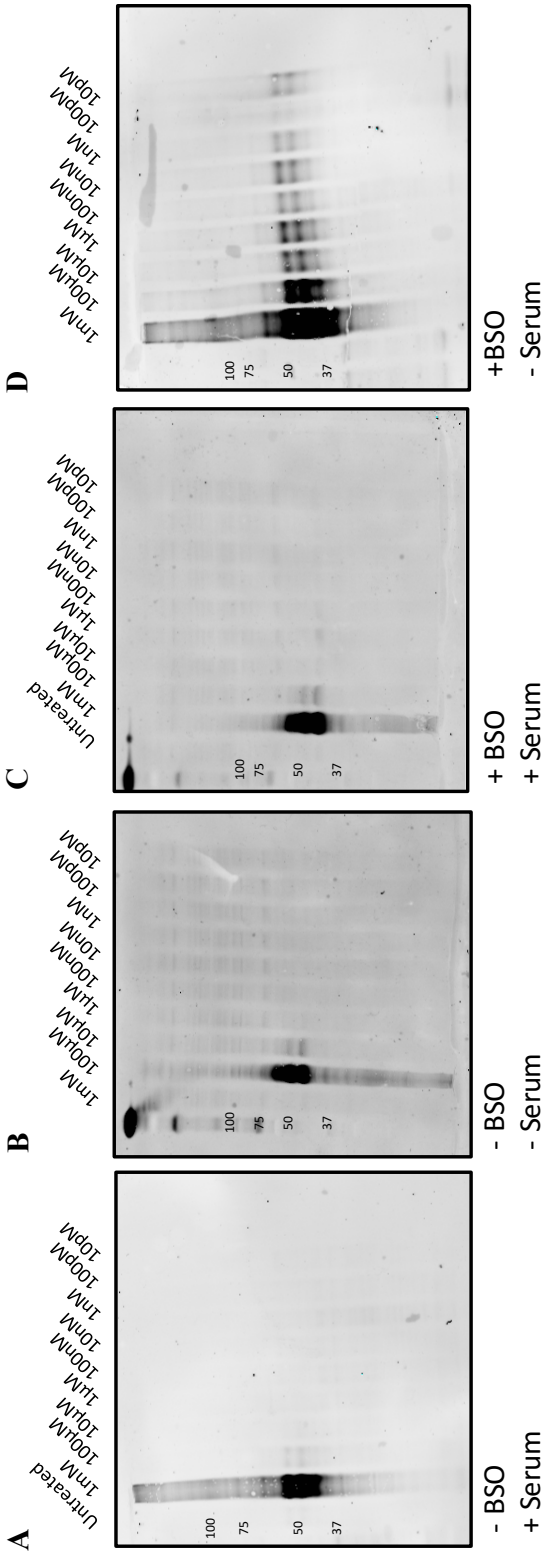

Figure 2.7 PTN western blot assay method development. A, B, C, 3-nitrotyrosine is only detectable in hepa1c1c cells with or without serum, and with 500μM BSO + serum after incubation with 100μM< peroxynitrite for 1 h. **D,** GSH depletion using 500μM BSO, in serum-free conditions increases susceptibility to peroxynitrite-induced PTN down to 10 pM concentrations.

2.3.8 PTN is present in both paracetamol- and FS-DILI

In order to establish whether mitochondrial damage was required for the formation of PTN, we examined whether PTN adducts are detectable in a CD-1 mouse model of paracetamol-DILI, a mitochondrial toxin, and a model of FS-DILI, a compound thought not to target the mitochondria (figure 2.8). Western blotting for 3-nitrotyrosine in liver tissue from mice treated with paracetamol, or vehicle for up to 8 h, demonstrates that there is a time-dependent increase in the formation of PTN up until 4 h, after which there is a marginal decrease in PTN. Similarly, when a 24 h time-course examining the effects of FS-DILI on PTN was examined, a time-dependent increase in nitration can be seen until 4 h post-dose, after which there is a brief fall in PTN levels, until 24 h, where PTN levels again increase. Interestingly, levels of PTN also appear to increase in the vehicle-dosed animals in the FS-study, possibly as a by-product of a pH change in the circulation driven by the alkaline vehicle.

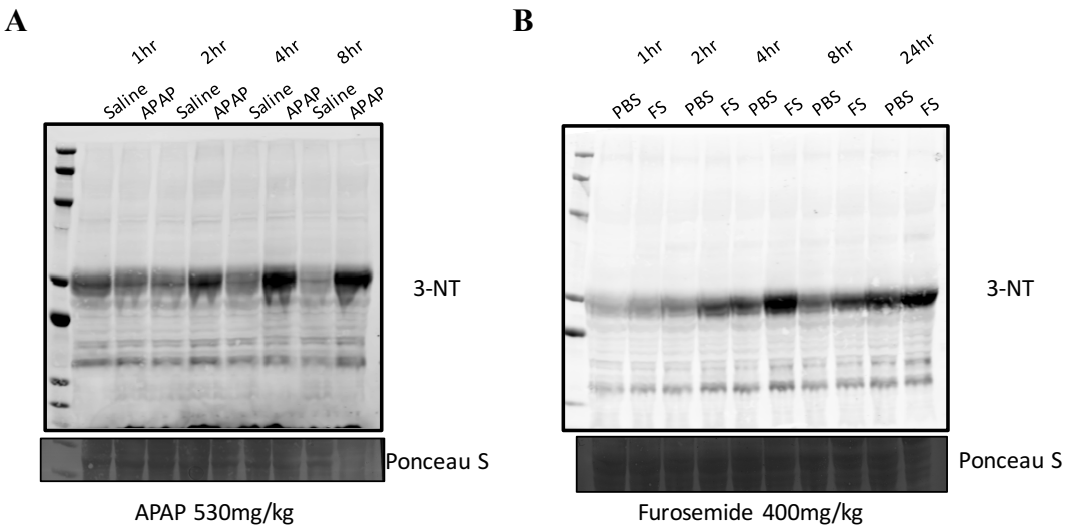

Figure 2.8 PTN is present in both paracetamol- and FS- DILI. Each time point displayed on the western blot represents a pool of either 4 mice (paracetamol) or 5 mice (furosemide). **A,** PTN increases in a time-dependent manner up to 4 h following 530 mg/kg paracetamol in CD-1 mice. **B,** PTN increases in a time-dependent manner up to 4 h, before declining at 8 h, followed by a further increase up to 24 h in CD-1 mice, after a 400 mg/kg dose of FS.

2.3.9 Quantification of PTN levels in paracetamol- and FS-DILI

To establish whether PTN was more prolific in either paracetamol- or FS-DILI, due to differential mechanisms of toxicity, we quantified PTN levels through titration of protein loading on a western blot, to establish PTN levels per µg of protein loaded at peak PTN in both types of injury (both at 4 h post-dose) (figure 2.9). After quantification through densitometry analysis of all bands present in each individual well of the blot, using Licor Biosciences densitometry software, peak PTN levels in each injury type were not statistically different, suggesting equivalent occurrence of PTN in each injury type (Average intensity value: paracetamol = 0.235 vs FS = 0.287).

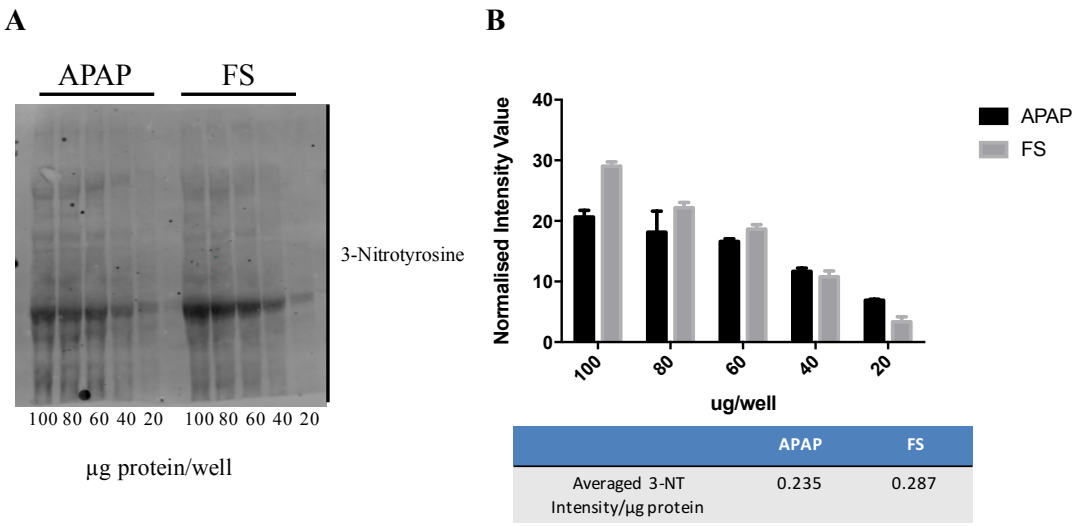

	APAP	FS
Averaged 3-NT Intensity/µg protein	0.235	0.287

Figure 2.9 PTN is present at equivalent levels in both paracetamol- and FS-DILI in CD-1 mice. A, protein loading titration of CD-1 mouse liver tissue administered with either 530 mg/kg paracetamol or 400 mg/kg FS for 4 h, probing for 3-nitrotyrosine. **B,** Quantification of 3-nitrotyrosine levels at peak PTN in paracetamol- and FS- DILI in CD-1 mice using densitometry.

2.3.10 Immunohistochemical detection of hepatic PTN adducts under basal conditions and in injury models

In order to localise the formation of PTN adducts in DILI, we aimed to establish an IHC assay to detect PTN in slices of fixed liver tissue (figure 2.10-14). To test the success of this method we produced a positive PTN control, by directly administering (37 mM) peroxynitrite to a fixed slice of healthy (non-dosed) liver tissue from a CD-1 mouse. PTN is clearly observable in regions in which the peroxynitrite was placed on the slide (brown stain), and absent in areas not incubated with peroxynitrite. However, it was observed that under basal (non-dosed mice) conditions PTN is present surrounding the portal vein (dark brown stain). Examination of PTN formation in paracetamol-DILI, demonstrated that PTN increases in a time-dependent manner until 4 h post-dose (Grade 5), after which it begins to decrease. PTN was visibly present in its highest levels in the cells surrounding the area of necrosis in the PC region. In FS-DILI, PTN increased in a time-dependent manner until 24h. PTN was similarly present in its highest levels on the periphery of the necrotic region (PC).

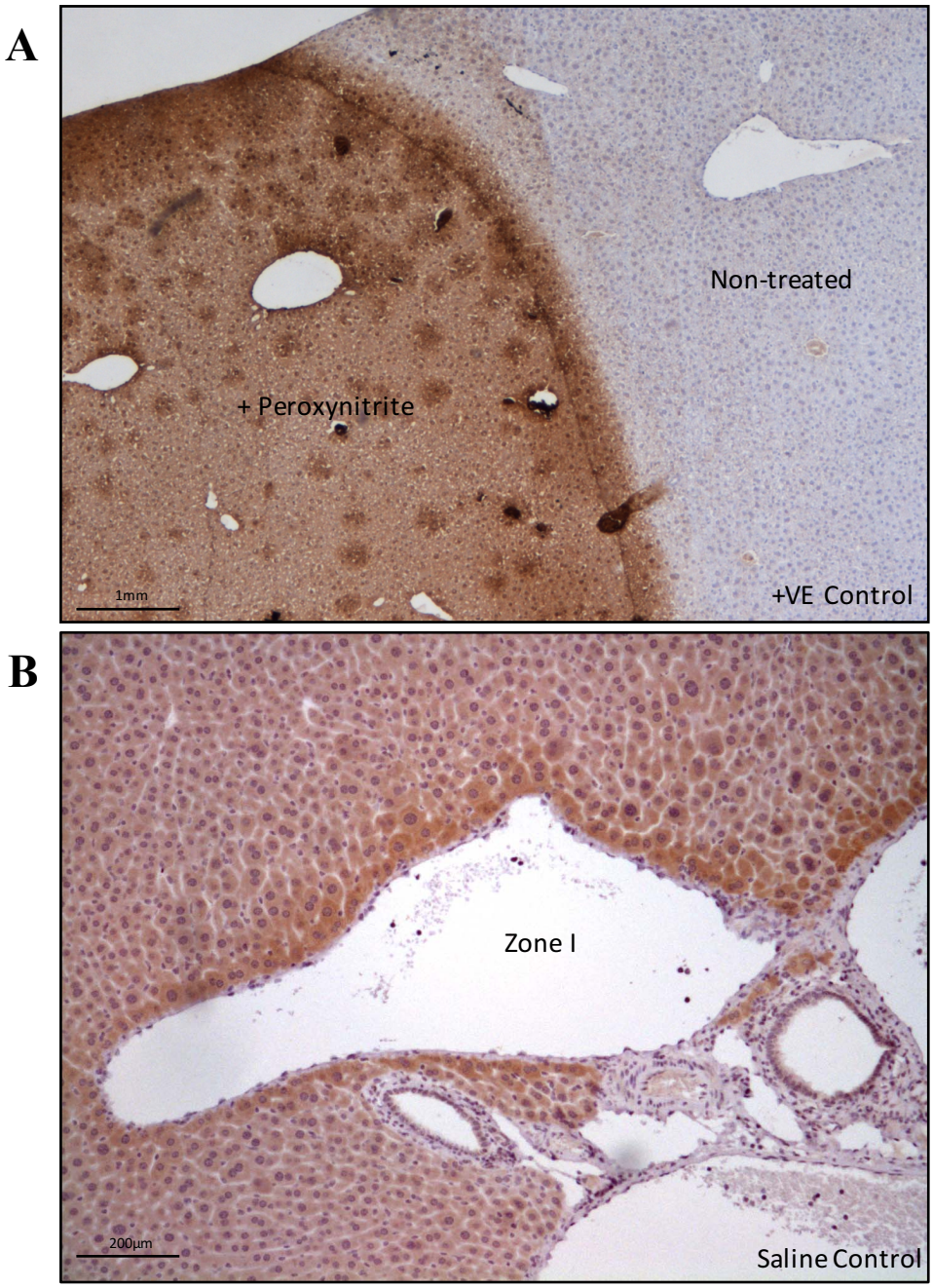

Figure 2.10 Detection of hepatic PTN (3-nitrotyrosine) using immunohistochemistry. **A,** Development of a positive control for nitration through direct application of peroxynitrite to liver tissue (Brown stain = 3-nitrotyrosine). **B,** IHC staining for 3-nitrotyrosine in liver tissue taken from healthy CD-1 mice demonstrates that high levels of PTN are present surrounding the portal vein under normal conditions.

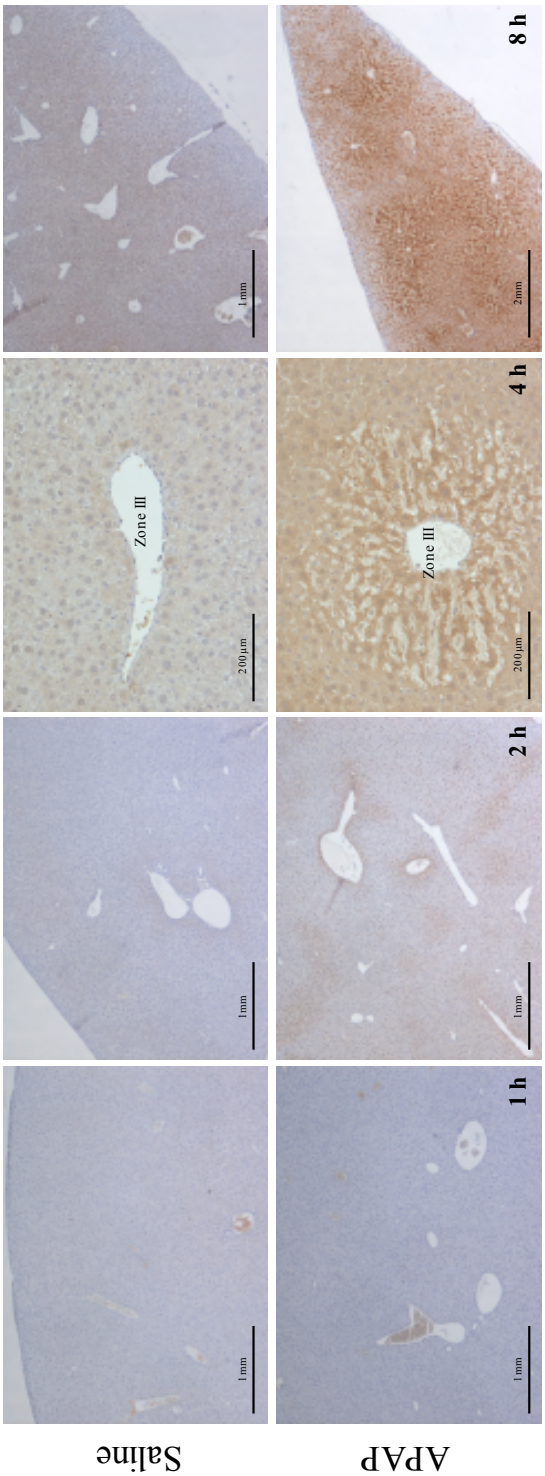

Figure 2.11 Detection of hepatic PTN (3-nitrotyrosine) using immunohistochemistry following 530 mg/kg paracetamol demonstrates that 3-nitrotyrosine levels increase in zone III of the liver in a time-dependent manner.

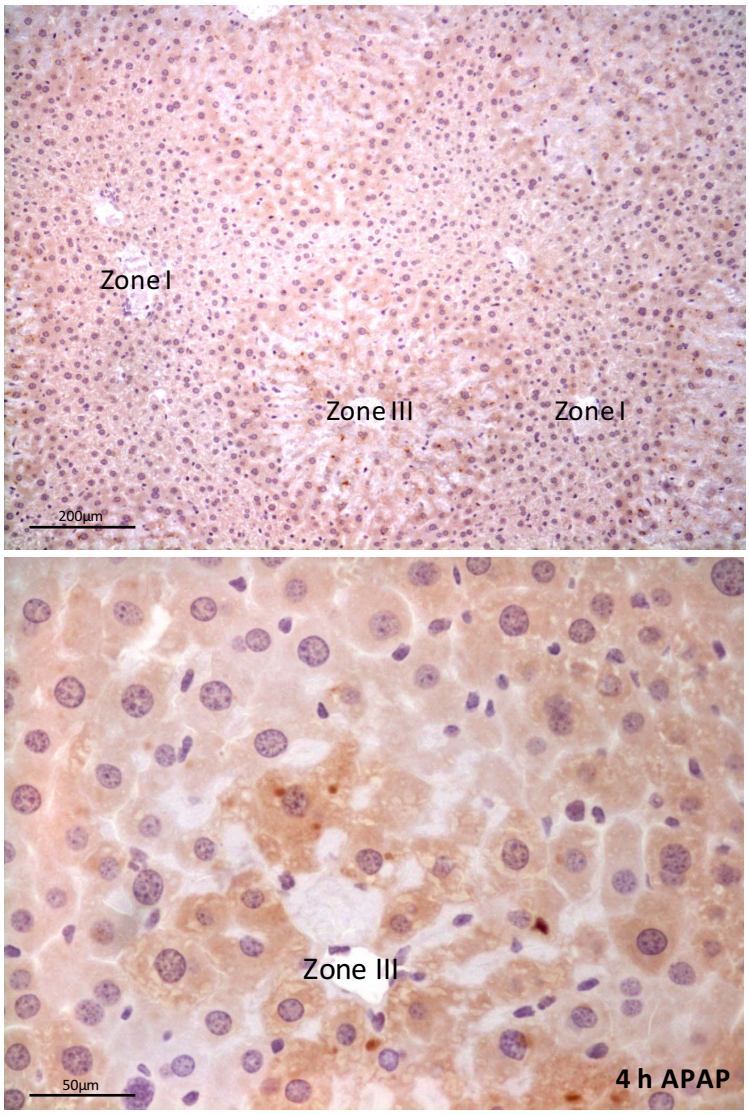

Figure 2.12 Detection of hepatic PTN (3-nitrotyrosine) using immunohistochemistry following 530 mg/kg paracetamol demonstrates the formation of PTN in cells surrounding the area of injury at 4 h post-dose.

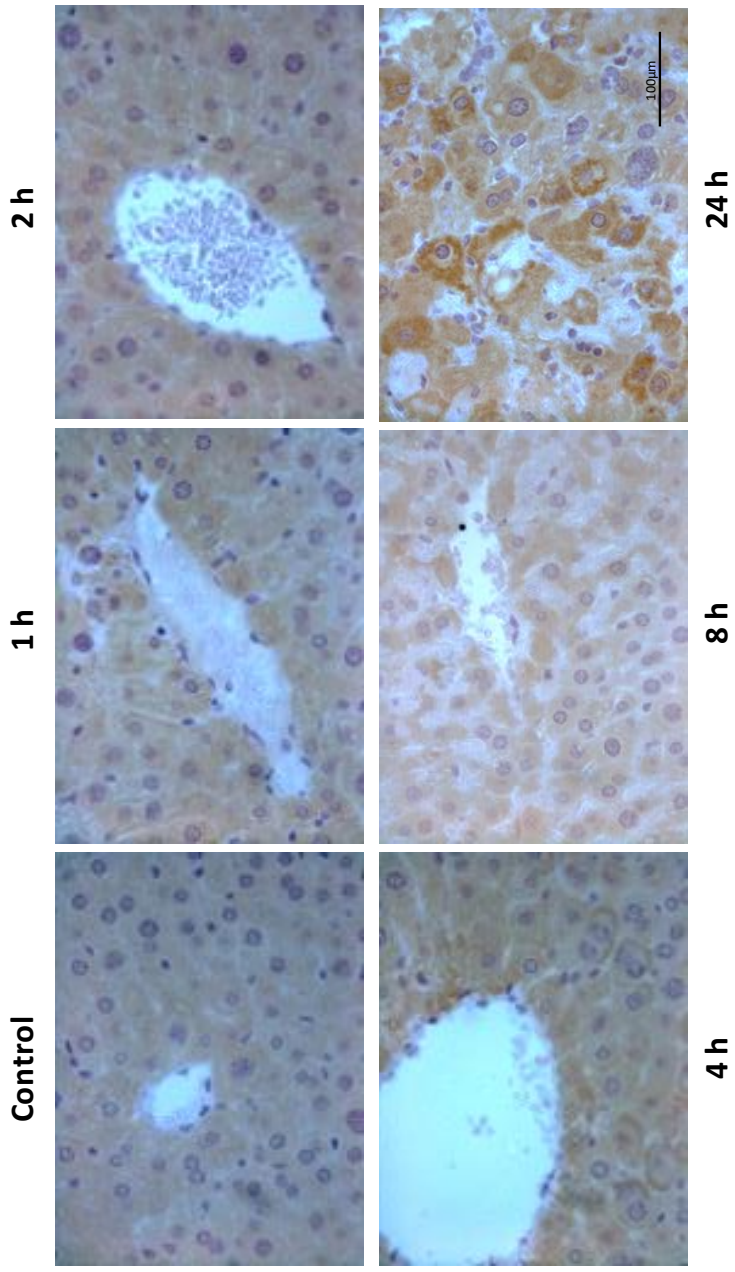

Figure 2.13 Detection of hepatic PTN using IHC in a mouse model of FS-DILI demonstrates that PTN increases in a time-dependent manner following 400 mg/kg FS.

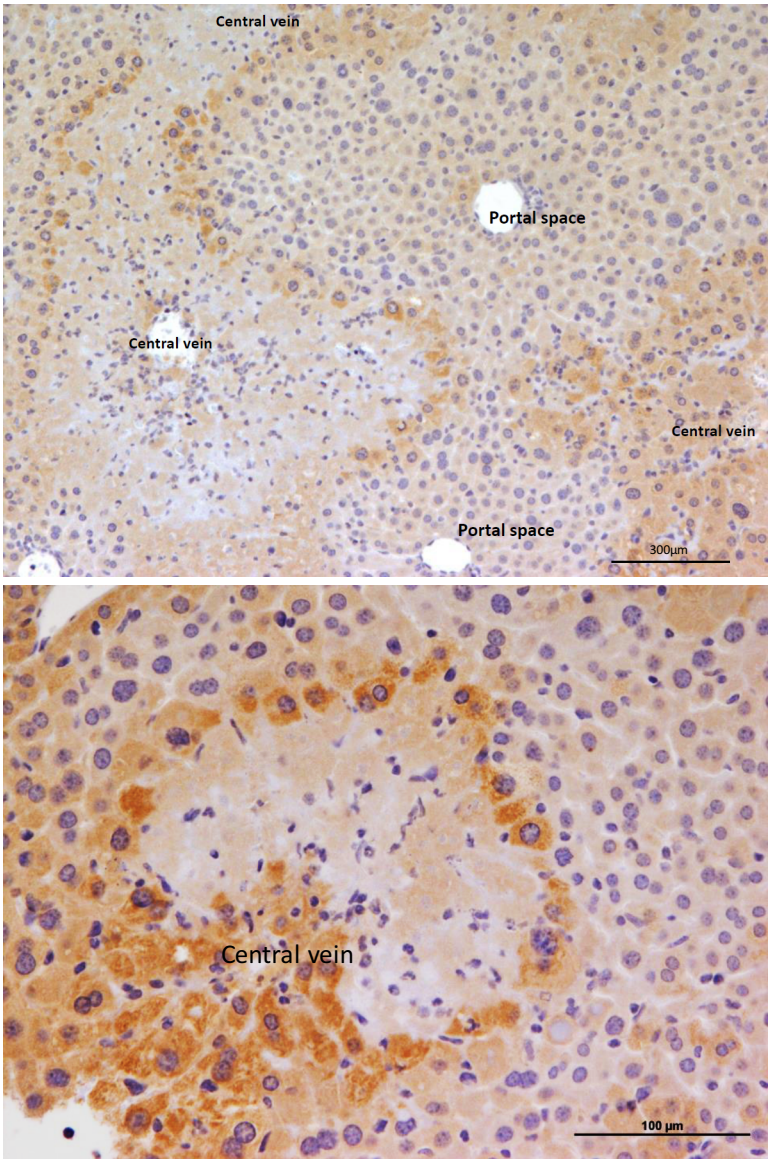

Figure 2.14 Detection of hepatic PTN (3-nitrotyrosine) using IHC in mice administered with 400 mg/kg FS for 24 h demonstrates that PTN is present in high levels on the periphery of the injured region.

2.4 DISCUSSION

PTN is a post-translational modification of protein tyrosine residues that is caused by the nitrating agent peroxynitrite. Peroxynitrite is usually formed in large amounts under oxidative stress conditions through the spontaneous reaction between nitric oxide and superoxide. PTN has previously been shown to be present in paracetamol-DILI early in the course of toxicity (Hinson et al. 1998), but there is no consensus on the cellular events which lead to its occurrence. Previous work in primary mouse hepatocytes has suggested that the MPT and thus mitochondrial injury plays a role in the formation of PTN in DILI (Burke et al. 2010). To examine this, we compared and contrasted DILI due to paracetamol and FS. Paracetamol is known to be a pericentral hepatotoxin which causes hepatotoxicity through damaging the mitochondria, leading to hepatocellular necrosis (McGill et al. 2012). In contrast, FS, also a pericentral hepatotoxin (Williams et al. 2007), is thought to cause necrosis through a pathway independent of the mitochondria, possibly through targeting the endoplasmic reticulum (Antoine et al. 2008; Qu et al. 2014). In utilising these compounds, we hypothesised that mitochondrial injury in paracetamol-DILI would lead to PTN, whereas FS, which is thought to leave the mitochondria intact should not cause PTN.

In order to test our hypothesis, we performed two time-course studies, in which CD-1 mice were either administered with a toxic dose of paracetamol (530 mg/kg) or FS (400 mg/kg), or vehicle. To confirm that each compound was hepatotoxic in our model, we carried out histological grading of the liver tissue, and measurement of serum ALT levels, the gold-standard circulating marker for assessment of hepatotoxicity. Histological assessment found that paracetamol-injury caused pericentral necrosis with increasing severity until 4 h post-dose, before beginning to resolve at 8 h post-dose. This is a contrast to previous studies examining paracetamol-DILI in mice, which found that the severity of injury continued to increase until 24 h post-dose (McGill et al. 2012). However, this may be caused by the previous models utilising fasted mice, whereas our model used fed mice, which may suggest that increased feeding aids the response to injury. Assessment of the FS dosed animals

similarly demonstrated necrosis in pericentral areas, which continued to worsen in severity until 24 h post-dose. Interestingly, although paracetamol and FS both target the pericentral region, they both cause distinctly different types of damage. Paracetamol cause an almost columnar pattern of injury radiating out from the central vein, affecting cells differentially. On the other hand, FS caused a wave of injury radiating outwards from the central vein which increased in size throughout the time-course, affecting all cells within the region. Both hepatotoxins were found to cause ALT elevations, in line with the previous literature (Jaeschke et al. 2012; McGill et al. 2012; Williams et al. 2007). Peak ALT levels in paracetamol-DILI were detected at 8 h post-dose, 4 h after peak injury was detectable in the liver tissue. Similarly, a significant ALT elevation was only detectable 24 h post FS dose, 20 h later than toxicity was detected using histology. This suggests that ALT has little use as a prognostic marker for DILI in experimental models, and that peak ALT levels should not be used to direct the selection of tissue samples for analysis.

A study previously examining FS-DILI in rodents suggested that FS did not cause depletion of cellular GSH *in vivo* (Wong et al. 2000), but did cause hepatotoxicity. GSH depletion is a critical cellular event in paracetamol-toxicity which allows the progression of toxicity (McGill et al. 2012), and it has been demonstrated that boosting GSH levels using *N*-acetylcysteine (NAC) or i.v. GSH provided protection from paracetamol-DILI (Whitehouse et al. 1985). However, a limitation of the study examining FS depletion of GSH was that the time-course only stretched to 5 h post-dose, whereas our study suggests that the toxicity is only beginning at 5 h post-dose. Therefore, to confirm that FS is able to cause toxicity without GSH depletion we assessed hepatic GSH content throughout our time-course, and compared this to paracetamol, a compound known to cause GSH depletion early in the course of injury. Assessment of cellular GSH levels following a toxic dose of paracetamol demonstrated that GSH was almost fully depleted by 1 h post-dose, a trend which continued until 8 h post-dose at which point GSH rebounded. This is expected, as paracetamol has been shown to induce the Nrf2 pathway, which regulates several of the enzymes involved in the biosynthesis of GSH

(Randle et al. 2008). Analysis of cellular GSH levels following a toxic dose of FS demonstrated that levels were not significantly different from the vehicle-dosed mice throughout the time-course until 24 h post-dose. At 24 h cellular GSH levels displayed a non-significant decrease, which may be explained by an overall decrease in the number of hepatocytes left within the liver due to the ongoing necrosis. Importantly, there was no early depletion of GSH, suggesting that GSH depletion does not play a role in the mechanism of FS-toxicity. Interestingly, in both models, GSH levels were decreased at 8 h post-dose in the vehicle treated animals. This can be explained by the fact that GSH is expressed in a cyclic manner under the control of the circadian clock (Tunon et al. 1992), in which GSH levels are lowest in the evening (matching our study; 8 h post-dose = 7 pm). This highlights the importance of using time-matched vehicle control animals in time-course studies.

Plasma GLDH is a mitochondrial membrane-associated protein involved in urea synthesis, and has previously been suggested to be a novel biomarker of DILI (Aubrecht et al. 2013; Schomaker et al. 2013a). However, this has been debated with one group suggesting that this marker is not a general marker of DILI, and is a marker of mitochondrial injury (Jaeschke and McGill 2013). In the Jaeschke group's study they were able to demonstrate that plasma GLDH was elevated after a toxic dose of paracetamol, but not after a toxic dose of FS (McGill et al. 2013). This was suggested to be due to mitochondrial damage in the case of paracetamol, and a lack of this following FS. Previous work within our group examining sub-cellular patterns of drug-protein covalent binding in different forms of DILI has also provided evidence to suggest this. It was found that paracetamol administration in mice led to a high level of covalent binding within the mitochondria of hepatocytes, whereas a toxic dose of FS had little effect on the mitochondria, but did cause covalent binding within the endoplasmic reticulum (Antoine et al. 2008). This led to our choice of paracetamol and FS as compounds to examine the role of the mitochondria in the formation of PTN. To confirm the previous work, in which GLDH was only measured at a single time-point in FS-injury, we profiled serum GLDH levels throughout the time-course of injury in both models. Similar to the previous study, we found

that paracetamol administration led to a time-dependent increase in serum GLDH levels, peaking at 8 h post-dose. Conversely, FS administration had little effect on serum GLDH levels until 24 h post-dose. At 24 h a highly variable increase in expression was documented, which was less marked than in comparison to that of paracetamol, suggesting either than some level of mitochondrial injury is occurring with FS or that there was some contamination of our serum samples with intact mitochondria which had been leaked out of the plasma membrane during necrosis. It has been previously suggested that this is a possibility and that this could be mitigated in future through the use of a high speed centrifugation step during the processing of serum in order to remove these intact mitochondria (McGill et al. 2013). Interestingly this may suggest that GLDH may have two utilities as a biomarker depending on the processing method chosen, one as a general injury marker and another as a mitochondrial injury marker, suggesting the importance of sample preparation method selection. Importantly serum GLDH did not strongly correlated to serum ALT, the gold-standard of liver injury suggesting either that it is not as sensitive as a marker of liver injury or that mitochondrial injury is more limited in FS-injury when compared to paracetamol-injury.

To build towards our goal of assessing PTN levels in paracetamol- and FS-DILI we first had to establish a method to detect PTN. We first sought to develop a positive control for PTN through the incubation of peroxynitrite with BSA, based on work performed in a previous study (Hinson et al. 2000). We then chose to develop a western blot method for detection of PTN, in the hope that this would also validate an antibody for immunohistochemistry. Analysis of a nitro-BSA standard curve (10 mM-1 pM) using an anti-3-nitrotyrosine antibody demonstrated that we were successful in detecting PTN by western blot. We then examined the role of GSH in the formation of PTN, through incubating a physiological concentration of GSH in the peroxynitrite/BSA reaction mix. Interestingly, we found that GSH was able to completely abolish the nitration of BSA up to concentrations of 1 mM peroxynitrite, suggesting that cellular GSH depletion may be necessary in order to see PTN formation, providing further evidence to support our hypothesis that FS may not lead to PTN, due to a

lack of GSH depletion. To build on this, we aimed to examine the role of cellular GSH in protection against peroxynitrite-mediated PTN in a hepatoma cell line (hepa1c1c), utilising BSO, an inhibitor of γ-GCL, an enzyme involved in biosynthesis, to deplete cellular GSH. Initially we found that depletion of GSH has little or no effect on the levels PTN after incubation with a range of peroxynitrite concentrations. However, upon removal of serum from the culture medium, we found that depletion of GSH using BSO increased PTN levels down to 1 pM (from 10 μM without GSH depletion). This provided further evidence that GSH depletion is necessary for the initiation of PTN.

In order to test our hypothesis that PTN will occur in paracetamol-DILI, due to GSH depletion and mitochondrial injury, and not in FS-DILI, due to a lack of both of these factors, we aimed to assess levels of PTN across our time-course models of DILI. Interestingly, we found that both paracetamol and FS lead to PTN in a time-dependent manner in our rodent models of DILI, disproving our hypothesis that this would not be found in FS-DILI. Furthermore, quantification of PTN levels in both types of DILI suggest that both produced equivalent levels of PTN, disproving our thoughts that levels in paracetamol-DILI would be higher due to increased ROS production during mitochondrial damage. We then assessed PTN in both models using IHC and found that the pattern of PTN closely followed the periphery of the area of injury, suggesting that PTN occurs before the cell undergoes necrosis.

To summarise, we have confirmed in mice that FS is able to cause hepatotoxicity without depleting GSH and without causing elevations in serum GLDH, whereas these both occur in paracetamol-DILI. We were also able to demonstrate that GSH is protective from PTN formation in both a simple chemical system, and in a cell-line model. Finally, we demonstrated that PTN occurs in both paracetamol- and FS-DILI despite their divergent pathways to toxicity, suggesting that PTN formation may not depend on the formation of ROS through mitochondrial damage, or on the depletion of GSH. Further work should be performed to identify the patterns of PTN in each model to assess whether both target similar proteins, or whether PTN can be related back to the organelles through which the drugs instigate toxicity.

This work could take the form of a similar study to Abdelmegeed et al. (2010), in which a proteomic approach was utilised to isolate nitrated proteins after paracetamol injury in mice. However, in this study, a 2D gel approach was used which limited the number of proteins available for analysis. Therefore a further study could use an affinity mass spectrometry approach, similar to the one used in Zhan et al. (2006) to isolate a large number of nitrated proteins for analysis using tandem mass spectrometry in order to compare the patterns of PTN in furosemide and paracetamol DILI.

CHAPTER 3

EXOSOME-BOUND AND PROTEIN-BOUND PROFILES OF LIVER-SPECIFIC MICRORNAS DURING DRUG-INDUCED LIVER INJURY IN HUMANS AND RATS

3.1 INTRODUCTION

Drug-induced liver injury (DILI) is the most prevalent form of adverse drug reaction seen within the clinic in the western world and is a major impediment to the development of new drugs. Because of this, sensitive and specific circulating biomarkers of DILI are required in the clinic to diagnose DILI, and also in the pharmaceutical industry to assess potential liver toxicity early in the development of new drugs. MicroRNAs hold many of the properties desired of biomarker candidates; they are organ-specific, species-conserved, stable in biofluids, and are easily quantifiable. Wang *et al* (2009) identified that two liver-enriched miRNAs, miR-122 and miR-192, were raised in the circulation in response to paracetamol-DILI, in both a time, and dose-dependent manner. Importantly, circulating miR-122 levels were elevated earlier in the course of DILI than plasma ALT. This provided the first evidence that miRNAs could be early markers of DILI, possibly providing prognostic value within the clinic. Work within our group has since demonstrated that both miR-122 and miR-192 are significantly raised in the plasma of patients suffering from acute paracetamol-induced liver injury and other forms of DILI (Starkey Lewis et al. 2011). Importantly, these microRNAs remained unchanged in patients undergoing chronic kidney injury, supporting the specificity of these markers. Further work has since suggested that miR-122 has prognostic value in patients admitted to hospital with suspected DILI due to paracetamol. miR-122 readings taken upon hospital admittance were able to predict peak toxicity ALT values, whereas admission ALT levels remained at baseline levels in all patients (Antoine et al. 2013a).

Although there is a great amount of evidence now available to suggest that miR-122 is an early marker of paracetamol-related DILI, there is little evidence to explain how miR-122 levels are raised in the circulation before other markers of DILI, such as ALT. Because of this, we aimed to examine in what form miR-122 was contained in within the circulation in order to shed further light on the release mechanism of this marker during DILI, in an attempt to explain its early elevation. Evidence now suggests that microRNAs can be held in several forms in the circulation, in extracellular vesicles, protein-complexes or lipid-complexes (Arroyo et al.

2011; Turchinovich et al. 2011; Vickers et al. 2011). Extracellular vesicles can be further sub-divided into apoptotic bodies, microvesicles (shedding vesicles) and exosomes (Extracellular vesicles are reviewed in: (Andaloussi et al. 2013). The work in this chapter focusses on the release of microRNAs within exosomes. Exosomes are nanovesicles (30-100 nm in diameter), which have been shown to be involved in immune regulation, and cell-cell signalling (Bianco et al. 2007; Valadi et al. 2007). Exosomes are actively released from the cell through the endosomal/multivesicular body pathway, through exocytosis. It has been demonstrated that their contents are not solely a reflection of the content of their parent cells contents, but that they are selectively packaged, and importantly they are able to laterally transfer their contents to other cells, which can then modulate the function of the recipient cell (Royo et al. 2013). We hypothesise that miR-122 is actively secreted from hepatocytes in exosomes early in the course of DILI, as an early biological response to paracetamol overdose. To examine this, we optimised a method to extract exosomes from the plasma/serum and profiled the content of miR-122 in both the exosomal fraction and the remaining serum/plasma throughout the course of DILI, in both rodent models of DILI, and human clinical samples from cases of DILI due to a variety of different drugs.

3.2 METHODS

3.2.1 Materials

All reagents unless otherwise stated were bought from Sigma Aldrich (St Louis, MO, USA). miRNeasy and RNeasy minElute kits were purchased from Qiagen (Venlo, Netherlands). Stem-loop reverse transcription primers and Taqman stem-loop reverse transcription primers/report (miRNA assays) were purchased from Life Technologies (Foster City, CA, USA). Thermo Infinity ALT Liquid Stable Reagent was purchased from Thermo (Waltham, MA, USA).

3.2.2 Experimental Animals

Rat studies were performed at Almirall, Barcelona under the following protocol. Male Wistar Han rats (6-8 weeks of age) were obtained from Charles River Laboratories (Lyon, France) and allowed 1 week to acclimate prior to the study. Six animals were housed per cage, on a 12 h light/dark cycle, temperature of 22 ± 2ºC and humidity of 55% ± 15%. Standard food and water were provided *ad libitum*. Care of animals was undertaken in compliance with the European Community Directive 86/609/CEE for the use of laboratory animals and with the Autonomous Catalan law (Decret 214/1997). All experimental procedures were approved by the Almirall Ethics Committee before initiation of the study. Rats were administered paracetamol (500, 1000, 1500 mg/kg) in 0.1% methylcellulose by oral gavage, at 0 h, 24 h, 48 h, 72 h and 96 h, followed by humane culling at 0 h, 2 h, 4 h, 6 h, 24 h, 48 h, 72 h, 96 h and 14 days following the first dose of paracetamol. Animals administered with paracetamol, which were immediately culled following dosing (0 h group) were used as the control group. Processed plasma samples were then shipped on dry ice to the Centre for Drug Safety Science (Liverpool, UK) for analysis.

3.2.3 Clinical Samples

NB: work performed on the Spanish DILI cohort was performed jointly with Joanna Clarke (MRC CDSS, PhD Student)

Plasma samples were obtained from ten individuals suffering from hepatocellular, mixed and cholestatic DILI by the Spanish DILI registry (Malaga, Spain) as part of the larger Spanish DILI cohort (Details available in Andrade et al 2005). Patients had been prescribed (or had ingested non-prescribed dietary supplements) a variety of different drugs and substances, including levofloxacin, methotrexate, co-amoxyclav, ciprofloxacin, methoxy-isoflavone, paracetamol, fenofibrate, simvastatin/co-amoxyclav, cocaine, erythromycin, sertraline, which led to DILI (Table 3.1). Plasma samples were taken at time of first admission to hospital ('baseline'), followed by a number of follow-up samples until recovery. The criteria for inclusion of subjects were: an increase in alanine transaminase (ALT) ≥3 times the upper limit of normal (xULN) or ≥2 xULN of alkaline phosphatase (ALP). However, 93% of the cases also fulfilled the more recent DILI criteria established by a recent study: ALT ≥5 xULN or ALT ≥3 xULN + total bilirubin (TBL) ≥2 xULN or ALP ≥2 xULN (Aithal et al. 2011). The pattern of liver injury was classified based on R value calculations as previously described (Benichou et al. 1990). A detailed description of the operational structure of the registry, data recording and case ascertainment has been reported elsewhere (Andrade et al. 2005).

Details of the healthy subjects in the therapeutic dose paracetamol trial can be found within (Watkins et al. 2006). Briefly, healthy volunteers were administered a therapeutic dose of paracetamol or a paracetamol-containing OTC analgesic daily for 14 days. Plasma ALT values were assessed daily, and in a later prospective study, miR-122 levels were also assessed in these samples. Subjects were then characterised as responders or non-responders based on ALT values. The criteria to be classed as a responder was displaying ALT values above the upper limit of normal, 40 U/L. Readings classed as above the upper the limit of normal are highlighted in red on table 3.2. 15 subjects were classed as responders in the study with marked elevations in ALT levels occurring at day 9 of the study, and miR-122 elevations occurring at day 8 (Thulin et al. 2013). Subjects 19, 33, 37 and 45 displayed values above the ULN, but were not classed as responders due to them either displaying these values consistently from day 1 of the study, suggesting a higher than normal basal level of ALT expression or that ALT

levels were raised by less than 10% throughout the study. Based on this, we assessed exosome-bound and exosome-free miR-122 at day 8 of this study in all subjects displayed on table 3.2. Ethical approval was obtained for all human studies.

Table 3.1 Details of Spanish DILI cohort samples used in our study. Patients were prescribed or ingested compounds and then displayed signs of liver injury related to these drugs. Liver injury types were catagorised into hepatocellular, mixed and cholestatic based on displayed biomarker levels. ALT expression was assessed in available samples and expressed as a times the upper limit of normal value. Values listed as a hyphen were classed as normal and in some cases samples were not available for analysis, and so no data was available.

Patient ID	Visit	ALT (x ULN)	Drug	Type of injury
678	Baseline	-	Co-amoxyclav	Cholestatic
	1	-		
687	1	7	Simvastatin/Coamoxy	-
714	Baseline	-	Co-amoxyclav	Hepatocellular
	1	5		
753	1	4	Paracetamol	Hepatocellular
758	1	12	Levofloxacin	Hepatocellular
	2	3		
759	1	60	Dietary supplement (*Camelia sinensis*)	Hepatocellular
762	Baseline	-	Methotrexate	Hepatocellular
	1	73		
	2	No data		
	3	10.5		
	4	No data		
764	Baseline	-	Ciprofloxacin	Hepatocellular
	1	19		
	2	12		
	3	7.7		
	4	No data		
768	Baseline	-	Co-amoxyclav	Mixed
	1	4		
769	Baseline	-	Cocaine	Hepatocellular
	1	25		
806	Baseline	-	Co-amoxyclav	Mixed
	1	2		
	2	1.8		
839	1	-	Co-amoxyclav	Cholestatic
	2	-		
860	1	6.8	Ciprofloxacin	Mixed
	2	8.5		
	3	5.3		
	4	2		
	5	-		
861	Baseline	-	Dietery supplement (methoxy-isoflavone)	Hepatocellular
	1	8		
909	Baseline	-	Fenofibrate	Cholestatic
	1	1.5		
945	1	-	Sertraline	Cholestatic
990	1	5	Erythromycin	Hepatocellular

Table 3.2 Human therapeutic dose paracetamol study ALT measurements. Plasma ALT (xULN) measurements for all subjects (non-responders and responders) in the therapeutic paracetamol dose trial cohort, from day 1 to day 14 (values highlighted in red were classed as above the upper limit of normal and patient IDs highlighted in red were classed as responders).

Subject	Response (Responder/non-responder)	ALT (xULN)													
		Day1	Day2	Day3	Day4	Day5	Day6	Day7	Day8	Day9	Day10	Day11	Day12	Day13	Day14
1	N	0.625	0.475	0.4	0.425	0.55	0.575	0.475	0.5	0.525	0.65	0.55	0.45	0.5	0.475
2	N	0.6	0.675	0.525	0.6	0.5	0.45	0.45	0.55	0.625	0.55	0.475	0.5	0.525	0.575
3	R	0.5	0.475	0.5	0.5	0.475	0.525	0.575	0.725	0.775	0.775	0.85	0.95	1	1
5	R	0.725	0.725	0.6	0.6	0.575	0.7	0.7	0.925	1.4	2.075	2.2	1.9	2	1.925
8	R	0.325	0.375	0.375	0.575	0.575	0.575	0.575	0.725	0.75	0.725	0.85	0.9	1.7	0.775
10	R	0.625	0.675	0.825	0.725	0.725	0.825	0.725	0.825	1.075	1.3	1.5	1.6	1.575	1.55
16	R	0.85	0.9	0.675	0.85	0.85	0.775	0.75	1.05	1.65	2.1	2.7	2.975	2.9	3
19	N	1.2	1.25	1.875	1.875	1.575	1.6	1.6	1.525	1.9	1.625	1.65	1.3	1	1.025
20	R	0.475	0.475	0.475	0.6	0.45	0.375	0.55	0.725	1.1	1.425	1.95	2.125	2.375	2.55
23	R	0.725	0.75	0.75	0.775	0.775	0.8	0.875	1.25	1.625	1.85	1.975	1.85	1.7	1.95
28	R	0.675	0.65	0.575	0.825	0.7	0.775	0.825	1.325	1.7	1.8	1.575	1.425	1.25	1.85
30	N	0.725	0.75	0.8	0.875	0.75	0.9	0.825	0.85	0.95	1	0.95	0.95	0.825	0.775
33	N	1.525	1.5	1.5	1.675	1.4	1.275	1.3	1.4	1.55	1.575	1.575	1.65	1.7	1.725
37	N	1.025	1.025	1.15	1.075	0.85	0.925	0.85	0.9	1.15	1.3	1.425	1.3	1.225	1.3
41	R	0.825	1	0.95	1	0.9	1.075	0.9	1.475	2.5	4.7	5.45	5.15	5.65	5.625
42	N	0.75	0.825	0.75	0.75	0.725	0.75	0.7	0.775	0.8	0.725	0.625	0.75	0.9	0.975
43	R	1.025	0.925	0.9	1	1	1.1	1.1	1.325	1.875	2.075	2.1	2.225	2.15	2.025
45	N	0.875	0.975	1.05	0.925	0.925	0.775	0.9	0.9	1.025	0.95	1.05	1.05	1.125	1.05
46	R	0.725	0.725	0.8	0.775	0.775	0.95	1.225	1.475	1.825	2.1	2.825	2.7	2.225	2.275
47	N	0.825	0.875	0.975	0.925	1	1.025	0.95	0.875	1.025	1	1.125	1.025	1.2	1.2
48	N	0.8	0.75	0.75	0.875	0.775	0.75	0.775	0.675	0.625	0.8	0.8	1	0.9	0.925
49	N	0.825	0.825	0.675	0.825	0.775	0.825	0.8	0.8	0.9	0.9	0.9	0.95	0.95	1.075
50	N	0.7	0.5	0.675	0.7	0.6	0.775	0.825	0.85	0.825	0.75	0.825	0.9	0.7	0.7
53	R	0.65	0.625	0.6	0.625	0.675	0.8	0.95	0.9	1.075	1.275	1.5	1.275	1.5	1.5
54	N	0.825	0.825	0.875	0.925	0.925	0.975	0.975	0.95	0.975	1.025	1.05	0.95	0.9	1
56	R	1.05	1.125	1.05	1.15	1.075	1.1	1.2	1.4	2	2.55	3.375	4.6	5.5	5.775
57	R	0.725	0.625	0.875	1	0.9	0.875	0.975	1.875	2.9	4.15	4.35	5.25	4.8	4.125
58	N	0.575	0.55	0.525	0.575	0.575	0.55	0.5	0.65	0.6	0.625	0.65	0.675	0.775	0.775
63	R	0.875	0.85	0.8	0.825	0.6	0.7	0.775	1.275	1.775	2.075	2.375	2.55	2.375	1.925
71	N	0.825	0.8	0.875	0.825	0.9	0.95	0.65	0.9	0.975	0.95	1	1	1	1.15
Responder	Average	0.71833325	0.72666675	0.71666675	0.78833325	0.73666675	0.79666675	0.84666675	1.15166675	1.60166675	2.065	2.37166675	2.49833325	2.58	2.5233325
	SD	0.1953629	0.20668875	0.1931105	0.18942267 5	0.18513187 5	0.20913655	0.21544527 5	0.3440135	0.60204025	1.09294825	1.25167275	1.43154725	1.50484925	1.51579375
Non-responder	Average	0.84666675	0.84	0.89333325	0.92333325	0.855	0.87333325	0.83833325	0.87333325	0.96333325	0.96166675	0.97666675	0.96333325	0.94833325	0.98166675
	SD	0.24655965	0.2720295	0.3863135	0.38469225	0.2989865	0.287456	0.30308925	0.27507575	0.3652135	0.321668	0.3556265	0.30747625	0.297079	0.308867

3.2.4 Serum ALT activity determination

Serum ALT activity was performed as in Chapter 2.

3.2.5 Exosome extraction from serum

Exosomes were extracted from serum, plasma and other biofluids using Exoquick (SBI, Cambridge, UK), Total Exosome Isolation Solution (Life Technologies, Foster City, USA), Exospin (Cell Guidance Systems, Stevenage, UK) or through ultracentrifugation (see (Pisitkun et al. 2004). Briefly, serum was centrifuged to remove dead cells and then incubated with a volume of the exosome isolation solution for the manufacturers indicated time. This solution was then centrifuged at the manufacturers indicated speed and time until the exosome fraction of the serum formed a pellet. The supernatant was then aspirated by pipette and saved for analysis. The exosome pellet was then suspended in a volume of nuclease-free water, equal to the starting volume of bio-fluid (for detailed work-flow see figure 3.1). Exosomes and supernatant were then characterised through western blotting for exosome markers (CD63 and TSG101). Additionally, exosomes were characterised through transmission electron microscopy using a negative staining protocol developed by Dr Alison Beckett (Department

of Physiology, University of Liverpool) and Dr Marion Pope (Department of Veterinary Pathology, University of Liverpool).

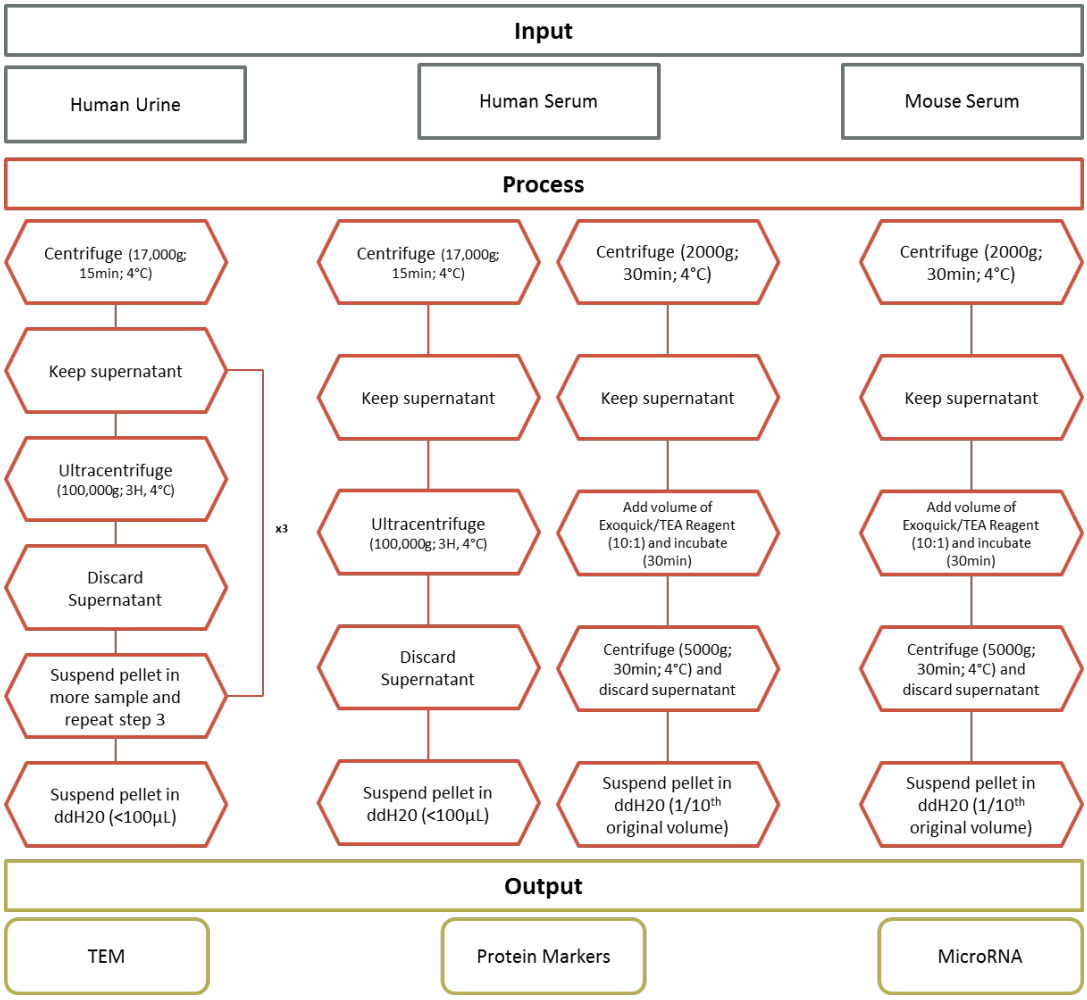

Figure 3.1. Work-flow of exosome-isolation methods, including ultracentrifugation and exosome isolation kits.

3.2.6 miRNA extraction from serum

miRNA was extracted from serum using a miRNeasy kit (Qiagen, Venlo, Netherlands), following the manufacturer's instructions with minor modifications. In brief, 40 µL of sample was diluted to 200 µL with nuclease-free water, and was then combined with 700 µL of QIAzol. The sample was then left to incubate for 5min to ensure complete nucleo-protein dissociation, before addition of 10 µL of (5 fM) Cel-lin-4 (Integrated DNA Techologies, Cambridge, USA) as a 'spike-in' technical control. 140 µL of chloroform was then added and the samples were centrifuged at 12,000 g for 15 minutes at 4 ºC. 350 µL of the upper aqueous

phase was the removed and mixed with an equal volume of 70% ethanol, before being added to a miRNeasy minispin column. The column was spun for 15s at >8,000 g at room temperature and the flow-through, containing the small-RNA fraction was kept.

3.2.7 miRNA Purification

The small-RNA fraction was removed and added to a fresh 2 mL Eppendorf tube, to which 450 µL 100% ethanol was also added. This solution was then added 700 µL at a time to a Qiagen MinElute column, in which the small-RNA fraction was immobilised. The column was then washed with RWT (700 µL) and RPE buffer (500 µL), before the final wash with 500 µL 80% ethanol. The column was then dried thoroughly in the centrifuge (column lids open, >8,000 g, 5 min, RT) and then was transferred to a new 1.5 mL collection tube. The small RNA fraction was then eluted in 14 µL of nuclease-free water and stored at -80 ºC until reverse transcription.

3.2.8 Quantitative Polymerase Chain Reaction Analysis

miRNA and snRNA levels were measured using Taqman-based quantitative polymerase chain reaction (qPCR). The small RNA elute obtained from miRNA Purification step was reverse transcribed to cDNA using specific stem-loop reverse transcription primers (Life Technologies, Foster City, CA) for each miRNA species, following the manufacturer's instructions. 1.33 µL of cDNA was used in the PCR mixture with specific stem-loop PCR primers (Life Technologies, Foster City, CA) in a total volume of 20 µL. Levels of miRNA were measured by the fluorescent signal produced from the Taqman probes on an Applied Biosystems Viia-7 (Life Technologies, Foster City, CA). miRNA levels were then normalised to either Cel-lin-4 (a technical normaliser) or various endogenous normalisers, such as snRNA U6 or hsa-Let-7d, as described elsewhere (Zhang et al. 2010). Alternatively, where no appropriate miRNA normalisation method was available miRNA levels were expressed as 40 minus the cycle threshold (Ct) reading for each sample. As a reference, work performed

previously by the author has suggested that miR-122 is usually detectable at negligible levels in non-DILI human serum samples (40-Ct level of <1).

3.2.9 Determination of Total Protein Concentration of Samples

Total protein concentration was determined using the method described by (Lowry et al. 1951).

3.2.10 Immunoblotting

Immunoblotting was performed as described in Chapter 2 using primary antibodies raised against TSG101 (Abcam ab83; 1:3000 overnight) and CD63 (Abcam ab134045; 1:10,000 overnight), followed by incubation for one hour with 1:10,000 anti-rabbit (Sigma A0545).

3.2.11 Statistical analysis

Statistical analysis was performed as described in Chapter 2.

3.3 RESULTS

3.3.1 Isolation and characterisation of exosomes from biofluids

In order to understand the role of exosomes in the release of miR-122 during paracetamol-DILI, we first sought to develop a robust and repeatable method for their isolation. Initially we chose human urine as a source to isolate exosomes from for convenience. Using an ultracentrifugation approach, we isolated exosomes from 66 ml of urine, and then confirmed their presence through TEM imaging, under a negative stain (Figure 3.2A). Measurement of the imaged vesicles confirmed the homogeneity of the solution for vesicles under 150 nm in diameter, suggesting that this was a pure population of exosomes. To further build towards our goal of analysing blood-bound miR-122, we aimed to extract exosomes from human plasma, due to the large volumes of substrate available. Analysis of the human plasma exosome fraction using TEM imaging confirmed the successful isolation of a pure population of <150 nm diameter nanovesicles using ultracentrifugation from >33 ml plasma. Due to the large volumes of starting solution required for the ultracentrifugation method, and because our aim was to examine miR-122 profiles in rodents, we looked to develop a method for exosome isolation requiring smaller volumes of biofluid. Three kits were initially identified, Exospin (Cell Targeting Systems, Cambridge, UK), Exoquick (Exiqon, Cambridge, UK) and Total exosome isolation solution (Life Technologies, Foster City, USA). Each kit was shown to be successful in isolating exosomes from a starting volume as low as 50 µL of human plasma, by TEM imaging (Figure 3.2B). Exosomes were then isolated from 50 uL rat plasma using each kit for characterisation. TEM imaging using a negative staining protocol was able to demonstrate that each kit had isolated a homogenous population of nanovesicles, (<150 nm in diameter) (Figure 3.2C; representative image of all three kits). To further enhance our confidence that we had isolated a pure population of exosomes, we assessed the expression of exosome markers in both the 'exosome-fraction' (the isolated exosomes) and the 'protein-rich' fraction (the remainder of the plasma), using immuno-blotting. Both CD63, and TSG101 (Figure 3.3) were found to be enriched in the exosome-fraction of the serum.

To examine the yield of exosomes produced from equal volumes of the same plasma sample by each different exosome-isolation kit, the protein expression in the exosome-fraction was measured using a protein assay (Lowry assay). The Exospin and Total exosome isolation solution on average produced a 5 μg/μL exosome solution, whereas the Exoquick kit was able to produce a ~8 μg/μL solution from an equal starting volume (Figure 3.4A).

To assess whether miR-122 was detectable in exosomes, and also to assess the distribution of exosome-bound and exosome-free miR-122 in the plasma of rats under basal conditions, we profiled miR-122 across both fractions in 35 healthy rats (Figure 3.4B). Analysis of baseline miR-122 content in all control animals demonstrated that the protein-rich fraction content of miR-122 is on average ~14-fold higher than in the exosome fraction ($p<0.01$) (Figure 3.4B), with the differences between the two fractions being highly variable between animals. However, in all animals, the protein-rich fraction contained more miR-122 than the exosome-fraction.

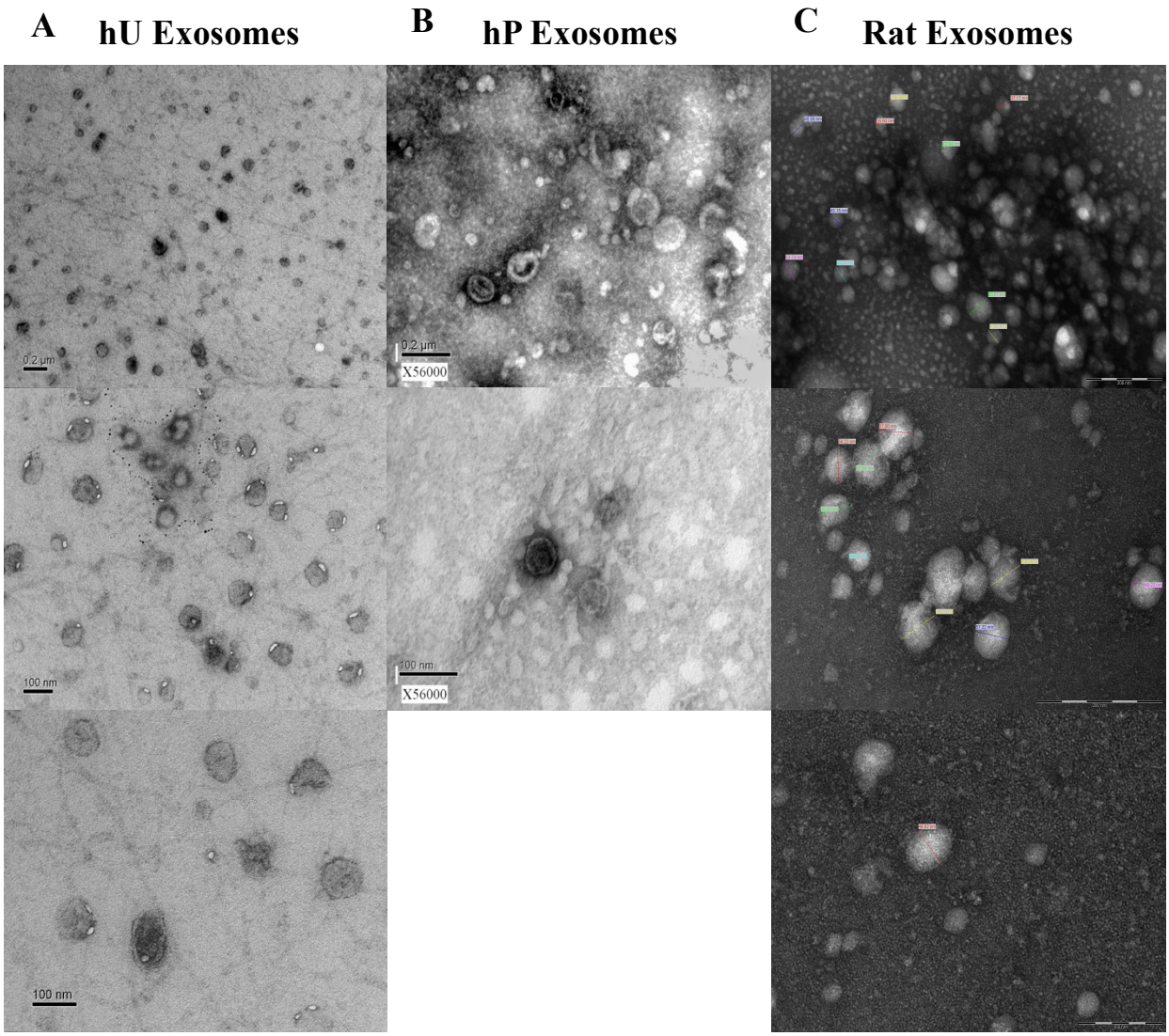

Figure 3.2 Transmission electron microscope images of exosomes extracted from human urine (A), human plasma (B) and rat plasma (C).

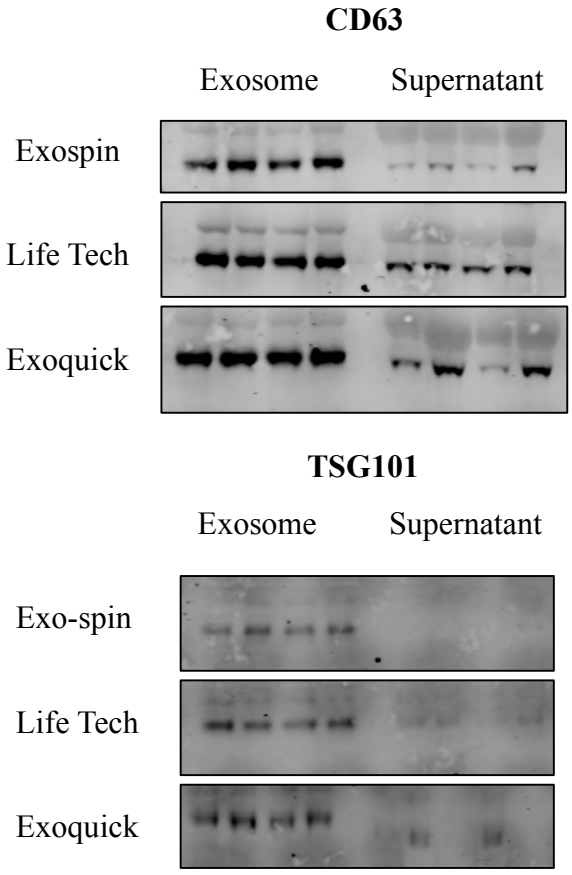

Figure 3.3 Analysis of the exosome markers CD63 and TSG101 in exosomes isolated from rat plasma using three different commercially available exosome-isolation kits, and in the retrospective plasma supernatant (Each lane displays exosomes or plasma-supernatant from a different individual rat).

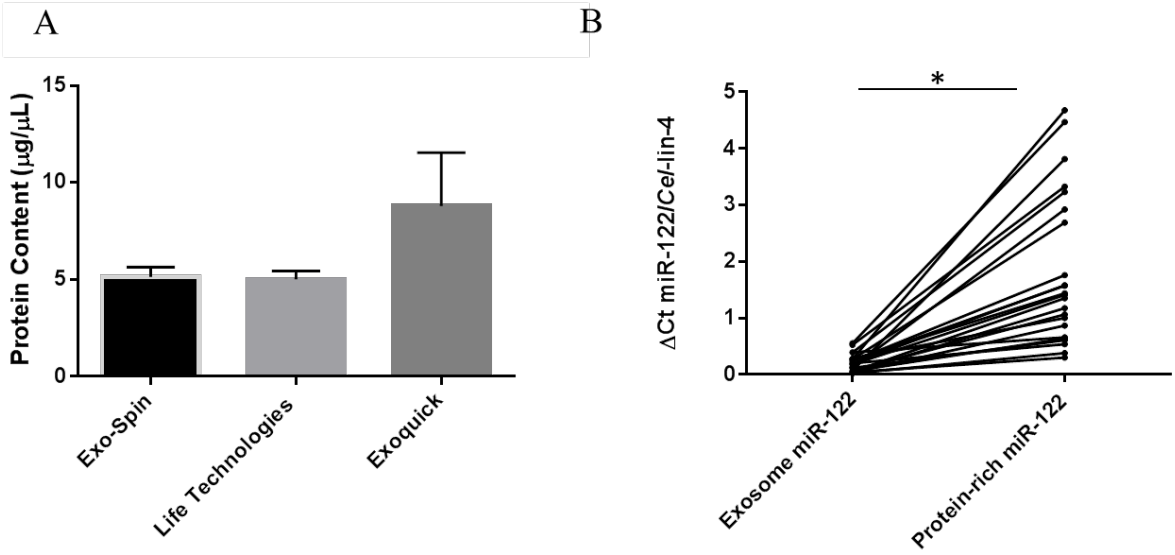

Figure 3.4 A, analysis of the total exosomal protein yields generated by each commercially available exosome-isolation kit from an equal starting volume of serum. **B,** Exosome-bound and exosome-free basal expression levels of miR-122 in 35 healthy non-dosed rats. MiR-122 is expressed at significantly higher levels in the protein-rich fraction when compared to the exosome fraction using a two-way t-test.

3.3.2 miR-122 and ALT are significantly elevated in the plasma of rats after 1500mg/kg paracetamol

In order to qualify miR-122 as an alternative marker of drug-induced hepatotoxicity, groups of rats (n = 6) were treated with a single dose of paracetamol (500, 1000 or 1500 mg/kg) and then sacrificed at 2, 4, 6 or 24 hours post administration. Other animals received a daily administration of paracetamol for 2, 3 or 4 days and were sacrificed 24 hours after the last administration. Body weight was monitored during the study and there was no difference in rats treated at 500 mg/kg compared to each corresponding vehicle group, whereas the body weight of the rats treated with 1000 and 1500 mg/kg was significantly reduced after 3 and 4 days of paracetamol administration (data not shown). The rats in the recovery group progressively gained weight from treatment day 4 until the fourteenth post-dosing day. No mortality was observed in the rats at any dose tested.

Conventional liver biomarkers were investigated in the plasma of all animals and the values were compared to the respective vehicle control groups for each treatment. Both aspartate aminotransferase (AST) (Table 3.3) and ALT levels began to increase after 24 hours after a single administration of 1500 mg/kg (AST: 1.8-fold, $p<0.05$; ALT: 2.0 fold, $p<0.001$) (figure 3.5). The levels of AST and ALT peaked to the same extent after 2 days daily administration of 1500 mg/kg (AST: 43.8-fold, $p>0.001$; ALT 44.3-fold, $p>0.001$) and then remained mildly elevated until day 3 and 4, respectively. Other biomarker measurements can be found in Table 3.3.

Analysis of alternative DILI biomarkers GLDH (figure 3.6) and miR-122 (Figure 3.7) revealed large dose-dependent changes from 24 hours: GLDH increased by 5-fold at 24 hours and peaked at day 2 in the 1500 mg/kg dose-group (24 h: 5.2-fold, $p>0.001$; day 2: 475.4-fold, $p>0.001$). GLDH-levels remained elevated until day 4 for the two highest dose-groups (day 3: 1000 mg/kg: 10.4-fold, $P>0.001$; 1500 mg/kg: 44.9-fold, $p>0.001$; day 4: 1000 mg/kg: 3.8-fold, $p>0.001$; 1500 mg/kg: 14.4-fold, $p>0.001$). Significant increases of miR-122 were observed after 24hrs treatment (1000 mg/kg: 7.0-fold, $p>0.01$; 1500 mg/kg: 17.7-fold,

p>0.001) and similarly, peaked at day 2 (1500 mg/kg: 79.9-fold, p>0.001) (figure 3.7). In contrast to the other liver markers, the levels of miR-122 had returned to baseline for all treatment groups by day 3.

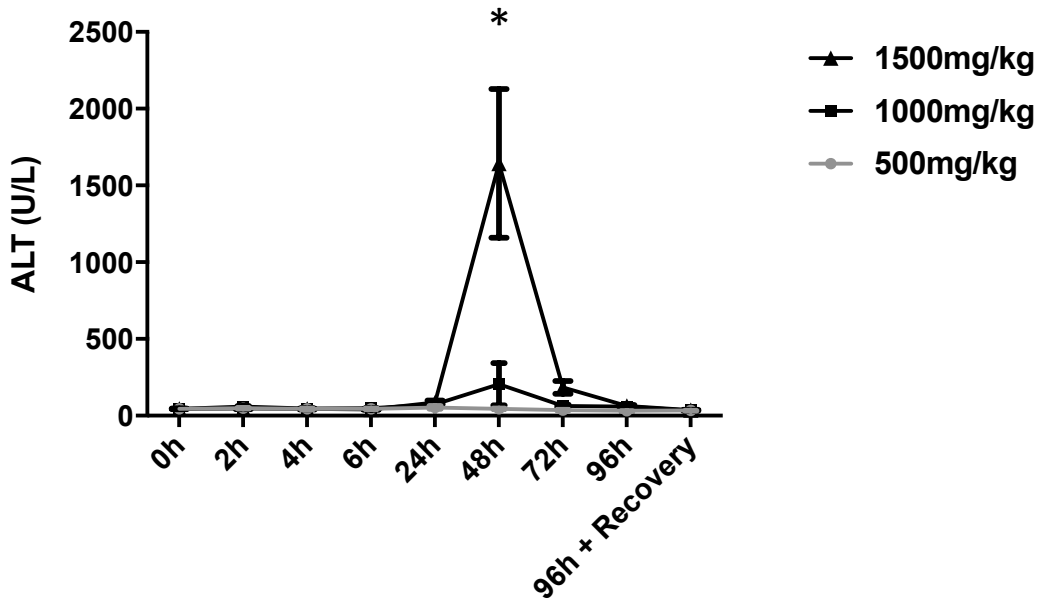

Figure 3.5 Plasma ALT is elevated after a toxic dose of paracetamol in a rat model of paracetamol-DILI. Plasma ALT levels are significantly elevated at 48 h post-dose in the 1500 mg/kg group, before returning to baseline levels by 96 h post-dose.

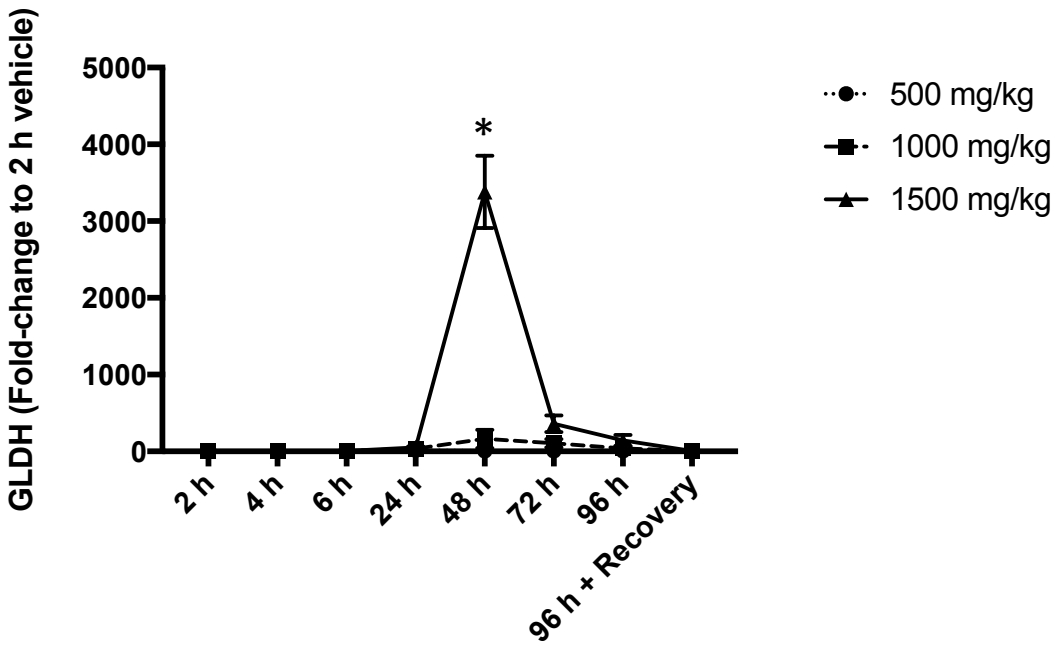

Figure 3.6 Fold-change in plasma GLDH relative to the 2 h vehicle mean.

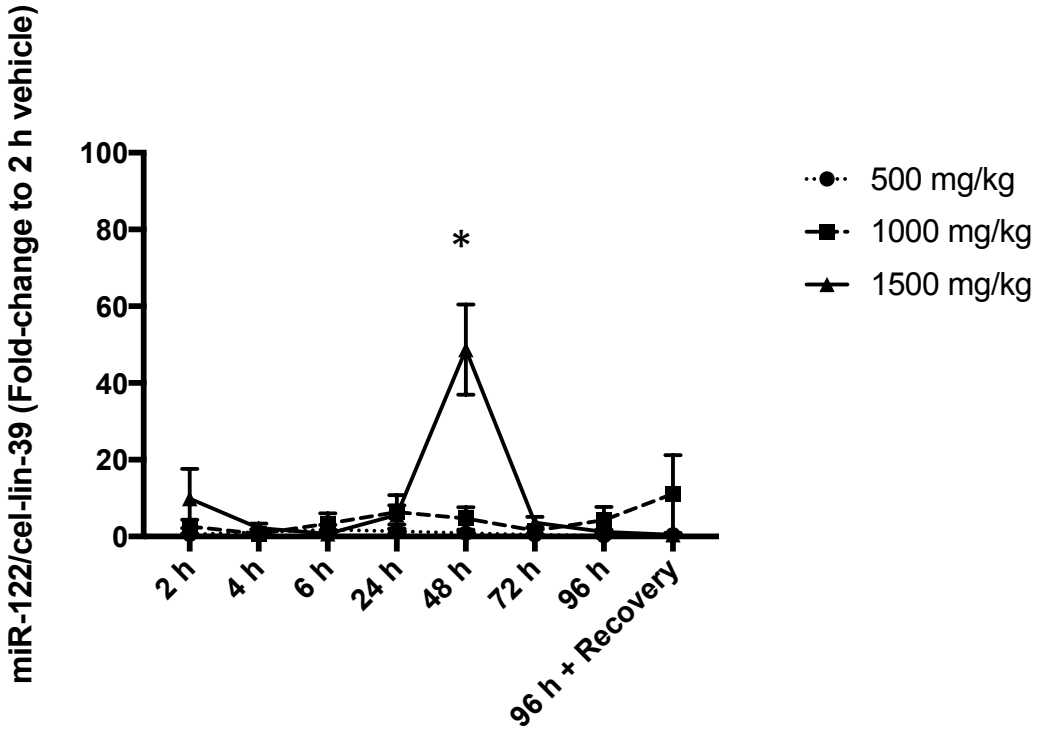

Figure 3.7 Total plasma miR-122 is elevated in rats administered with a toxic dose (1500 mg/kg) of paracetamol at 24 h post-dose, peaking at 48 h.

Table 3.3 Clinical chemistry values (expressed as fold-change to 2 h vehicle) for all biomarkers measured in the rat paracetamol-DILI study. Significance values were assessed based on the mean fold-difference between the treatment group and the 2 h vehicle group (*p < 0.05).

	Dose-group (mg/kg)	2H	4H	6H	24H	2D	3D	4D	R
	500	1.1	0.9	0.9	1.3	1.3	1.0	0.9	0.9
ALT	1000	1.2	1.1	0.9	1.6*	3.0*	1.9	1.6*	0.9
	1500	1.1	0.9	0.9	2.0*	44.3*	4.8*	1.8*	1.0
	500	1.0	0.9	0.9	1.0	1.0	0.9	0.9	0.9
AST	1000	1.0	0.9	1.0	1.2	2.3*	1.5	1.2	0.9
	1500	0.9	0.9	0.9	1.8*	43.8*	2.9*	1.2	1.1
	500	0.9	2.0*	1.6	1.3	0.8	0.7	0.7	0.8
ALP	1000	1.2	1.3	2.0*	2.2*	1.2	0.6	0.7	1.3
	1500	1.0	2.5*	1.8*	2.2*	2.0*	1.0	1.1	1.9*
	500	0.9	0.7	1.0	4.0*	3.3*	2.3	2.6	1.2
GGT	1000	1.5	0.9	1.6	2.6	8.5*	3.2*	2.1	1.0
	1500	0.7	1.4	1.5	2.0	0.7	5.4*	2.4	0.9
	500	1.3	1.2	1.3	1.2	1.3	2.3*	0.8	2.1*
BA	1000	0.8	0.9	0.9	0.8	2.3*	4.6*	2.2*	1.4
	1500	1.5	0.8	1.0	1.1	3.3*	3.3*	1.4	1.9
	500	1.0	1.1	1.1	1.0	0.8	1.2	1.3	0.8*
T-BIL	1000	1.1	1.5*	1.0	1.0	0.9	1.3*	1.2	1.1
	1500	1.1	1.1	1.0	1.0	1.1	1.3*	1.5*	1.2
	500	1.1*	1.1*	1.0	0.9*	1.0	1.0	1.0	1.0
Alb	1000	1.1*	1.2*	1.0	0.9*	1.0	1.0	1.0	1.1
	1500	1.1*	1.2*	1.1*	1.0	1.0	1.0	1.0	1.0
	500	1.1*	1.1*	1.1*	1.0	1.0	1.0	1.0	1.0
TP	1000	1.1*	1.2*	1.1*	0.95*	1.05*	1.0	1.0	1.0
	1500	1.1*	1.2*	1.1*	1.0	1.0	1.0	1.0	1.0
	500	0.9	1.0	0.9	0.9	1.0	1.0	1.0	1.0
LIP C	1000	1.0	1.0	0.9	1.1	1.0	1.1	1.0	1.0
	1500	1.4*	1.1	0.9	1.0	0.9	1.2	1.2	1.0
	500	0.9	0.8	0.9	0.7	0.5*	0.7	0.8	0.8
CK	1000	1.2	0.8	1.2	0.6*	0.6*	0.6*	0.9	0.8
	1500	0.7	0.9	1.0	0.8	0.4*	0.8	1.4	1.1
	500	0.9	1.0	1.0	1.3	1.1	1.3	1.0	1.1
GLDH	1000	1.1	0.9	1.2	2.0	9.9*	10.4*	3.8*	1.0
	1500	1.2	1.0	1.1	5.2*	475.4*	44.9*	14.4*	1.4
	500	0.4	0.5	0.5	4.2	0.9	0.4	0.2*	1.5
miR-122	1000	0.9	0.3	0.9	7.0*	3.0	0.6	1.5	4.3
	1500	2.2	1.4	0.5	17.7*	79.9*	3.5	0.6	1.6

3.3.3 miR-122 is released in both exosome-bound and non-exosome bound forms under basal-conditions and in DILI

To establish whether miR-122 is present in a specific compartment of the plasma in DILI, and moreover, whether fractionation of the plasma into exosomes and the 'protein-rich' fraction (remainder of plasma) increased the sensitivity of miR-122 as a biomarker, we isolated exosomes from the plasma of all rats in the 1500 mg/kg group of the rat paracetamol-DILI study for microRNA profiling analysis. Both fractions were subject to analysis of their miR-122 content, and it was found that both exhibited an almost matching profile (when expressed as fold-change to control average), with both peaking at 48 h post-dose, at ~130-fold times control values (exosome-bound 48 h vs control: $p<0.001$, exosome-free 48 h vs control: $P<0.001$) (Figure 3.8A). Expression profiles throughout the course of injury in both fractions are highly correlative ($R^2 = 0.781$; $p <0.0001$) (Figure 3.8B). On average the exosome-bound miR-122 content was 13.1% of the total plasma miR-122, with the remainder being present in the protein-rich fraction. The exosome-bound miR-122 content increased at the later time-points (72, 96 and 96 h + recovery) to represent 22.2% (SD = 38.42%), 27.1% (SD = 21.96%) and 38.5% (SD = 35.42%) of the total plasma miR-122, however due to a high level of variation between animals, these values are not statistically significant (ANOVA). The average exosome miR-122 content in the earlier time-points (2-48 h) was ~5% (SD = 3.1%) of the total plasma miR-122 (Figure 3.8C).

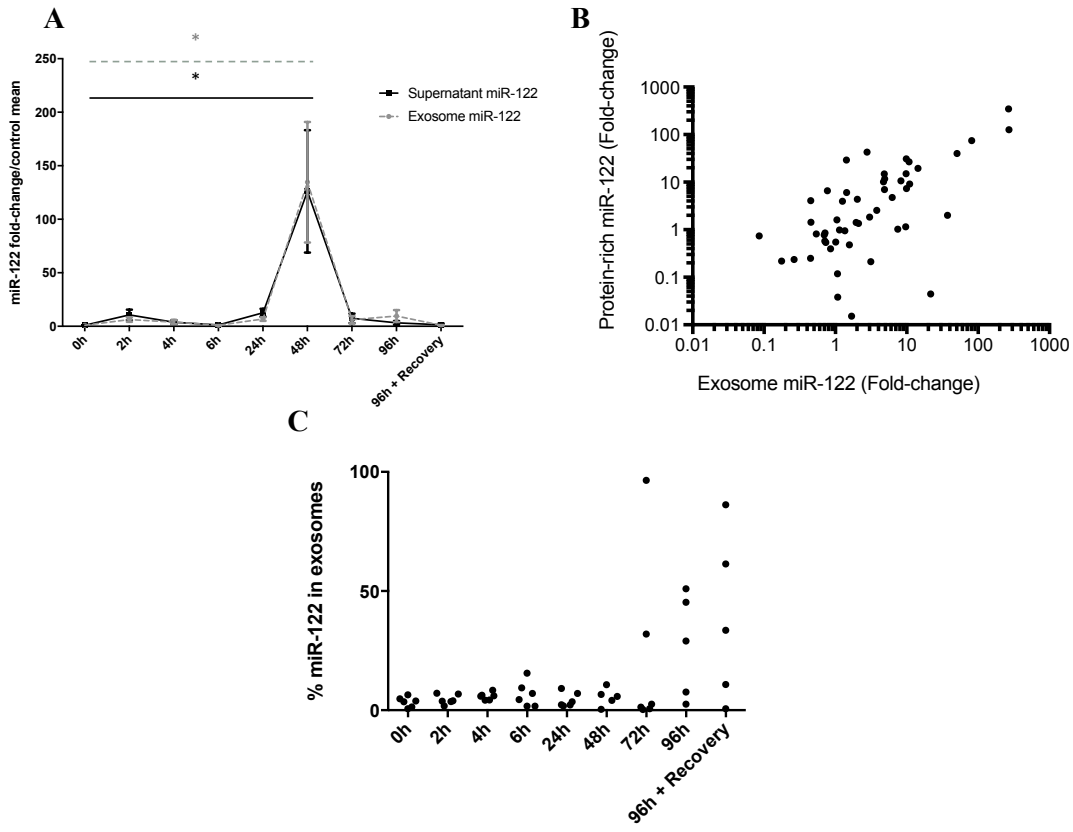

Figure 3.8 A, Profile of exosome-bound and exosome-free miR-122 throughout the course of paracetamol injury in rats. Exosome-bound and exosome-free miR-122 are expressed in the plasma of rats in similar profiles throughout the course of paracetamol-DILI when expressed as fold-change to control samples (animals administered paracetamol and immediately culled). **B, Correlation analysis of exosome-bound and exosome-free miR-122 expressed as fold-change to the mean of the normalised control group samples**. Exosome-bound and exosome-free miR-122 are strongly correlated throughout the course of paracetamol-DILI. **C, Analysis of the percentage of the total serum miR-122 contained within exosomes.** The percentage miR-122 contained within the exosome-bound fraction remains at ~13% throughout the course of DILI. However, from 72 h onwards a small highly variable, but marginally significant elevation of the proportion of miR-122 contained within the exosome fraction can be seen.

3.3.4 miR-192 is raised in both the exosome-fraction and plasma-supernatant fraction in paracetamol-DILI in rats

To examine the release of another liver-enriched miRNA, miR-192 which has previously been shown to be released into the circulation during paracetamol DILI in rodents and humans (Wang et al. 2009; Starkey Lewis et al. 2011), we profiled this marker in both the exosome-rich and protein-rich fractions of plasma taken from the 1500 mg/kg dose group (figure 3.9). Similarly, to miR-122, miR-192 was detectable in both fractions of the plasma and significantly elevated in both fractions at 48 h following a toxic dose of paracetamol (exosome-bound miR-192: $p < 0.01$, exosome-free miR-192: $p < 0.01$). Both the exosome and exosome-free fraction displayed similar expression profiles of miR-192 throughout the course of injury (Pearson R = 1.00, $p<0.0001$), with no significant differences being found at any time point between the exosome-bound and exosome-free fraction of miR-122 (time exosome-bound miR-192 vs time exosome-free miR-192, n = 6). Analysis of the relative quantities of miR-192 contained within exosomes and free-from exosomes (from equal starting volumes) illustrated that exosome-bound miR-192 accounts for 4.9% of the total plasma miR-192 on average, with little difference between time-points in the study (Average = 4.9%, S.D. = 4.2%; Range = 0.7-18.5%).

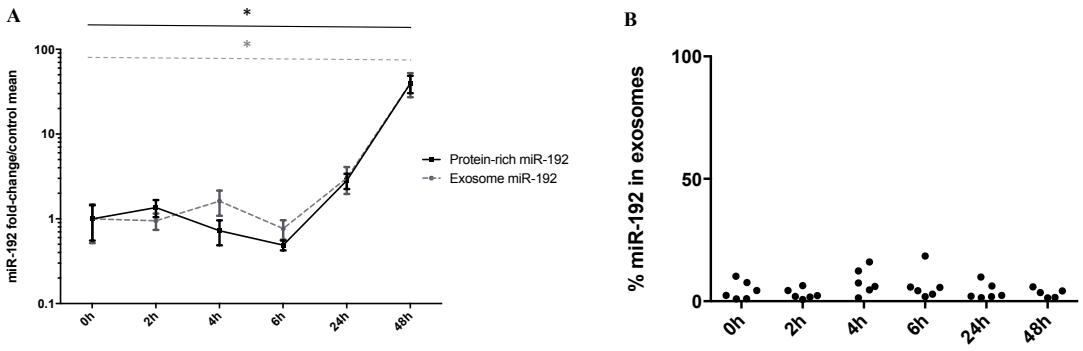

Figure 3.9 A, Exosome-bound and exosome-free miR-192 profiles follow a similar expression trend throughout DILI. **B,** The percentage of the total miR-192 in the plasma contained within exosomes remains constant throughout paracetamol-DILI.

3.3.5 Exosomal release of miR-122 is not the cause of early transient elevations of this biomarker in a human study examining biomarker elevations after therapeutic doses of paracetamol

A study was previously undertaken in which healthy subjects were administered with a therapeutic (4 g/day) dose of paracetamol for 14 days. Blood samples were taken daily to examine for elevations in conventional liver biomarkers, such as ALT. Subjects were then grouped into responders (those with ALT elevations), and non-responders (those-without) (Watkins et al. 2006). Responders were defined as those individuals who displayed plasma ALT levels of above 3 times the upper limit of normal (40 U/L) during the study period (Table 3.2). These samples were then subject to miR-122 analysis in another study (Thulin et al. 2014) and elevations of miR-122 were seen in responders as early as 8 days after paracetamol, one day in advance of ALT elevations. To examine the possibility of differential forms of miR-122 release in this model, exosomes were extracted from the plasma of healthy volunteers administered 8 days of paracetamol (figure 3.10). Successful exosome isolation was confirmed through western blotting for exosome markers and visualisation of exosomes using TEM (Data not shown). Profiling of miR-122 in the exosome and protein-rich fractions in both responders and non-responders, demonstrated a lack of correlation between the two fractions (Pearson R = 0.025, N.S.). Comparison of the exosome-bound (Mean: 17.69, S.D.: 49.60) and exosome-free miR-122 (Mean: 2.96, S.D.: 4.66) levels in the responsive subjects similarly demonstrated that the fractions were not correlative (Pearson R = -0.1; N.S.), but neither was shown to be statistically significantly different from the other ($p = 0.3$).

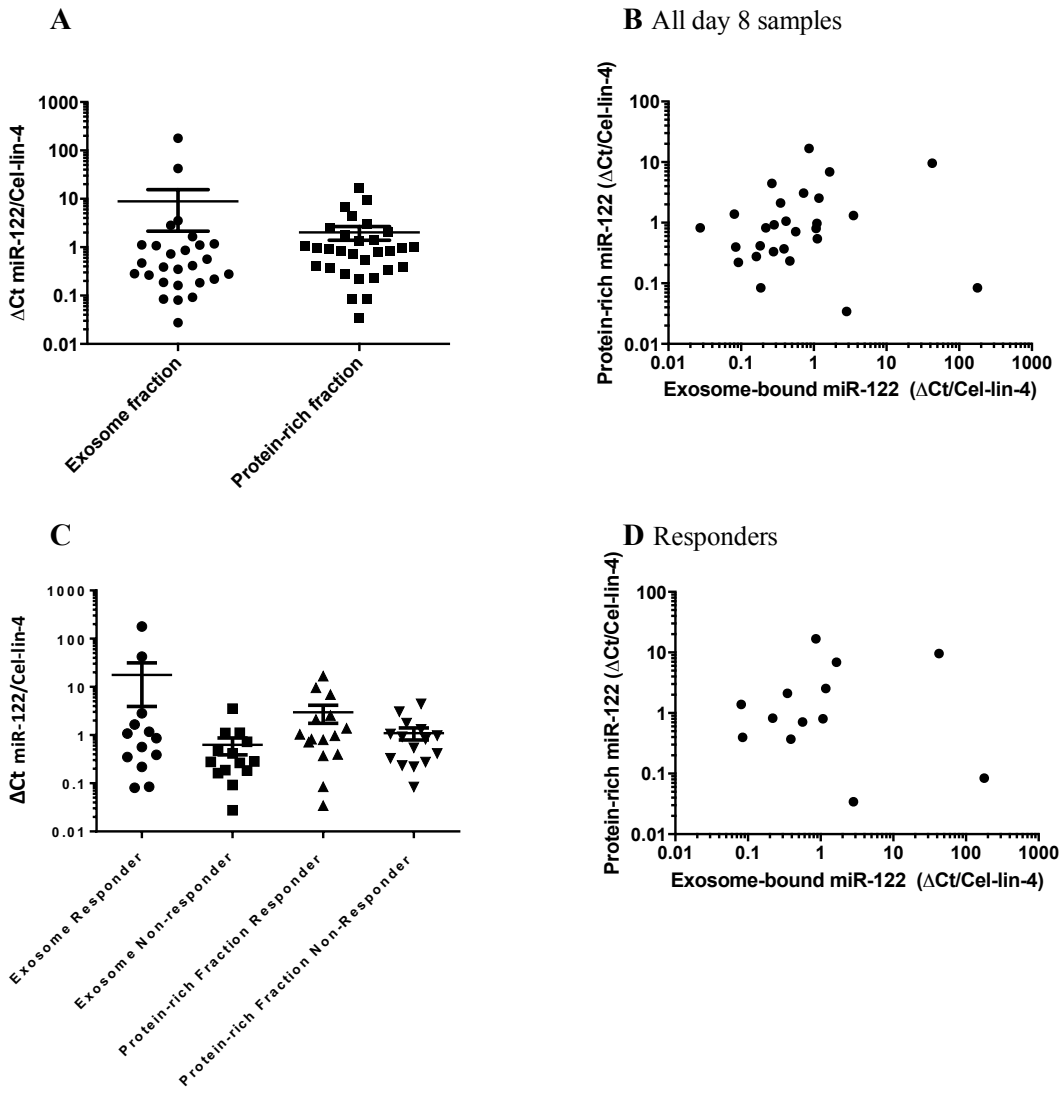

Figure 3.10 A, miR-122 expression in the exosome-fraction and the protein-rich fraction of subjects administered with a therapeutic dose of paracetamol (4 g/day) for 8 days. **B,** Correlation analysis of the exosome-bound and exosome-free expression levels of miR-122. **C,** Expression analysis of exosome-bound and exosome-free miR-122 in responders (those with ALT rises after paracetamol) and non-responders (those with no ALT response). **D,** Correlation analysis of exosome-bound and exosome-free miR-122 levels in patients with displayed an ALT response after therapeutic doses of paracetamol.

3.3.6 Different forms of liver injury do not cause any differentiation between the exosomal and protein-rich content of miR-122 in human patients after exposure to different hepatotoxic drugs

As our initial hypothesis was not supported by our study examining forms of miR-122 release during acute injury in rats, we aimed to examine the mechanisms behind miR-122 release in non-acute forms of DILI and under sub-toxic conditions in order to fully establish the role of exosomes in miR-122 release. To examine whether miR-122 is preferentially released from the liver in exosomes during different forms of DILI, 31 human plasma samples from patients (See table 3.1 for details of samples assessed) suffering hepatocellular, mixed or cholestatic DILI were obtained from the Spanish DILI registry (Malaga, Spain). Exosomes were then isolated and characterised as previously described, then miR-122 was profiled in each fraction to assess whether either fraction was better able to predict the type of injury. Correlation analysis of all samples from all injury types and drugs indicated that the exosome-bound and exosome-free profiles of miR-122 strongly correlated (Pearson $R = 0.612$, $p < 0.0005$) (Fig 3.11A). Similarly, correlation analysis of only the samples taken from each patient at peak exosome-free miR-122 levels, demonstrated that the exosome-bound and exosome-free fractions of miR-122 are strongly correlated (Pearson $R = 0.637$, $p < 0.005$) (Figure 3.11D). Analysis of first presentation samples (listed as 'baseline' on table 3.1) demonstrated that there was a weak negative correlation between exosome-bound and exosome-free miR-122 (Pearson $R = -0.252$, $p = 0.3$ N.S.) (Figure 3.11B). However, samples analysed in this category were highly clustered, with a low overall difference in expression between the highest and lowest readings making it difficult to assess any possible relationships or differences between the exosome-bound and exosome-free miR-122. To examine whether different injury types (cholestatic, mixed and hepatocellular) caused different profiles of miR-122 release, the results were categorised based on the aetiology. Exosome-bound and exosome-free miR-122 profiles in hepatocullar injury patients were correlative (Pearson $R = 0.636$, $p < 0.01$) (Figure 3.11B+C). Mixed injury samples displayed a non-significant trend towards correlation

(Pearson R = 0.556, N.S., n = 8) and those with cholestatic injury showed little correlation between the exosome-bound and exosome-free fractions (Pearson R = 0.042, N.S.) (Fig 3.12A). Individual patient profiles of exosome-bound and exosome-free miR-122 (expressed as 40-Ct) were then subject to comparison to each other, and also to ALT (xULN) values measured previously (figure 3.13). In 4 out of 6 cases of hepatocellular DILI both the exosome-bound and exosome-free profiles of miR-122 were closely matched. In 1 out of the 6, specifically patient 769, exosome-bound and exosome-free miR-122 displayed an opposite trend, with exosome-bound increasing and exosome-free decreasing. However, the dynamic change in this sample was small in both assessments. In the case of patient 764, there is a clear fall in exosome-free miR-122 expression in sample 2, in comparison to the smooth increase in exosome-bound miR-122. Due to the limited number of ALT samples in the hepatocellular group, meaningful comparisons could only be obtained from patients 758,762 and 764. In all cases, peak ALT was matched in time by peak exosome-free miR-122 and in two out of three cases, was also matched by peak exosome-bound miR-122. Similarly, the overall direction of expression change was similar between ALT, exosome-bound miR-122 and exosome-free miR-122 in two out of three cases, and in three out of three cases for the comparison of exosome-free miR-122 to ALT. In all mixed injury cases exosome-bound miR-122 and exosome-free miR-122 followed similar expression trends (patient 768, 806, 860), and in the case of 860, ALT also followed a similar expression trend. Interestingly, in patient 806, ALT expression was seen to fall between sample 1 and 2 (ALT: 2.0 vs 1.8 xULN), whereas miR-122 levels remained consistent in both fractions. In the patients displaying cholestatic injury little trend could be seen between the exosome-bound and exosome-free miR-122 fractions, with two patients (839, 678) displaying opposite expression trends and one patient (909) displaying a stable expression levels of exosome-bound miR-122, with increasing levels of exosome-free miR-122. In all cases, cholestatic patients did not show ALT elevations and therefore it was not possible to obtain this comparison.

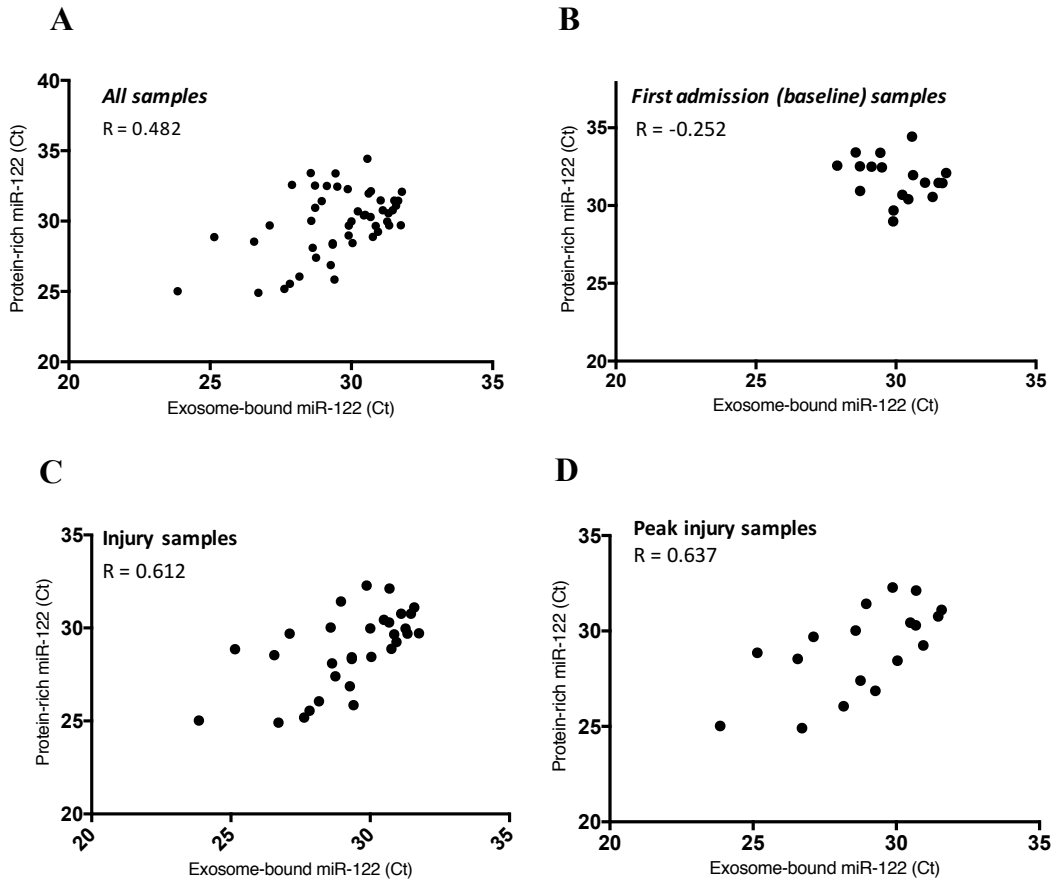

Figure 3.11 A, Correlation analysis of miR-122 expression in samples taken from all patients within the cohort at all time-points. **B,** Correlation analysis of the baseline/control samples taken from each patient before any obvious signs of injury are present. **C,** Correlation analysis of samples taken from patients displaying signs of injury. **D,** Correlation analysis of samples taken at the peak of injury from all patients, assessed using peak ALT (xULN) values.

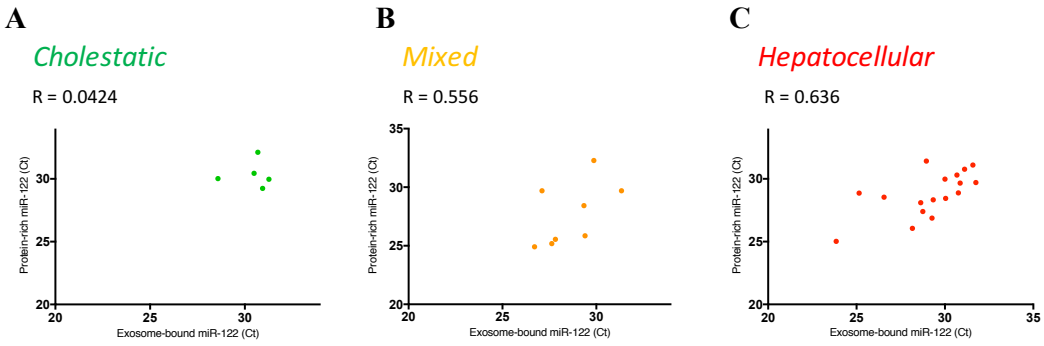

Figure 3.12 A, Correlation analysis of exosome-bound and exosome-free miR-122 expression in cholestatic injury patients. **B,** Correlation analysis of exosome-bound and exosome-free miR-122 expression in mixed injury patients. **C,** Correlation analysis of exosome-bound and exosome-free miR-122 in hepatocellular injury patients.

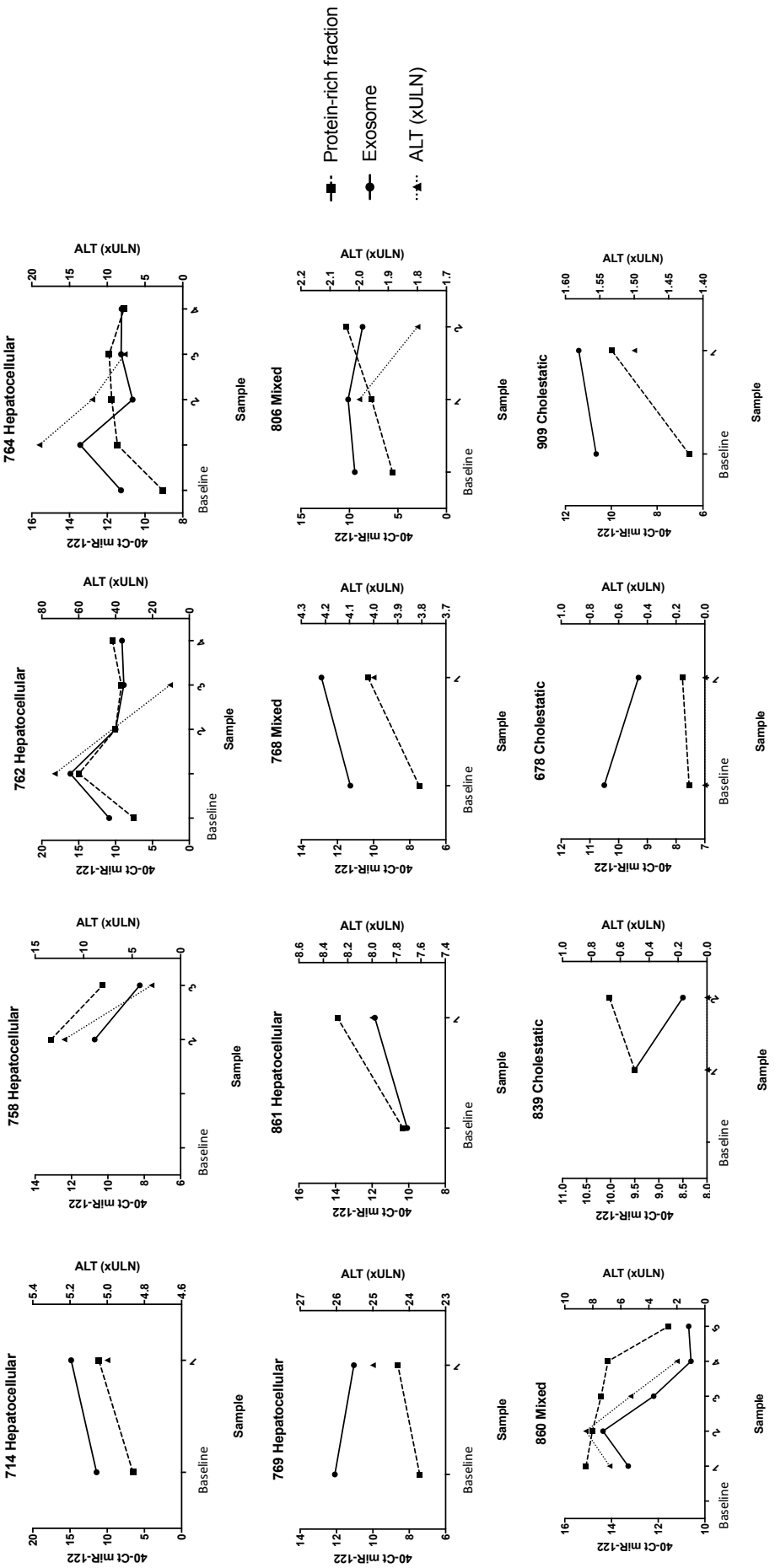

Figure 3.13 Individual patient profiles of exosome-bound, exosome-free miR-122 (Expressed as 40-Ct value) and ALT (xULN).

3.4 DISCUSSION

To investigate our hypothesis that early detection of circulating miR-122 in DILI is possible due to its active release in exosomes, it was first necessary to develop a method to separate exosomes from the remainder of the plasma/serum. Through testing several commercially available kits for exosome extraction, alongside well established non-kit based methods, we identified that three commercially available kits produced an equivalent quantity, and purity of exosomes from a smaller volume of serum than was possible to use with the centrifugation method. Based on this, we selected Life Technologies Total Exosome Isolation Solution for the remainder of the studies within the chapter.

In order to assess whether miR-122 is raised early in the circulation within exosomes, we first had to select an appropriate experimental model, taking into account the current literature examining miR-122 as a marker of DILI, and also encompassing the necessary longitudinal capability to detect its early release. Initially, our chosen model was a rat model of paracetamol-induced liver injury, in which non-fasted rats were administered by oral gavage in order to elongate the time-course of paracetamol injury. This is demonstrated by peak miR-122 and ALT levels only being achieved by 48 h post-dose, whereas in an equivalent fasted, I.P. dosing study in mice, this would be expected as early as 8 h, as seen in chapter 2 of this thesis. Importantly, total plasma miR-122 was elevated to a significantly greater level in the plasma at 24 h after paracetamol (17.7-fold), when compared to ALT (2-fold), adding further evidence to the previous literature which suggests that miR-122 is an early marker of DILI.

To test our hypothesis that miR-122 is released early within exosomes, we then examined the profiles of miR-122 expression in both exosomes and the remainder of the plasma. Analysis of the basal expression of miR-122, and miR-192, another liver-enriched microRNA, suggests that the majority of these microRNAs are contained in an exosome-free form. This is not unexpected, and it has previously been shown in a study examining basal levels of a number of microRNAs that the majority are free from vesicles under normal conditions (Turchinovich et al. 2011). Our analysis of the profiles of both fractions throughout the time-course of

paracetamol-DILI demonstrates for the first time that miR-122 is released in equivalent profiles both bound to exosomes, and un-bound throughout the course of DILI. However, the exosomal quantity of miR-122 was ~13% on average of the total plasma miR-122 content throughout the time-course. This suggests that in paracetamol-DILI, miR-122 is being released in multiple forms, which may suggest that this is a product of necrotic cellular membrane damage, which leads to a non-selective release of this marker into the circulation. This complements work performed in a previous study (Bala et al. 2012) in mice, which suggested that the majority of miR-122 is released in the exosome-free fraction after a toxic I.P. dose of paracetamol. This together suggests that measurement of exosomal miR-122 in this rodent model does not add any further prognostic use in DILI, over measuring whole plasma/serum miR-122. However, interestingly the percentage of the total plasma miR-122 contained within the exosome-fraction increased from 72 h onwards, peaking at an average of 38%, three times the average baseline level. Although this result was not statistically significant due to high levels of variation between the rats, several hypotheses could be generated from this. First, miR-122 packaged in exosomes may be more stable than exosome-free miR-122, allowing the packaged miR-122 to remain in the plasma after injury resolves. This is supported by studies examining the stability of exosome-bound miRNAs, which have now suggested that these miRNAs remain stable in the circulation for much longer than ones un-bound (Ge et al. 2014). However, the finding that exosome-bound miR-192 levels remained constant throughout the time-course, may suggest that both forms of miRNA packaging are equally stable in the circulation. Second, could be the reverse of our initial hypothesis, that the liver actively secretes exosome-bound miR-122 in the regenerative stages of injury to increase the proliferative response of the remaining hepatocytes. Both however would need to be experimentally verified.

As our rat model provided evidence against our initial hypothesis, we developed a new hypothesis that miR-122 is not selectively released in exosomes following a toxic dose of paracetamol, due to the severity of the injury involved, but this marker may be released in

exosomes following a low, non-toxic dose of paracetamol. There is evidence to support the release of both miR-122 and other miRNAs in exosomes during alcohol-induced liver injury, which is a much slower form of injury than paracetamol, in which cellular energy and transport functions are still active (Bala et al. 2012). To examine this hypothesis, we obtained plasma samples from healthy individuals who were administered with a therapeutic dose of paracetamol daily for 14 days (Watkins et al. 2006). Previously, these samples have shown that some individuals within this trial displayed transient ALT elevations at as early as 9 days after paracetamol. A study following this then demonstrated that miR-122 was also elevated in these responders at around one day earlier than ALT (on average) (Thulin et al. 2014). Once again, we tested whether this early release, with no signs of toxicity, is due to an active release of miR-122 through the exosome pathway. In our analysis miR-122 was elevated in both fractions, and similarly to the rat model, no statistically significant difference could be seen between exosome and non-exosome bound miR-122 in the plasma of the patients which responded to paracetamol. This once again suggests that after sub-toxic doses of paracetamol, miR-122 is not selectively released in exosomes over other pathways of miRNA release. The lack of correlation between the two plasma fractions may explained by the small dynamic range of miR-122 expression in this study, and also the expected levels of inter-individual variations that are seen in human trials.

Finally, we aimed to test the hypothesis that miR-122 may be released in different compartments during different types of DILI. To examine this, we obtained human plasma samples from the Malaga DILI registry, which comprises individuals who have been prescribed a variety of hepatotoxic drugs and have displayed mixed, hepatocellular or cholestatic injury. To account for the different number of blood samples taken from each patient, direct comparisons between patients were taken at peak ALT values, and individual longitudinal plasma miR-122 profiles were compared separately. Similarly to both of the previous studies, our analysis demonstrated that exosome and non-exosome miR-122 profiles are highly correlative when all samples taken from hepatocellular injury patients were

compared. In contrast, mixed injury displayed a weaker relationship, and in cholestatic injury the correlation between the two different fractions was low. However, it is likely this that can be attributed to the low dynamic range of the change in miR-122 in cholestatic injury, due to miR-122 largely being associated with hepatocyte injury, and not injury of the bile ducts. Interestingly, when individual patient profiles were analysed and compared with each other, and also ALT, there was little overriding trend amongst patients suffering each individual type of injury, and no distinguishing factor in exosome-bound or exosome-free profiles of miR-122 could be found to clearly separate the different types of injury. Similarly, when ALT profiles were compared to the profiles of each miR-122 fraction, no distinguishing trend could be found, with peak ALT measurements matching those of both miR-122 fractions in the majority of samples involving hepatocyte injury, supporting our previous conclusions drawn from our rat study. In fact, the only distinguishing factor found was that ALT was not elevated in patients undergoing cholestatic injury and that elevations in miR-122 in both fractions were minimal in comparison to mixed and hepatocellular injury. This however is of no surprised as it has been suggested that miR-122 expression is highly enriched in hepatocytes (Lagos-Quintana et al. 2002; Kia et al. 2015) and therefore in cholestatic injury, where hepatocyte injury will initially be considerably less than in the other forms of injury, it is no surprise that a hepatocyte-injury marker would not be elevated (Padda et al. 2011).

Another interesting finding in our study examining forms of human liver injury, was that exosome-bound miR-122 expression actually decreased in two out of the three patients undergoing cholestatic injury and levels were maintained in the third, in comparison to exosome-free miR-122 expression which actually increased. An explanation for this could be the slow progressive nature of cholestatic injury in which hepatocyte injury is usually secondary to bile duct injury (Padda et al. 2011), meaning that cell-signalling may play more of a role than in more acute forms of injury. Therefore, it is possible that hepatocytes are actively slowing the release of exosomes which contain miR-122 as an adaptive response to the oncoming injury. This finding is a contrast to much of the previous literature which is

examining the release of exosomes as signalling or shuttling vehicles which are able to transport intracellular molecules to recipient cells to elicit a response (Herrera et al. 2010; Mittelbrun et al. 2011), and is therefore relatively unexplored.

In summary, we have examined whether the exosomal pathway is implicated in the early release of miR-122 during DILI in both rats and humans. Although miR-122 levels are raised in exosomes during DILI, exosome-free miR-122 levels also are raised similarly, suggesting that there is not one specific pathway for miR-122 release. This suggests that there is little prognostic value added through the fractionation of plasma to exosomes, over what is gained from miR-122 measurement in the whole plasma. Despite our findings which suggest a limited prognostic use for exosome-bound miR-122, studies examining slower, more progressive forms of liver injury, such as alcohol-induced liver injury (ALD), have produced different findings. In one example, it was found that exosome-bound miR-122, and miR-155, a miRNA associated with inflammation were elevated in the exosome-bound fraction over the protein-rich fraction during ALD (Bala et al. 2012). This result supports our previous suggestion that that exosomal release of miRNAs may be more of a factor in progressive forms of liver injury, in which cell-cell signalling and inflammation is a more predominant factor.

Future work could look to further examine the pathways of miR-122 release, through further fractionation of the exosome-free fraction into microvesicles, protein complexes and lipid complexes in order to assess whether miR-122 is associated with all of these release pathways, or whether it is selectively associated to any one of these. Additionally, work could be undertaken to manipulate the levels of exosome release in DILI using exosome release blockers (Mittelbrun et al. 2011) to fully understand the functional effects of these molecules.

CHAPTER 4

ANALYSIS OF ZONAL MICRORNA EXPRESSION PROFILES BASALLY AND IN PARACETAMOL-INDUCED LIVER INJURY IN THE RAT

4.1 INTRODUCTION

The liver by mass is almost 60% hepatocytes, which are responsible for the production of albumin, and the metabolism of endogenous compounds, and drugs. Hepatocytes are a heterogeneous species, with their phenotype being dependent on their proximity to a portal or central vein (Reviewed by (Colnot and Perret 2011). Zone I hepatocytes (periportal) are rich in glutathione, express low levels of cytochrome P450 enzymes, and contain high levels of phase II metabolism enzymes. In contrast, zone III hepatocytes, located in the oxygen-poor pericentral regions, express a low levels of glutathione, but high levels of cytochrome P450 enzymes. Because of this zone III hepatocytes are particularly susceptible to toxicity caused by certain drugs, such as paracetamol, due to increased bioactivation of the compound, but reduced excretion (Anundi et al. 1993). Some zonated processes, such as glycolysis and gluconeogenesis are subject to environmental regulation, by factors such as differential oxygen content between the hepatic zones, and because of this are reversible through changes in the local blood content (Berkowitz et al. 1995; Braeuning et al. 2006; Gebhardt 1992; Häussinger et al. 1991). Other zonated processes, such as ammonia detoxification are also subject to transcriptional regulation, which is not reversible through changing external environmental conditions (Tygstrup et al. 1962). Studies since utilising knock-out models have now attributed this master zonal regulation to the Wnt/Beta-Catenin pathway (Benhamouche et al. 2006b; Cadoret et al. 2002).

microRNAs (miRNAs) are small non-coding RNAs (20-22nt) that are able to regulate gene expression through translational repression or mRNA degradation. miRNAs regulate various biological processes, such as lipid metabolism (Esau et al. 2006), apoptosis (Cimmino et al. 2005), and carcinogenesis (Lu et al. 2005). It is not currently understood whether gene-regulation at a miRNA level plays a role in zonation within the liver. Yamaura *et al,* examined hepatic zonal miRNA profiles basally, and in different forms of DILI in rats, demonstrating that 49 miRNAs are differentially expressed between zone I and zone III regions of the liver (27 up-regulated in PV, 22 down-regulated) (Yamaura et al. 2014), however no analysis of

the downstream function of this expression was undertaken. Therefore, this chapter aims to identify and characterise miRNAs which are significantly differentially expressed between different regions of the liver, and importantly, link this expression to possible downstream targets within the liver to establish the role of miRNA gene regulation in hepatic zonation. An additional aim is to address contrasting results within the literature examining whether miR-122, a biomarker of DILI is lost from the liver during liver injury. To address this, we aimed to profile miR-122 and other miRNAs in both zone I and III after paracetamol treatment in rats, in order to establish both whether miR-122 is lost from injured areas, and whether other miRNA expression changes occur during injury within either region. The rat was chosen as our species of investigation in order to allow sufficient zonal tissue collection for the study discussed within this chapter and a recently published partner study (Holman et al. 2016).

4.2 METHODS

4.2.1 Animal use

Sprague Dawley rats were chosen for use in this study based on their previous use by the Hamner Institutes for Health Sciences in similar studies. 6-8 week old Sprague Dawley rats (200-250 g) were obtained from Charles River (Raleigh, NC), housed in pairs, and left to acclimatise for 1 week prior to use. Food and water was available *ad libumtum,* and animals were kept in a 12 h light-dark cycle. All animal work was approved by the Institutional Animal Care and Use Committee, and was carried out under Hamner Institutes for Health Sciences regulations.

4.2.2 Study Design

This study was performed at the Hamner Institutes for Health Sciences (Raleigh-Durham, NC, USA) as a collaborative effort between the MRC Centre for Drug Safety Sciences and the Hamner Institute for Drug Safety Sciences. Food was removed from the housing of 120x Sprague Dawley rats prior to the study commencing. After 16 h, rats were administered with either vehicle (0.5% methylcellulose in water), 500 mg/kg paracetamol in vehicle, or 1400 mg/kg paracetamol in vehicle by oral gavage. Rats were then culled at 1, 2, 4, 8, and 24 h post-dosing, in groups of 5 per treatment. Blood was then collected and stored in EDTA-plasma tubes for subsequent plasma separation. Liver tissue was also collected and the lobes were separated. The left and median lobes were then processed for histology, including H&E and immunohistochemistry.

4.2.3 Clinical Chemistry

Approximately 250 µl of plasma was used for clinical chemistry analysis. Plasma was selected to maximize the spectrum of analytes that can be measured in this study. Chemistries were assessed using standard assays on a CLC 720 clinical chemistry analyzer (Carolina Liquid Chemistries, Winston Salem, NC). Analysis includes ALT, aspartate aminotransferase (AST),

alkaline phosphatase (ALP), glutamate dehydrogenase (GLDH), albumin (ALB), blood urea nitrogen (BUN), creatinine (CR) and total and direct bilirubin.

4.2.4 Laser Capture Microdissection

Slices from both the left and median liver lobes of each animal were frozen in OCT medium within a cryomold by gradual submersion in liquid nitrogen. Cryomolds were then placed onto dry ice until they can be stored at approximately at ≤ -70 °C. For sectioning, tissue blocks were mounted onto a brass chuck and sectioned into 12 µM sections using a cryostat set at approximately -12℃. Approximately 2-5 sections from the interior portion of the liver slices were immediately affixed to membrane slides (Molecular Machines & Industries, Haslett, MI), followed by fixation in EtOH and staining with hemotoxylin. LCM was conducted utilizing an Olympus 1X81 microscope and MMI Cell Cut Plus software (Molecular Machines & Industries, Haslett, MI). Within median liver sections, periportal (zone 1) and pericentral (zone 3) hepatic cells were isolated separately and the area of tissue collected was recorded for the purpose of data normalization. A zone of four hepatocytes depth was collected surrounding the portal and central veins in order to ensure the specificity of zones collected. Sections were collected on diffuser caps (Molecular Machines & Industries) and subsequently immersed into RLT buffer (Qiagen, Valencia, CA), a guanidine isothiocycanate-containing lysis buffer, and stored at ≤ -70°C.

4.2.5 Taqman microRNA profiling

Total RNA was isolated from select tissue sections using the miRNeasy Micro Kit (Qiagen, Valencia, CA) in accordance with manufacture's recommended protocol. Isolated RNA was reverse transcribed using the TaqMan MicroRNA Reverse Transcription Kit and the Megaplex Reverse Transcription Rodent Pools Set V. 3.0 (Life Technologies, Foster City, CA). The resulting cDNA was pre-amplified using TaqMan PreAmp Master Mix and MegaPlex Preamp Rodent Pools Set V. 3.0 (Life Technologies, Foster City, CA) following

the manufacturer's instructions. MiRNA profiling was then conducted using TaqMan Rodent miRNA Set A and B V. 3.0 Arrays and Taqman Universal Master Mix II, No UNG (Life Technologies) following the manufacturer's specifications. Quantitative real time PCR (qRT-PCR) of these arrays was then performed using a Viia-7 Real-Time PCR System (Applied Biosystems).

4.2.6 Taqman microRNA qPCR

Pre-amplified and reverse transcribed microRNA samples (See above) were subject to qPCR validation. Briefly, equal quantities of cDNA were analysed examining individual microRNAs using Taqman microRNA assays (Life Technologies, Foster City, CA) and universal Taqman master mix (Life Technologies), on a Viia-7 qPCR platform.

4.2.7 Total RNA extraction and analysis

Total RNA extraction was performed as described above. Pre-amplification of the total RNA content was performed using a MiScript Preamp PCR kit (Qiagen, Venlo, Netherlands) under the manufacturer's protocol. Total RNA was then quantified using a Nanodrop (Thermo Scientific) and loaded in equal quantity onto a 384-well qPCR plate. Specific primers (Eurofins) then combined with universal SYBR master-mix reagent (Sigma), and added to the cDNA. The content of the specific genes was then quantified using a Viia-7 qPCR platform (Applied Biosystems).

4.2.8 In situ hybridization of miR-122

MiR-122 was localised using double-DIG labelled miRCURY LNA microRNA detection probes (Exiqon A/S, Vedbaek, Denmark). The in situ hybridization procedure was performed on a fully-automated Ventana Discovery Ultra (Roche diagnostics AG, Rotkreuz, Switzerland). All reagents were provided by Roche Diagnostics. Briefly, whole liver sections were de-paraffinized at 62 °C for 12 minutes before proteinase K digestion step (Exiqon A/S, Vedbaek, Denmark) treatment (37 °C, 24 min). The antimiR-122 probe (25 pmoles) was then

incubated at 54 °C for 3 h with de-paraffinized sections. Sections were then washed with 3 × 8 mins cycles of saline sodium citrate, an acidic salt buffer solution at increasing stringency per cycle (2.0×, 1.0×, 0.5×) to control acidity. A negative scramble control was also used in place of the antimiR-122 probe, which is an antimiR probe targeted against a sequence non-existent miRNA sequence. The secondary antibody (alkaline phosphatase-linked Sheep anti-DIG, dilution 1:500 in antibody diluent) was then incubated at 37 °C for 32 mins. Chromogenic detection was performed using the BlueMap® kit as per the manufacturer's instructions. The substrate was allowed to develop for 6 h before counterstaining with Red Stain II for 4 mins. Slides were manually washed before mounting on laboratory-grade glycerol gelatin (Sigma-Aldrich, Buchs, Switzerland). Slides were scanned using a Nanozoomer 2.0-HT digital slide scanner (Hamamatsu photonics, Hamamatsu, Japan). Images were captured using NDP.view2 software (Hamamatsu photonics, Hamamatsu, Japan).

4.2.9 Expression analysis, statistical analysis and pathway mapping

Initial data processing was carried out using Expression Suite Software (Life Technologies, Foster City, USA) and Graph Pad Prism for statistical analysis, in which groups were compared using multiple t-tests followed by a Holm-Sidak correction for multiple comparisons. P values below 0.05 were considered as statistically significant. Data is expressed as mean fold change (FC) which denotes the mean fold difference of the score of the test group versus the control group. Pathway mapping was then carried out using Ingenuity Pathway Analysis Software (Qiagen, Venlo, Netherlands) in order to identify downstream targets of miRNAs in order to suggest functional outcomes of differentially expressed miRNAs. P values were developed in IPA from previous study data and mathematically predicated targets. RQ values denotes the log-transformed fold-difference to control.

4.3 RESULTS

4.3.1 CPS1, GS, CYP2E1 and PCK are expressed differentially in periportal and pericentral regions

Zone I and Zone III hepatic tissue was dissected using LCM from four healthy Sprague Dawley rats in order to assess differential RNA expression profiles between the two regions. The tissue was initially subject to analysis of mRNA expression through qPCR to examine the profiles of previously established zonally expressed genes, including *cyp2e1*, glycogen synthase (*gs*), phosphoenolpyruvate carboxyinase (*pck*) and carbamoyl-synthase 1 (*cps1*) (figure 4.1). As has previously been shown, *pck* and *cps1*, zone I markers, had their highest expression levels in zone I tissue (Bartels et al. 1993). Conversely, *cyp2e1* and *gs* were expressed at their highest in zone III.

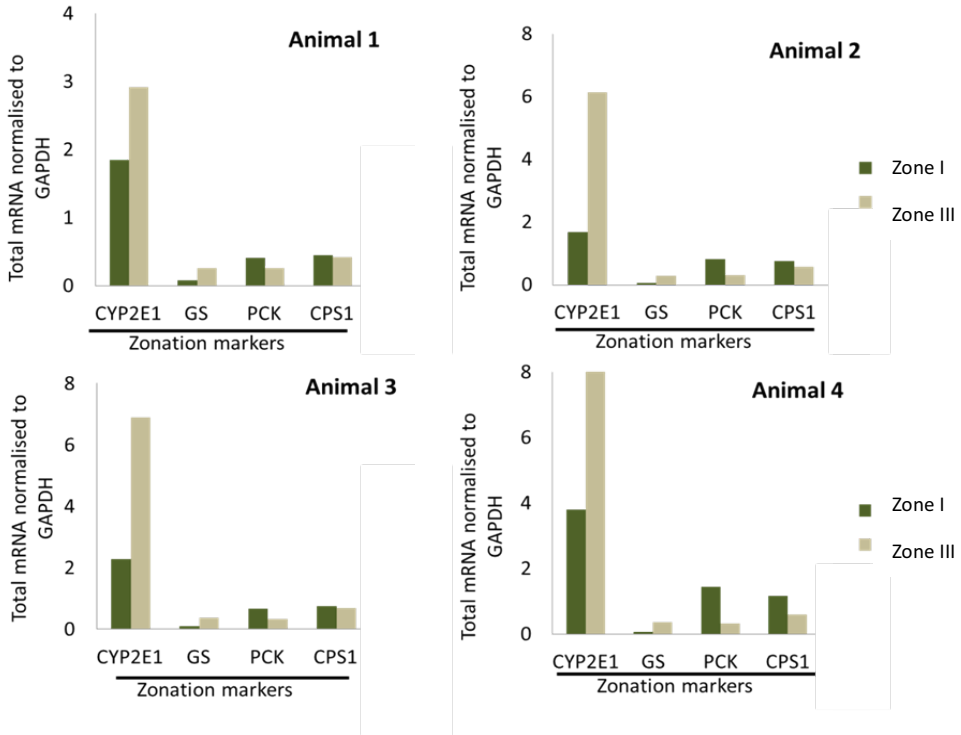

Figure 4.1 mRNA expression of zonally expressed genes from four individual animals

4.3.2 45 microRNAs are differentially expressed between pericentral and periportal regions of the liver in healthy Sprague Dawley rats

After confirmation of the correct expression profiles of previously characterised zonally expressed genes, thus confirming the correct dissection of zone I and III tissue, a global miRNA expression analysis was performed on both regions of the liver from four healthy (non-dosed) rats. Our miRNA analysis was able to detect 421 individual miRNA species detected in three or more rats from a specific region. Comparison of the profiles of both regions using a correlation analysis demonstrates that the miRNA profiles of either region highly correlate (Pearson $R = 0.923$; $p<0.001$). Importantly, several outliers can be seen on the correlation plot, suggesting the differential expression of some miRNAs (figure 4.2A). Volcano plot analysis confirms the significant differential expression of 45 microRNAs when zone III is compared to zone I (figure 4.2B). Analysis of the individual microRNAs which were found to be differentially expressed demonstrates that eight miRNAs are up-regulated in zone III, when compared to zone I, and 41 miRNAs are down-regulated (Figure 3). miR-671-3p is the most statistically significant up-regulated miRNA in Zone III ($p = 0.009$), whereas miR-203 is the most statistically significant down-regulated ($p = 0.0009$) (table 4.1). Three randomly selected miRNAs, miR-138, miR-16 and let-7f were then quantified using RT-qPCR in the same samples as those used in the above study in order to validate the results generated using miRNA arrays (figure 4.4). As was the case in the array data, miR-138 was expressed at higher levels in zone III, whereas miR-16 and let-7f were expressed at higher levels in zone I.

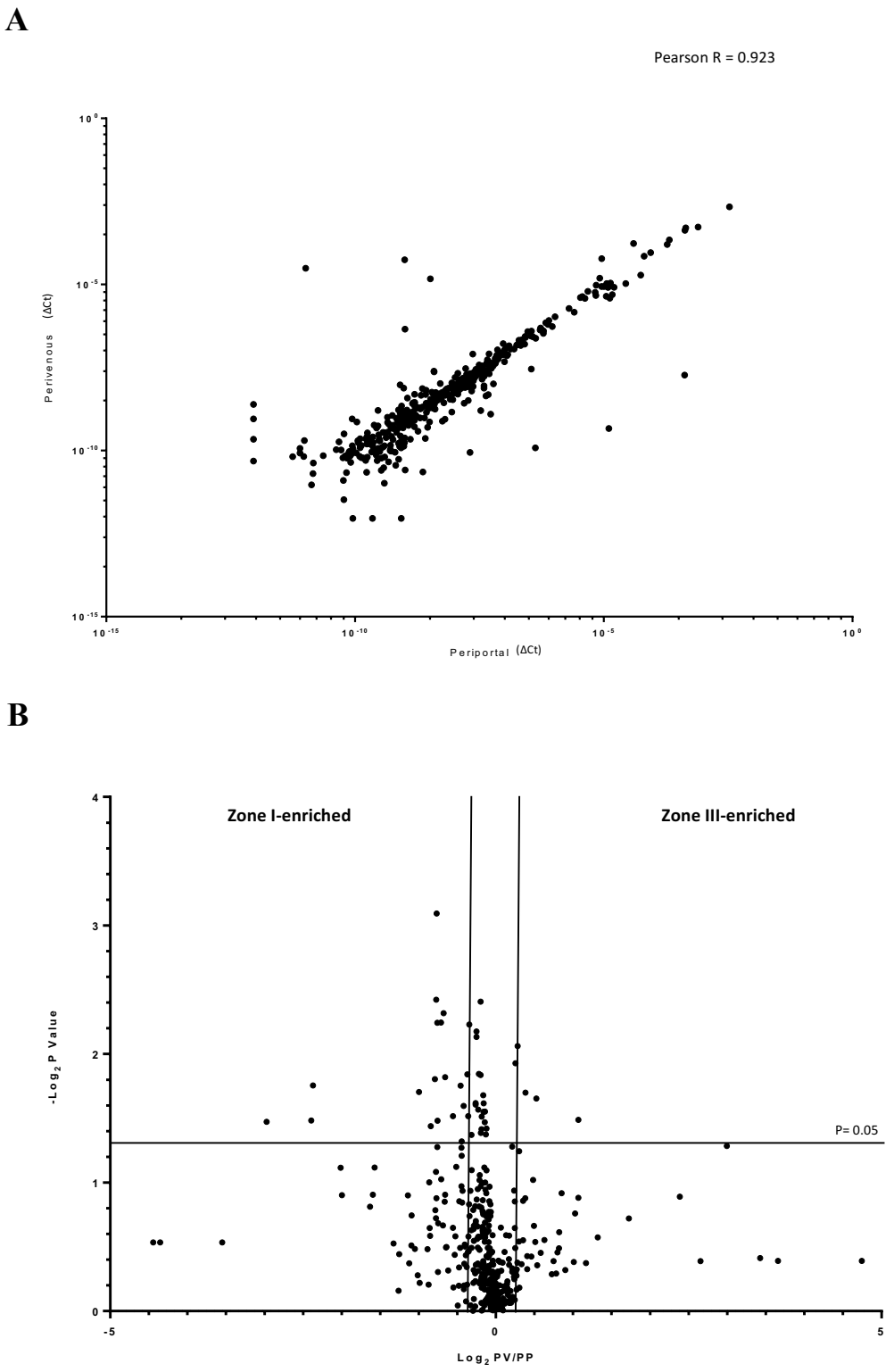

Figure 4.2 Comparison of hepatic microRNA expression between zone I, and zone III. A, Correlation of zone I and zone III microRNAs shows that the two profiles strongly correlate**. B,** Volcano plot analysis of zone I and zone III microRNA expression (zone III vs I) comparing negative log 2 p-value to log 2 fold-change to zone I, demonstrates that 45 miRNAs are significantly differentially expressed between the two regions ($p < 0.05$). Cut off lines denote a two-fold difference in expression level (vertical) and a negative log 2 p-value of 1.3 ($p = 0.05$, horizontal). Significantly different miRNAs fall above the horizontal cut-off line.

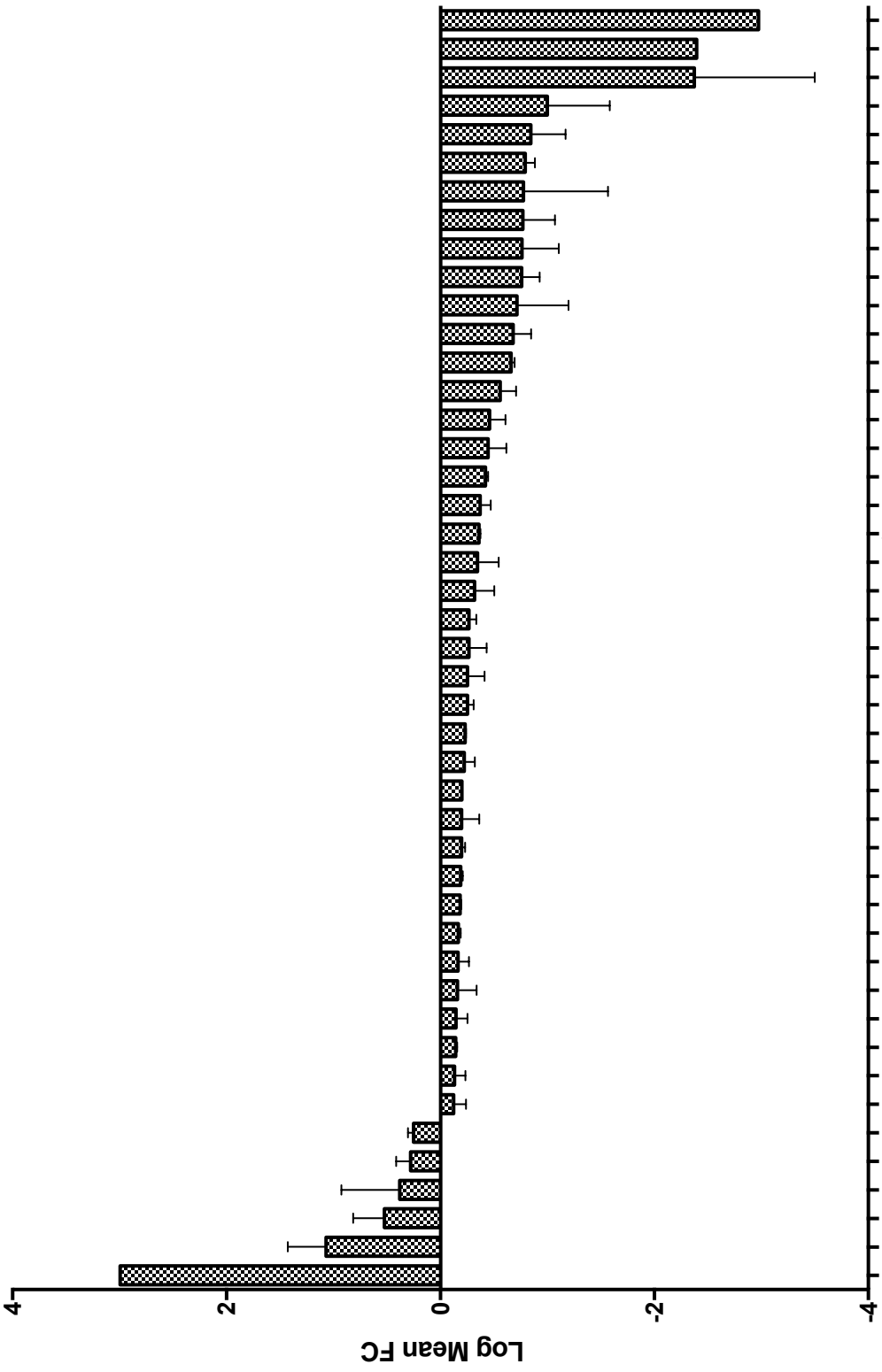

Figure 4.3 Statistically significant differentially expressed microRNAs identified by a global comparison of microRNA profiles in hepatic zone I and III (Expressed as fold-change, zone III/zone I).

Table 4.1. Statistically significant differentially expressed microRNAs identified by a global comparison of microRNA profiles in hepatic zone I and III. Expressed as fold-difference between miRNA expression zone III versus zone I. Red = highly expressed in specific zone, Orange = marginally overexpressed in specific zone compared to comparator zone, Green = under-expressed in zone compared to comparator zone.

Zone III>Zone I

Target Name	Mean fold-change	P value
mmu-miR-671-3p	1.9	0.009
mmu-miR-375	1.8	0.01
mmu-miR-139-3p	2.4	0.02
mmu-miR-1195	3.4	0.02
mmu-miR-1935	11.8	0.03
mmu-miR-211	990.9	0.05

Zone I>Zone III

Target Name	Mean fold-change	P value
mmu-miR-203	0.2	0.0009
mmu-miR-218	0.2	0.004
mmu-let-7b	0.6	0.004
rno-miR-547	0.2	0.005
*mmu-miR-31**	0.2	0.006
mmu-miR-184	0.2	0.006
rno-miR-146B	0.5	0.006
mmu-miR-99b	0.6	0.007
mmu-miR-16	0.6	0.007
snoRNA135	0.6	0.01
mmu-miR-335-3p	0.4	0.01
mmu-miR-30d	0.6	0.02
mmu-miR-129-3p	0.2	0.02
mmu-miR-183	0.2	0.02
mmu-miR-31	0.004	0.02
mmu-miR-215	0.3	0.02
mmu-miR-200c	0.1	0.02
mmu-let-7c	0.7	0.02
mmu-miR-15a	0.5	0.02
mmu-let-7d	0.7	0.02
mmu-miR-130a	0.5	0.03
mmu-miR-32	0.4	0.03
mmu-let-7a	0.6	0.03
mmu-miR-301b	0.7	0.03
mmu-miR-15b	0.7	0.03
mmu-let-7f	0.4	0.03
mmu-miR-802	0.3	0.03
mmu-miR-125b-5p	0.7	0.03
*hsa-miR-9**	0.004	0.03
mmu-miR-207	0.2	0.03
mmu-miR-23a	0.001	0.03
mmu-let-7e	0.7	0.03
mmu-miR-450a-5p	0.1	0.04
mmu-miR-101a	0.8	0.04
mmu-let-7i	0.7	0.04
mmu-miR-322	0.6	0.04
mmu-let-7g	0.7	0.04
mmu-miR-29a	0.5	0.04
mmu-miR-434-3p	0.4	0.05

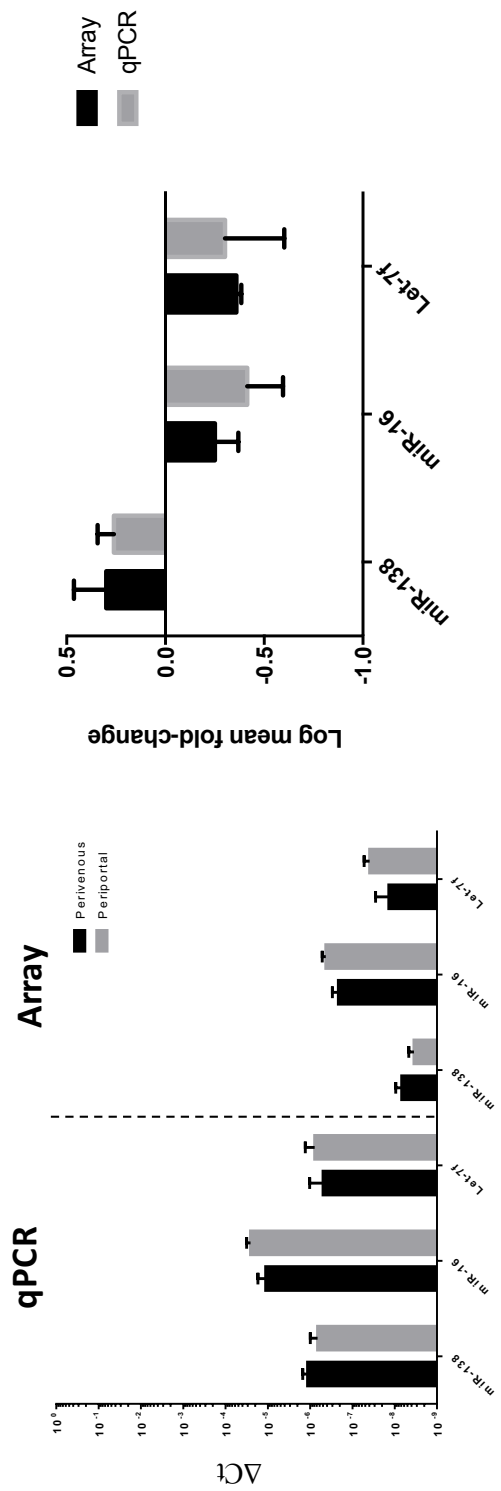

Figure 4.4 Validation of a random selection of statistically significant differentially expressed microRNAs using qPCR to compare against results generated from array cards.

4.3.3 Two microRNAs are present exclusively within zone I or zone III

Global miRNA analysis in zone I and zone III liver tissue from healthy rats was able to identify two miRNAs and one pre-cursor miRNA present exclusively within one zone of the liver (negligible level of detection in the other) (table 4.2). miR-211 ($p = 0.05$) was only detectable in zone III, whereas miR-23a ($p = 0.03$) and the precursor miRNA miR-9* ($p = 0.03$) were only detectable in zone I.

Table 4.2 MicroRNAs detected significantly in only one hepatic region

Zone III Specific

Target Name	Mean FC	P value
mmu-miR-211	990.9372	0.05

Zone I Specific

Target Name	Mean FC	P value
*hsa-miR-9**	0.004054132	0.03
mmu-miR-23a	0.001067765	0.03

**opposing strand of precursor-microRNA*

4.3.4 Six microRNAs target the mRNAs of well-characterised zonally expressed proteins

Differentially expressed miRNAs were subject to a target analysis using Ingenuity Pathway Analysis (IPA) and target scan to identify mRNA transcripts of known zonally expressed genes targeted by differentially expressed miRNAs from our analysis (table 4.3). A single up-regulated miRNA and five down-regulated miRNAs were found to be predicted to target six characterised zonally expressed genes. The genes were found to have roles in arginine degradation, xenobiotic metabolism signalling, the pentose phosphate pathway, glycerol degradation I and the TCA cycle II.

Table 4.4 Identification of differentially expressed microRNAs which target the mRNA transcripts of genes known to be expressed in a zonal. Fold-change (FC) represents the fold-difference in expression between zone I and zone III in healthy rats. Evidence is based on a ranking system of mild, moderate and highly predicted based on mathematical likelihood of each miRNA sequence targeted a mRNA species.

Target mRNA	miRNA ID	Mean fold-change	Evidence	mRNA function/pathway
Arg1	mmu-miR-218	-5.951	Moderate (predicted)	Arginine Degradation I (Arginase Pathway), Arginine Degradation VI (Arginase 2 Pathway), Citrulline Biosynthesis, Super-pathway of Citrulline Metabolism, Urea Cycle
Arg2	mmu-let-7f	-2.280	High (predicted)	Arginine Degradation I (Arginase Pathway), Arginine Degradation VI (Arginase 2 Pathway), Citrulline Biosynthesis, LXR/RXR Activation, Super-pathway of Citrulline Metabolism, Urea Cycle
Ahrr	mmu-miR-125b-5p	-1.521	High (predicted)	Aryl Hydrocarbon Receptor Signalling, Xenobiotic Metabolism Signalling
G6pd	mmu-miR-16	-1.778	Moderate (predicted)	Pentose Phosphate Pathway, Pentose Phosphate Pathway (Oxidative Branch)
	mmu-miR-138	1.624	High (predicted)	
Gk5	mmu-let-7f	-2.280	High (predicted)	Glycerol Degradation I
	mmu-miR-125b-5p	-1.521	High (predicted)	
	mmu-miR-138	1.624	High (predicted)	
Idh3a	mmu-miR-16	-1.778	High (predicted)	TCA Cycle II (Eukaryotic)
	mmu-miR-218	-5.951	High (predicted)	

Arg1 – arginase 1; *Arg2* – arginase 2; *Ahrr* – aryl-hydrocarbon receptor repressor; *G6pd* – glucose-6-phosephate dehydrogenase; *Gk5* – glucokinase 5 (***Not zonal at mRNA level; Katz et al, 1977***); *Idh3a* – isocitrate dehydrogenase 3A

4.3.5 Pathway analysis identifies the top canonical pathways regulated by differentially expressed microRNAs

Up-regulated and down-regulated microRNAs were then individually subject to a global mRNA target screen, followed by an analysis of their involvement in biological function and canonical pathways using Ingenuity Pathway Analysis (IPA, Qiagen, Venlo, Netherlands). In both of the individual analyses, the top statistically significant canonical pathway was shown to be the molecular mechanisms of cancer (table 4.4). The Wnt/β-Catenin pathway was found to be in the top ten canonical pathways perturbed by up- and down-regulated miRNAs (Zone I > Zone III = 8^{th}; Zone III > Zone I = 5^{th}). Other significantly perturbed pathways of interest include HGF signalling, STAT3, ERM/MAPK, TGF-B, PI3K/AKT (all I > III), PKA (Both I and III).

Table 4.5 Top 50 canonical pathways associated with differentially expressed microRNAs

PP>PV miRNA target pathways in PV		
Rank	Ingenuity Canonical Pathways	-log(p-value)
1	Molecular Mechanisms of Cancer	16.8
2	Axonal Guidance Signaling	14.7
3	HGF Signaling	11.0
4	STAT3 Pathway	10.5
5	Cardiac Hypertrophy Signaling	9.82
6	Glioblastoma Multiforme Signaling	9.75
7	Protein Kinase A Signaling	9.72
8	Wnt/β-catenin Signaling	9.34
9	ERK/MAPK Signaling	9.15
10	B Cell Receptor Signaling	8.96
11	PTEN Signaling	8.56
12	Glioma Signaling	8.35
13	Breast Cancer Regulation by Stathmin1	8.33
14	p53 Signaling	8.23
15	ErbB Signaling	8.04
16	IGF-1 Signaling	8.03
17	IL-8 Signaling	7.99
18	TGF-β Signaling	7.83
19	Mouse Embryonic Stem Cell Pluripotency	7.79
20	Chronic Myeloid Leukemia Signaling	7.66
21	Role of NFAT in Cardiac Hypertrophy	7.5
22	HER-2 Signaling in Breast Cancer	7.45
23	NGF Signaling	7.42
24	Regulation of the Epithelial-Mesenchymal Transition Pathway	7.38
25	Pancreatic Adenocarcinoma Signaling	7.35
26	SAPK/JNK Signaling	7.28
27	Signaling by Rho Family GTPases	7.21
28	Insulin Receptor Signaling	7.1
29	Colorectal Cancer Metastasis Signaling	7.01
30	Regulation of IL-2 Expression in Activated and Anergic T Lymphocytes	6.93
31	IL-6 Signaling	6.92
32	UVA-Induced MAPK Signaling	6.91
33	Prolactin Signaling	6.89
34	GDNF Family Ligand-Receptor Interactions	6.87
35	PEDF Signaling	6.87
36	Ephrin Receptor Signaling	6.79
37	EGF Signaling	6.5
38	Ovarian Cancer Signaling	6.48
39	LPS-stimulated MAPK Signaling	6.44
40	Protein Ubiquitination Pathway	6.44
41	RANK Signaling in Osteoclasts	6.41
42	FGF Signaling	6.41
43	p70S6K Signaling	6.4
44	UVB-Induced MAPK Signaling	6.4
45	PI3K/AKT Signaling	6.38
46	HIPPO signaling	6.29
47	FLT3 Signaling in Hematopoietic Progenitor Cells	6.24
48	Role of Osteoblasts, Osteoclasts and Chondrocytes in Rheumatoid Arthritis	6.14
49	Role of Macrophages, Fibroblasts and Endothelial Cells in Rheumatoid Arthritis	6.06
50	T Cell Receptor Signaling	6.06

PV>PP miRNA target pathways in PV		
Rank	Ingenuity Canonical Pathways	-log(p-value)
1	Molecular Mechanisms of Cancer	9.29
2	Ephrin Receptor Signaling	7.29
3	Axonal Guidance Signaling	7.22
4	Signaling by Rho Family GTPases	5.45
5	Wnt/β-catenin Signaling	4.97
6	Protein Kinase A Signaling	4.65
7	Regulation of the Epithelial-Mesenchymal Transition Pathway	4.44
8	RhoGDI Signaling	4.4
9	cAMP-mediated signaling	4.23
10	Ephrin B Signaling	4.04
11	G-Protein Coupled Receptor Signaling	4
12	Notch Signaling	3.92
13	Adipogenesis pathway	3.67
14	CXCR4 Signaling	3.48
15	p53 Signaling	3.44
16	RAR Activation	3.42
17	Phospholipase C Signaling	3.38
18	Colorectal Cancer Metastasis Signaling	3.37
19	Glioblastoma Multiforme Signaling	3.33
20	Semaphorin Signaling in Neurons	3.25
21	Cardiac Hypertrophy Signaling	3.22
22	Role of Macrophages, Fibroblasts and Endothelial Cells in Rheumatoid Arthritis	3.14
23	Thrombin Signaling	3.13
24	IL-8 Signaling	2.98
25	IL-1 Signaling	2.94
26	Sphingosine-1-phosphate Signaling	2.83
27	Melanocyte Development and Pigmentation Signaling	2.73
28	TR/RXR Activation	2.7
29	Chronic Myeloid Leukemia Signaling	2.64
30	Cellular Effects of Sildenafil (Viagra)	2.55
31	Circadian Rhythm Signaling	2.55
32	Basal Cell Carcinoma Signaling	2.47
33	GABA Receptor Signaling	2.47
34	Cell Cycle: G1/S Checkpoint Regulation	2.31
35	Agrin Interactions at Neuromuscular Junction	2.29
36	Calcium Signaling	2.27
37	Role of Osteoblasts, Osteoclasts and Chondrocytes in Rheumatoid Arthritis	2.26
38	Acute Myeloid Leukemia Signaling	2.25
39	RhoA Signaling	2.24
40	Leptin Signaling in Obesity	2.14
41	Relaxin Signaling	2.14
42	Ovarian Cancer Signaling	2.11
43	Reelin Signaling in Neurons	2.08
44	DNA Methylation and Transcriptional Repression Signaling	2.07
45	Angiopoietin Signaling	2.05
46	Role of NFAT in Cardiac Hypertrophy	2.03
47	GNRH Signaling	2.03
48	VEGF Signaling	2.02
49	Death Receptor Signaling	2.02
50	Neuroprotective Role of THOP1 in Alzheimer's Disease	2.01

4.3.6 The master zonation regulating pathway, the Wnt/β-Catenin pathway is targeted by nine differentially expressed microRNAs

Analysis of the top canonical pathways perturbed by up- and down-regulated miRNAs identified the Wnt/β-Catenin pathway as a top 10 significantly perturbed pathway in both of the individual analyses (table 4.4). Up-regulated miRNAs are defined as miRNAs with a significantly higher expression level in zone III when compared to zone I, conversely, down-regulated miRNAs are defined as those with a significantly lower expression in zone III when compared to zone I. To further examine the role of miRNAs in the Wnt/β-Catenin pathway, an mRNA target filter analysis was performed in order to identify individual mRNAs targeted (predicted or observed) by the differentially expressed miRNAs. Three up-regulated miRNAs (miR-138-5p, miR-1913 and miR-671-3p) were found to target 45 mRNAs (predicted) associated with the Wnt/β-Catenin Pathway, including WNT isoforms, SOX isoforms and CD44 (table 4.5 and figure 4.5). Six down-regulated miRNAs were found to target 109 mRNAs (13 experimentally observed, 96 predicted) associated with the Wnt/β-Catenin signalling pathway (table 4.6 and figure 4.6).

Table 4.6 Up-regulated miRNAs in zone III known or predicted to target genes associated with the Wnt/β-Catenin signalling pathway

ID	Mean FC	Symbol	Evidence
miR-138-5p	1.624	ACVR2A	High (predicted)
		ACVR2B	High (predicted)
		AKT3	Moderate (predicted)
		CD44	Moderate (predicted)
		DVL2	Moderate (predicted)
		DVL3	Moderate (predicted)
		EP300	Moderate (predicted)
		GNAO1	Moderate (predicted)
		MARK2	High (predicted)
		MDM2	High (predicted)
		PPARD	High (predicted)
		RARA	High (predicted)
		SOX12	High (predicted)
		SOX13	High (predicted)
		SOX4	High (predicted)
		SOX5	High (predicted)
		SOX7	Moderate (predicted)
		SOX8	Moderate (predicted)
		SOX9	High (predicted)
		TCF3	High (predicted)
		TCF4	High (predicted)
		WNT2B	Moderate (predicted)
miR-1913	2.000	ACVR1C	Moderate (predicted)
		AKT2	High (predicted)
		APC2	Moderate (predicted)
		CDH5	High (predicted)
		CSNK1D	Moderate (predicted)
		EP300	Moderate (predicted)
		FRZB	High (predicted)
		FZD9	Moderate (predicted)
		HNF1A	Moderate (predicted)
		KREMEN2	Moderate (predicted)
		LEF1	Moderate (predicted)
		RARA	Moderate (predicted)
		RARG	High (predicted)
		SMO	Moderate (predicted)
		SOX6	Moderate (predicted)
		SRC	Moderate (predicted)
		TAB1	High (predicted),Moderate (predicted)
		WNT3A	High (predicted)
		WNT4	Moderate (predicted)
		WNT8B	Moderate (predicted)
		WNT9B	Moderate (predicted)
miR-671-3p	1.910	WNT3A	Moderate (predicted)
		WNT5A	Moderate (predicted)

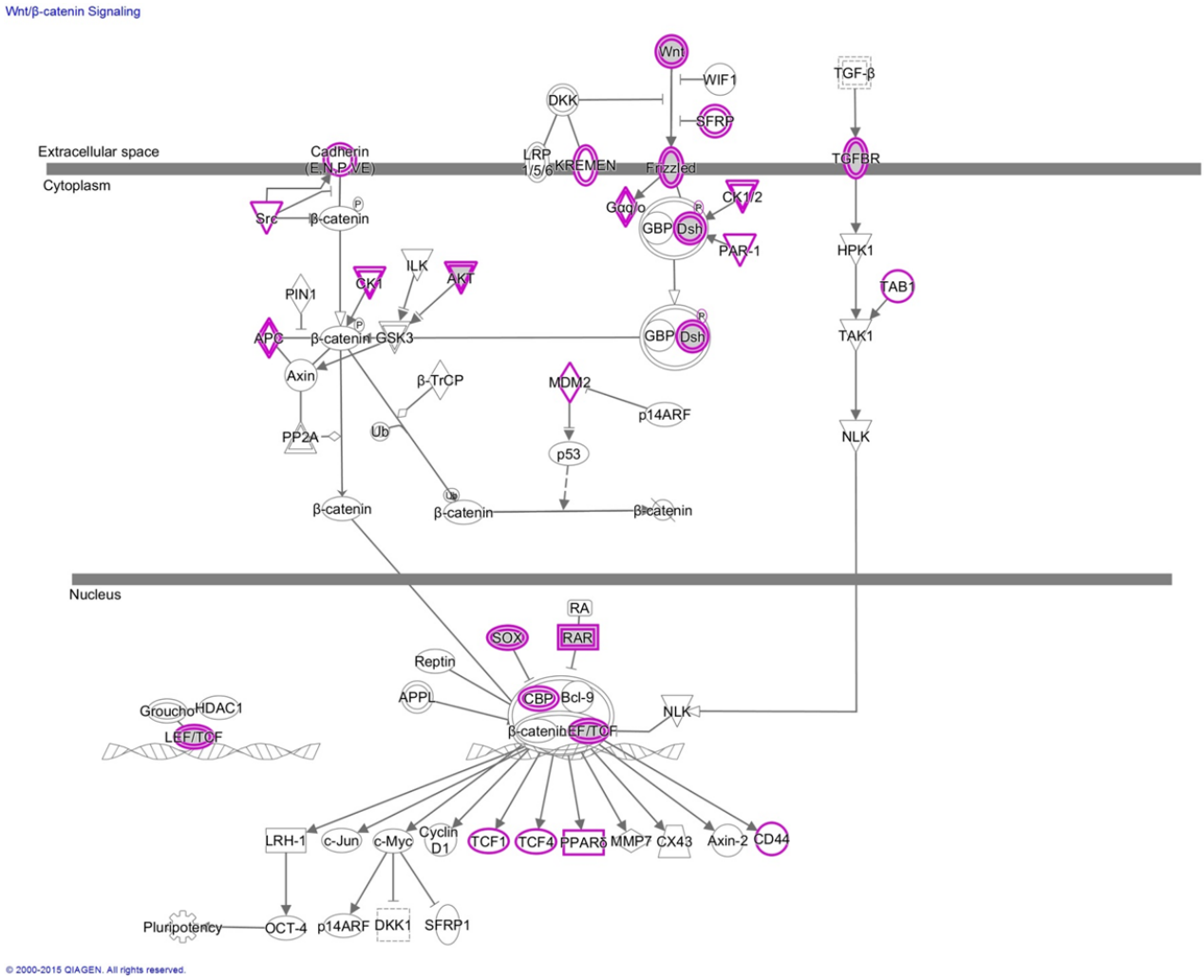

Figure 4.5. mRNA members of the Wnt/β-Catenin Pathway (highlighted in purple) targeted by miRNAs which were expressed at higher levels in zone III (in comparison to zone I) in healthy rats

Table 4.7 Down-regulated miRNAs in zone III known or predicted to target genes associated with the Wnt/β-Catenin signalling pathway

ID	Mean FC	Symbol	Evidence
mmu-let-7f	-2.280	ACVR1B	High (predicted)
		ACVR1C	High (predicted)
		ACVR2A	High (predicted)
		ACVR2B	High (predicted)
		AKT2	High (predicted)
		APC2	High (predicted)
		CCND1	Experimentally Observed, High (predicted)
		CDH1	Moderate (predicted)
		CSNK1D	Experimentally Observed
		DKK3	High (predicted)
		DVL3	High (predicted)
		FZD3	High (predicted)
		FZD4	High (predicted)
		KREMEN1	High (predicted)
		MYC	Experimentally Observed
		NLK	High (predicted)
		PPP2R2A	High (predicted)
		SOX13	High (predicted)
		SOX6	High (predicted)
		TGFBR1	Experimentally Observed,High (predicted)
		TGFBR3	High (predicted)
		TP53	High (predicted)
		WNT1	Experimentally Observed, High (predicted)
mmu-miR-125b-5p	-1.521	ACVR1C	High (predicted)
		APC	High (predicted)
		APPL1	Moderate (predicted)
		BMPR2	High (predicted)
		CDH12	Moderate (predicted)
		CDH5	Experimentally Observed,High (predicted)
		CDKN2A	Experimentally Observed
		CSNK1G1	High (predicted)
		CSNK2A1	High (predicted)
		DVL3	High (predicted)
		MARK2	High (predicted)
		PPP2CA	High (predicted)
		PPP2R1B	Moderate (predicted)
		PPP2R4	High (predicted)
		PPP2R5C	High (predicted)
		SFRP5	Moderate (predicted)
		SMO	Experimentally Observed
		SOX11	High (predicted)
		TLE3	High (predicted)
		TP53	Experimentally Observed,Moderate (predicted)
miR-129-1-3p	-4.551	BMPR2	Moderate (predicted)
		DKK2	Moderate (predicted)
		FZD10	Moderate (predicted)
		GJA1	Moderate (predicted)
		MAP3K7	Moderate (predicted)
		SOX10	Moderate (predicted)
		TGFBR3	Moderate (predicted)
miR-16-5p	-1.778	ACVR2A	High (predicted)
		ACVR2B	High (predicted)
		AKT3	High (predicted)
		AXIN2	High (predicted)
		BTRC	High (predicted)
		CCND1	Experimentally Observed,High (predicted)
		DVL1	Moderate (predicted)
		FRZB	Moderate (predicted)
		FZD10	High (predicted)
		FZD4	High (predicted)
		FZD6	High (predicted)
		JUN	Experimentally Observed
		LRP6	High (predicted)
		PPM1L	Moderate (predicted)
		PPP2R1A	High (predicted)
		PPP2R1B	Moderate (predicted)
		PPP2R5C	Experimentally Observed,High (predicted)
		RARB	High (predicted)
		SOX5	High (predicted)
		SOX6	High (predicted)
		TCF3	High (predicted)
		TGFBR3	High (predicted)
		TLE4	High (predicted)
		WIF1	Moderate (predicted)
		WNT3A	Experimentally Observed,High (predicted)
		WNT4	High (predicted)
		WNT5B	High (predicted)
		WNT7A	High (predicted)
miR-218-5p	-5.951	BCL9	High (predicted)
		CDH2	High (predicted)
		CSNK1E	High (predicted)
		DKK2	High (predicted)
		FZD4	High (predicted)
		GNAO1	High (predicted)
		GSK3B	High (predicted)
		MARK2	High (predicted)
		PPP2R2A	High (predicted)
		PPP2R2C	High (predicted)
		PPP2R4	High (predicted)
		PPP2R5A	High (predicted)
		RARA	High (predicted)
		SFRP2	High (predicted)
		SOX11	High (predicted)
		SOX5	High (predicted)
		SOX6	High (predicted)
		TCF4	High (predicted)
		TGFB2	Moderate (predicted)
		WNT2B	High (predicted)
miR-329-3p	-2.783	AKT2	High (predicted)
		AKT3	Moderate (predicted)
		BCL9	Moderate (predicted)
		BMPR2	High (predicted)
		BTRC	Moderate (predicted)
		CSNK1G3	High (predicted)
		CSNK2A1	High (predicted)
		H2BFM	Moderate (predicted)
		NLK	Moderate (predicted)
		PPP2R2C	High (predicted)
		SOX17	High (predicted)
		TCF7L1	High (predicted)
		WNT1	High (predicted)
		WNT3	High (predicted)

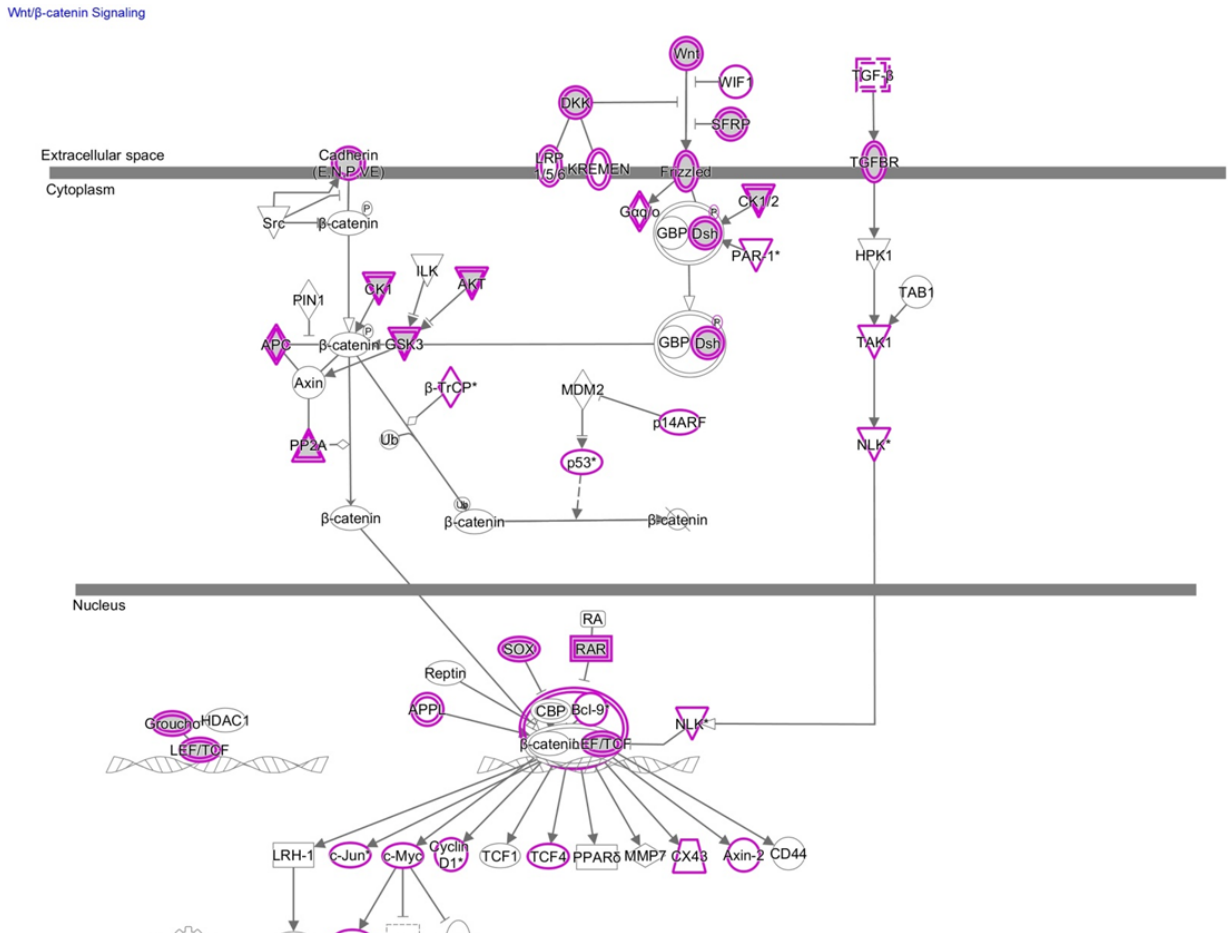

Figure 4.6. mRNA members of the Wnt/β-Catenin Pathway (highlighted in purple) targeted by under-expressed miRNAs in zone III (in comparison to zone I) in healthy rats

4.3.7 miR-122 is expressed at lower levels in zone III regions of the liver following paracetamol administration in rats

In order to assess whether previously seen elevations in circulating miR-122 during paracetamol-injury are a product of miR-122 loss from the liver, we profiled miR-122 individually using qPCR in zone I and zone III LCM-dissected liver tissue samples from rats administered with a toxic dose of paracetamol (1400 mg/kg), a sub-toxic dose (500 mg/kg) and vehicle for 24H (figure 4.7). MiR-122 expression was found to be significantly lower than control (vehicle zone III) in zone III of rats administered a high dose of paracetamol for 24 h (Control zone III vs 1400 mg/kg paracetamol zone III: $p<0.05$), with two out of the 5 rats measured displaying a lower response to paracetamol. Although not significant, zone I in the 1400 mg/kg dose rats, and both zone I and III in the low dose rats also displayed a varied level of response to paracetamol. *In situ* hybridisation of miR-122 in the livers of rats administered with 1500 mg/kg paracetamol for 48 h displays a marked loss of miR-122 from hepatocytes in zone III regions when compared to vehicle control, with little or no change in zone I miR-122 content (figure 4.8B).

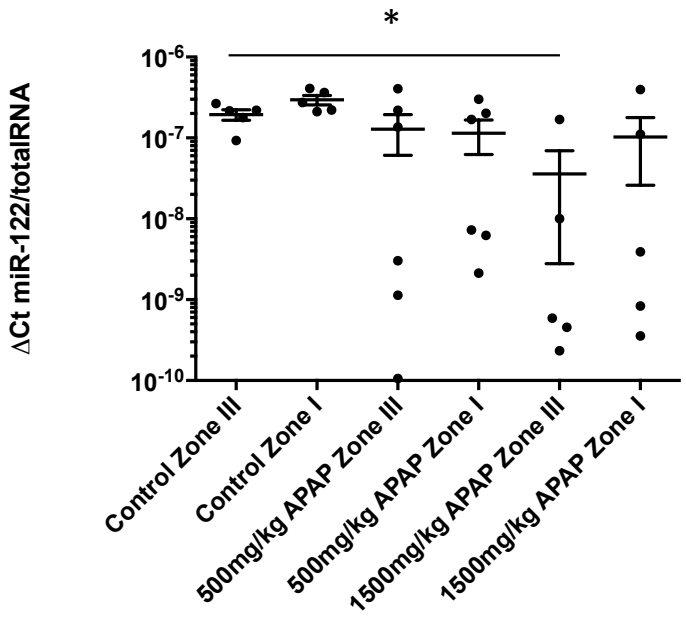

Figure 4.7 Zonal analysis of miR-122 expression basally, and after mild or toxic dose of paracetamol, expressed as ΔCt normalised to the total RNA loaded. Rats were administered either a low-dose (500 mg/kg) or a high-dose (1500 mg/kg) of paracetamol for 24 h, after which their livers were subject to LCM to excise zone I and zone III of the liver for analysis. MiR-122 levels were then measured in each zone and compared back to vehicle control animals. It was found that all paracetamol groups displayed a varied response to APAP, but only the high-dose zone III group showed a significant response to paracetamol ($p < 0.05$).

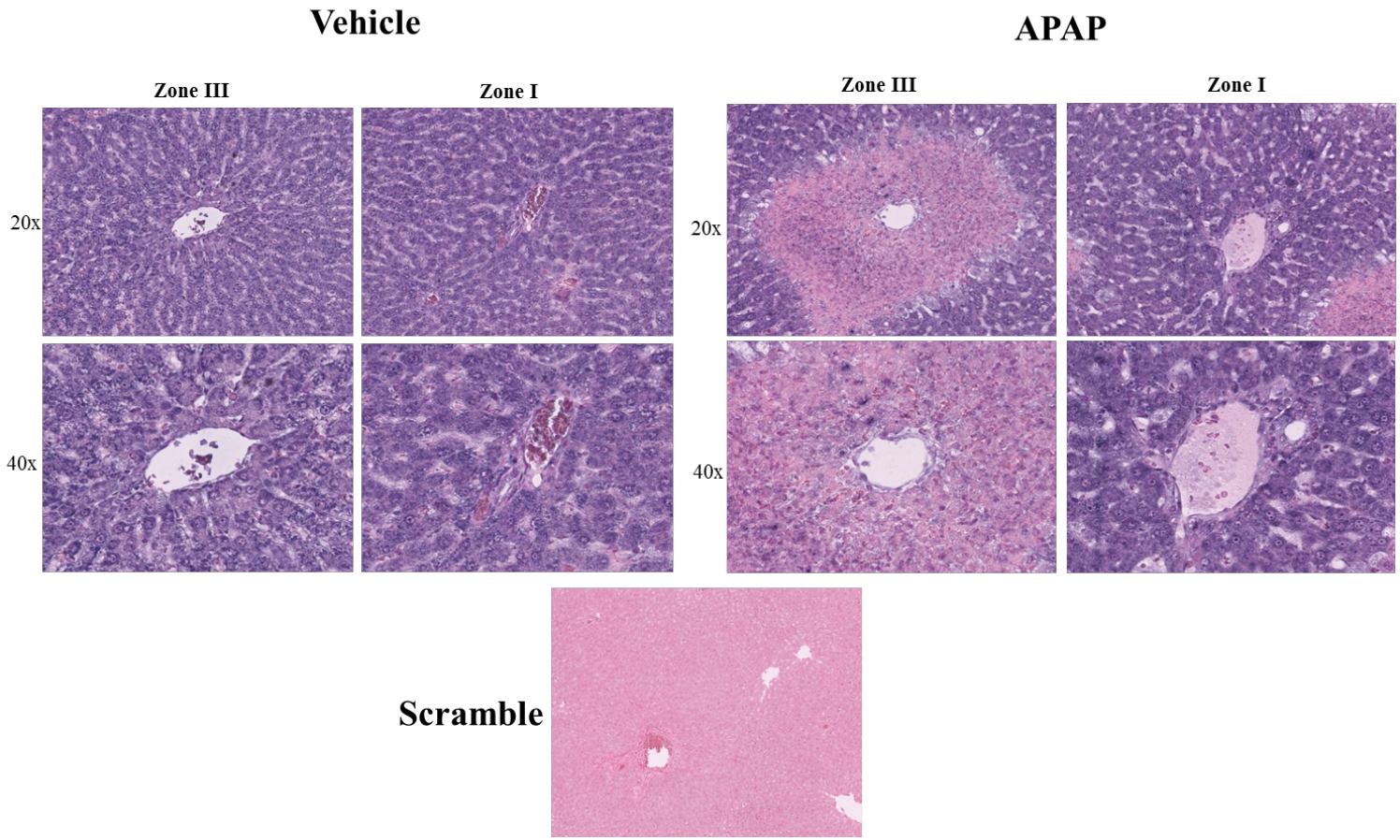

Figure 4.8 *In situ* hybridisation (ISH) of miR-122 in the liver of rats administered with vehicle or 1500mg/kg paracetamol for 48 h. ISH of zone I and zone III of the livers of rats administered 1500 mg/kg paracetamol for 48 h displays that miR-122 (purple stain) expression is decreased in zone III regions following paracetamol, when compared to control (vehicle). A scramble control targeting a nonsense miRNA sequence was used in order to assess that non-specific binding was not occurring during the staining process.

4.3.8 Differential changes in microRNA expression between zone I and III 24H after a toxic dose (1400mg/kg) of paracetamol

In order to assess whether paracetamol causes changes in the tissue expression of miRNAs other than miR-122, we performed a separate global miRNA analysis of hepatic zone I, and zone III (n = 4), 24 h after administration of 1400 mg/kg paracetamol. ALT levels were seen to significantly elevated at 24 h post-dose similar to the findings in chapter 3 (figure 4.9). Correlation analysis of all detected miRNAs (421) between zone I and zone III suggested that there was a lack of correlation between the miRNA profiles of the two zones after 24 h paracetamol (Pearson R = 0.005; p = 0.918) (figure 4.10A). MiRNA profiles in each region from paracetamol-dosed rats were then compared to profiles from the same region in healthy non-dosed rats. Analysis of changes in the miRNA profile caused by paracetamol in zone I, demonstrated that miRNAs were both up and down regulated after paracetamol, with a greater number being significantly up-regulated (figure 4.10B and C, figure 4.11A and B). Analysis of significantly changed ($p < 0.05$) miRNAs in zone I demonstrated that the expression of 43 miRNAs was changed, with 32 being up-regulated, and 11 being down-regulated. The same analysis of zone III demonstrates an even distribution of up- and down-regulated miRNAs when compared using a volcano plot. Expression analysis of significantly changed miRNAs demonstrates that the expression of 42 miRNAs was changed by paracetamol, with 22 being up-regulated, and 20 being down-regulated.

To gain a greater understanding of the consequences of the dysregulation of these miRNAs, we performed a pathway analysis using IPA (Qiagen, Venlo, Netherlands) on the significantly changed miRNAs from each zone (analysis was performed separately for each zone). miRNA target filter analysis suggested that the significantly deregulated miRNAs from zone I, and zone III targeted 1874 and 3562 mRNAs, respectively. Analysis of these mRNAs using the IPA tox functions analysis was then performed. miRNAs changed in zone I were found to target mRNAs involved in both liver proliferation (6 out of top 20 significant pathways), and liver damage (14 out of top 20). Those changed in zone III were found to target mRNAs

involved in liver damage/necrosis (15 out of top 20) and liver proliferation/hyperproliferation (5 out of top 20) (table 4.9).

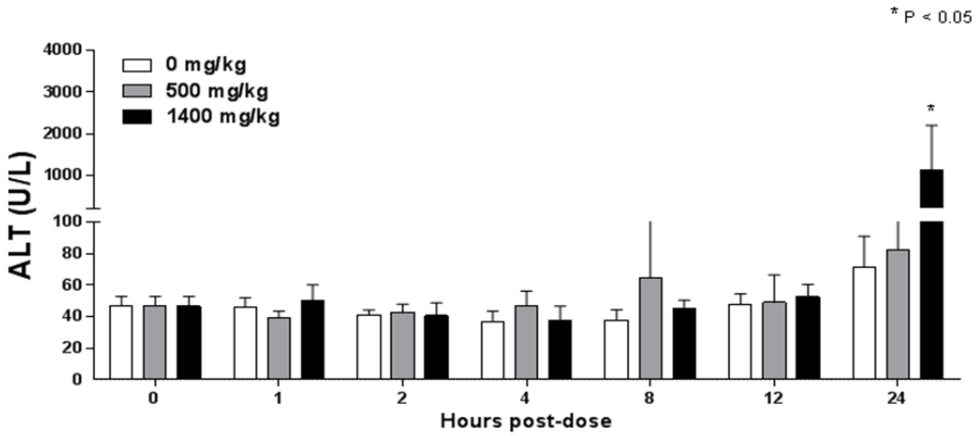

Figure 4.9. Plasma ALT activity in rats administered with vehicle, 500 mg/kg paracetamol or 1400 mg/kg paracetamol for up to 24 h

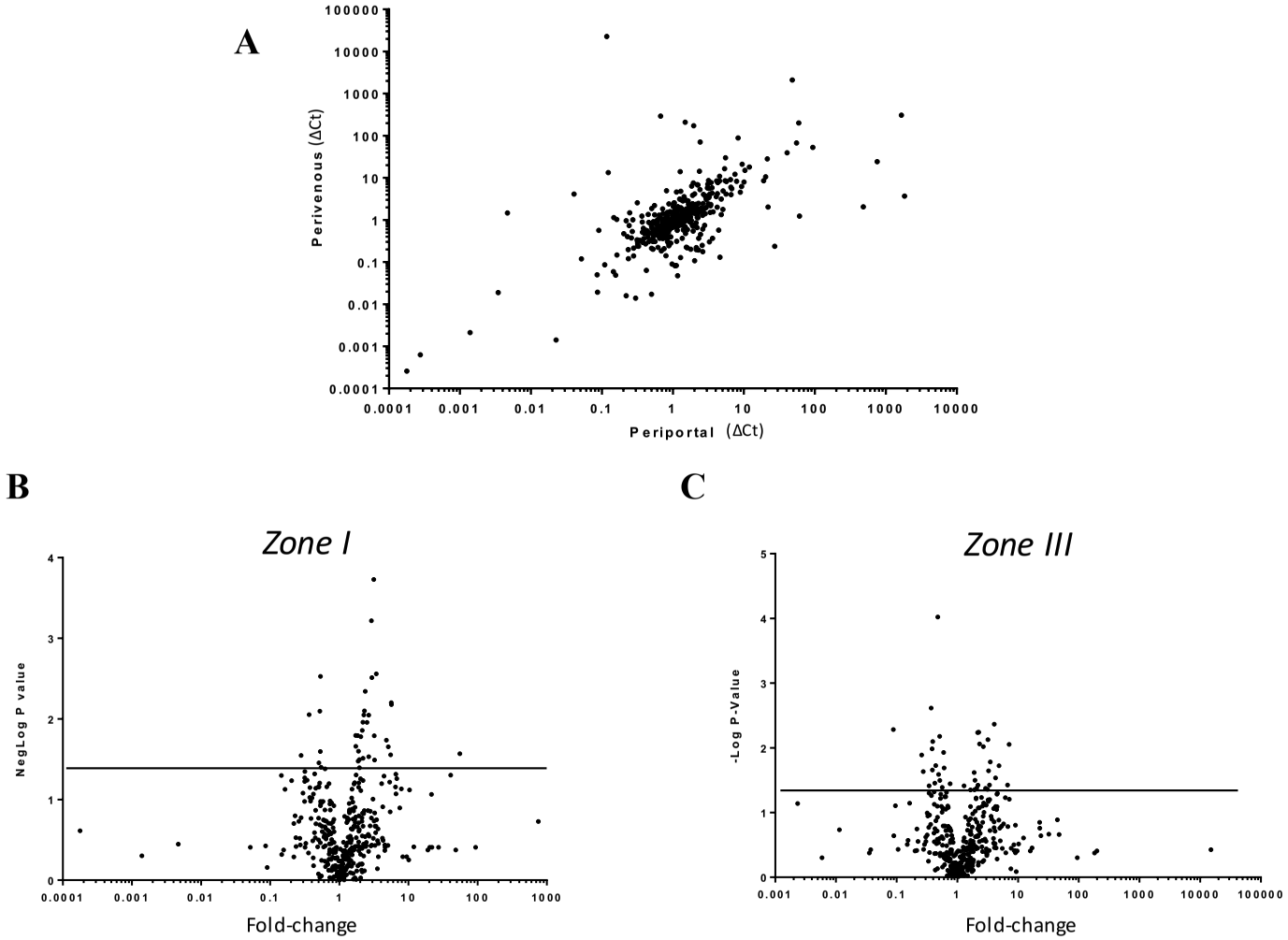

Figure 4.10 Global analysis of zonal changes in micrRNA expression after a toxic dose of paracetamol. A, Correlation analysis of zone I (ΔCt) and zone III (ΔCt) suggests that the global miRNA profiles do not correlate strongly after paracetamol. **B,** Volcano plot analysis of changes in zone I microRNA content (compared to healthy controls) demonstrates that the expression of 43 miRNAs is significantly changed after paracetamol. The horizontal cut-off denotes a negative log p-value of 1.3 (p = 0.05). **C,** Volcano plot analysis of changes in in zone III microRNA content (compared to healthy controls) demonstrates that the expression of 42 miRNAs is significantly changed after paracetamol

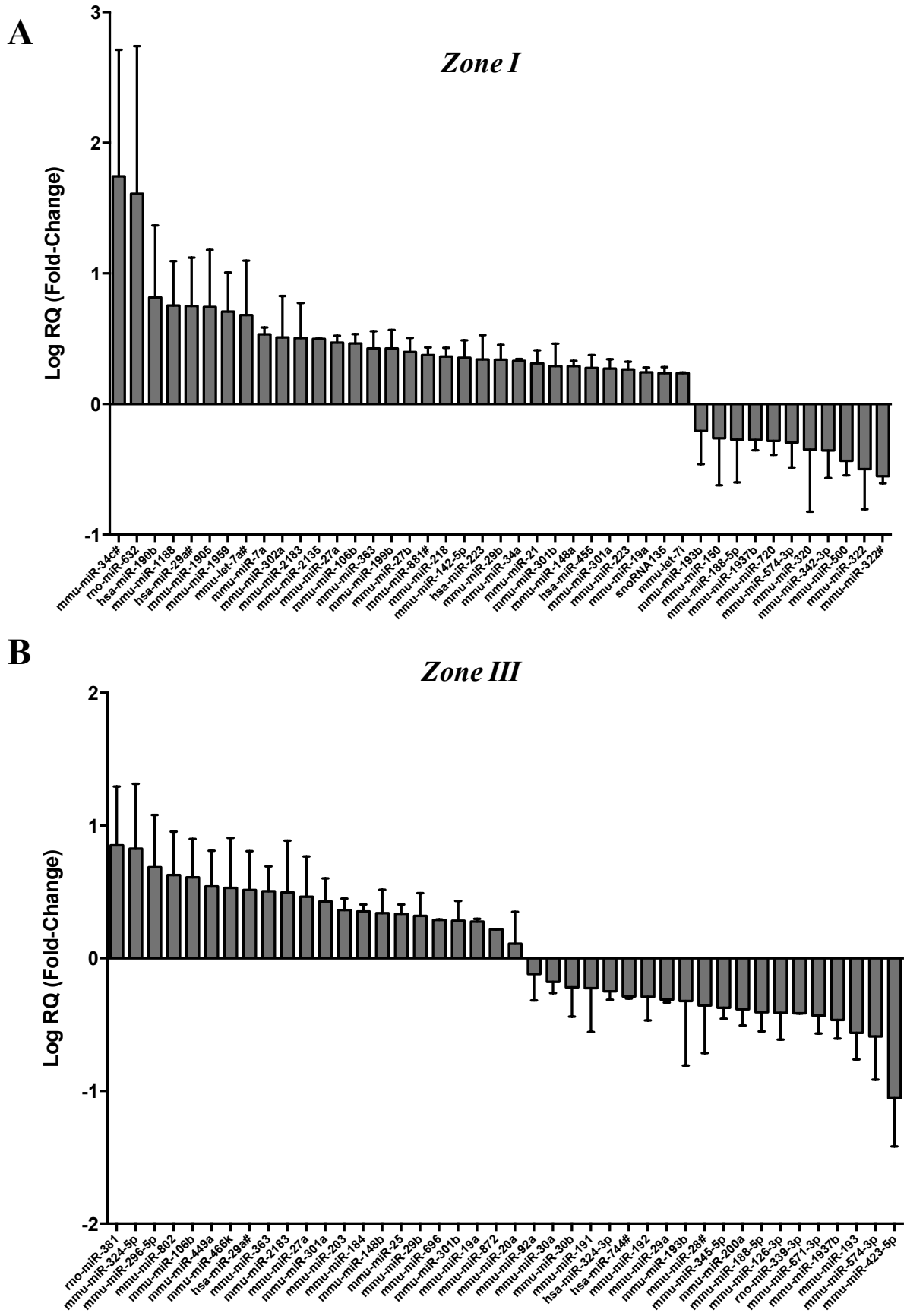

Figure 4.11 Global analysis of microRNA expression changes (expressed as log fold-change) in zone I (N=4) and III (N=5) after paracetamol administration demonstrates that 43, and 42 miRNAs are significantly changes in zone I and III, respectively.

Table 4.8 Global analysis of microRNA expression changes in zone I and III after paracetamol administration demonstrates that 43, and 42 miRNAs are significantly changes in zone I and III, respectively. MicroRNAs are ranked based on significance following a t-test with a multiple comparison correction. The colour scheme is representative of the log fold change value, with red denoting higher values and green denoting lower value.

Zone I

MicroRNA	Log mean FC	P-value
mmu-miR-2135	0.498284	1.87E-04
mmu-miR-106b	0.463169	6.07E-04
mmu-miR-7a	0.533233	0.002759
mmu-miR-188-5p	-0.27306	0.002972
mmu-miR-27a	0.469341	0.003077
mmu-miR-881#	0.374683	0.004546
hsa-miR-29a#	0.750349	0.006288
mmu-miR-1188	0.75397	0.006634
mmu-miR-218	0.363416	0.007951
mmu-miR-720	-0.28329	0.008011
mmu-miR-500	-0.43622	0.008864
mmu-miR-142-5p	0.35363	0.008946
mmu-miR-363	0.425581	0.008958
mmu-miR-29b	0.339467	0.010986
mmu-miR-27b	0.39882	0.011048
mmu-miR-34a	0.330143	0.013892
mmu-let-7i	0.235897	0.016067
mmu-miR-223	0.265513	0.016089
mmu-miR-2183	0.504251	0.016158
mmu-miR-21	0.311291	0.016605
mmu-let-7a#	0.680176	0.018392
snoRNA135	0.236505	0.021836
mmu-miR-1959	0.708225	0.022222
hsa-miR-455	0.275429	0.025206
mmu-miR-1937b	-0.27508	0.025429
mmu-miR-34c#	1.7426	0.027089
mmu-miR-1905	0.742131	0.02792
mmu-miR-322#	-0.5532	0.028365
mmu-miR-199b	0.424953	0.029477
hsa-miR-223	0.341687	0.030739
mmu-miR-148a	0.29057	0.031881
mmu-miR-302a	0.508629	0.032296
mmu-miR-301a	0.271173	0.033343
mmu-miR-574-3p	-0.29609	0.03513
mmu-miR-150	-0.26318	0.039712
mmu-miR-301b	0.290901	0.040429
mmu-miR-193b	-0.20752	0.041694
mmu-miR-322	-0.49954	0.044986
mmu-miR-342-3p	-0.35639	0.048106
mmu-miR-320	-0.35024	0.048386
hsa-miR-190b	0.815669	0.048529
mmu-miR-19a	0.243137	0.049696
rno-miR-632	1.609827	0.049935

Zone III

MicroRNA	Log mean FC	P-value
mmu-miR-193b	-0.32175	9.49E-05
mmu-miR-671-3p	-0.43143	0.002431
mmu-miR-106b	0.609032	0.004299
mmu-miR-423-5p	-1.05377	0.005229
mmu-miR-184	0.352014	0.005738
mmu-miR-25	0.334719	0.005808
mmu-miR-192	-0.29031	0.006656
mmu-miR-363	0.504574	0.007482
mmu-miR-188-5p	-0.40698	0.007999
mmu-miR-203	0.364351	0.008684
rno-miR-381	0.851833	0.00884
mmu-miR-301a	0.427693	0.009583
rno-miR-339-3p	-0.41512	0.010375
mmu-miR-191	-0.2252	0.011811
mmu-miR-574-3p	-0.58932	0.01288
mmu-miR-449a	0.542134	0.016489
mmu-miR-28#	-0.35547	0.018775
mmu-miR-296-5p	0.685784	0.018874
mmu-miR-30b	-0.21877	0.020515
mmu-miR-126-3p	-0.4115	0.022048
hsa-miR-29a#	0.514485	0.022691
mmu-miR-193	-0.56161	0.023265
mmu-miR-19a	0.276489	0.024145
mmu-miR-29a	-0.31054	0.025711
mmu-miR-802	0.627383	0.029205
mmu-miR-696	0.289174	0.031698
hsa-miR-744#	-0.2875	0.031968
mmu-miR-345-5p	-0.37249	0.035093
mmu-miR-92a	-0.11912	0.035934
mmu-miR-324-5p	0.826174	0.037468
mmu-miR-466k	0.529936	0.037604
mmu-miR-148b	0.340575	0.0377
mmu-miR-1937b	-0.46487	0.038669
mmu-miR-20a	0.109977	0.038691
hsa-miR-324-3p	-0.25007	0.040811
mmu-miR-29b	0.319012	0.0419
mmu-miR-27a	0.463916	0.042202
mmu-miR-2183	0.495618	0.043801
mmu-miR-301b	0.282612	0.04435
mmu-miR-872	0.217312	0.044732
mmu-miR-200a	-0.38353	0.047969
mmu-miR-30a	-0.17841	0.048714

Table 4.9 Significantly changed microRNAs in zone I and III are associated with toxicological functions identified by IPA, such as liver proliferation (highlighted green) and liver damage (highlighted red). Significantly perturbed miRNAs following APAP were analysed using a miRNA targetscan followed by a downstream Ingenuity Tox Functions analysis in order to identify toxicological pathways predicted to be affected by these miRNAs. Significance was based on the number of downstream molecules predicted to be targeted and the concentration of molecules in specific pathways associated with these toxicological functions. The Tox Functions analysis suggested in the case of both zone I and zone III that the most predicted toxicological functions to be occurring were liver hyperplasia, hyperproliferation, proliferation, necrosis and cell death.

Zone I

Categories	Diseases or Functions Annotation	p-Value	# Molecules
Liver Hyperplasia/Hyperproliferation	liver tumor	4.69E-25	592
Liver Proliferation	proliferation of liver cells	1.66E-24	65
Liver Hyperplasia/Hyperproliferation	liver cancer	1.36E-23	583
Liver Necrosis/Cell Death	necrosis of liver	2.71E-23	76
Hepatocellular Carcinoma, Liver Hyperplasia/Hyperproliferation	hepatocellular carcinoma	6.91E-23	566
Liver Steatosis	hepatic steatosis	1.74E-21	76
Liver Inflammation/Hepatitis	inflammation of liver	1.52E-19	76
Liver Necrosis/Cell Death	cell death of liver cells	5.31E-19	62
Liver Proliferation	proliferation of hepatocytes	6.12E-19	50
Liver Necrosis/Cell Death	apoptosis of liver cells	1.56E-16	50
Liver Necrosis/Cell Death	necrosis of liver parenchyma	1.74E-15	49
Liver Necrosis/Cell Death	cell death of hepatocytes	5.30E-15	48
Liver Necrosis/Cell Death	apoptosis of hepatocytes	1.65E-13	41
Liver Damage	damage of liver	6.86E-12	61
Liver Regeneration	regeneration of liver	9.82E-12	27
Liver Damage	injury of liver	1.42E-10	50
Liver Cirrhosis	Cirrhosis	1.68E-10	44
Liver Fibrosis	fibrosis of liver	2.01E-09	32
Liver Cirrhosis	cirrhosis of liver	2.91E-09	37

Zone III

Categories	Diseases or Functions Annotation	p-Value	# Molecules
Liver Proliferation	proliferation of liver cells	2.40E-28	88
Liver Necrosis/Cell Death	cell death of liver	6.58E-27	105
Liver Necrosis/Cell Death	necrosis of liver	1.56E-26	104
Liver Steatosis	hepatic steatosis	1.94E-26	108
Liver Proliferation	proliferation of hepatocytes	5.09E-25	72
Liver Inflammation/Hepatitis	inflammation of liver	8.99E-25	110
Liver Hyperplasia/Hyperproliferation	liver tumor	1.25E-24	890
Liver Hyperplasia/Hyperproliferation	liver cancer	1.97E-22	874
Hepatocellular Carcinoma, Liver Hyperplasia/Hyperproliferation	hepatocellular carcinoma	9.58E-22	848
Liver Necrosis/Cell Death	cell death of liver cells	1.18E-21	85
Liver Necrosis/Cell Death	apoptosis of liver	1.38E-19	70
Liver Necrosis/Cell Death	apoptosis of liver cells	2.45E-19	69
Liver Damage	damage of liver	2.06E-17	95
Liver Necrosis/Cell Death	cell death of hepatocytes	3.56E-17	66
Liver Necrosis/Cell Death	apoptosis of hepatocytes	1.31E-16	58
Liver Damage	injury of liver	1.62E-14	76
Liver Fibrosis	fibrosis of liver	4.31E-14	50
Liver Cirrhosis	Cirrhosis	4.88E-13	64
Liver Cirrhosis	cirrhosis of liver	3.94E-12	55

4.4 DISCUSSION

MiRNAs have been shown to be potential circulating markers of drug-induced liver injury, however, little is known about changes in the tissue content of miRNAs in the liver during injury. Therefore, we undertook a study to identify zonal miRNA changes in pericentral (zone 3) and periportal (zone 1) hepatocytes during paracetamol-induced injury in rats.

Initially, we aimed to establish baseline zonal miRNA expression profiles through performing a global miRNA expression analysis in four healthy non-dosed rats. Although, Yamaura *et al* (2014) had previously carried out a similar analysis, we felt their use of a single array for each group in the analysis limited the robustness of their study and created difficulties in our identification of statistically significant differentially expressed miRNAs between the liver regions. Therefore, we looked to repeat this analysis with adequate numbers for appropriate statistical analysis, to ensure robustness in our identification of zone-specific miRNAs.

Our global zonal miRNA analysis was able to detect 421 miRNAs which were identified in three or more rats in a single zone. Of these miRNAs we assessed that 45 were significantly differentially expressed between zone I and zone III, with 8 being up-regulated in zone III, and 41 being down-regulated. Similarly to Yamaura *et al*, we detected over 40 differentially expressed miRNAs, importantly however, only 9 of these miRNAs overlapped, and three of these had the opposite expression trend (miR-200c, miR-31*, miR-184). A possible explanation for this could be due to differences in study design, due to our study having multiple replicates allowing for statistical analysis and elimination of non-significant changes in miRNA expression. Another possible cause could be our choice of using fasted rats, whereas the previous study utilised fed rats. It has previously been established that blood content is a driver of many zonated processes, including gluconeogenesis and glycolysis; therefore, it is possible that miRNA expression is also affected by this. To account for this, we compared our differentially expressed miRNAs to a list of miRNAs generated in Yamaura's study which were altered in their comparison of fed and fasted rats. We found that 14 of our

45 differentially expressed miRNAs were altered in the previous study by fasting, suggesting that fasting may partially explain the discrepancies in results between the two studies (Table 4.10). Interestingly, this suggests that miRNA expression may be under the control of both environmental factors, such as food consumption, but could also be under the control of transcriptional mechanisms independent of external factors. It has previously been demonstrated that the zonal expression pattern of some proteins remains, even in conditions were the blood content was reversed between zone I and zone III, supporting that this may be also the case with miRNA expression (Tygstrup et al. 1962).

Table 4.10 Comparison of Yamaura *et al* (2014) to our study. MiRNAs detected in our study have been demonstrated to be regulated by feeding/fasting

	CDSS Study	Yamaura Study		
microRNA	Zone I or Zone III	Differentially expressed?	Affected by fasting in Zone I	Affected by fasting in Zone III
mmu-let-7b	Zone I	Zone I	Yes (Down-regulated)	
mmu-miR-31*	Zone I	**Zone III**		Yes (Down-regulated)
mmu-miR-99b	Zone I	**No**	Yes (Down-regulated)	Yes (Up-regulated)
mmu-miR-335-3p	Zone I	Zone I		Yes (Up-regulated)
mmu-miR-200c	Zone I	**Zone III**		Yes (Up-regulated)
mmu-let-7c	Zone I	Zone I	Yes (Down-regulated)	
mmu-miR-130a	Zone I	Zone I	Yes (Down-regulated)	
mmu-miR-301b	Zone I	**No**	Yes (Down-regulated)	
mmu-miR-125b-5p	Zone I	**No**	Yes (Down-regulated)	
mmu-let-7e	Zone I	**No**	Yes (Down-regulated)	
mmu-let-7i	Zone I	Zone I	Yes (Down-regulated)	
mmu-miR-29a	Zone I	**No**	Yes (Down-regulated)	Yes (Down-regulated)
mmu-miR-375	Zone III	**No**	Yes (Down-regulated)	Yes (Down-regulated)
mmu-miR-138	Zone III	**No**	Yes (Down-regulated)	

Another aim of our study was to identify zone-specific miRNAs that could provide use as biomarkers of zone-specific liver damage, as well as providing possible candidates for miRNA regulators of zonation. We were able to identify 3 molecules expressed in only one zone, miR-211, miR-23a and the precursor miRNA miR-9*. Although further validation is required in injury models of zone-specific injury, possibly comparing the zone III toxin paracetamol to the zone I toxin methapyrilene, these miRNAs offer potential use as mechanistic biomarkers of liver injury.

In order to assess the relevance of differential miRNA expression in the liver, we undertook pathway analysis of the significantly differentially expressed miRNAs in order to identify

possible biological pathways perturbed by these molecules, as well as specific mRNA targets. In our canonical analysis, 'the molecular mechanisms of cancer' was identified as the most significantly perturbed pathway. Although this is seemingly unrelated, this is not surprising as many miRNAs are commonly deregulated in cancer and therefore it is common for this type of analysis to identify this pathway as the most significant result, largely due to it being a heavily studied area. Importantly, the Wnt/β-Catenin pathway was identified in both our analysis of down-regulated microRNAs (in zone III) and up-regulated miRNAs in the top ten most perturbed pathways. The Wnt/β-Catenin pathway has previously been implicated as being the master transcriptional regulator of zonation within the liver in studies utilising beta-catenin and APC KO models to remove zonation from the liver (Benhamouche et al. 2006). This provided the first evidence that miRNAs may be implicated in the regulation of zonation, however it is also possible that their zonated expression is a product of this transcriptional pathway. In order to further elucidate the role of miRNAs in the Wnt/β-Catenin pathway within the liver, we performed a target filter search to identify potential downstream mRNA targets of the differentially expressed miRNAs in our study. This analysis identified 109 mRNA targets of 9 of the differentially expressed miRNAs, further suggesting that miRNAs may be involved in the regulation of this pathway. However, to fully understand the role of miRNAs in this pathway, studies must be undertaken to manipulate the levels of these miRNAs in order to establish a cause and effect relationship between these molecules and the potential mRNA targets.

Studies examining hepatic miR-122 concentrations following paracetamol-administration have thus far produced mixed results, with one suggesting that hepatic miR-122 content is decreased in paracetamol-injury (Wang et al. 2009), and one suggesting that this is not the case (Bala et al. 2012). One possible explanation for the findings in Bala et al (2012) is that total hepatic miR-122 was measured, however it is probable that miR-122 is only lost from hepatocytes in the area surrounding zone III, the area undergoing damage in paracetamol-injury. Therefore, measurement of total hepatic miR-122 may mask the magnitude of the

change in miR-122 levels within the liver. In order to resolve this, we aimed to both quantify and visualise hepatic miR-122 during paracetamol-DILI in specific regions of the liver, using both LCM followed by qPCR and *in situ* hybridisation of miR-122. Quantification of hepatic miR-122 levels in zone I and III demonstrates that there is a reduction of miR-122 in hepatic zone III of rats administered a toxic dose of paracetamol for 24 h. Interestingly, we also detected variable non-significant reduction of hepatic miR-122 after a high dose of paracetamol in zone I, and a low-dose of paracetamol in both zone I and III. This mixed response could be explained by inter-individual variation in the rats used and possible differences in the re-feeding patterns of the rats after fasting. To further confirm this reduction in zone III miR-122 levels, in situ hybridisation was performed on the livers of rats administered with a toxic dose of paracetamol (48 h). Even more clearly than our zonal qPCR analysis, we saw a marked loss of miR-122 from zone III areas after paracetamol, with no obvious loss of miR-122 in zone I regions. Therefore, through two different methods we have demonstrated that hepatic miR-122 is reduced during paracetamol-injury.

After establishing that miR-122 levels change within the liver following paracetamol in a zonal manner, we aimed to examine whether the expression of other miRNAs were also altered following a toxic dose of paracetamol. We hypothesised that miRNAs would be lost indiscriminately from zone III due to the ongoing necrosis and breakdown of cells, whereas miRNA levels in zone I would be altered as a possible adaptive response to the ongoing damage in zone III. In order to do this, we performed a global microRNA profiling experiment on hepatic zone I and III of rats administered 1400 mg/kg paracetamol, and then compared these expression profiles back to those found in healthy non-dosed controls. Comparison of the miRNA profiles in zone I and zone III from rats administered with paracetamol suggested that there was little correlation between the two global profiles, in contrast to that of healthy controls, in which both were found to be highly correlative. This suggested that, as expected the zones were responding differently to paracetamol-treatment. When a comparative analysis was carried out between zones in paracetamol-dosed and healthy rats, we found that 43 and

42 miRNAs were changed significantly in zone I, and zone III respectively. It is interesting that an almost equivalent number of miRNAs were changed in zone I, as in zone III, despite no injury occurring in this area, suggesting that living cells in this region are responding to the damage ongoing in zone III. We found that the majority of miRNAs in zone I were up-regulated (32 out of 43), further confirming that these expression changes were not due to necrotic damage and were due to an active response from the cells. When a downstream analysis was performed using IPA, examining the mRNA targets of these miRNAs, we found that the top three functions associated with targets were liver hyperplasia/hyperproliferation, liver proliferation and liver necrosis. This suggests that although there are functions associated with toxicity occurring, the most significant functions occurring in zone I at this point are proliferative, suggesting that this region may be adapting to paracetamol. Analysis of zone III miRNA expression changes after paracetamol demonstrated that 22 out of 42 miRNAs were down-regulated, which fits with the hypothesis that large-scale necrosis would cause a loss of miRNA from this region of the liver. However, the finding that 20 miRNAs were up-regulated was less expected, which suggests that there is some form of transcriptional response to the injury in this region. This is reflected when IPA was used to examine the top Tox Functions occurring in this region. The most significant function occurring in this region was found to be liver proliferation, with the second and third being cell death, and necrosis, suggesting that although widespread damage is occurring, so is an adaptive response to this.

This suggests that a form of adaptation is occurring in unaffected regions of the liver, which may be as a response to compensate for the loss of zone III hepatocytes. These findings from both our study and the Yamaura study led us to generate two hypotheses for further investigation. First, that damaged hepatocytes in zone III have elicited this response in zone I hepatocytes through cell-cell signalling. Studies previously mentioned in chapter 3 have highlighted the complexity of cell-cell signalling through exosomal transport, which is just a single form of cell-cell communication. This was further highlighted by a study which demonstrated that hepatocyte-derived exosomes were able to longitudinally transfer RNA to

hepatic stellate cells, eliciting increased expression of nitric oxide synthase 2 (Royo et al. 2013), and another which suggested that mice undergoing ischemia/reperfusion treated with hepatocyte-derived extracellular vesicles, demonstrated a higher level of hepatocyte proliferation (Nojima et al. 2014). Therefore, it is possible that stressed hepatocytes in zone III may use this form of cell-cell communication in order to produce an adaptive response in other cells in zone I. Further work could be performed utilising exosome release-blocking agents, such as manumycin-A (Mittelbrunn et al. 2011) in order to assess the role of exosomal cell-cell signalling on microRNA expression in zone I, to fully understand whether this is part of an adaptive response in the liver. Our second hypothesis was that these changes in miRNA expression are driven directly by paracetamol in zone I hepatocytes, but due to zonal gene expression, zone I hepatocytes are not damaged, while zone III hepatocytes are. In paracetamol injury, hepatocytes in zone I will be similarly exposed to the same dose of paracetamol, as those hepatocytes in zone III. However, they are not susceptible to injury due to decreased CYP2E1 expression, and increased GSH expression. However, it may be possible that the parent-drug may elicit a form of active response. The role of the parent compound may be established using analogues of paracetamol, such as AMAP, which have previously been used to examine the role of covalent binding in paracetamol-toxicity (Qiu et al. 2001).

In summary we have evaluated zonal profiles of miRNAs within the liver, identifying potential candidates for use as zonal biomarkers, we have established that miR-122 is lost from the liver during paracetamol-DILI, and we have found global miRNA profiles also change differentially between the zones after paracetamol. Further work should aim to validate these findings using simpler qPCR-based methods, followed by functional work to examine the role of these identified microRNAs in the regulation of zonation. Also, in order to validate the use of potential zone-specific miRNA biomarkers, work should now be performed using models of zonal injury, such as the comparison of paracetamol and methapyrilene toxicity in order to assess whether the expression of these markers is changed in the circulation in the correct pattern following injury. It will also be critical for these markers to undergo assessment in

human liver tissue in order to establish, first, that these miRNAs are present in humans and second, that they are expressed in a similar zonal manner.

CHAPTER 5

ISOLATION OF MOUSE BILIARY EPITHELIAL CELLS FOR GLOBAL MICRORNA ANALYSIS AND CANDIDATE BIOMARKER IDENTIFICATION

5.1 INTRODUCTION

The biliary system is responsible for the production of bile components, and the transport of bile into the duodenum. Biliary epithelial cells (BEC), which comprise of 3-5% of the total hepatic cell count, form the three-dimensional structure of the bile ducts which span from small intrahepatic bile ducts, through to the large extra-hepatic bile duct network (Sherlock 1998). BEC are a heterogeneous species which range from small-BEC, which line the intrahepatic bile ducts, to large BEC which form the extra-hepatic bile duct network (Kanno et al. 2000). BEC are susceptible to injury caused by a number of toxins, including flucloxacillin (Lakehal et al. 2001), 5-fluorodeoxyuridine (Hohn et al. 1985) and fenofibrate (Hajdu et al. 2009). BEC are differentially susceptible to drug-induced liver injury (DILI), with small BEC being prone to 'vanishing bile duct syndrome' (VBD) (Desmet 1997; Strazzabosco et al. 2000), and large BEC being prone to direct drug-induced damage leading to cholestasis (Alpini et al. 1996; Lazaridis et al. 2004; Strazzabosco et al. 2000). VBD is characterised by the progressive, permanent loss of the intrahepatic bile duct structure, leading to long-term cholestasis (Desmet 1997). Small BEC also possess a high level of plasticity and are able to transdifferentiate into periportal (zone 1) hepatocytes, suggesting their importance in hepatocyte regeneration after injury (Limaye et al. 2008; Watanabe et al. 2008).

Current circulating biomarkers of bile duct injury and cholestasis include alkaline phosphatase (ALP), γ-glutamyl transferase (GGT), and total bilirubin (T-BIL) (Dufour et al. 2000; Nishio et al. 2000; Ramaiah 2007). Each of these markers suffers from either a lack of specificity, possibility of false positives, or a lack of prognostic value. Therefore, new candidate biomarkers which are specific to BEC, and can be demonstrated to have prognostic value would be of great use in the diagnosis of bile duct injury and cholestasis, both in the clinic, and in drug development. MicroRNAs have previously demonstrated potential as biomarkers drug-induced liver injury, with miR-122 specifically being shown to be a prognostic, specific and sensitive marker of hepatocellular necrosis in paracetamol-, heparin- and alcohol-induced liver injury (Antoine et al. 2013b; Starkey Lewis et al. 2011). Other work has demonstrated

that miR-122 is not the only organ-enriched miRNA, with others such as miR-1 (heart), let-7i (brain) and miR-194 (kidney) being enriched in other organs (Ai et al. 2010; Balakathiresan et al. 2012; Sharkey et al. 2012). Therefore, we hypothesised that BEC may be enriched in specific miRNAs, which may have potential as circulating biomarkers of bile duct injury. To examine the potential of miRNAs as biomarkers of BEC/bile duct injury, and also whether miRNA profiles in both hepatocytes, and BEC can be linked to the overall function of these cell types, we isolated each cell type and performed a global microRNA profiling analysis in order to elucidate the basal microRNA profiles of these cell types. We then sought to identify miRNAs which were enriched in BEC over hepatocytes for future validation as potential bile duct injury biomarkers.

5.2 METHODS

5.2.1 Animals

The protocols described within this thesis were performed by personal licence holders according to the regulations defined within the project licence granted under the Animals (Scientific Procedures) Act 1986 and approved by the University of Liverpool ethics committee. CD-1 mice were purchased from Charles River (Manston, UK) or Harlan and housed at a constant temperature and humidity with free access to food and water. Mice were allowed to acclimatise for at least 7 days before any experimental procedure and were kept in a 12-hour light/dark cycle (Lights on: 08:00/Lights off: 20:00).

5.2.2 Isolation of hepatocytes from mouse liver

Hepatocytes were isolated by a modified two-step collagenase perfusion method, as previously described in Li et al. (2010). Briefly, mice were anaesthetised using pentobarbital (1 µL/g), after which a V-shaped transverse incision was made on the abdomen to reveal the intestinal cavity. The intestines were then moved to the left to reveal the hepatic portal vein and vena cava. A small clamp was then used to close the hepatic artery and the hepatic portal vein was cannulised using an 18 G winged catheter. The liver was then perfused for 9 minutes using a wash buffer (10x Ca^{2+}-free Hanks Balanced Salt Solution, 5.8 mM HEPES, 4.5 mM $NaHCO_3$) to remove circulating blood before being digested by digestion buffer (wash buffer, 0.05% w/v collagenase, 0.068% w/v trypsin inhibitor, 5 mM $CaCl_2$) for 5 minutes. Following the digestion, the liver was excised into a petri dish, washed with wash buffer and the liver capsule was disrupted using blunt forceps to release the digested cells. The cell suspension was then filtered through a 100 µm cell strainer to remove the vasculature resulting in a mixture of parenchymal and non-parenchymal cells.

The cell suspension was centrifuged to pellet hepatocytes (30 g for 2 minutes at 4 °C). The hepatocyte pellet was then re-suspended in wash buffer and the centrifugation step was repeated to pellet the hepatocytes. This step was twice repeated before cells were counted and

viability was assessed using a trypan blue exclusion method (20 µL trypan blue: 100 µL cells). Only isolations with a viability of above 85% were used for experiments. Hepatocytes were then pelleted (30 g for 2 minutes at 4 °C) and re-suspended in 700 uL of Qiazol for RNA analysis.

5.2.3 Isolation of mouse biliary epithelial cells

A mouse hepatocyte isolation was first performed (see above). The remaining liver capsule and vascular bed (minus hepatocytes) was retained, and finely diced using a scalpel. The diced tissue was then suspended in a collagenase solution (1 g/L collagenase type A, Roche, Switzerland in RPMI medium, Sigma Aldrich) for 1 h. The digested tissue was then pelleted by centrifugation (500 g for 5 min), and re-suspended in a cell dissociation medium (800 mg/L Trypsin in 1x PBS) for 20 min. The dissociated cell solution was then passed through a 22 G needle three times and incubated with a monoclonal antibody targeted at epithelial cell adhesion marker (EPCAM, 1 µL/mL, Abcam, Cambridge, UK) for 1 h (37 °C). The cell solution was then incubated with Dynabeads (Life Technologies, CA, USA) coated with sheep anti-rabbit monoclonal secondary antibodies (1 h, 4 °C). The solution containing BEC bound to Dynabeads was then subject to a magnetic field to remove contaminants, followed by washing with 1x PBS (repeat 5x). The purified BEC bound to Dynabeads were then suspended in 700 µL Qiazol (Qiagen, Venlo, Netherlands) or 1x PBS.

5.2.4 Determination of Total Protein Concentration of Samples

Total protein concentration was determined as described in previous chapters.

5.2.5 Immunoblotting and immunohistochemistry

Immunoblotting and immunohistochemistry was performed as described in chapter 2 using antibodies targeted against epithelial cell adhesion marker (EPCAM; Abcam ab32392; 1 h at 1:5000), keratin-19 (K-19; Abcam ab52625; 1 h at 1:10,000), γ-glutamylcysteine ligase catalytic subunit (GCLC; Abcam ab41463; 1 h at 1:10,000), albumin and cytochrome P450

2E1 (cyp2e1; Abcam ab28146; overnight at 1:5000). Antibodies were then incubated with their corresponding species of horseradish peroxidase conjugated secondary antibody for 1 h at a dilution of 1:10,000.

5.2.6 miRNA extraction and purification

miRNA was extracted and purified using the method described in Chapter 3.

5.2.8 Global microRNA quantification in BEC and Hepatocytes

A global microRNA analysis was performed on isolated BEC and hepatocytes using the Agilent microRNA hybridisation array platform, as per the manufacturer's guidelines (Agilent Biosystems, CA, USA).

5.2.9 Expression analysis, statistical analysis and pathway mapping

Initial data processing was carried out using GeneSpring (Agilent), or using the R^2-based AgiMicroRna software (Bioconductor) and Graph Pad Prism for statistical analysis. Groups were compared using multiple t-tests followed by a Bonferroni multiple comparisons correction, with significance being set at $p < 0.05$. Pathway mapping was carried out using the Ingenuity Pathway Analysis Software (Qiagen, Venlo, Netherlands) miRNA targetscan method.

5.3 RESULTS

5.3.1 A modified to two-step perfusion method, followed by antibody purification is able to produce a pure population of BEC and hepatocytes

To validate the anti-*Epcam* antibody selected for BEC immunoprecipitation (IP), immunohistochemistry was performed on sections of healthy mouse liver tissue using this antibody (figure 5.1A). The sections clearly display areas of staining (brown stain) surrounding the large bile ducts in the portal region of the liver, and also staining within the tissue surrounding hepatocytes, suggesting the detection of intrahepatic BEC. Upon successful validation of the IP antibody, BEC and hepatocytes were isolated from CD-1 mice using a modified two-step collagenase perfusion method, followed by characterisation. Analysis of the BEC markers, *Epcam* and keratin-19 (*k-19*) demonstrated that these markers were enriched in isolated BEC lysates, and not detectable in hepatocyte lysates (figure 5.1B). Conversely, the hepatocyte markers, albumin and glutamate-cysteine ligase, catalytic-subunit (*Gclc*), were enriched in hepatocytes over BEC. Analysis of *cyp2e1*, a member of the cytochrome P450 family demonstrated that this marker was expressed at higher levels in hepatocytes, with a low-level of expression in BEC (figure 5.1B).

A

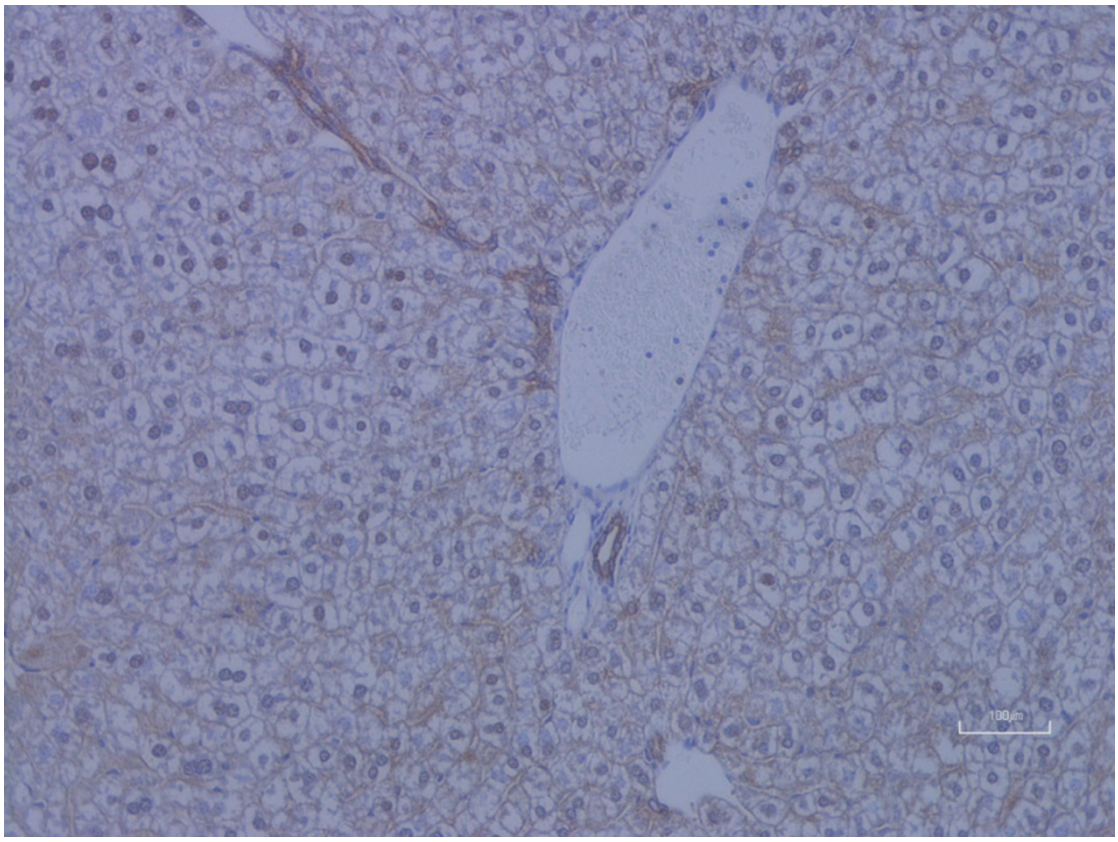

B

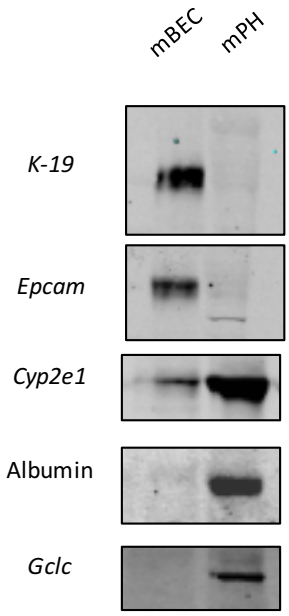

Figure 5.1 IP antibody validation and characterisation of BEC. A, Immunohistochemical staining of healthy mouse liver sections using an anti-EPCAM antibody to target *Epcam* (brown-stain), a cell-surface marker present on the cell-membrane of BEC. **B,** Western blot analysis of the BEC markers, *K-19* and *Epcam*, and the hepatocyte markers albumin and *Gclc*, as well as *Cyp2e1*.

5.3.2 Global microRNA analysis of BEC and hepatocytes identifies differential rank expression profiles between the cell types

In order to identify possible microRNA biomarkers of BEC injury, we performed a global miRNA profiling analysis in both BEC, and hepatocytes in order to establish rank expression profiles of miRNAs, and possible differentially expressed miRNAs. Global miRNA expression analysis in healthy BEC identified 111 individual miRNA species, with the top three ranked miRNA being miR-5109 (Mean intensity/MI: 503267.4, S.D.: 133149.2), miR-6243 (MI: 278441.5, S.D.: 162571.1), and miR-1224-5p (MI: 78147.22, S.D.: 65911.07) (Figure 2). Global miRNA expression analysis in healthy hepatocytes identified 33 individual miRNA species, with the top three ranked miRNA being miR-122-5p (MI: 15340.3, S.D.: 1308.3), miR-5109 (MI: 13548.3, S.D.: 1139.3), and miR-6243 (MI: 9871.2, S.D.: 1105.2) (figure 5.3).

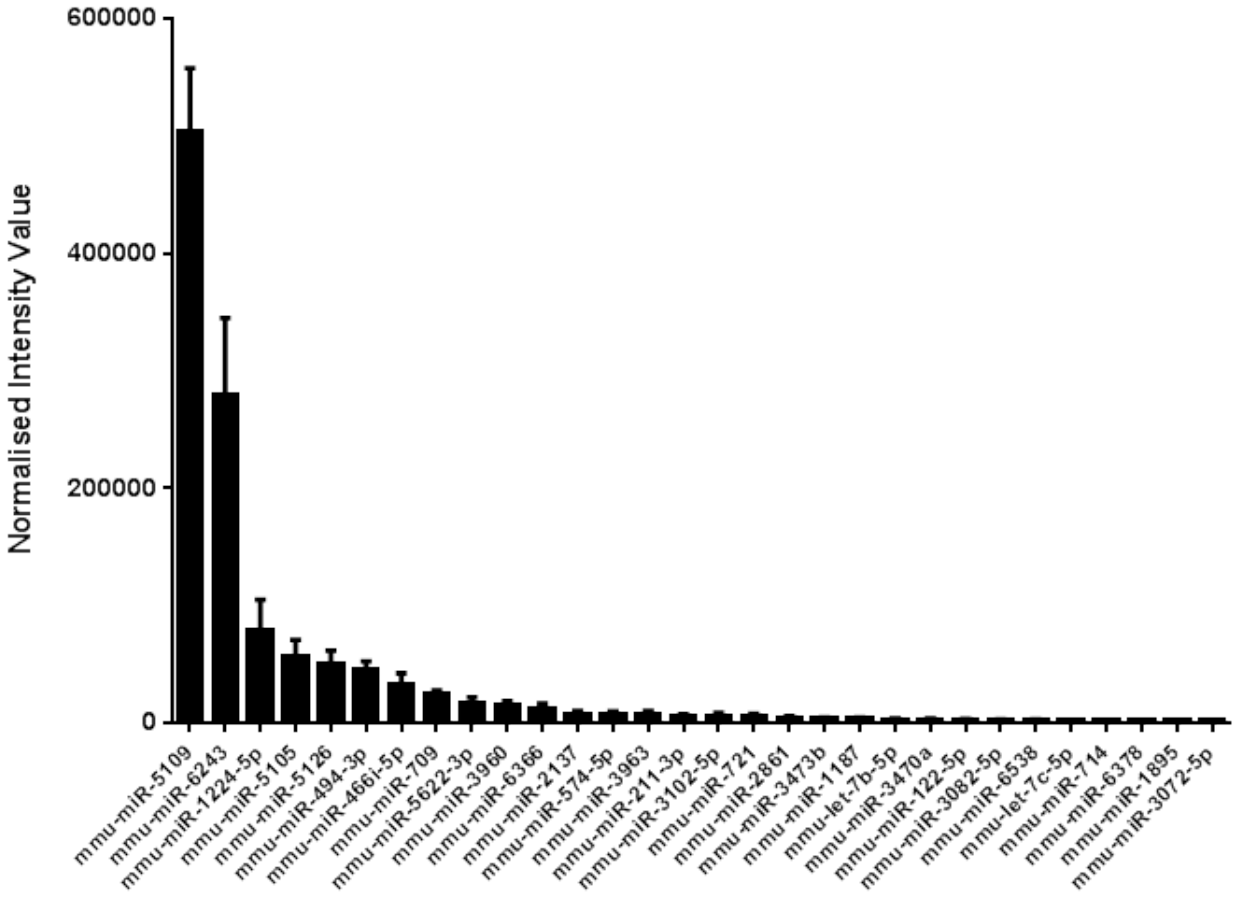

Figure 5.2 Rank expression profile of primary mouse BEC microRNAs. Normalised intensity values represent the mean of normalised intensity values generated off n = 5 individual array plates. Normalised values are generated using multiple incorporated standard miRNAs on each array plate and Agilent GeneSpring pre-processing software

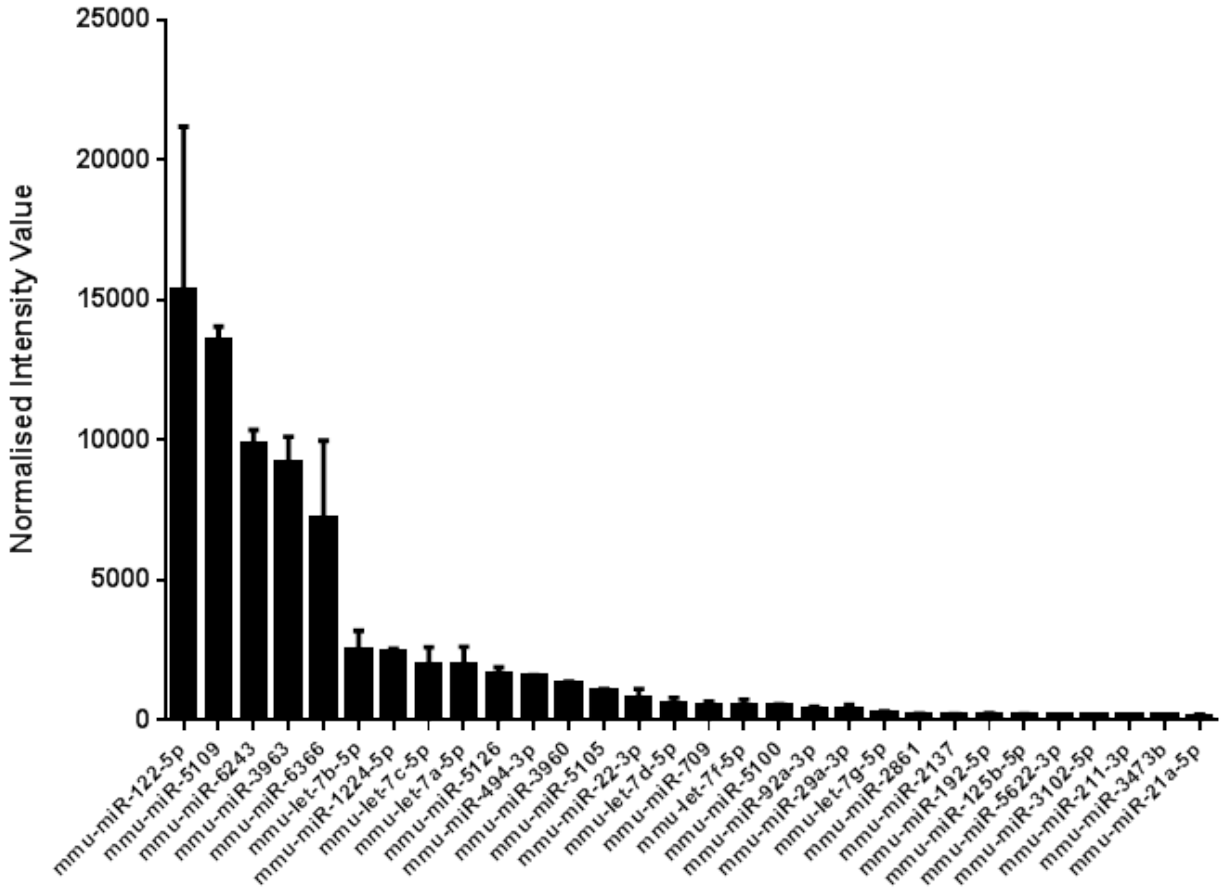

Figure 5.3 Primary mouse hepatocyte rank microRNA expression profile. Normalised intensity values represent the mean of normalised intensity values generated off n = 5 individual array plates. Normalised values are generated using multiple incorporated standard miRNAs on each array plate and Agilent GeneSpring pre-processing software

5.3.3 BEC and hepatocyte enriched miRNAs

To identify miRNAs which were differentially expressed between BEC and hepatocytes, the global miRNA profiles of each cell type were subject to comparison, and statistical analysis using multiple t-tests, followed by a multiple comparisons correction to identify significantly enriched miRNAs in either cell type. Comparison of the two profiles revealed that 92 miRNAs were significantly up-regulated in BEC over hepatocytes and of these miRNAs 85 were only detectable at a negligible level within hepatocytes, suggesting relative enrichment in BEC (figure 5.4 and table 5.1). Conversely, 25 miRNAs were upregulated in hepatocytes over BEC, of which 8 miRNAs were detected in hepatocytes, which were not detected in BEC (miR-194-5p, miR-378b, miR-365-3p, miR-455-3p, miR-378d, miR-107-3p, miR-130a-3p, miR-192-5p). Several miRNAs were found to be significantly enriched in BEC over hepatocytes, including miR-574-5p (Fold-change: 7416.2, $p < 0.05$), miR-721 (FC: 5734.4; $p < 0.05$), and miR-1187 (FC: 3310.9, $p < 0.05$) (figure 5.5). MicroRNAs were also detected that were significantly enriched in hepatocytes over BEC, including miR-107-3p (FC: 93.3, $p < 0.05$), miR-194-5p (FC: 72.9, $p < 0.05$) and miR-378b (FC: 61.7, $p < 0.05$) (figure 5.6). The previously examined hepatocyte-enriched miRNA, miR-122 was found to be present in both cell types, but enriched in hepatocytes over BEC (FC: 5.4, $p < 0.05$). Another characterised hepatocyte-enriched miRNA, miR-192 was only detectable in hepatocytes and not in BEC (MI: 172.84; S.D.: 163.3).

Table 5.1 MicroRNAs detectable in BEC, but not in hepatocytes. Average values represent the mean normalised intensity reading obtained from the analysis of n = 5 mice per group (individual array plates per mouse)

Name	Average	S.D.
mmu-miR-574-5p	7416.2	5880.9
mmu-miR-721	5734.4	4680.5
mmu-miR-1187	3310.9	2586.8
mmu-miR-3470a	2880.6	2296.7
mmu-miR-3082-5p	2412.9	1795.8
mmu-miR-714	1864.9	1125.5
mmu-miR-1895	1763.8	460.4
mmu-miR-3072-5p	1524.3	375.4
mmu-miR-328-5p	1446.8	851.6
mmu-miR-1306-3p	1335.7	761.0
mmu-miR-5112	1265.0	844.7
mmu-miR-3102-5p.2-5p	1222.3	257.9
mmu-miR-5107-5p	1214.7	379.9
mmu-miR-1904	1077.0	355.4
mmu-miR-6368	1075.2	450.7
mmu-miR-3472	1011.1	705.7
mmu-miR-3095-3p	909.2	461.4
mmu-miR-467f	811.7	281.7
mmu-miR-1982-5p	780.3	629.8
mmu-miR-466h-3p	772.1	228.0
mmu-miR-5128	755.7	403.0
mmu-miR-1897-5p	750.1	266.3
mmu-miR-3099-3p	723.8	384.6
mmu-miR-712-5p	636.8	368.9
mmu-miR-5119	617.7	143.4
mmu-miR-760-3p	585.9	417.0
mmu-miR-1196-5p	579.0	210.8
mmu-miR-669p-3p	565.8	214.5
mmu-miR-669n	540.8	493.2
mmu-miR-3473a	537.8	178.0
mmu-miR-1894-3p	533.8	248.9
mmu-miR-149-3p	532.3	236.9
mmu-miR-6385	521.6	330.2
mmu-miR-5130	517.4	320.9
mmu-miR-705	491.9	105.0
mmu-miR-3077-5p	473.5	273.1
mmu-miR-370-3p	463.5	172.2
mmu-miR-1934-3p	461.5	62.4
mmu-miR-1231-5p	433.2	101.2
mmu-miR-680	428.9	156.3
mmu-miR-1906	423.7	172.6
mmu-miR-1896	418.3	82.6
mmu-miR-6405	409.0	141.2

Name	Average	S.D.
mmu-miR-6418-5p	404.6	311.4
mmu-miR-652-5p	395.3	301.5
mmu-miR-6392-3p	391.3	350.4
mmu-miR-466q	373.3	142.1
mmu-miR-1892	328.6	183.8
mmu-miR-125a-3p	322.4	262.6
mmu-miR-483-5p	315.8	166.3
mmu-miR-690	292.0	117.0
mmu-miR-32-3p	247.9	236.3
mmu-miR-5113	243.2	184.4
mmu-miR-706	237.4	126.3
mmu-miR-468-3p	227.7	220.5
mmu-miR-5131	211.2	159.0
mmu-miR-3572-5p	211.0	131.5
mmu-miR-681	205.8	123.3
mmu-miR-691	193.3	157.7
mmu-miR-3067-3p	191.2	99.9
mmu-miR-6352	190.9	115.9
mmu-miR-450a-2-3p	176.0	81.1
mmu-miR-1967	163.1	92.7
mmu-miR-6240	162.6	110.4
mmu-miR-466f-3p	160.7	64.2
mmu-miR-1940	157.6	102.2
mmu-miR-466i-3p	153.3	75.0
mmu-miR-3110-3p	149.3	102.0
mmu-miR-669c-3p	139.4	74.6
mmu-miR-6370	139.0	122.6
mmu-miR-423-5p	126.0	96.8
mmu-miR-6354	123.6	66.5
mmu-miR-6349	120.5	73.5
mmu-miR-6343	111.6	61.9
mmu-miR-3473e	102.7	63.0
mmu-miR-1971	98.8	64.6
mmu-miR-6351	90.3	49.5
mmu-miR-5132-5p	86.8	49.3
mmu-miR-5103	74.1	43.9
mmu-miR-3075-5p	68.8	66.2
mmu-miR-195a-3p	62.4	59.7
mmu-miR-5118	43.4	32.6
mmu-miR-6394	38.9	35.7
mmu-miR-327	28.9	18.9
mmu-miR-30c-1-3p	27.6	15.0

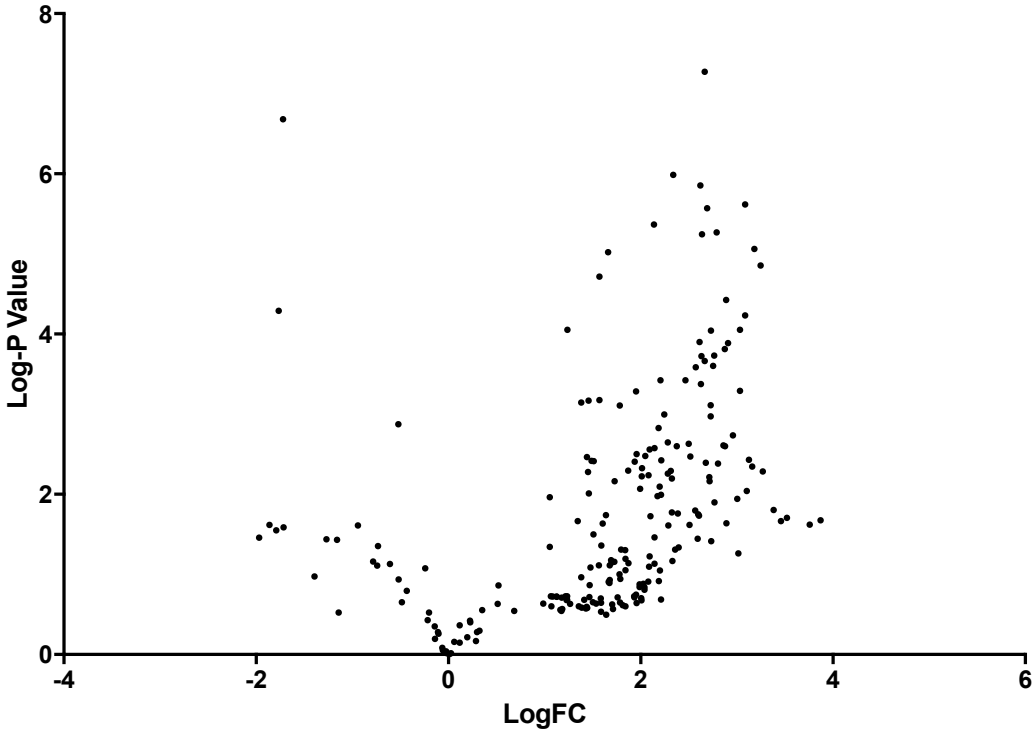

Figure 5.4 Volcano plot comparison of the global microRNA profile of BEC, compared to hepatocytes. Comparison of negative $\log_2$ P-value versus $\log_2$ fold-change of mean values taken from n = 5 mice per group. Each individual data point represents an individual miRNA species. Significance is set at $p<0.05$ ($-\log_2 p<1.3$).

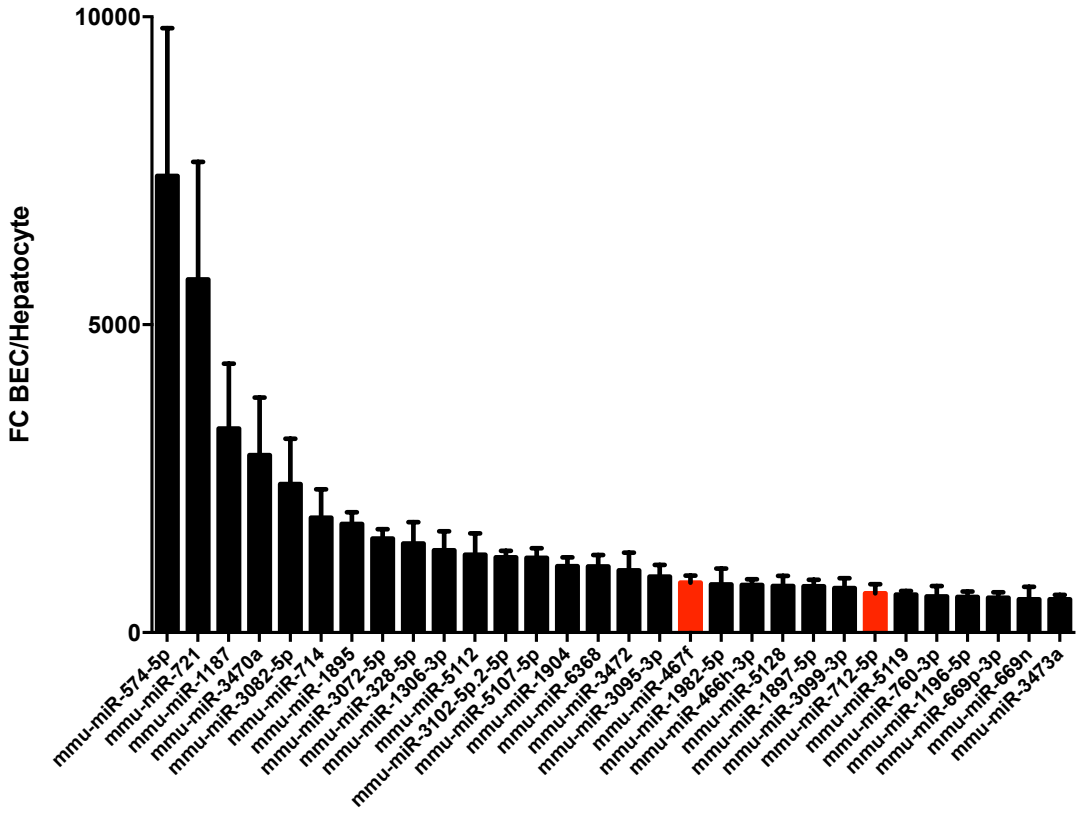

Figure 5.5 BEC microRNA profile in comparison to the microRNA profile of hepatocytes. Mean fold-change (FC) values represent the mean calculated intensity value derived from n = 5 array plates (n = 5 mice per group) for the group (BEC), divided by the same value derived from the other group (hepatocytes). The three most significantly enriched miRNAs in BEC over hepatocytes were found to be miR-574-5p, miR-721 and miR-1187. The miRNAs highlighted in red, miR-467f and miR-712-5p have been identified in a recent study examining markers of cholestatic injury as being elevated (miR-467f: 5-fold elevated, miR-712: 3-fold) in the circulation during ANIT injury (Church et al. 2015)

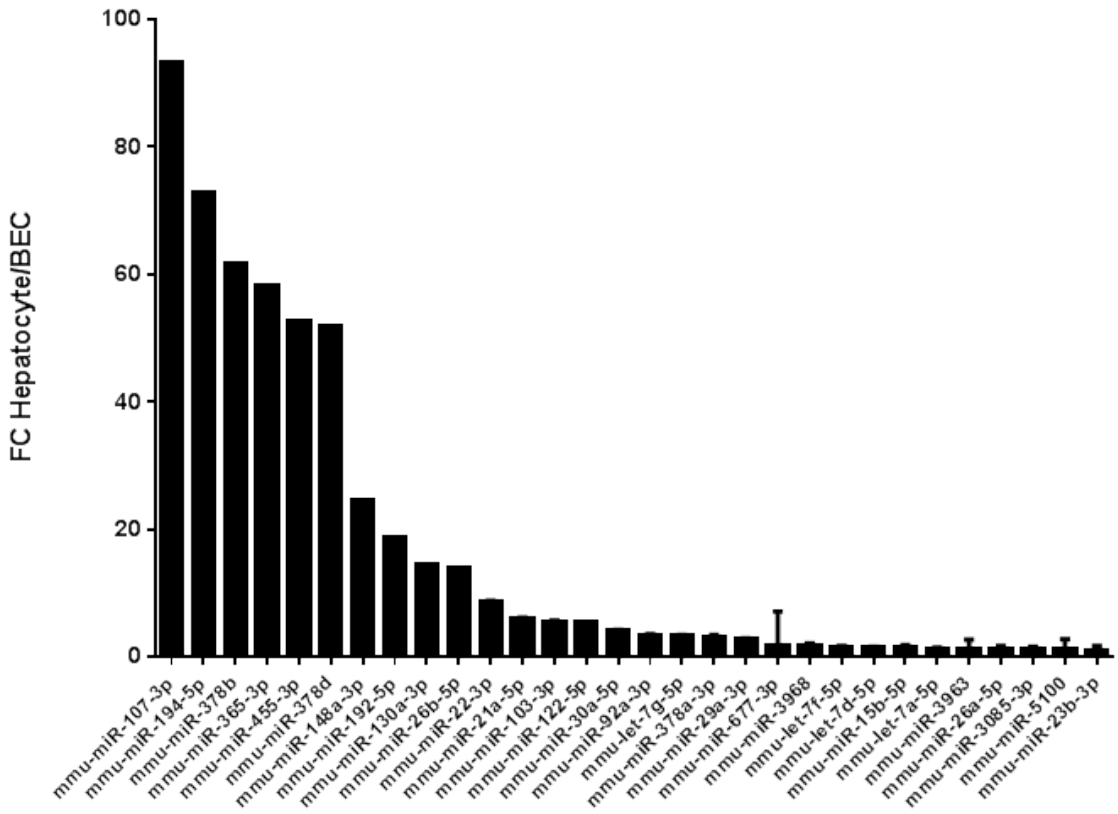

Figure 5.6 Hepatocyte microRNA profile compared to the microRNA profile of BEC. Mean fold-change (FC) values represent the mean calculated intensity value derived from n = 5 array plates (n = 5 mice per group) for the group (hepatocytes), divided by the same value derived from the other group (BEC)

5.4. DISCUSSION

The current biomarkers of BEC/bile duct injury are prone to false positive readings, are not specific to BEC, and have little prognostic value. Therefore, new biomarkers with better characteristics would be useful within the clinic and industry in order to diagnose bile duct injury early in its course. MicroRNAs have previously been shown to be useful prognostic markers in several forms of DILI, due to their organ specificity, stability, and ability to be detected in the circulation earlier in the course of injury than the current gold-standard markers of DILI. This phenomenon is not solely restricted to the liver, with other studies demonstrating that miRNAs are enriched within other organs, such as the heart and kidneys. Because of this, we hypothesised that a miRNA species may be enriched, or even be specific to BEC cells, offering the possibility that it may be used as a circulating biomarker of BEC injury.

In order to identify possible miRNA biomarkers of BEC injury we performed a global microRNA profiling analysis of primary isolated BEC and hepatocytes, in order to determine whether each cell type displays a differential miRNA expression profile, and also whether any miRNAs are enriched in BEC. Our global microRNA analysis indicated that miR-5109, miR-6243, miR-5105 were highly expressed in both cell types, however post-analysis, it has now been demonstrated that these miRNA are derived from a fragments of large sub-unit ribosomal RNA (Castellano and Stebbing 2013), therefore they cannot be considered for further analysis. This highlights the speed at which the field of miRNAs is developing, and also the importance of validating the existence of miRNAs detected when using global profiling studies. After removal of these miRNA from the analysis, we found that the top three ranked miRNAs in BEC were miR-1224-5p, miR-5126 and miR-494-3p, and in hepatocytes were miR-122-5p, miR-3963 and miR-6366.

The detection of miR-122-5p as the most enriched miRNA in hepatocytes was expected, as it has previously been suggested that this species makes up ~70% of the miRNA content of the liver (Lagos-Quintana et al. 2002), and has previously been shown to be the most enriched

miRNA in primary human hepatocytes (Kia et al. 2014). Both miR-3963 and miR-6366 are recently discovered miRNAs which have yet to be fully investigated in context to the liver. It has previously been demonstrated that miR-3963 has a role in myogenic differentiation in a myoblast cell line (Katase et al. 2015).

Interestingly, each of these miRNAs was also detected within BEC cells, with miR-122-5p, miR-3963 and miR-6366 being the 19th, 14th, and 11th most enriched miRNAs in BEC. This suggests that none of these markers can be classed as truly hepatocyte specific, and that miR-122 is a liver-tissue-specific biomarker, as it is present in at least two liver cell types. Therefore, we have generated the following hypotheses to explain this, first, although the method for BEC extraction contains several purification steps, there may be some residual hepatocyte carry-over, due to the sheer abundance of both hepatocytes in the liver, and miR-122 in the hepatocytes (Wang et al. 2009). Therefore, only a small number of hepatocytes left within the sample could produce this result. Second, miR-122 may be present within BEC, as previously much of the work examining miR-122 expression has only focussed on whole liver tissue (Lagos-Quintana et al. 2001); making the assumption that miR-122 is only present within hepatocytes without validation. Our hypothesis is not without reason, as it has been shown that small BEC are able to transdifferentiate to become zone I hepatocytes, demonstrating that these cells share the same lineage (Limaye et al. 2008). And finally, it may be possible that our extraction method may also have isolated oval cells (liver progenitor cells), which may express a low-level of miR-122, due to them representing the cells which are able to differentiate to form hepatocytes (LeCluyse et al. 2012).

Similarly, the three most enriched miRNAs in BEC were also detectable within the hepatocytes, with miR-1224-5p, miR-5126, and miR-494-3p being the 7th, 10th and 11th most enriched miRNAs in hepatocytes in our analysis, suggesting that they will not offer value as a BEC-specific miRNA. Additionally, miR-1224-5p has previously been suggested to be a circulating biomarker several forms of cancer, including primary colon cancer (Ogata-Kawata et al. 2014), miR-5126 has been detected in adipose and brain tissue (Tao et al. 2015; Zhao et

al. 2015), and miR-494-3p has been implicated in prostate cancer (Shen et al. 2014), suggesting a lack of organ/cell-specificity.

To eliminate miRNAs which were present in both hepatocytes and BEC, we performed a comparison analysis of the two global microRNA profiles, in order to identify miRNAs enriched, or only detected in one cell type, in order to increase the possibility of discovering a cell-specific miRNA. In this analysis we were able to identify 106 miRNAs which were enriched in BEC over hepatocytes, and 11 miRNAs which were enriched in hepatocytes over BEC. Of these miRNAs, 85 were only detected in BEC, and 8 others were only detected in hepatocytes. The three most enriched miRNAs detected only in BEC were miR-574-5p, miR-721, and miR-1187. Examination of the literature surrounding these molecules suggests that miR-574 has been implicated in non-small cell lung cancer (Foss et al. 2011), and miR-721 in stimulation of iPS cell generation (Pfaff et al. 2011), suggesting that neither is specific for BEC. Investigation of the literature examining miR-1187 suggests this microRNA is down regulated in the liver in acute liver failure, and that use of a miR-1187 mimic is able to inhibit caspase-8 activation and apoptosis in hepatocytes in acute liver failure, however there is little knowledge presented of whether this miRNA is present within hepatocytes in the liver or within non-parenchymal cells (Yu et al. 2012). In fact, of the 85 miRNAs detected only in BEC, all were found to be implicated in pathologies or processes elsewhere in the body, suggesting that our analysis was unable to find a completely BEC-specific miRNA. However, future studies will evaluate whether there is sufficient enrichment in BEC that may make these miRNAs sufficiently BEC-selective to be useful cell markers. Interestingly, in a recent study which aimed to examine hepatobiliary injury and biliary hyperplasia, two miRNAs which were identified as BEC-enriched in our study, namely miR-467f (5-fold increase) and miR-721 (3-fold) were demonstrated to be elevated in the plasma of rats administered the model hepatotoxin alpha-napthylisothiocynate (ANIT), and FB004BA, a proprietary compound synthesised by Bayer (Bayer Pharmaceuticals, Germany) known to cause hepatobiliary injury (Church et al. 2015). ANIT is of particular interest because it is understood to initially cause

BEC injury, leading to secondary development of hepatocellular injury, followed by a recovery phase which entails cellular regeneration and compensatory biliary hyperplasia (Kossor et al. 1993), making it an ideal compound to investigate potential biomarkers of biliary cell injury. Unfortunately, due to methodological difference between our study and the study performed by Church et al. (2015), a number of the miRNAs we identified as BEC-enriched were not investigated in their study. Therefore, if a study was performed using a wider range of miRNA species similar to the study performed using ANIT, more potential biomarkers may be identified from the work performed within our study.

A limitation of our study was that we isolated BEC as a single species, however as previously discussed in this thesis, BEC are a heterogeneous species which differ depending on their location along the biliary tract (Glaser et al. 2006). Due to this heterogeneity, BEC are differentially affected by DILI-causing compounds. Therefore, to build on this relatively simplistic experiment, counter-flow elutriation could be utilised in order to separate different BEC species, based on their size, in order to identify differential expression of microRNAs between different BEC species. This could then be used to identify markers of different types of biliary tract injury. An additional limitation may be a product of the use of the microRNA array platform, limiting our analysis to only previously known miRNAs, and not potentially new species, which may have been identified with sequencing approach. Therefore, a possible direction for the future would be to build on the global microRNA profile of this cell type using an approach which would allow the identification of novel miRNA sequences.

In summary, we were able to identify different global miRNA profiles of BEC and hepatocytes in CD-1 mice. Further future work, after the limitations of this study were addressed could aim to examine the utility of BEC-enriched miRNAs, which were not detectable in hepatocytes as biomarkers of BEC injury in complex cell culture systems which have incorporated this cell type to mimic the overall structure of the liver.

CHAPTER 6

CONCLUDING DISCUSSION

6. GENERAL DISCUSSION

As described throughout this thesis, our aim to identify, examine and validate novel biomarkers of DILI was driven by the current lack of sensitive and specific biomarkers to diagnose this pathology (Reviewed by Hornby et al. (2014)). In this chapter we briefly outline the major findings of this thesis, the implications of our findings, possible future work and finally, we discuss future perspectives on the wider field as a whole.

6.1 MAJOR FINDINGS

We approached our major goal from several perspectives, first, we investigated mechanisms behind the early release of miR-122 in DILI (Antoine et al. 2013a; Harrill et al. 2012; Starkey Lewis et al. 2011; Wang et al. 2009). In our study we aimed to understand whether miR-122 was released actively in exosomes early in DILI, however in our study we found no evidence to suggest that this was the case, but we did find that the percentage of this marker in exosomes began to rise in the recovery phase of DILI, which suggests possible implications in hepatic regeneration. Our results are in line with current research which suggested that miR-122 is mainly contained free-from exosomes which no specific exosome-bound release in acute forms of DILI (Bala et al. 2012).

Our second aim was to identify new miRNA biomarkers of DILI through examination of cell-specific, and hepatic zonal miRNA profiles. To do this we sought to develop methods for the isolation of hepatic non-parenchymal cells, and also specific areas of the hepatic architecture. Our study examining zonation in hepatic miRNA expression demonstrated that certain miRNAs are expressed in a zonal pattern, with several being highly enriched in either zone I or zone III. This suggests the potential for miRNAs to not only predict hepatic injury, but also to provide an insight into in which zone injury is occurring. Our study also suggested a possible role for microRNAs in the regulation of zonation, through modulation of the Wnt/β-catenin pathway, the molecular driver of zonation (Burke et al. 2009), hinting at the possible mechanistic role of miRNAs in liver zonation. Then in chapter 5, we provided the first view

of the global microRNA expression profile of BEC, and compared this to that of hepatocytes, in order to identify cell-specific enriched miRNAs. Despite the preliminary stages of this work, we were able to identify several miRNAs which were enriched in BEC over hepatocytes, and even more interestingly several more of these have recently been shown to be elevated in the circulation in an ANIT model of biliary tract injury (Church et al. 2015).

Finally, we aimed to gain a greater understanding of the mechanisms behind the formation of 3-NT adducts in DILI through utilising paracetamol and FS rodent models of DILI. The major finding of our study was that although the two hepatotoxins cause injury through separate pathways, they both lead to 3-NT formation suggesting that there are multiple mechanisms for the occurrence of this adduct, both through and independent of the mitochondria.

6.2 IMPLICATIONS OF FINDINGS AND FUTURE DIRECTIONS

Aside from our main hypotheses which have been discussed in depth in each chapter and briefly above, there is the possibility that our findings will have implications for the wider fields of DILI and DILI biomarkers, which will now be outlined in the following section.

Our finding that exosome-bound miR-122 is elevated in the recovery phase of DILI may suggest that these molecules may have a use in drug-development for the prediction of mechanisms surrounding DILI, or moreover as therapeutic molecules in their own right (Reviewed in Suntres et al. (2013), with studies now demonstrating that exosomes derived from stem-cells or perturbed cells may be able to modulate an adaptive or proliferative response in recipient cells (Herrera et al. 2010; Tan et al. 2014). There is already some evidence to suggest that extracellular vesicles may accelerate a proliferative response. In a study examining the hepatectomy model in rats, the authors were able to show that administration of human liver stem cell-derived microvesicles accelerated hepatic regeneration following hepatectomy (Herrera et al. 2010). Another study demonstrated that exosomes sourced from hepatocytes treated with alcohol are able to directly transfer miR-122 to monocytes, inhibiting the HO-1 pathway and sensitising the cells to LPS (Momen-Heravi

et al. 2015). This, in contrast to the first study mentioned, may suggest that miR-122 is actively being shed in DILI to active the hepato-protective HO-1 pathway in perturbed hepatocytes. However, further work examining the effects of blocking exosome release, using molecules such as manumycin (Mittelbrun et al. 2011), during the recovery phase of injury should be undertaken in order to fully establish a cause-and-effect role of circulating exosomes in an adaptive response to injury. If it was possible to establish this link, miR-122 could have an important therapeutic role as a promoter of liver regeneration. Interestingly, the targeting of miR-122 is not novel however, as pharmaceutical companies are currently developing an antagonist of miR-122 in order to block the replication of the Hepatitis C virus (Bhat et al. 2013; Regulus Therapeutics: http://www.regulusrx.com/therapeutic-areas/rg-101/), in which miR-122 has previously been shown to play a role (Fukuhara et al. 2012). Similarly, a number of studies are now studying the potential of exosomes as therapeutic targets and as a method of drug delivery (Reviewed by Johnsen et al. 2014). Therefore, this taken as a whole, suggests that exosome-bound miRNA research in the future may be better directed towards examining mechanisms of injury, and the modulatory effects of these molecules, rather than seeking out exosome-bound miRNAs as biomarkers of acute injury.

A current major focus of the DILI field is the development of complex cell culture models in order to reduce the use of animal models and also to improve on the relative lack of availability of cell culture models which accurately predict DILI. Current model systems such as HepG2, a human hepatoma cell line and Hepa1c, a mouse hepatoma cell line which are still commonly used in toxicity studies, have long lives in culture, but lack in the expression of many important drug metabolism enzymes, such as CYP2E1 (cyp2e1), limiting their true predictive ability (Wu and Cederbaum 2008). Conversely, primary human hepatocytes, the current gold standard cell culture model for the examination of DILI are the closest match to human hepatocytes *in situ*, but they de-differentiate quickly which limits their useful life (Rowe et al. 2010; Heslop et al. 2016). Because of this, groups are now focussed on producing cell culture systems which contain multiple cell-types in organ-like systems in the hope that if conditions

are more closely matched to those *in vivo* then cells will maintain their phenotype and metabolic activity for longer period (Maschmeyer et al. 2015). Examples of which are the LiverChip which incorporates Kupffer cells, endothelial cells, stellate cells and hepatocytes on a single microfluidic chip arranged similarly to the liver acinus (Bushan et al. 2013), and bioprinted human liver tissue developed by Organovo, a California-based biotechnology company which involves 3D printing of multiple liver cell types in a normal liver like structure (Murphy et al. 2015). Our work in developing a method for BEC isolation may offer its use for the production of these liver models, in order for them to contain bile duct-like structures in order to more closely match the phenotype of the parent liver, if it is found that our method is transferable to human liver tissue. Additionally, if it can be established that a miRNA, or a group of miRNAs are involved in driving the zonal phenotype, possibly through the Wnt//β-Catenin pathway, it is possible that our work may have wider long-term implications in the development of *in vitro* models for the examination of DILI. If this was the case, it may be possible to generate zone I-like, or zone III-like hepatocytes using miRNA knock-down, or transfection approaches to manipulate miRNA levels within these cells, it would be of great use in the assessment of new compounds. Inhibitors of miRNAs, such as Antagomirs, have been used previously to silence the function of miR-16, miR-122, miR-192 and miR-194 *in vivo* in order to gain a greater understanding of the roles of these molecules, demonstrating the feasibility of this approach (Krutzfelt et al. 2005).

A further outcome of our work may be that zonal- and cell-enriched miRNAs may have the potential to identify zone-specific or cell-specific injury in pre-clinical models, in clinical trials and also in the complex cell-culture systems mentioned previously. However, limitations of these markers may become apparent because of their lack of liver-specificity, due to their expression in other cell-types and organs (Chitnis et al. 2012; Packer et al. 2008). However, this issue could be mitigated through the use of a panel of miRNAs, encompassing miR-122, in order to diagnose general hepatocyte injury, and then zone-specific markers in order to identify the localisation of the injury. This could be progressed further through the use of cell-

specific biomarkers, such as the miRNAs identified in our study examining BEC, to develop a full miRNA panel capable of identifying general injury, the zone in which injury is taking place and any other cell types undergoing injury. This approach is not novel and has previously been suggested for the identification of types of cancer (Wang et al. 2015; Zheng et al. 2014; Tan et al. 2014a) and has been used as a standard approach in DILI for a number of years in which ALT, AST and bilirubin were used in combination (Kaplowitz et al. 2006).

6.2 FUTURE PERSPECTIVES ON PROGRESSING MICRORNAS AS DILI BIOMARKERS

6.2.1 Barriers to the progress of miRNA biomarkers towards use in the clinic

Much of the work within this thesis has focussed on the development of miRNAs as biomarkers of DILI, however before these markers can truly become challengers to the current gold standard biomarker of DILI, ALT, several points must be addressed.

Despite the work in this thesis and in the wider literature, the greatest hindrance towards the development of miRNAs as clinical biomarkers are the assays which are used to quantify them. The most common technique for miRNA quantification is reverse transcription-quantitative PCR (RT-qPCR), which despite having a high level of sensitivity, is inappropriate for clinical use as it can take up to 8 hours to perform the assay (Kramer et al. 2011). In the case of paracetamol acute liver injury, the onset of toxicity may be rapid and therefore this test would be too slow to provide prognostic value (Starkey Lewis et al. 2011). In comparison, the assay to detect ALT is relatively simple requiring little sample preparation and extremely quick, with the time between sampling and results being as little as 90 minutes (Reviewed by Huang et al. 2006). Another consideration is cost, analysis of a single miRNA sample can currently cost as much as £20, whereas this cost can be as little as £1 for analysis of serum ALT, creating another barrier to the progression of miR-122 towards becoming a mainstream biomarker. To facilitate the transition of miRNAs from a proof-of concept biomarker to a true clinical bedside test, a fast, robust, simple and sensitive new clinical assay must be developed

for the rapid quantification of miRNAs in accessible biofluids. Several novel assays are currently in development for the detection of miRNAs that would be more suitable in a clinical setting, however none have yet undergone the rigorous testing required for use. Recently, a group developed a label-free method to quantify miRNAs through the use of gold nanoparticle networks and a duplex-specific nuclease (DSN) which allowed detection of miRNAs at sub-femtomolar levels, with almost no sample preparation required (Shen et al. 2013). Another group, Cissel *et al,* have developed a microtiter plate assay to quantify miRNAs, using *Renilla-luciferase* labelled microRNA as a competitor to free microRNA for binding to a complementary microRNA probe. An assay which takes a total of 1.5 hours, requires no PCR amplification step and is sensitive down to a femtomolar level (Cissel et al. 2008). In addition to those examples, many other novel methods for microRNA quantification have emerged, in which silicon nanowire biosensors (Zhang et al. 2009), universal tagged probes and time-resolved fluorescence technology (Jiang et al. 2012), and solution-phase detection of miRNAs (Broyles et al. 2012) are all used to detect miRNAs with high levels of sensitivity. However, until one of these methods is fully validated and accepted, miRNAs as biomarkers will remain a concept within the clinic and not a reality.

Another consideration for progressing miR-122 to becoming a mainstream biomarker, is the establishment of a baseline level of miR-122 within humans, much like the ULN value used for ALT, as little is currently know about inter-individual variability in this biomarker. Inter-individual variation of miRNAs was first documented in a study using significance analysis, in which 4 miRNAs were identified that were 63-95% higher in females, compared to males (Duttagupta et al. 2011). In another study, Wang *et al* demonstrated differences in miRNA content of human male serum samples; specifically, miR-130b and miR-18b were slightly higher in males compared to females (Wang et al. 2010). The significance of this in DILI is still unknown and will require further study. This however, highlights the need for studies which assess baseline levels across different population groups and patient groups for

individual miRNAs. This information would then allow clinicians to set an upper limit of normal for each of these biomarkers across a population.

6.3 FINAL THOUGHTS AND CONCLUSION

To conclude, our overall aim was to investigate novel biomarkers of DILI, which we addressed through examining release forms of miR-122, zonal and cellular hepatic miRNA profiles, and cellular patterns of 3-NT formation in DILI, with our findings suggesting that future work should be focussed on understanding the regulatory roles of these potential biomarkers, as well as their combined use alongside other current biomarkers.

6.3 FINAL COMMENTS

Finally, the hypotheses addressed in this thesis will be commented on individually:

Hypothesis 1

Paracetamol and FS both produce necrosis in centrilobular regions of the liver, but both compounds cause this toxicity through distinct routes. We hypothesise that formation of 3-nitrotyrosine adducts, a marker of oxidative stress, will occur during paracetamol injury, but will not occur during FS injury, due to lack of mitochondrial damage in FS injury.

Comment: *We were able to successfully develop a western blot and IHC method for the detection of 3-nitrotyrosine adducts. However, in contrast to our hypothesis we found that 3-NT adducts were detectable in both paracetamol-, and FS-DILI despite the divergent routes of toxicity. In order to further understand the cause of this, a proteomic assessment of the 3-NT adductome should be performed to assess whether any localisation of 3-NT adducts is present within the cell, in order to assess the causative factor of the nitration.*

Hypothesis 2

miR-122 is detectable earlier in the course of DILI than conventional DILI markers due to its mechanism of release. We hypothesise that miR-122 is released actively from the liver in exosomes upon receiving a toxic insult in order to adapt to circumvent DILI.

Comment: *Analysis of the profiles of exosome-bound and exosome-free miR-122 throughout the course of a rat model of paracetamol-DILI, suggested that miR-122 is in fact released in similar profiles in both fractions. This suggests that our initial hypothesis was incorrect and that miR-122 release is likely to be due to non-specific release after loss of plasma membrane integrity. Further work must be done in less severe models of DILI in order to assess the relevance of active miRNA release into the circulation as a method of cell-cell signalling.*

Hypothesis 3

Liver microRNAs are expressed zonally depending on their proximity to a portal or ventral vein, and these expression changes will be related to hepatocyte phenotype and function in these regions. Upon liver injury by paracetamol, we expect to observe changes in microRNA expression in the region surrounding the central vein, however we also hypothesise that expression changes may occur away from this region in order to adapt to the oncoming toxicity.

Comment: *Analysis of the global microRNA profiles of zone I and zone III of the liver suggests that miRNAs are indeed differentially expressed depending on the location across the port-central axis. Interestingly, the differentially expressed miRNAs can also be related back to the Wnt/Beta-Catenin pathway, the molecular driver of zonation, which suggests that miRNAs may play a role in the zonated phenotype of the liver. Further work involving the manipulation of these miRNAs will have to be performed in order to fully understand their role in zonation.*

Hypothesis 4

Intrahepatic biliary epithelial cells, which undergo damage during cholestatic injury, will contain a unique microRNA profile, differing from the surrounding hepatocytes. This profile will allow the selection of specific markers of BEC which will provide use as biomarkers of damage to this cell type in cell models, pre-clinical animal models, and possibly within the clinic.

Comment: *A method was successfully established for the isolation of BEC from mouse liver, and global profiles of hepatocyte and BEC miRNAs were generated. However, all miRNAs identified only in BEC had also been implicated in other forms of tissue/cell injury in prior studies, suggesting that none would be a suitable marker of BEC-specific injury. Further work must be done to establish whether any of these miRNAs could offer use as an in vitro marker of BEC-injury.*

BIBLIOGRAPHY

Abdelmegeed MA, Jang S, Banerjee A, Hardwick JP, Song B-J (2013) Robust protein nitration contributes to paracetamol-induced mitochondrial dysfunction and acute liver injury. Free Radical Biology and Medicine 60(0):211-222

Agouni A, Lagrue-Lak-Hal AH, Ducluzeau PH, et al. (2008) Endothelial dysfunction caused by circulating microparticles from patients with metabolic syndrome. The American journal of pathology 173(4):1210-1219

Ai J, Zhang R, Li Y, et al. (2010) Circulating microRNA-1 as a potential novel biomarker for acute myocardial infarction. Biochemical and biophysical research communications 391(1):73-77

Aklillu E, Persson I, Bertilsson L, Johansson I, Rodrigues F, Ingelman-Sundberg M (1996) Frequent distribution of ultrarapid metabolizers of debrisoquine in an ethiopian population carrying duplicated and multiduplicated functional CYP2D6 alleles. Journal of Pharmacology and Experimental Therapeutics 278(1):441-446

Aithal GP, Watkins PB, Andrade RJ, et al. (2011) Case definition and phenotype standardization in drug-induced liver injury. Clinical Pharmacology & Therapeutics 89(6):806-815

Alam J, Stewart D, Touchard C, Boinapally S, Choi AM, Cook JL (1999) Nrf2, a Cap'n'Collar transcription factor, regulates induction of the heme oxygenase-1 gene. Journal of Biological Chemistry 274(37):26071-26078

Alpini G, Roberts S, Kuntz SM, et al. (1996) Morphological, molecular, and functional heterogeneity of cholangiocytes from normal rat liver. Gastroenterology 110(5):1636-1643

Anand AC, Nightingale P, Neuberger JM (1997) Early indicators of prognosis in fulmitant hepatic failure: an assessment of the King's criteria. Journal of hepatology 26(1):62-68

Andaloussi SE, Mäger I, Breakefield XO, Wood MJ (2013) Extracellular vesicles: biology and emerging therapeutic opportunities. Nature Reviews Drug Discovery 12(5):347-357

Andrade RJ, Lucena MI, Fernández, M. C., et al. (2005) Drug-induced liver injury: an analysis of 461 incidences submitted to the Spanish registry over a 10-year period. Gastroenterology 129(2):512-521

Antoine DJ (2008) Molecular and Chemical Biomarkers of Drug-Induced Hepatic Apoptosis, Necrosis and Inflammation. PhD Thesis. University of Liverpool

Antoine DJ, Dear JW, Lewis PS, et al. (2013) Mechanistic biomarkers provide early and sensitive detection of paracetamol-induced acute liver injury at first presentation to hospital. Hepatology 58(2):777-787

Anundi I, Lähteenmäki T, Rundgren M, Moldeus P, Lindros KO (1993) Zonation of paracetamol metabolism and cytochrome P450 2E1-mediated toxicity studied in isolated periportal and perivenous hepatocytes. Biochemical pharmacology 45(6):1251-1259

Apostolova N, Gomez-Sucerquia LJ, Alegre F, et al. (2013) ER stress in human hepatic cells treated with Efavirenz: mitochondria again. Journal of hepatology 59(4):780-789

Arasu P, Wightman B, Ruvkun G (1991) Temporal regulation of lin-14 by the antagonistic action of two other heterochronic genes, lin-4 and lin-28. Genes & development 5(10):1825-1833

Arroyo JD, Chevillet JR, Kroh EM, et al. (2011) Argonaute2 complexes carry a population of circulating microRNAs independent of vesicles in human plasma. Proceedings of the National Academy of Sciences 108(12):5003-5008

Asahina K, Tsai SY, Li P, et al. (2009) Mesenchymal origin of hepatic stellate cells, submesothelial cells, and perivascular mesenchymal cells during mouse liver development. Hepatology 49(3):998-1011

Aubrecht J, Schomaker SJ, Amacher DE (2013) Emerging hepatotoxicity biomarkers and their potential to improve understanding and management of drug-induced liver injury. Genome Med 5(9):85

Auman JT, Chou J, Gerrish K, et al. (2007) Identification of genes implicated in methapyrilene-induced hepatotoxicity by comparing differential gene expression in target and nontarget tissue. Environmental health perspectives:572-578

Baker LA, Lee KC, Jimenez CP, et al. (2015). Circulating microRNAs Reveal Time Course of Organ Injury in a Porcine Model of Acetaminophen-Induced Acute Liver Failure. PloS one 10(5): e0128076.

Bala S, Petrasek J, Mundkur S, et al. (2012) Circulating microRNAs in exosomes indicate hepatocyte injury and inflammation in alcoholic, drug-induced, and inflammatory liver diseases. Hepatology 56(5):1946-1957

Balakathiresan N, Bhomia M, Chandran R, Chavko M, McCarron RM, Maheshwari RK (2012) MicroRNA let-7i is a promising serum biomarker for blast-induced traumatic brain injury. Journal of neurotrauma 29(7):1379-1387

Bartels H, Freimann S, Jungermann K (1993) Predominant periportal expression of the phosphoenolpyruvate carboxykinase gene in liver of fed and fasted mice, hamsters and rats studied by in situ hybridization. Histochemistry 99(4):303-309

Bedard K, MacDonald N, Collins J, Cribb A (2004) Cytoprotection following endoplasmic reticulum stress protein induction in continuous cell lines. Basic & clinical pharmacology & toxicology 94(3):124-131

Benhamouche S, Decaens T, Godard C, et al. (2006a) Apc tumor suppressor gene is the "zonation-keeper" of mouse liver. Developmental cell 10(6):759-770

Benhamouche S, Decaens T, Perret C, Colnot S (2006b) Wnt/beta-catenin pathway and liver metabolic zonation: a new player for an old concept. Médecine sciences 22(11):904

Benichou, C (1990) Criteria of drug-induced liver disorders. Report of an international consensus meeting. Journal of hepatology 11(2):272-276

Benichou C, Danan G, Flahault A (1993) Causality assessment of adverse reactions to drugs—II. An original model for validation of drug causality assessment methods: case reports with positive rechallenge. Journal of clinical epidemiology 46(11):1331-1336

Berkowitz CM, Shen CS, Bilir BM, Guibert E, Gumucio JJ (1995) Different hepatocytes express the cholesterol 7α-hydroxylase gene during its circadian modulation in vivo. Hepatology 21(6):1658-1667

Bernstein RE (1980) Isoniazid hepatotoxicity and acetylation during tuberculosis chemoprophylaxis. American Review of Respiratory Disease 121(3):429-430

Berry MN, Barritt GJ, & Edwards AM (1991) Isolated Hepatocytes: Preparation, Properties and Applications: Preparation, Properties and Applications (Vol. 21). Elsevier

Bianco NR, Kim SH, Morelli AE, et al. (2007) Modulation of the immune response using dendritic cell-derived exosomes. Immunological Tolerance: Methods and Protocols 443-455

Bihrer V, Friedrich-Rust M, Kronenberger B, et al. (2011) Serum miR-122 as a biomarker of necroinflammation in patients with chronic hepatitis C virus infection. The American journal of gastroenterology 106(9):1663-1669

Bioulac-Sage P, Le Bail B, Balabaud C (1999) Liver and biliary tract histology. Textbook of Hepatology: From Basic Science to Clinical Practice, Third Edition:9-19

Bjornsson ES & Jonasson JG (2013). Drug-induced cholestasis. Clinics in liver disease 17(2): 191-209

Boelsterli UA (2003) Diclofenac-induced liver injury: a paradigm of idiosyncratic drug toxicity. Toxicology and applied pharmacology 192(3): 307-322

Boelsterli UA, Lim PL (2007) Mitochondrial abnormalities—a link to idiosyncratic drug hepatotoxicity? Toxicology and applied pharmacology 220(1):92-107

Bogaards J, Bertrand M, Jackson P, et al. (2000) Determining the best animal model for human cytochrome P450 activities: a comparison of mouse, rat, rabbit, dog, micropig, monkey and man. Xenobiotica 30(12):1131-1152

Bogert PT, LaRusso NF (2007) Cholangiocyte biology. Current opinion in gastroenterology 23(3):299-305

Bohnsack MT, Czaplinski K, Gorlich D (2004) Exportin 5 is a RanGTP-dependent dsRNA-binding protein that mediates nuclear export of pre-miRNAs. RNA 10(2):185-191

Boulanger CM, Amabile N, Tedgui A (2006) Circulating Microparticles: A Potential Prognostic Marker for Atherosclerotic Vascular Disease. Hypertension 48(2):180-186

Boyer TD, Wright TL, Manns MP (2011) Zakim and Boyer's hepatology: a textbook of liver disease. Elsevier Health Sciences.

Bradford MM (1976) A rapid and sensitive method for the quantitation of microgram quantities of protein utilizing the principle of protein-dye binding. Analytical biochemistry 72(1-2):248-254

Bradford LD, Kirlin WG (1998) Polymorphism of CYP2D6 in Black populations: implications for psychopharmacology. The International Journal of Neuropsychopharmacology 1(02):173-185

Braeuning A, Ittrich C, Köhle C, et al. (2006) Differential gene expression in periportal and perivenous mouse hepatocytes. FEBS Journal 273(22):5051-5061

Bralet M-P, Branchereau S, Brechot C, Ferry N (1994) Cell lineage study in the liver using retroviral mediated gene transfer. Evidence against the streaming of hepatocytes in normal liver. The American journal of pathology 144(5):896

Brooks KB (1986) IgE Enhances B Cell-Derived Exosomal Induced T Cell Proliferation. Virginia Commonwealth University Richmond, Virginia

Broyles D, Cissell K, Kumar M, Deo S (2012) Solution-phase detection of dual microRNA biomarkers in serum. Analytical and Bioanalytical Chemistry 1(1):543-50

Buege JA, Aust SD (1978) Microsomal lipid peroxidation. Methods in enzymology 52:302-310

Burke AS, MacMillan-Crow LA, Hinson JA (2010) Reactive nitrogen species in paracetamol-induced mitochondrial damage and toxicity in mouse hepatocytes. Chemical research in toxicology 23(7):1286-1292

Burke ZD, Reed KR, Phesse TJ, Sansom OJ, Clarke AR, Tosh D (2009) Liver zonation occurs through a β-catenin–dependent, c-Myc–independent mechanism. Gastroenterology 136(7):2316-2324

Bhushan A, Senutovitch N, Bale SS, et al. (2013) Towards a three-dimensional microfluidic liver platform for predicting drug efficacy and toxicity in humans. Stem Cell Research Therapeutics, 4:16.

Cadoret A, Ovejero C, Terris B, et al. (2002) New targets of beta-catenin signaling in the liver are involved in the glutamine metabolism. Oncogene 21(54):8293-8301

Castellano L, Stebbing J (2013) Deep sequencing of small RNAs identifies canonical and non-canonical miRNA and endogenous siRNAs in mammalian somatic tissues. Nucleic acids research 41(5):3339-3351

Chen TS, Lai RC, Lee MM, Choo ABH, Lee CN, Lim SK (2010) Mesenchymal stem cell secretes microparticles enriched in pre-microRNAs. Nucleic Acids Research 38(1):215-224

Chen W, Koenigs LL, Thompson SJ, et al. (1998) Oxidation of Paracetamol to Its Toxic Quinone Imine and Nontoxic Catechol Metabolites by Baculovirus-Expressed and Purified Human Cytochromes P450 2E1 and 2A6. Chemical Research in Toxicology 11(4):295-301

Chendrimada TP, Gregory RI, Kumaraswamy E, et al. (2005) TRBP recruits the Dicer complex to Ago2 for microRNA processing and gene silencing. Nature 436(7051):740-744

Chitnis NS, Pytel D, Bobrovnikova-Marjon E, et al. (2012) miR-211 is a prosurvival microRNA that regulates chop expression in a PERK-dependent manner. Molecular cell 48(3):353-364

Cimmino A, Calin GA, Fabbri M, et al. (2005) miR-15 and miR-16 induce apoptosis by targeting BCL2. Proceedings of the National Academy of Sciences of the United States of America 102(39):13944-13949

Cissell KA, Rahimi Y, Shrestha S, et al. (2008) Bioluminescence-based detection of microRNA, miR21 in breast cancer cells. Analytical Chemistry 1(7):2319-25

Cocucci E, Racchetti G, Meldolesi J (2009) Shedding microvesicles: artefacts no more. Trends in cell biology 19(2):43-51

Cogger VC, McNerney GP, Nyunt T, et al. (2010) Three-dimensional structured illumination microscopy of liver sinusoidal endothelial cell fenestrations. Journal of structural biology 171(3):382-388

Cohen G (1997) Caspases: the executioners of apoptosis. Biochem j 326:1-16

Colnot S, Perret C (2011) Liver zonation Molecular pathology of liver diseases. Springer:7-16

Conde-Vancells J, Rodriguez-Suarez E, Embade N, et al. (2008) Characterization and comprehensive proteome profiling of exosomes secreted by hepatocytes. Journal of proteome research 7(12):5157-5166

Conde-Vancells J, Rodriguez-Suarez E, Gonzalez E, et al. (2010) Candidate biomarkers in exosome-like vesicles purified from rat and mouse urine samples. PROTEOMICS-Clinical Applications 4(4):416-425

Copple IM, Goldring CE, Kitteringham NR, Park BK (2010) The keap1-nrf2 cellular defense pathway: mechanisms of regulation and role in protection against drug-induced toxicity Adverse Drug Reactions. Springer:233-266

Cortez MA, Calin GA (2009) MicroRNA identification in plasma and serum: a new tool to diagnose and monitor diseases.

Cribb AE, Peyrou M, Muruganandan S, Schneider L (2005) The endoplasmic reticulum in xenobiotic toxicity. Drug metabolism reviews 37(3):405-442

Cullen BR (2004) Transcription and processing of human microRNA precursors. Molecular cell 16(6):861-865

Cullinan SB, Diehl JA (2004) PERK-dependent activation of Nrf2 contributes to redox homeostasis and cell survival following endoplasmic reticulum stress. Journal of Biological Chemistry 279(19):20108-20117

Cullinan SB, Gordan JD, Jin J, Harper JW, Diehl JA (2004) The Keap1-BTB protein is an adaptor that bridges Nrf2 to a Cul3-based E3 ligase: oxidative stress sensing by a Cul3-Keap1 ligase. Molecular and cellular biology 24(19):8477-8486

Cullinan SB, Zhang D, Hannink M, Arvisais E, Kaufman RJ, Diehl JA (2003) Nrf2 is a direct PERK substrate and effector of PERK-dependent cell survival. Molecular and cellular biology 23(20):7198-7209

Daly AK, Donaldson PT, Bhatnagar, et al. (2009) HLA-B* 5701 genotype is a major determinant of drug-induced liver injury due to flucloxacillin. Nature genetics 41(7):816-819

Datta J, Kutay H, Nasser MW, et al. (2008) Methylation mediated silencing of MicroRNA-1 gene and its role in hepatocellular carcinogenesis. Cancer research 68(13):5049-5058

Davies MH, Harrison RF, Elias E, Hübscher SG (1994) Antibiotic-associated acute vanishing bile duct syndrome: a pattern associated with severe, prolonged, intrahepatic cholestasis. Journal of hepatology 20(1):112-116

De La Puente MAG, Calderón E, Espinosa R, Rincón M, Varela JM. (2001) Fatal hepatotoxicity associated with enalapril. Annals of Pharmacotherapy 35(11):1492-1492

DeLeve LD (1997). Glutathione defense in non-parenchymal cells. In Seminars in liver disease 18(4):403-413

DeLeve LD (2007) Hepatic microvasculature in liver injury. In: Seminars in liver disease 27:390-400

Desmet V (1997) Vanishing bile duct syndrome in drug-induced liver disease. Journal of hepatology 26:31-35

Dinkova-Kostova AT, Holtzclaw WD, Cole RN, et al. (2002) Direct evidence that sulfhydryl groups of Keap1 are the sensors regulating induction of phase 2 enzymes that protect against carcinogens and oxidants. Proceedings of the National Academy of Sciences 99(18):11908-11913

Dufour DR, Lott JA, Nolte FS, Gretch DR, Koff RS, Seeff LB (2000) Diagnosis and monitoring of hepatic injury. II. Recommendations for use of laboratory tests in screening, diagnosis, and monitoring. Clinical chemistry 46(12):2050-206

Dulley JR, Grieve PA (1975) A simple technique for eliminating interference by detergents in the Lowry method of protein determination. Analytical biochemistry 64(1):136-141

DuRose JB, Scheuner D, Kaufman RJ, Rothblum LI, Niwa M (2009) Phosphorylation of eukaryotic translation initiation factor 2α coordinates rRNA transcription and translation inhibition during endoplasmic reticulum stress. Molecular and cellular biology 29(15):4295-4307

Duttagupta R, Jiang R, Gollub J, et al. (2011) Impact of cellular miRNAs on circulating miRNA biomarker signatures. PLoS One 6(6):e20769

Earnshaw WC, Martins LM, Kaufmann SH (1999) Mammalian caspases: structure, activation, substrates, and functions during apoptosis. Annual review of biochemistry 68(1):383-424

Esau C, Davis S, Murray SF, et al. (2006) miR-122 regulation of lipid metabolism revealed by in vivo antisense targeting. Cell Metabolism 3(2):87-98

Fabris L, Cadamuro M, Okolicsanyi L (2009) The patient presenting with isolated hyperbilirubinemia. Digestive and Liver Disease 41(6):375-381

Fontana RJ (2008). Acute liver failure including acetaminophen overdose. Medical Clinics of North America 92(4):761-794

Fontana RJ, Hayashi PH, Barnhart H, et al. (2015) Persistent Liver Biochemistry Abnormalities Are More Common in Older Patients and those With Cholestatic Drug Induced Liver Injury. The American journal of gastroenterology 110: 1450-1459

Foss KM, Sima C, Ugolini D, Neri M, Allen KE, Weiss GJ (2011) miR-1254 and miR-574-5p: serum-based microRNA biomarkers for early-stage non-small cell lung cancer. Journal of Thoracic Oncology 6(3):482-488

Fredriksson L, Wink S, Herpers B, et al. (2014) Drug-induced endoplasmic reticulum and oxidative stress responses independently sensitize toward TNFα-mediated hepatotoxicity. Toxicological Sciences 140(1):144-159

Frier BM, Stewart WK. (1977). Cholestatic jaundice following chlorpropamide self-poisoning. Clinical toxicology 11(1):13-17

Fu D, Wakabayashi Y, Lippincott-Schwartz J, Arias IM (2011) Bile acid stimulates hepatocyte polarization through a cAMP-Epac-MEK-LKB1-AMPK pathway. Proceedings of the National Academy of Sciences 108(4):1403-1408

Fukuhara T, Kambara H, Shiokawa M, et al. (2012) Expression of microRNA miR-122 facilitates an efficient replication in nonhepatic cells upon infection with hepatitis C virus. Journal of virology 86(15):7918-7933

Funk C, Pantze M, Jehle L, et al. (2001) Troglitazone-induced intrahepatic cholestasis by an interference with the hepatobiliary export of bile acids in male and female rats. Correlation with the gender difference in troglitazone sulfate formation and the inhibition of the canalicular bile salt export pump (Bsep) by troglitazone and troglitazone sulfate. Toxicology 167(1):83-98

García-Monzón C, Majano PL, Zubia I, Sanz P, Apolinario A, Moreno-Otero R (2000) Intrahepatic accumulation of nitrotyrosine in chronic viral hepatitis is associated with histological severity of liver disease. Journal of hepatology 32(2):331-338

Ge Q, Zhou Y, Lu J, Bai Y, Xie X, Lu Z (2014) miRNA in plasma exosome is stable under different storage conditions. Molecules 19(2):1568-1575

Gebhardt R (1992) Metabolic zonation of the liver: regulation and implications for liver function. Pharmacology & therapeutics 53(3):275-354

Gibson GG, Skett P (2001) Introduction to drug metabolism. Nelson Thornes

Girard M, Jacquemin E, Munnich A, Lyonnet S, Henrion-Caude A (2008) miR-122, a paradigm for the role of microRNAs in the liver. Journal of hepatology 48(4):648-656

Glaser S, Francis H, DeMorrow S, et al. (2006) Heterogeneity of the intrahepatic biliary epithelium. World journal of gastroenterology: World Journal of Gastroenterology 12(22):3523-3536

Graham DJ, Green L, Senior JR, Nourjah P (2003a). Troglitazone-induced liver failure: a case study. The American journal of medicine 114(4):299-306

Graham DJ, Drinkard CR, Shatin D (2003b). Incidence of idiopathic acute liver failure and hospitalized liver injury in patients treated with troglitazone. The American journal of gastroenterology 98(1):175-179

Gramantieri L, Ferracin M, Fornari F, et al. (2007) Cyclin G1 is a target of miR-122a, a microRNA frequently down-regulated in human hepatocellular carcinoma. Cancer research 67(13):6092-6099

Green DR, Reed JC (1998) Mitochondria and apoptosis. Science 281(5381):1309

Hajdu D, Aiglová K, Vinklerová I, Urbánek K (2009) Acute cholestatic hepatitis induced by fenofibrate. Journal of clinical pharmacy and therapeutics 34(5):599-602

Harrill A, Roach J, Fier I, et al. (2012) The effects of heparins on the liver: application of mechanistic serum biomarkers in a randomized study in healthy volunteers. Clinical Pharmacology & Therapeutics 92(2):214-220

Häussinger D, Lamers W, Moorman A (1991) Hepatocyte heterogeneity in the metabolism of amino acids and ammonia. Enzyme 46(1-3):72-93

Hayes JD, McLellan LI (1999) Glutathione and glutathione-dependent enzymes represent a co-ordinately regulated defence against oxidative stress. Free radical research 31(4):273-300

Hengstler JG, Van der Burg B, Steinberg P, Oesch F (1999) Interspecies differences in cancer susceptibilty and toxicity 1*. Drug metabolism reviews 31(4):917-970

Herrera M, Fonsato V, Gatti S, et al. (2010) Human liver stem cell-derived microvesicles accelerate hepatic regeneration in hepatectomized rats. Journal of cellular and molecular medicine 14(6b):1605-1618

Heslop JA, Rowe C, Walsh J, Sison-Young R, Jenkins R, Kamalian L, Park BK (2016) Mechanistic evaluation of primary human hepatocyte culture using global proteomic analysis reveals a selective dedifferentiation profile. Archives of Toxicology 1-14

Hinson JA, Michael SL, Ault SG, Pumford NR (2000) Western blot analysis for nitrotyrosine protein adducts in livers of saline-treated and paracetamol-treated mice. Toxicological sciences 53(2):467-473

Hinson JA, Pike SL, Pumford NR, Mayeux PR (1998) Nitrotyrosine−Protein Adducts in Hepatic Centrilobular Areas following Toxic Doses of Paracetamol in Mice. Chemical Research in Toxicology 11(6):604-607

Holman NS, Mosedale M, Wolf KK, LeCluyse EL, Watkins PB (2016). Sub-toxic alterations in hepatocyte-derived exosomes: an early step in drug-induced liver injury? Toxicological Sciences, kfw047

Horie T, Ono K, Nishi H, et al. (2010) Acute doxorubicin cardiotoxicity is associated with miR-146a-induced inhibition of the neuregulin-ErbB pathway. Cardiovascular research 87(4):656-664

Hornby RJ, Starkey Lewis P, Dear J, Goldring C, Park BK (2014) MicroRNAs as potential circulating biomarkers of drug-induced liver injury: key current and future issues for translation to humans. Expert review of clinical pharmacology 7(3):349-362

Hoofnagle, J. H., Serrano, J., Knoben, J. E., et al. (2013). LiverTox: A website on drug-induced liver injury. Hepatology 57(3):873-874

Hsu S-h, Wang B, Kota J, et al. (2012) Essential metabolic, anti-inflammatory, and anti-tumorigenic functions of miR-122 in liver. The Journal of clinical investigation 122(8):2871

Huang XJ, Choi YK, Im HS, et al. (2006) Aspartate aminotransferase (AST/GOT) and alanine aminotransferase (ALT/GPT) detection techniques. Sensors 6(7):756-782

Hussaini SH, Farrington EA (2007) Idiosyncratic drug-induced liver injury: an overview. Expert Opinion on Drug Safety 6(6):673-684

Ito Y, Bethea NW, Abril ER, Mccuskey RS (2003) Early hepatic microvascular injury in response to paracetamol toxicity. Microcirculation 10(5):391-400

Ito Y, Sørensen KK, Bethea NW, et al. (2007) Age-related changes in the hepatic microcirculation in mice. Experimental gerontology 42(8):789-797

Jaeschke H, Bajt ML (2006) Intracellular signaling mechanisms of paracetamol-induced liver cell death. Toxicological sciences 89(1):31-41

Jaeschke H, McGill MR (2013) Serum Glutamate Dehydrogenase—Biomarker for Liver Cell Death or Mitochondrial Dysfunction? Toxicological Sciences

Jaeschke H, McGill MR, Ramachandran A (2012) Oxidant stress, mitochondria, and cell death mechanisms in drug-induced liver injury: lessons learned from paracetamol hepatotoxicity. Drug metabolism reviews 44(1):88-106

James LP, Mayeux PR, Hinson JA (2003) Paracetamol-induced hepatotoxicity. Drug metabolism and disposition 31(12):1499-1506

Jiang L, Duan D, Shen Y, Li J (2012) Direct microRNA detection with universal tagged probe and time-resolved fluorescence technology. Biosensors and Bioelectronics 1(1):291-5

Johnsen KB, Gudbergsson JM, Skov MN, et al. (2014) A comprehensive overview of exosomes as drug delivery vehicles—endogenous nanocarriers for targeted cancer therapy. Biochimica et Biophysica Acta (BBA)-Reviews on Cancer 1846(1):75-87

Jollow D, Mitchell J, Potter W, Davis D, Gillette J, Brodie B (1973) Paracetamol-induced hepatic necrosis. II. Role of covalent binding in vivo. Journal of Pharmacology and Experimental Therapeutics 187(1):195-202

Jopling CL, Yi M, Lancaster AM, Lemon SM, Sarnow P (2005) Modulation of Hepatitis C Virus RNA Abundance by a Liver-Specific MicroRNA. Science 309(5740):1577-1581

Jungermann K (1995) Zonation of metabolism and gene expression in liver. Histochemistry and cell biology 103(2):81-91

Jungermann K, Keitzmann T (1996) Zonation of Parenchymal and Nonparenchymal Metabolism in Liver. Annual Review of Nutrition 16(1):179-203

Jy W, Horstman LL, Jimenez JJ, Ahn YS (2004) Measuring circulating cell-derived microparticles. Journal of Thrombosis and Haemostasis 2(10):1842-1843

Kanduc D, Mittelman A, Serpico R, et al (2002) Cell death: apoptosis versus necrosis. International journal of oncology 21(1):165-170

Kanno N, LeSage G, Glaser S, Alvaro D, Alpini G (2000) Functional heterogeneity of the intrahepatic biliary epithelium. Hepatology 31(3):555-561

Kaplowitz N (2006) Rules and laws of drug hepatotoxicity. Pharmacoepidemiology and drug safety 15(4):231-233

Katase N, Terada K, Suzuki T, Nishimatsu S-i, Nohno T (2015) miR-487b, miR-3963 and miR-6412 delay myogenic differentiation in mouse myoblast-derived C2C12 cells. BMC cell biology 16(1):13

Kenna JG, Neuberger J, Williams R (1987) Specific antibodies to halothane-induced liver antigens in halothane-associated hepatitis. British journal of anaesthesia 59(10):1286-1290

Kia R, Kelly L, Sison-Young RL, et al. (2014) MicroRNA-122: a novel hepatocyte-enriched in vitro marker of drug-induced cellular toxicity. Toxicological Sciences 144(1):173-185

Kmiec Z (2001) Cooperation of liver cells in health and disease: with 18 tables, vol 161. Springer Science & Business Media

Koek GH, Stricker BH, Blok APR, et al. (1994) Flucloxacillin-associated hepatic injury. Liver 14(5):225-229

Kolios G, Valatas V, Kouroumalis E (2006) Role of Kupffer cells in the pathogenesis of liver disease. World Journal of Gastroenterology 12(46):7413

Koutedakis Y, Raafat A, Sharp NC, Rosmarin MN, Beard MJ, Robbins SW (1993) Serum enzyme activities in individuals with different levels of physical fitness. The Journal of sports medicine and physical fitness 33(3):252

Kozomara A, Griffiths-Jones S (2011) miRBase: integrating microRNA annotation and deep-sequencing data. Nucleic Acids Research 39:152–7

Krämer N, Löfström C, Vigre H, et al. (2011) A novel strategy to obtain quantitative data for modelling: combined enrichment and real-time PCR for enumeration of salmonellae from pig carcasses. International Journal of Food Microbiology 145:S86-S95

Krützfeldt J, Rajewsky N, Braich, R., et al. (2005) Silencing of microRNAs in vivo with 'antagomirs'. Nature 438(7068):685-689.

Kubo M, Yonemoto K, Ninomiya T, et al. (2007) Liver enzymes as a predictor for incident diabetes in a Japanese population: the Hisayama study. Obesity 15(7):1841-1850

Kutay H, Bai S, Datta J, et al. (2006) Downregulation of miR-122 in the rodent and human hepatocellular carcinomas. Journal of cellular biochemistry 99(3):671-678

Labbe G, Pessayre D, Fromenty B (2008) Drug-induced liver injury through mitochondrial dysfunction: mechanisms and detection during preclinical safety studies. Fundamental & clinical pharmacology 22(4):335-353

Labowitz JK, Silverman WB. (1997). Case report: Cholestatic jaundice induced by ciprofloxacin. Digestive diseases and sciences 42(1):192-194

Lagarriga J, Buenrrostro C, Rodríguez P, Castañeda J (1976) Hepatinecrosis caused by furosemide. Special lesions of various species? Revista de gastroenterologia de Mexico 42(3):117-125

Lagos-Quintana M, Rauhut R, Yalcin A, Meyer J, Lendeckel W, Tuschl T (2002) Identification of tissue-specific microRNAs from mouse. Current Biology 12(9):735-739

Lakehal F, Wendum D, Barbu V, et al. (1999) Phase I and phase II drug-metabolizing enzymes are expressed and heterogeneously distributed in the biliary epithelium. Hepatology 30(6):1498-1506

Larosche I, Lettéron P, Berson A, et al. (2010) Hepatic mitochondrial DNA depletion after an alcohol binge in mice: probable role of peroxynitrite and modulation by manganese superoxide dismutase. Journal of Pharmacology and Experimental Therapeutics 332(3):886-897

Lazaridis KN, Strazzabosco M, LaRusso NF (2004) The cholangiopathies: disorders of biliary epithelia. Gastroenterology 127(5):1565-1577

LeCluyse EL, Witek RP, Andersen ME, Powers MJ (2012) Organotypic liver culture models: meeting current challenges in toxicity testing. Critical reviews in toxicology 42(6):501-548

Lee SS, Buters JT, Pineau T, Fernandez-Salguero P, et al. (1996) Role of CYP2E1 in the hepatotoxicity of acetaminophen. Journal of Biological Chemistry 271(20):12063-12067

Lee J, Kim J, Lee S, Kim K (2009) Role of protein tyrosine nitration in neurodegenerative diseases and atherosclerosis. Arch Pharm Res 32(8):1109-1118

Lee K-L, Kenney FT (1970) Induction of alanine transaminase by adrenal steroids in cultured hepatoma cells. Biochemical and biophysical research communications 40(2):469-475

Lee Y, Ahn C, Han J, et al. (2003) The nuclear RNase III Drosha initiates microRNA processing. Nature 425(6956):415-419

Lewis DF, Ioannides C, Parke DV (1998) Cytochromes P450 and species differences in xenobiotic metabolism and activation of carcinogen. Environmental health perspectives 106(10):633

Lewis JH, Larrey D, Olsson R, Lee WM, Frison L, Keisu M (2008) Utility of the Roussel Uclaf Causality Assessment Method (RUCAM) to analyze the hepatic findings in a clinical trial program: evaluation of the direct thrombin inhibitor ximelagatran. International journal of clinical pharmacology and therapeutics 46(7):327-339

Li W-C, Ralphs KL, Tosh D (2010) Isolation and culture of adult mouse hepatocytes Mouse Cell Culture. Springer, p 185-196

Limaye PB, Bowen WC, Orr AV, Luo J, Tseng GC, Michalopoulos GK (2008) Mechanisms of hepatocyte growth factor–mediated and epidermal growth factor–mediated signaling in transdifferentiation of rat hepatocytes to biliary epithelium. Hepatology 47(5):1702-1713

Lindblom P, Rafter I, Copley C, et al. (2007) Isoforms of alanine aminotransferases in human tissues and serum—Differential tissue expression using novel antibodies. Archives of Biochemistry and Biophysics 466(1):66-77

Lindros KO (1997) Zonation of cytochrome P450 expression, drug metabolism and toxicity in liver. General Pharmacology: The Vascular System 28(2):191-196

Lowry OH, Rosebrough NJ, Farr AL, Randall RJ (1951) Protein measurement with the Folin phenol reagent. J biol Chem 193(1):265-275

Lu J, Getz G, Miska EA, et al. (2005) MicroRNA expression profiles classify human cancers. nature 435(7043):834-838

Rodríguez LAG, Stricker BH, Zimmerman HJ (1996) Risk of acute liver injury associated with the combination of amoxicillin and clavulanic acid. Archives of internal medicine 156(12):1327-1332

MacMillan-Crow LA, Crow JP, Thompson JA (1998) Peroxynitrite-Mediated Inactivation of Manganese Superoxide Dismutase Involves Nitration and Oxidation of Critical Tyrosine Residues†. Biochemistry 37(6):1613-1622

Malhotra JD, Kaufman RJ (2007) Endoplasmic reticulum stress and oxidative stress: a vicious cycle or a double-edged sword? Antioxidants & redox signaling 9(12):2277-2294

Mantena S, Vaughn D, Andringa K, et al. (2009) High fat diet induces dysregulation of hepatic oxygen gradients and mitochondrial function in vivo. Biochem J 417:183-193

Marciniak SJ, Yun CY, Oyadomari S, et al. (2004) CHOP induces death by promoting protein synthesis and oxidation in the stressed endoplasmic reticulum. Genes & development 18(24):3066-3077

Marzioni M, Glaser SS, Francis H, Phinizy JL, LeSage G, Alpini G Functional heterogeneity of cholangiocytes. In: Seminars in liver disease, 2002. vol 22. p 227-240

Maschmeyer I, Lorenz, AK, Schimek K, et al. (2015) A four-organ-chip for interconnected long-term co-culture of human intestine, liver, skin and kidney equivalents. Lab on a Chip 15(12):2688-2699

Matsunaga N, Nakamura N, Yoneda N, Qin T, et al. (2004) Influence of feeding schedule on 24-h rhythm of hepatotoxicity induced by acetaminophen in mice. Journal of Pharmacology and Experimental Therapeutics 311(2):594-600

McGill MR, Sharpe MR, Williams CD, Taha M, Curry SC, Jaeschke H (2012) The mechanism underlying paracetamol-induced hepatotoxicity in humans and mice involves mitochondrial damage and nuclear DNA fragmentation. The Journal of Clinical Investigation 122(4):1574-1583

Meister A, Anderson ME (1983) Glutathione. Annual review of biochemistry 52(1):711-760

Mesri M, Altieri DC (1999) Leukocyte microparticles stimulate endothelial cell cytokine release and tissue factor induction in a JNK1 signaling pathway. Journal of Biological Chemistry 274(33):23111-23118

Minamide Y, Horiea T, Tomaru A, Awazu S (1998) Spontaneous chemiluminescence production, lipid peroxidation, and covalent binding in rat hepatocytes exposed to paracetamol. Journal of pharmaceutical sciences 87(5):640-646

Mitchell J, Jollow D, Potter W, Gillette J, Brodie B (1973) Paracetamol-induced hepatic necrosis. IV. Protective role of glutathione. Journal of Pharmacology and Experimental Therapeutics 187(1):211-217

Mitchell J, Nelson W, Potter W, Sasame H, Jollow D (1976) Metabolic activation of furosemide to a chemically reactive, hepatotoxic metabolite. Journal of Pharmacology and Experimental Therapeutics 199(1):41-52

Mitchell JR, Potter WZ, Hinson JA, Jollow DJ (1974) Hepatic necrosis caused by furosemide. Letters to Nature 251:508-511

Mitchell PS, Parkin RK, Kroh EM, et al. (2008) Circulating microRNAs as stable blood-based markers for cancer detection. Proceedings of the National Academy of Sciences 105(30):10513-10518

Mittelbrunn M, Gutiérrez-Vázquez C, Villarroya-Beltri C, et al. (2011) Unidirectional transfer of microRNA-loaded exosomes from T cells to antigen-presenting cells. Nature communications 2:282

Miyaki S, Sato T, Inoue A, et al. (2010) MicroRNA-140 plays dual roles in both cartilage development and homeostasis. Genes & development 24(11):1173-1185

Molinari M, Watt KD., Kruszyna T, et al. (2006). Acute liver failure induced by green tea extracts: case report and review of the literature. Liver transplantation 12(12):1892-1895.

Momen-Heravi F, Bala S, Kodys K, Szabo G (2015) Exosomes derived from alcohol-treated hepatocytes horizontally transfer liver specific miRNA-122 and sensitize monocytes to LPS. Scientific reports 5

Morrison GR, Karl IE, Schwartz R, et al. (1965). The quantitative histochemistry of the normal human liver lobule. The Journal of laboratory and clinical medicine 65(2): 248-256

Mühlberger N, Kraft W (1994). Diagnostic value of glutamate dehydrogenase determination in the dog. Tierarztliche Praxis 22(6):567-573

Murphy EJ, Davern TJ, Obaid S, et al. (2000). Troglitazone-induced fulminant hepatic failure. Digestive diseases and sciences 45(3):549-553

Murphy K, Dorfman S, Smith N, et al. (2015) U.S. Patent No. 8,931,880. Washington, DC: U.S. Patent and Trademark Office

Nguyen T, Sherratt PJ, Pickett CB (2003) Regulatory mechanisms controlling gene expression mediated by the antioxidant response element. Annual review of pharmacology and toxicology 43(1):233-260

Nilsson J, Skog J, Nordstrand A, et al. (2009) Prostate cancer-derived urine exosomes: a novel approach to biomarkers for prostate cancer. British journal of cancer 100(10):1603-1607

Nishio A, Keeffe EB, Ishibashi H, Gershwin EM (2000) Diagnosis and treatment of primary biliary cirrhosis. Medical Science Monitor 6(1):RA181-RA193

Noce R, Paredes BE, Pichler WJ, Krähenbühl S (2000) Acute generalized exanthematic pustulosis (AGEP) in a patient treated with furosemide. The American journal of the medical sciences 320(5):331-333

Nojima H, Wilson G, Quillin R, et al. (2014) Hepatocyte-derived exosomes regulate liver recovery and regeneration after ischemia/reperfusion in mice (398.3). The FASEB Journal 28(1 Supplement):398.3

Notenboom RG, Moorman AF, Lamers WH (1997) Developmental appearance of ammonia-metabolizing enzymes in prenatal murine liver. Microscopy research and technique 39(5):413-423

O'Brien PJ, Slaughter MR, Polley SR, Kramer K (2002) Advantages of glutamate dehydrogenase as a blood biomarker of acute hepatic injury in rats. Laboratory Animals 36(3):313-321

O'Grady JG, Alexander GJ, Hayllar KM, Williams R (1989) Early indicators of prognosis in fulminant hepatic failure. Gastroenterology 97(2):439-445

Ogata-Kawata H, Izumiya M, Kurioka D, et al. (2014) Circulating exosomal microRNAs as biomarkers of colon cancer. PLoS One 9(4):e92921

Ohmori S, Shiraki K, Inoue H, et al. (2003) Clinical characteristics and prognostic indicators of drug-induced fulminant hepatic failure. Hepato-gastroenterology 50(53):1531-1534

Ohshima H, Friesen M, Brouet I, Bartsch H (1990) Nitrotyrosine as a new marker for endogenous nitrosation and nitration of proteins. Food and chemical toxicology 28(9):647-652

Ong MM, Latchoumycandane C, Boelsterli UA (2007) Troglitazone-induced hepatic necrosis in an animal model of silent genetic mitochondrial abnormalities. Toxicological Sciences 97(1):205-213

Oosthuyzen W, Sime NEL, Ivy JR, et al. (2013) Quantification of human urinary exosomes by nanoparticle tracking analysis. The Journal of physiology 591(23):5833-5842

Ørom UA, Nielsen FC, Lund AH (2008) MicroRNA-10a Binds the 5′UTR of Ribosomal Protein mRNAs and Enhances Their Translation. Molecular cell 30(4):460-471

Ostapowicz G, Fontana RJ, Schiødt FV, et al. (2002) Results of a prospective study of acute liver failure at 17 tertiary care centers in the United States. Annals of internal medicine 137(12):947-954

Ozer J, Ratner M, Shaw M, Bailey W, Schomaker S (2008) The current state of serum biomarkers of hepatotoxicity. Toxicology 245(3):194-205

Packer AN, Xing Y, Harper SQ, Jones L, Davidson BL (2008) The bifunctional microRNA miR-9/miR-9* regulates REST and CoREST and is downregulated in Huntington's disease. The Journal of Neuroscience 28(53):14341-14346

Padda MS, Sanchez M, Akhtar AJ, Boyer JL (2011) Drug-induced cholestasis. Hepatology 53(4):1377-1387

Pan B-T, Johnstone RM (1983) Fate of the transferrin receptor during maturation of sheep reticulocytes in vitro: selective externalization of the receptor. Cell 33(3):967-978

Park BK, Boobis A, Clarke S, et al. (2011) Managing the challenge of chemically reactive metabolites in drug development. Nature Reviews Drug Discovery 10(4):292-306

Parker WA, Shearer CA (1979). Phenytoin hepatotoxicity: A case report and review. Neurology 29(2):175-175

Parola M, Pinzani M (2009) Fibrogenesis & Tissue Repair 2:4

Passonneau JV, Lowry OH (1993) Enzymatic analysis: a practical guide

Pasquinelli AE, Reinhart BJ, Slack F, et al. (2000) Conservation of the sequence and temporal expression of let-7 heterochronic regulatory RNA. Nature 408(6808):86-89

Patten CJ, Thomas PE, Guy RL, et al. (1993) Cytochrome P450 enzymes involved in paracetamol activation by rat and human liver microsomes and their kinetics. Chemical research in toxicology 6(4):511-518

Pauli A, Rinn JL, Schier AF (2011) Non-coding RNAs as regulators of embryogenesis. Nature Reviews Genetics 12(2):136-149

Penna A, Buchanan N (1991) Paracetamol poisoning in children and hepatotoxicity. British Journal of Clinical Pharmacology 32(2):143-9

Pfaff N, Fiedler J, Holzmann A, et al. (2011) miRNA screening reveals a new miRNA family stimulating iPS cell generation via regulation of Meox2. EMBO reports 12(11):1153-1159

Pfeiffer S, Lass A, Schmidt K, Mayer B (2001) Protein Tyrosine Nitration in Cytokine-activated Murine Macrophages: Involvement of a peroxidase/nitrate pathway rather than peroxynitrate. Journal of Biological Chemistry 276(36):34051-34058

Pfeiffer S, Schmidt K, Mayer B (2000) Dityrosine Formation Outcompetes Tyrosine Nitration at Low Steady-state Concentrations of Peroxynitrite: Implications for tyrosine modification by nitric oxide/superoxide in vivo. Journal of Biological Chemistry 275(9):6346-6352

Pisitkun T, Shen R-F, Knepper MA (2004) Identification and proteomic profiling of exosomes in human urine. Proceedings of the National Academy of Sciences of the United States of America 101(36):13368-13373

Ponto LLB, Schoenwald RD (1990) Furosemide (frusemide). Clinical pharmacokinetics 18(6):460-471

Qiu Y, Benet LZ, Burlingame A (2001) Identification of hepatic protein targets of the reactive metabolites of the non-hepatotoxic regioisomer of paracetamol, 3'-hydroxyacetanilide, in the mouse in vivo using two-dimensional gel electrophoresis and mass spectrometry Biological Reactive Intermediates VI. Springer, p 663-673

Qu B, Li Q-T, Wong KP, Tan TM, Halliwell B (2001) Mechanism of clofibrate hepatotoxicity: mitochondrial damage and oxidative stress in hepatocytes. Free Radical Biology and Medicine 31(5):659-669

Qu Q, Liu J, Zhou H-H, Klaassen CD (2014) Nrf2 protects against furosemide-induced hepatotoxicity. Toxicology 324:35-42

Radi R (2004) Nitric oxide, oxidants, and protein tyrosine nitration. Proceedings of the National Academy of Sciences 101(12):4003-4008

Raha A, Tew KD (1996) Glutathione S-transferases. In Drug resistance (83-122).

Ramadori G, Moriconi F, Malik I, Dudas J (2008) Physiology and pathophysiology of liver inflammation, damage and repair. J Physiol pharmacol 59(Suppl 1):107-117

Ramaiah SK (2007) A toxicologist guide to the diagnostic interpretation of hepatic biochemical parameters. Food and chemical toxicology 45(9):1551-1557

Ramakrishnaiah V, Thumann C, Fofana I, et al. (2013) Exosome-mediated transmission of hepatitis C virus between human hepatoma Huh7. 5 cells. Proceedings of the National Academy of Sciences 110(32):13109-13113

Randle LE, Goldring CE, Benson CA, et al. (2008) Investigation of the effect of a panel of model hepatotoxins on the Nrf2-Keap1 defence response pathway in CD-1 mice. Toxicology 243(3):249-260

Rang HP, Ritter JM, Flower RJ, Henderson G (2014) Rang & Dale's Pharmacology. Elsevier Health Sciences

Rao RV, Ellerby H, Bredesen DE (2004) Coupling endoplasmic reticulum stress to the cell death program. Cell Death & Differentiation 11(4):372-380

Rappaport A (1977) Microcirculatory units in the mammalian liver. Their arterial and portal components. Bibliotheca anatomica(16 Pt 2):116

Rautou P-E, Mansouri A, Lebrec D, Durand F, Valla D, Moreau R (2010) Autophagy in liver diseases. Journal of hepatology 53(6):1123-1134

Read A, Harrison C, Sherlock S (1961) Chronic chlorpromazine jaundice: with particular reference to its relationship to primary biliary cirrhosis. The American journal of medicine 31(2):249-258

Reed DJ, Fariss MW (1984) Glutathione depletion and susceptibility. Pharmacological reviews 36(2):25S-33S

Ren X-Y, Li Y-N, Qi J-S, Niu T (2008) Peroxynitrite-induced protein nitration contributes to liver mitochondrial damage in diabetic rats. Journal of Diabetes and its Complications 22(5):357-364

Rochon J, Protiva P, Seeff LB, et al. (2008) Reliability of the Roussel Uclaf Causality Assessment Method for assessing causality in drug-induced liver injury. Hepatology 48(4):1175-1183

Rodes J BJ-P, Blei A, Reichen J, Rizzetto M. (2007) Textbook of Hepatology: From Basic Science to Clinical Practice. Wiley-Blackwell Publishing

Royo F, Schlangen K, Palomo L, et al. (2013) Transcriptome of extracellular vesicles released by hepatocytes. PloS one 8(7)

Rowe C, Goldring CE, Kitteringham NR, et al. (2010) Network analysis of primary hepatocyte dedifferentiation using a shotgun proteomics approach. Journal of proteome research 9(5):2658-2668

Rushmore TH, Tony Kong A (2002) Pharmacogenomics, regulation and signaling pathways of phase I and II drug metabolizing enzymes. Current drug metabolism 3(5):481-490

Sabatier F, Darmon P, Hugel B, et al. (2002) Type 1 and type 2 diabetic patients display different patterns of cellular microparticles. Diabetes 51(9):2840-2845

Sacerdoti D, Gatta A, McGiff JC (2003) Role of cytochrome P450-dependent arachidonic acid metabolites in liver physiology and pathophysiology. Prostaglandins & other lipid mediators 72(1):51-71

Sanges D, Marigo V (2006) Cross-talk between two apoptotic pathways activated by endoplasmic reticulum stress: differential contribution of caspase-12 and AIF. Apoptosis 11(9):1629-1641

Sanz-Cameno P, Medina J, García-Buey L, et al. (2002) Enhanced intrahepatic inducible nitric oxide synthase expression and nitrotyrosine accumulation in primary biliary cirrhosis and autoimmune hepatitis. Journal of hepatology 37(6):723-729

Savill J, Fadok V, Henson P, Haslett C (1993) Phagocyte recognition of cells undergoing apoptosis. Immunology today 14(3):131-136

Schenker S, Speeg Jr KV, Perez A, Finch J (2001) The effects of food restriction in man on hepatic metabolism of paracetamol. Clinical Nutrition 20(2):145-150

Schomaker S, Warner R, Bock J, et al. (2013) Assessment of Emerging Biomarkers of Liver Injury in Human Subjects. Toxicological Sciences 132(2):276-283

Schrenk D, Eisenmann-Tappe I, Gebhardt R, et al. (1991) Drug metabolizing enzyme activities in rat liver epithelial cell lines, hepatocytes and bile duct cells. Biochemical pharmacology 41(11):1751-1757

Seggie J, Saunders SJ, Kirsch RE, et al. (1979). Patterns of hepatic injury induced by methyldopa. South African medical journal 55(3): 75-83

Sharkey JW, Antoine DJ, Park BK (2012) Validation of the isolation and quantification of kidney enriched miRNAs for use as biomarkers. Biomarkers 17(3):231-239

Sharma K, Karl B, Mathew AV, et al. (2013) Metabolomics reveals signature of mitochondrial dysfunction in diabetic kidney disease. Journal of the American Society of Nephrology 24(11):1901-1912

Shen W, Deng H, Ren Y, Gao Z (2013) A real-time colorimetric assay for label-free detection of microRNAs down to sub-femtomolar levels. Chemical Communications 49(43):4959-61

Shen HM (2014) Necrotic Cell Death. P. Vandenabeele (Ed.). Springer New York.

Shen Pf, Chen Xq, Liao Yc, et al. (2014) MicroRNA-494-3p targets CXCR4 to suppress the proliferation, invasion, and migration of prostate cancer. The Prostate 74(7):756-767

Sherlock S (1998) Overview of chronic cholestatic conditions in adults: terminology and definitions. Clinics in liver disease 2(2):217-233

Shi Q, Hong H, Senior J, Tong W (2010) Biomarkers for drug-induced liver injury. Expert Review of Gastroenterology & Hepatology 4(2):225-234

Simon, J. B., Manley, P. N., Brien, J. F., et al. (1984). Amiodarone hepatotoxicity simulating alcoholic liver disease. New England Journal of Medicine 311(3):167-172

Singh R (2010) Autophagy and regulation of lipid metabolism Sensory and Metabolic Control of Energy Balance. Springer, p 35-46

Smith MT, Wills ED (1981) Effects of dietary lipid and phenobarbitone on the distribution and concentration of cytochrome P-450 in the liver studied by quantitative cytochemistry. FEBS letters 127(1):33-36

Sokal, E. M., Trivedi, P., Portmann, B., et al. (1989). Developmental changes in the intra-acinar distribution of succinate dehydrogenase, glutamate dehydrogenase, glucose-6-phosphatase, and NADPH dehydrogenase in the rat liver. Journal of pediatric gastroenterology and nutrition 8(4): 522-527

Souza JM, Daikhin E, Yudkoff M, Raman CS, Ischiropoulos H (1999) Factors Determining the Selectivity of Protein Tyrosine Nitration. Archives of Biochemistry and Biophysics 371(2):169-178

Starkey Lewis PJ, Dear J, Platt V, et al. (2011) Circulating microRNAs as potential markers of human drug-induced liver injury. Hepatology 54(5):1767-1776

Stern-Ginossar N, Elefant N, Zimmermann A, et al. (2007) Host immune system gene targeting by a viral miRNA. Science 317(5836):376-381

Strazzabosco M, Spirlì C, Okolicsanyi L (2000) Pathophysiology of the intrahepatic biliary epithelium. Journal of gastroenterology and hepatology 15(3):244-253

Stricker BC, Van Den Broek JWG, Keuning J, et al. (1989). Cholestatic hepatitis due to antibacterial combination of amoxicillin and clavulanic acid (Augmentin). Digestive diseases and sciences 34(10):1576-1580

Suntres ZE, Smith MG, Momen-Heravi F, et al. (2013) Therapeutic uses of exosomes. Exosomes Microvesicles 1(5)

Tajiri K, Shimizu Y (2008) Practical guidelines for diagnosis and early management of drug-induced liver injury. World Journal of Gastroenterology 14(44):6774

Tan Y, Ge G, Pan T, et al. (2014a) A serum microRNA panel as potential biomarkers for hepatocellular carcinoma related with hepatitis B virus. PloS one 9(9):e107986

Tan CY, Lai RC, Wong W, Dan YY, Lim S-K, Ho HK (2014b) Mesenchymal stem cell-derived exosomes promote hepatic regeneration in drug-induced liver injury models. Stem Cell Res Ther 5:76

Tao C, Huang S, Wang Y, et al. (2015) Changes in white and brown adipose tissue microRNA expression in cold-induced mice. Biochemical and biophysical research communications

Tay Y, Zhang J, Thomson AM, Lim B, Rigoutsos I (2008) MicroRNAs to Nanog, Oct4 and Sox2 coding regions modulate embryonic stem cell differentiation. Nature 455(7216):1124-1128

Taylor JW, Stein MN, Murphy MJ, & Mitros FA (1984). Cholestatic liver dysfunction after long-term phenytoin therapy. Archives of neurology 41(5):500.

Taylor DD, Gercel-Taylor C (2005) Tumour-derived exosomes and their role in cancer-associated T-cell signalling defects. British journal of cancer 92(2):305-311

Taylor DD, Zacharias W, Gercel-Taylor C (2011) Exosome isolation for proteomic analyses and RNA profiling Serum/Plasma Proteomics. Springer, p 235-246

Testa B, Krämer SD (2008) The Biochemistry of Drug Metabolism–An Introduction. Chemistry & biodiversity 5(11):2171-2336

Théry C, Boussac M, Véron P, et al. (2001) Proteomic analysis of dendritic cell-derived exosomes: a secreted subcellular compartment distinct from apoptotic vesicles. The Journal of Immunology 166(12):7309-7318

Thomas DD, Espey MG, Vitek MP, Miranda KM, Wink DA (2002) Protein nitration is mediated by heme and free metals through Fenton-type chemistry: An alternative to the NO/O reaction. Proceedings of the National Academy of Sciences 99(20):12691-12696

Thorgeirsson S, Sasame H, Mitchell J, Jollow D, Potter W (1976) Biochemical changes after hepatic injury from toxic doses of paracetamol or furosemide. Pharmacology 14(3):205-217

Thulin P, Nordahl G, Gry M, et al. (2014) Keratin-18 and microRNA-122 complement alanine aminotransferase as novel safety biomarkers for drug-induced liver injury in two human cohorts. Liver International 34(3):367-378

Thummel KE, Lee CA, Kunze KL, Nelson SD, Slattery JT (1993) Oxidation of paracetamol to N-acetyl-p-aminobenzoquinone imine by Human CYP3A4. Biochemical Pharmacology 45(8):1563-1569

Timbrell J (1999) Principles of biochemical toxicology. CRC Press

Tórtora V, Quijano C, Freeman B, Radi R, Castro L (2007) Mitochondrial aconitase reaction with nitric oxide, S-nitrosoglutathione, and peroxynitrite: Mechanisms and relative contributions to aconitase inactivation. Free Radical Biology and Medicine 42(7):1075-1088

Traber PG, Chianale J, Gumucio JJ (1988) Physiologic significance and regulation of hepatocellular heterogeneity. Gastroenterology 95(4):1130-1143

Tsai W-C, Hsu S-D, Hsu C-S, et al. (2012) MicroRNA-122 plays a critical role in liver homeostasis and hepatocarcinogenesis. The Journal of clinical investigation 122(8):2884

Tunon M, Gonzalez P, Lopez P, Salido G, Madrid J (1992) Circadian rhythms in glutathione and glutathione-S transferase activity of rat liver. Archives Of Physiology And Biochemistry 100(1):83-87

Turchinovich A, Weiz L, Langheinz A, Burwinkel B (2011) Characterization of extracellular circulating microRNA. Nucleic Acids Research 39(16):7223-7233

Turko IV, Murad F (2002) Protein Nitration in Cardiovascular Diseases. Pharmacological Reviews 54(4):619-634

Turner I, Eckstein R, Riley J, Lunzer M (1988) Prolonged hepatic cholestasis after flucloxacillin therapy. The Medical journal of Australia 151(11-12):701-705

Turner R, Lozoya O, Wang Y, et al. (2011) Human hepatic stem cell and maturational liver lineage biology. Hepatology 53(3):1035-1045

Tygstrup N, Winkler K, Mellemgaard K, Andreassen M (1962) Determination of the hepatic arterial blood flow and oxygen supply in man by clamping the hepatic artery during surgery. Journal of Clinical Investigation 41(3):447

Tynes RE, Philpot RM (1987) Tissue-and species-dependent expression of multiple forms of mammalian microsomal flavin-containing monooxygenase. Molecular pharmacology 31(6):569-574

Ugele B, Kempen H, Kempen J, et al. (1991) Heterogeneity of rat liver parenchyma in cholesterol 7 alpha-hydroxylase and bile acid synthesis. Biochem J 276:73-77

Uzi D, Barda L, Scaiewicz V, et al. (2013) CHOP is a critical regulator of paracetamol-induced hepatotoxicity. Journal of hepatology 59(3):495-503

Valadi H, Ekström K, Bossios A, Sjöstrand M, Lee JJ, Lötvall JO (2007) Exosome-mediated transfer of mRNAs and microRNAs is a novel mechanism of genetic exchange between cells. Nature cell biology 9(6):654-659

Vandeputte C, Guizon I, Genestie-Denis I, et al. (1994) A microtiter plate assay for total glutathione and glutathione disulfide contents in cultured/isolated cells: performance study of a new miniaturized protocol. Cell biology and toxicology 10(5-6):415-421

Vassallo JD, Hicks SM, Daston GP, Lehman-McKeeman LD (2004) Metabolic detoxification determines species differences in coumarin-induced hepatotoxicity. Toxicological Sciences 80(2):249-257

Vickers KC, Palmisano BT, Shoucri BM, Shamburek RD, Remaley AT (2011) MicroRNAs are transported in plasma and delivered to recipient cells by high-density lipoproteins. Nature cell biology 13(4):423-433

Villarroya-Beltri C, Gutiérrez-Vázquez C, Sánchez-Cabo F, et al. (2013) Sumoylated hnRNPA2B1 controls the sorting of miRNAs into exosomes through binding to specific motifs. Nature communications 4

Walker R, McElligott T (1981) Furosemide induced hepatotoxicity. The Journal of pathology 135(4):301-314

Wang G-K, Zhu J-Q, Zhang J-T, et al. (2010) Circulating microRNA: a novel potential biomarker for early diagnosis of acute myocardial infarction in humans. European Heart Journal 1(6):659-66

Wang K, Zhang S, Marzolf B, et al. (2009) Circulating microRNAs, potential biomarkers for drug-induced liver injury. Proceedings of the National Academy of Sciences 106(11):4402-4407

Wang X, Thomas B, Sachdeva R, et al. (2006) Mechanism of arylating quinone toxicity involving Michael adduct formation and induction of endoplasmic reticulum stress. Proceedings of the National Academy of Sciences of the United States of America 103(10):3604-3609

Wang Y, Gao J, Zhang D, Zhang J, Ma J, Jiang H (2010) New insights into the antifibrotic effects of sorafenib on hepatic stellate cells and liver fibrosis. Journal of hepatology 53(1):132-144

Wang J, Chen J, Chang P, et al. (2009) MicroRNAs in plasma of pancreatic ductal adenocarcinoma patients as novel blood-based biomarkers of disease. Cancer prevention research 2(9):807-813

Ward RM, Bates BA, Benitz WE, et al. (2001) Acetaminophen toxicity in children. Pediatrics 108(4)

Watanabe S, Yaginuma R, Ikejima K, Miyazaki A (2008) Liver diseases and metabolic syndrome. Journal of gastroenterology 43(7):509-518

Watkins PB., Whitcomb RW (1998) Hepatic dysfunction associated with troglitazone. New England Journal of Medicine 338(13):916-917

Watkins PB (2005) Idiosyncratic liver injury: challenges and approaches. Toxicologic pathology 33(1):1-5

Watkins PB, Kaplowitz N, Slattery JT, et al. (2006) Aminotransferase elevations in healthy adults receiving 4 grams of paracetamol daily: A randomized controlled trial. JAMA 296(1):87-93

Westphal JF, Vetter D, Brogard JM. (1994) Hepatic side-effects of antibiotics. Journal of Antimicrobial Chemotherapy 33(3):387-401

Whitehouse LW, Wong LT, Paul CJ, et al. (1985) Postabsorption antidotal effects of N-acetylcysteine on acetaminophen-induced hepatotoxicity in the mouse. Canadian journal of physiology and pharmacology 63(5):431-437

Wightman B, Bürglin TR, Gatto J, Arasu P, Ruvkun G (1991) Negative regulatory sequences in the lin-14 3'-untranslated region are necessary to generate a temporal switch during Caenorhabditis elegans development. Genes & development 5(10):1813-1824

Williams DP, Antoine DJ, Butler PJ, et al. (2007) The metabolism and toxicity of furosemide in the Wistar rat and CD-1 mouse: a chemical and biochemical definition of the toxicophore. Journal of Pharmacology and Experimental Therapeutics 322(3):1208-1220

Williams GT, Smith CA (1993) Molecular regulation of apoptosis: genetic controls on cell death. Cell 74(5):777-779

Wimmer, M., Luttringer, C., Colombi, M. (1990). Enzyme activity patterns of phosphoenolpyruvate carboxykinase, pyruvate kinase, glucose-6-phosphate-dehydrogenase and malic enzyme in human liver. Histochemistry 93(4): 409-415

Wirth PJ, Bettis CJ, Nelson WL (1976) Microsomal metabolism of furosemide evidence for the nature of the reactive intermediate involved in covalent binding. Molecular pharmacology 12(5):759-768

Wisse E (1970) An electron microscopic study of the fenestrated endothelial lining of rat liver sinusoids. Journal of ultrastructure research 31(1):125-150

Wisse E, De Zanger R, Charels K, Van Der Smissen P, McCuskey R (1985) The liver sieve: considerations concerning the structure and function of endothelial fenestrae, the sinusoidal wall and the space of Disse. Hepatology 5(4):683-692

Wisse, E., Luo, D., Vermijlen, D., Kanellopoulou, C., et al. (1996). On the function of pit cells, the liver-specific natural killer cells. In Seminars in liver disease 17(4):265-286

Witek RP, Yang L, Liu R, et al. (2009) Liver Cell–Derived Microparticles Activate Hedgehog Signaling and Alter Gene Expression in Hepatic Endothelial Cells. Gastroenterology 136(1):320-330.e2

Wong SG, Card JW, Racz WJ (2000) The role of mitochondrial injury in bromobenzene and furosemide induced hepatotoxicity. Toxicology letters 116(3):171-181

Woodhead JL, Howell BA, Yang Y, et al. (2012) An analysis of N-acetylcysteine treatment for acetaminophen overdose using a systems model of drug-induced liver injury. Journal of Pharmacology and Experimental Therapeutics 342(2):529-540

Woolf TF (1999). Handbook of drug metabolism. Marcel Dekker

Wu YM, Joseph B, Berishvili E, Kumaran V, Gupta S (2008) Hepatocyte transplantation and drug-induced perturbations in liver cell compartments. Hepatology 47(1):279-287

Wu D, Cederbaum AI (2008). Development and properties of HepG2 cells that constitutively express CYP2E1. Alcohol: Methods and Protocols 137-150

Xie G, Wang L, Wang X, Wang L, DeLeve LD (2010) Isolation of periportal, midlobular, and centrilobular rat liver sinusoidal endothelial cells enables study of zonated drug toxicity. American Journal of Physiology-Gastrointestinal and Liver Physiology 299(5):G1204-G1210

Xu H, He JH, Xiao ZD, et al. (2010) Liver-enriched transcription factors regulate MicroRNA-122 that targets CUTL1 during liver development. Hepatology 52(4):1431-1442

Xu Y, Xia F, Ma L, et al. (2011) MicroRNA-122 sensitizes HCC cancer cells to adriamycin and vincristine through modulating expression of MDR and inducing cell cycle arrest. Cancer letters 310(2):160-169

Yamaura Y, Nakajima M, Tatsumi N, et al. (2014) Changes in the expression of miRNAs at the pericentral and periportal regions of the rat liver in response to hepatocellular injury: Comparison with the changes in the expression of plasma miRNAs. Toxicology 322:89-98

Yano Y, Kambayashi J, Shiba E, et al. (1994) The role of protein phosphorylation and cytoskeletal reorganization in microparticle formation from the platelet plasma membrane. Biochem J 299:303-308

Yu DS, An FM, Gong BD, et al. (2012) The regulatory role of microRNA-1187 in TNF-α-mediated hepatocyte apoptosis in acute liver failure. International journal of molecular medicine 29(4):663-668

Yu K, Geng X, Chen M, et al. (2014) High daily dose and being a substrate of cytochrome P450 enzymes are two important predictors of drug-induced liver injury. Drug Metabolism and Disposition 42(4):744-750

Zamzami N, Kroemer G (2001) The mitochondrion in apoptosis: how Pandora's box opens. Nature Reviews Molecular Cell Biology 2(1):67-71

Zhan X, Desiderio DM (2006) Nitroproteins from a human pituitary adenoma tissue discovered with a nitrotyrosine affinity column and tandem mass spectrometry. Analytical biochemistry 354(2):279-289

Zhang G-J, Chua JH, Chee R-E, Agarwal A, Wong SM (2009) Label-free direct detection of MiRNAs with silicon nanowire biosensors. Biosensors and Bioelectronics 24(8):2504-2508

Zhang Y, Jia Y, Zheng R, et al. (2010) Plasma microRNA-122 as a biomarker for viral-, alcohol-, and chemical-related hepatic diseases. Clinical chemistry 56(12):1830-1838

Zhao YY, Wang WA, Hu H (2015) Treatment with recombinant tissue plasminogen activator alters the microRNA expression profiles in mouse brain after acute ischemic stroke. Neurological Sciences:1-8

Zheng G, Du L, Yang X, et al. (2014). Serum microRNA panel as biomarkers for early diagnosis of colorectal adenocarcinoma. British journal of cancer 111(10):1985-1992

Zhou H, Gurley EC, Jarujaron S, et al. (2006) HIV protease inhibitors activate the unfolded protein response and disrupt lipid metabolism in primary hepatocytes. American Journal of Physiology-Gastrointestinal and Liver Physiology 291(6):G1071-G1080

Zimmerman HJ (1999) Hepatotoxicity: the adverse effects of drugs and other chemicals on the liver. Lippincott Williams & Wilkins

Zimmerman, HJ (1976). Various forms of chemically induced liver injury and their detection by diagnostic procedures. Environmental health perspectives 15(3)

Review

EXPERT REVIEWS

MicroRNAs as potential circulating biomarkers of drug-induced liver injury: key current and future issues for translation to humans

Expert Rev. Clin. Pharmacol. 7(3), 349–362 (2014)

Robert James Hornby[1], Philip Starkey Lewis[1], James Dear[2,3], Chris Goldring*[1] and Kevin Park[1]

[1]*MRC Centre for Drug Safety Science, Department of Molecular and Clinical Pharmacology, Sherrington Buildings, University of Liverpool, L69 3GE, UK*
[2]*NPIS Edinburgh, Royal Infirmary of Edinburgh, Edinburgh, UK*
[3]*University of Edinburgh/British Heart Foundation Centre for Cardiovascular Science, Edinburgh, UK*
**Author for correspondence: Chrissy@liv.ac.uk*

Drug-induced liver injury (DILI) is a common form of adverse drug reaction seen within the clinic. Sensitive, specific and non-invasive biomarkers of liver toxicity are required to help diagnose hepatotoxicity and also to identify safety liabilities during drug development. Limitations exist in the current gold standard DILI biomarkers: alanine aminotransferase is not liver-specific and therefore gives rise to false-positive signals. Interest has grown in the potential of microRNAs (miRNAs) as biomarkers of DILI. Some miRNAs display remarkable organ specificity, can be measured sensitively and are stable in a wide range of biofluids. However, little is currently known about the mechanisms through which miRNAs are released from cells. Furthermore, a clinically suitable method to measure miRNAs has not yet been developed. This review aims to highlight the current research surrounding these markers and areas in which further work is required to establish these markers within clinical and pre-clinical settings.

KEYWORDS: acetaminophen • DILI • exosome • hepatocyte • injury • liver • miR-122 • miRNA

Drug-induced liver injury

The liver is the main organ responsible for the detoxification of xenobiotics and natural toxins. Due to the biotransformational capacity of the liver, it is prone to generating chemically reactive metabolites, which makes the liver particularly susceptible to drug-induced liver injury (DILI) [1]. DILI is a complex disease that can be classified into two subcategories, type A and type B. Type A DILI occurs in a predictable and dose-dependent manner, usually at supratherapeutic doses, such as in the case of acetaminophen (APAP) overdose. In contrast, type B DILI is idiosyncratic in nature and usually occurs at a therapeutic dose. The susceptibility of a patient to DILI can be influenced by host factors including age, sex, nutrition, poly-pharmacy (including alcohol), co-morbidity and genetics. To date, over 1000 different drugs have been associated with hepatotoxicty independent of drug class or disease indication (National Institute of Health Database of drugs and supplements associated with liver toxicity [2,3]). DILI is a common adverse drug reaction seen within the clinic in Europe and the USA, representing a major impediment to the generation and accessibility of new medicines [1]. It is a major clinical concern and led to 40,393 deaths in the USA alone in 2010 [4]. Because of this, sensitive biomarkers of DILI are required to facilitate in its diagnosis, direct treatment strategy within the clinic and also detect safety liabilities reliably during drug development. A biomarker by definition is 'a characteristic that is objectively measured and evaluated as an indicator of normal biological processes, pathogenic processes or pharmacological responses to a therapeutic intervention'. For a biomarker to be of clinical use, it must have both biological and bioanalytical sensitivity, tissue/organ specificity, easy accessibility and it must display a change early enough for a therapeutic intervention to

 10.1586/17512433.2014.904201 ISSN 1751-2433

Table 1. The ideal characteristics of a potential biomarker of drug-induced liver injury.

Characteristic	
Specificity	The biomarker should be informative of the status of a specific organ or pathology
Sensitivity	The biomarker should be sensitive enough to detect liver injury early and without false positive
Translatable	The biomarker should be applicable to both humans and pre-clinical species to aid the process of new drug development
Detectable	The biomarker assay should be easy and quick to measure in the clinic without the need for specialist equipment
Repeatable	The biomarker assay should be robust and data should be reproducible between laboratories
Non-invasive	The biomarker must be present within accessible biofluids for ease of access
Diagnostic	The biomarker should be easy to interpret to allow clinicians to design a treatment strategy

be effective. Furthermore, a prognostic marker would direct in patient management to help the physician provide appropriate treatment (Table 1) (see review [5]).

Clinical & pre-clinical biomarkers of DILI

The current gold-standard biomarkers of liver injury are alanine aminotransferase (ALT) and aspartate aminotransferase (AST) [6]. These enzymes are involved in amino acid biosynthesis and are released into the circulation following hepatocyte cell membrane breakdown during necrosis. Despite these markers being the gold standard, they suffer from a lack of liver specificity; ALT exists in two isoforms (ALT1 and ALT2), which are expressed in heart, kidney and muscle tissue to different degrees. Therefore, these enzymes may not only report on liver injury. ALT1 has been demonstrated to be expressed in high levels in human liver tissue, as well as being the most abundant isoform detectable in human serum. Importantly however, ALT1 is also detectable in high levels in kidney and muscle tissue, which would hamper the use of an isoform-specific assay [7]. As a product of this, ALT has previously been demonstrated to be elevated in cases of muscle injury [8]. A variety of studies have also demonstrated that ALT levels may become raised in humans undertaking extreme endurance sports events [9]. Additionally, ALT can be raised by hyperalimentation [10] and basal expression can be induced by drugs [11]. ALT2 does not offer use as a biomarker of liver injury, as it is expressed at negligible levels in the liver [7].

Due to the clear lack of an appropriate clinical biomarker to detect DILI, the usual method of practice in clinics in the UK is to establish a causal relationship between the drug in question and the possible diagnosis of liver damage. To establish this relationship, several qualitative scoring systems have been developed, a commonly used example of which is the Roussel Uclaf Causality Assessment Method/Council for International Organizations of Medical Sciences scale, which was developed by Danan and Benichou [12]. The Roussel Uclaf Causality Assessment Method/Council for International Organizations of Medical Sciences scale takes the type of liver injury into account (hepatocellular, cholestatic or mixed) and is a qualitative system that scores on seven criteria: temporal relationship, clinical course, risk factors, concomitant drugs, non-drug etiologies, likelihood of reaction based on published research and response to re-challenge [13]. The score developed from this scale then allows clinicians to categorize patients based on their risk of developing DILI. The limitations of this system have now been highlighted in several studies, which suggest that the lack of a clear scoring method and non-intuitive output have limited the reliability of this system [14,15]. In the UK, the current method of practice is to assess the risk of poor outcome (i.e., development of liver failure) in cases of liver injury using the King's College Criteria, developed at the Liver Unit, King's College Hospital, London [16]. The King's College Criteria is also qualitative system, which takes into account blood pH, serum creatitine, grade of encephalopathy and prothrombin time to assess patient's prognosis of outcome [16,17].

Outside of the clinic, in pre-clinical drug development, the current FDA-endorsed approach in the USA is the combination of four markers, ALT, AST, alkaline phosphatase and total bilirubin, which provides an integrated assessment of liver function. This approach is based on Hy's law, which states that if a drug causes ALT/AST levels to increase to >3× upper limit of normal (ULN) and total bilirubin levels to increase above 2× ULN and there is not an obvious indication of viral hepatitis or other obvious cause, a drug is likely to cause hepatotoxicity. Despite this approach, each of these markers is limited by the possibility that they may also rise in other indications, aside from liver injury [18]. AST, similar to ALT, is liable to rise in muscle injury [6]; bilirubin detection can also be a by-product of erythrocyte hemolysis through macrophage-mediated recycling of the released hemoglobin into unconjugated bilirubin and also several other non-DILI-related conditions [19,20]. Serum alkaline phosphatase, a marker of cholestasis, is also not liver-enriched and may rise in bone diseases and in pregnancy [21].

Recently, interest has grown surrounding a class of small non-coding RNAs, miRNA as potential blood-based biomarkers. miRNAs are small (~22 nucleotides long), RNA-based molecules, which are implicated in gene regulation at a translational level [22]. Having been discovered in the early 1990s as key regulators of development [23–25], recent work has suggested they may play a role in the pathology of a wide range of diseases. miRNAs have also been found to be

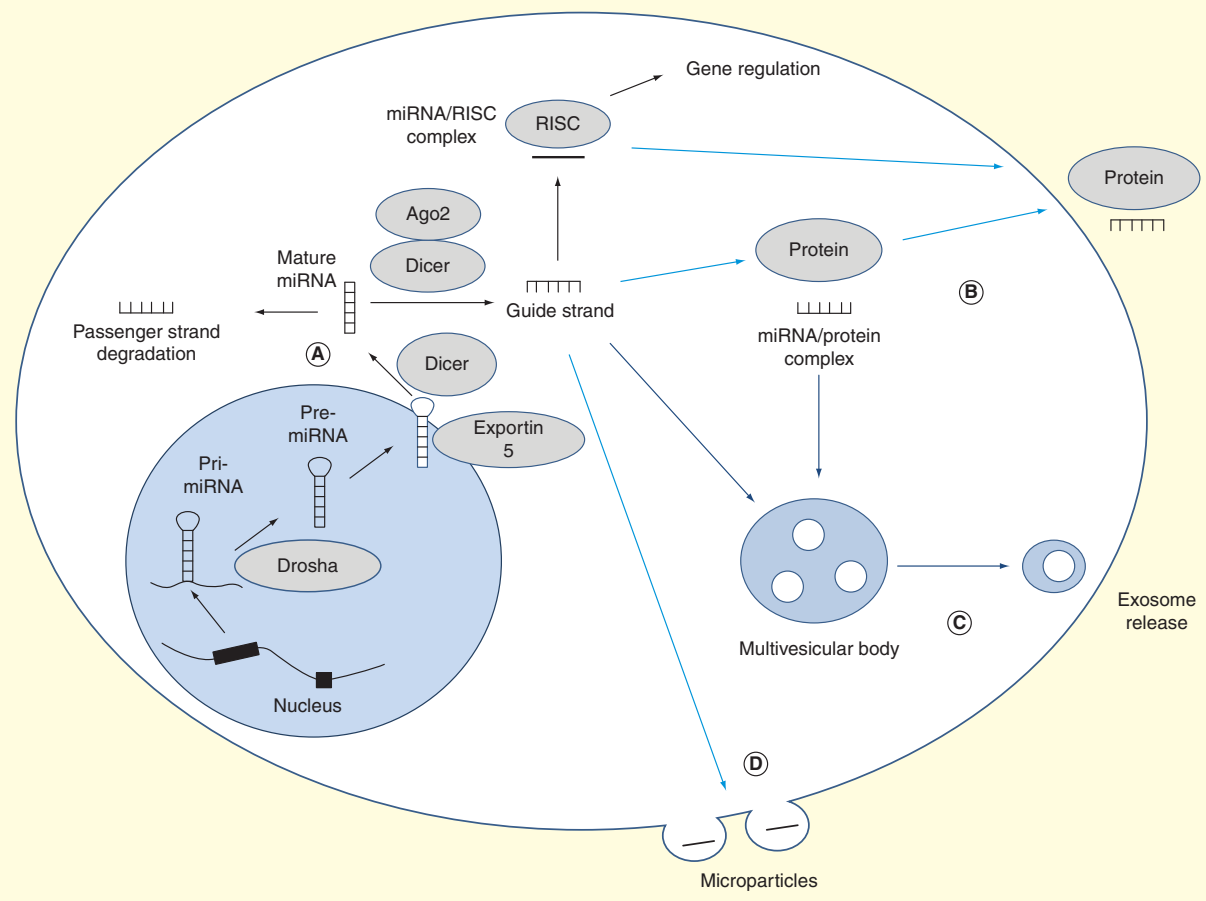

Figure 1. Mechanisms of miRNA processing, function and release into the circulation. (A) miRNA transcription, processing and function. **(B)** miRNA/protein complex formation and export from the cell through current unclear mechanisms. **(C)** miRNA packaging into exosomes in the multivesicular body and subsequent release from the cell through exocytosis. **(D)** miRNA release in microparticles budding from the cell membrane.
Ago2: Argonaute 2; RISC: RNA-induced silencing complex.

present and highly stable in biofluids, such as blood and urine, so can be easily accessed in a non-invasive manner. The stability of miRNAs has been attributed to the various forms in which they are released from cells, including in vesicle-encapsulated forms [26] and protein-bound complexes [26,27]. Some miRNAs demonstrate remarkable tissue enrichment, such as miR-218 in the brain/muscle [28], miR-1 in the heart [29] and miR-122 is present almost exclusively in the liver, representing approximately 70% of the total liver miRNA content [30].

miRNAs are usually encoded by intron sections of DNA and are initially formed as pri-miRNAs (~thousands of nucleotides in length), which are cleaved within the nucleus by Drosha, a class 2 RNase III enzyme [31], to form pre-miRNAs (~70 nucleotides). Pre-miRNAs are actively exported from the nucleus to the cytosol through transporters such as exportin 5 [32]. Within the cytosol, pre-miRNAs form a RNA-induced silencing complex (RISC) with proteins such as argonaute 2 (Ago2) [33], where they are then cleaved further by Dicer, an endoribonuclease, to liberate mature single-stranded miRNAs (reviewed extensively in [34]). Mature miRNA/RISC complexes target specific mRNAs through antisense recognition via the miRNA sequence and thereby regulate RNA translation through a variety of mechanisms (Figure 1) [35,36]. miRNAs play an important role in embryogenesis [37], cell differentiation [38], tissue homeostasis [39], carcinogenesis [40], cardiotoxicity [41] and viral infections [42]. Importantly, miRNAs can be also highly conserved between species [43]. Because of this, they have great potential as translational biomarkers in pre-clinical models, as well as in the clinic.

This review aims to highlight the current knowledge surrounding miRNAs as biomarkers of DILI and provides a prospective outlook on the clinical impact that these markers may have in the coming years.

APAP-induced liver injury

Because of the unpredictable nature of idiosyncratic DILI, no single experimental model or compound is currently available to examine mechanisms of this indication. Therefore, other models must be utilized to understand the mechanisms of this complex indication and discover novel biomarkers of DILI. APAP, the most commonly used analgesic and antipyretic in the world, is a potent liver toxin in both humans and rodents when taken at supratherapeutic doses, causing damage in a well-defined and dose-dependent manner. This predictable nature explains why much of the literature surrounding potential biomarkers of DILI has focused on APAP as a 'model-compound' to examine mechanisms of liver injury and also potential translational biomarkers to diagnose DILI. Additionally, in 2012–13 there were approximately 46,000 documented cases of APAP overdose in English emergency rooms (National Health Service Information Centre – Hospital Episode Statistics for England). Similarly, in the USA, 100,000 cases of APAP poisoning per year were documented, representing a major issue to public health and also to the healthcare budget [44].

In the case of APAP overdose in the clinic, an increase in serum ALT activity is not usually observed until at least 12 h after APAP ingestion, therefore, ALT is not useful as an early prognostic marker to determine an appropriate treatment regimen. Due to the lack of an early biological marker that can be used prognostically, the current method to stratify patients who are at risk of developing severe liver injury is to measure plasma APAP concentration using the Rumack-Matthew nomogram [45]. However, such a chemical readout has limitations since it assumes equal risk among patients, which is clearly not the case. Therefore, an early biological readout that could provide 'patient-specific' prognostic value would be hugely beneficial to the clinical management of APAP-induced acute liver injury (ALI). The limitation of the APAP nomogram was highlighted in a recent letter to the editor in which a case-report of a 25-year-old male who had consumed an APAP overdose was documented. The male presented at the Royal infirmary of Edinburgh 4.5 h after ingesting a single dose of co-codamol (60–70 tablets, 30–35 g of APAP, 480–560 mg codeine) and blood was taken to assess the APAP content. The APAP content in the blood was shown to be 107 mg/l and this was deemed low risk by the UK guidelines (Rumack-Matthew nomogram; original high-risk cut-off was 200 mg/l [45]) at that time and because of this the patient was discharged. The patient then re-presented at hospital 43 h later showing signs of hepatotoxicity. Since then, the UK guidelines have been lowered to classify 100 mg/l APAP as requiring treatment; however, in countries such as North America, New Zealand and Australia, which still classify 150 mg/l APAP as the cutoff, this patient would still be sent home after first presentation [46].

miRNAs as potential biomarkers of DILI

Initially, many of the studies examining the potential of miRNAs to serve as biomarkers focused on the use of these molecules to detect cancer [47]. However, recent studies have demonstrated the utility of some liver-enriched miRNAs, in particular miR-122, as possible markers of DILI and other forms of liver injury. A growing body of evidence shows that miR-122 plays an important role in the physiology of the hepatocyte. Several web-based algorithms predict that miR-122 may target several thousand genes, but most of these are yet to be experimentally verified (for experimentally verified miRNA target prediction database, refer to [48]). Studies utilizing antisense oligonucleotides in mice to inhibit miR-122 have established its role in the regulation of lipid and cholesterol metabolism [49]. It was observed that when miR-122 function is abolished, the translation of important enzymes in these processes becomes deregulated, such as cholesterol 7α-hydroxylase [49]. Additionally, studies in human hepatocellular carcinoma (HCC) cell lines have demonstrated that miR-122 has been associated with hepatocyte differentiation through post-transcriptional repression of CUTL1, a transcriptional repressor of genes involved in cell differentiation [36].

In pathological states, it has been shown that miR-122 may play a role in the development of cancerous tumors and in hepatitis C virus (HCV) infection ([50]; reviewed by [51]). In a study examining the replication of HCV, it was observed that HCV was unable to replicate in cell lines that did not express miR-122 (HepG2) when compared with cell lines that were miR-122 positive (Huh 7). This was further explored utilizing antisense strategies to knock-down miR-122 expression, which consistently noted impaired HCV replication [50]. Interestingly, miR-122 is now being investigated as a drug target for HCV in Phase II studies [52]. In HCC, miR-122 is specifically downregulated in both humans and rodents [53], and interestingly, has been demonstrated to modulate cyclin G1 in HCC-derived cell lines. Further studies in primary tumor cells lines have demonstrated an inverse expression relationship between miR-122 and *cyclin* G1, suggesting that downregulation of miR-122 in HCC may affect the cell cycle [54]. Mice that are genetically deficient of miR-122 are viable but develop spontaneous liver lesions and HCCs early in life [55,56]. Therefore, it is clear that miR-122 plays an important role in liver biology and defines the phenotype of the mature hepatocyte (Figure 2).

Due to the large abundance and remarkable liver enrichment of miR-122, several studies examined the use of this miRNA to serve as a circulating biomarker of liver injury. In a study examining APAP-induced ALI in mice, the authors were able to demonstrate that miR-122 as well as another liver-enriched miRNA, miR-192, detected liver injury earlier and at lower toxic doses, than ALT activity when measured in serum [57]. To test the translational potential of miR-122 and miR-192 as biomarkers of DILI, a study examining these markers in 53 patients admitted to hospital after taking an APAP overdose was performed. We demonstrated that miR-122 and miR-192 were raised in serum when compared with healthy controls. Another observation in this study was that miR-122 levels return to baseline between 3 and 7 days after initial hospitalization, whereas serum ALT levels remained elevated [58]. This suggests that miR-122 has a shorter circulatory half-life, which may allow miR-122 to closely

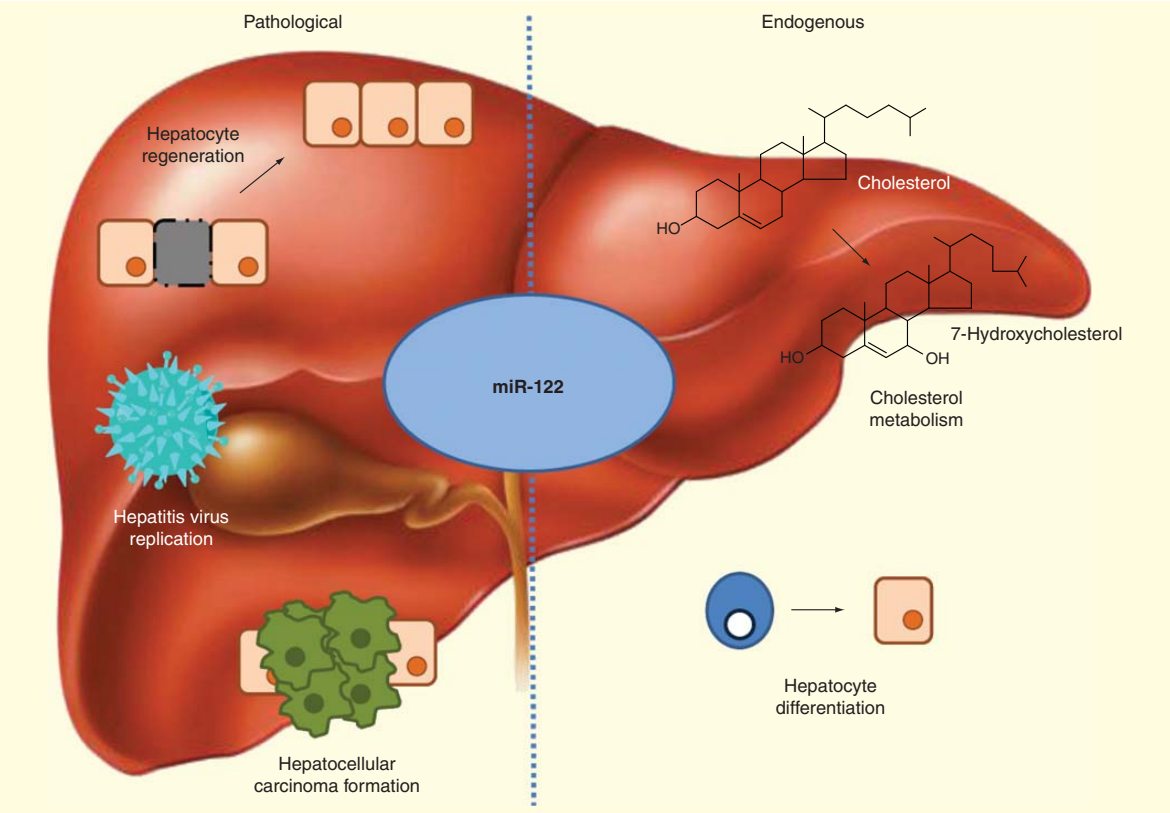

Figure 2. The endogenous and pathological roles of miR-122. Under endogenous conditions, miR-122 is involved in the regulation of 7α-hydroxylase translation, an enzyme that converts cholesterol into 7-hydroxycholesterol in cholesterol metabolism. miR-122 is also involved in the regulation of hepatocyte differentiation and maintenance of hepatocyte phenotype in endogenous conditions. In pathological conditions, miR-122 has been suggested to have a role in hepatocyte regeneration after injury, hepatitis virus replication and also in the formation of hepatocellular carcinoma.

reflect the actual state of the liver more than a biomarker, which remains in the circulation for a long period of time without degradation. More recently, a study examining the utility of several mechanistic biomarkers of DILI in patients who had ingested a single toxic dose of APAP demonstrated that initial miR-122 levels at hospital presentation were able to predict maximum ALT activity and peak international normalized ratio score during the hospital stay of the patient, while initial ALT activity could not. This highlighted for the first time that miR-122 is raised very early during liver injury in man, and may provide prognostic value to identify patients who develop liver injury [59]. Moreover, miR-122 was raised as early as 4 h after a toxic APAP dose, almost 8 h before an increase in ALT levels is usually detected in serum. The importance of this was highlighted in a recent letter to the editor described in an earlier section of the review [46]. Despite the patient being classified as 'low-risk' when assessed using the Rumack-Matthew nomogram [45], on retrospective analysis of blood biomarkers taken upon first presentation at the hospital, miR-122 levels were measured to be approximately 50× ULN, while ALT levels remained at baseline. Importantly, in this case miR-122 would have directed clinicians to administer *N*-acetylcysteine treatment, instead of sending the patient home and allowing the progression of the toxicity [46].

Importantly, Starkey-Lewis *et al.* [58] demonstrated that miR-122 may also be a sensitive marker of DILI caused by other drugs, aside from APAP. In a single case of clarithromycin-induced liver injury, serum miR-122 was demonstrated to be elevated, correlating with serum ALT, similar to APAP-induced DILI. Since this initial study, circulating miR-122 levels have been demonstrated to report on other drugs associated with DILI, such as heparin [60] and in several experimental models associated with liver injury in rodents, including galactosamine- and alcohol-induced liver injury [8]. In a study examining the effects of chronic subcutaneous heparin injections in 48 healthy male subjects, which the authors proposed caused mild hepatocyte necrosis, miR-122 was demonstrated to rise in the serum, peaking 7 days after the study began. These results were said to be consistent with hepatocyte leakage in necrotic

conditions and importantly the dynamic range of miR-122 was higher than that of alternative protein biomarkers, such as ALT (peak miR-122: 8–16× baseline; peak ALT: <1–12× baseline) [60]. These data collectively suggest that miR-122 could be a liver-specific, early and sensitive marker of DILI within the clinic, which may be able to predict the severity of the pathology.

In addition to the utility of miR-122 as a biomarker of DILI, it has also been demonstrated to be used as a marker of viral hepatitis. Zhang *et al.* was able to show that plasma miR-122 levels change in a disease–severity relationship in patients infected with hepatitis B virus, showing a strong correlation with plasma ALT activity [8]. Additionally, miR-122 levels were raised earlier in the plasma and correlated strongly with histological grading. The strength of miR-122 as a biomarker (vs ALT) was tested using a ROC analysis and a multivariate logistic regression analysis, which suggested that miR-122 is a stronger biomarker of hepatitis B virus-associated liver injury than ALT [8]. In a different study examining patients with chronic hepatitis C viral infection (CHC), serum miR-122 levels were shown to strongly correlate with serum ALT levels in patients undergoing necroinflammation associated with CHC [61]. However, miR-122 did not correlate with changes in liver function and also the fibrosis stage of hepatitis, suggesting in CHC, miR-122 is a marker of cellular damage and not overall liver function [61]. An additional study testing the value of miRNAs as biomarkers to distinguish between HCC and chronic viral hepatitis using a ROC analysis was able to support miR-122 as a strong biomarker of cellular damage. However, miR-122 was only able to distinguish patients with chronic viral hepatitis from healthy controls and not from patients with HCC, once again suggesting that miR-122 is a marker of hepatocyte damage [62].

miRNA stability in circulation & forms of release

Despite the RNA-based structure of miRNAs, which can be degraded quickly by cellular RNases, miRNAs are extremely stable in biofluids [47]. Stability is an ideal quality for a biomarker, as clinical samples in their very nature are unlikely to be collected, processed and stored in exactly the same way, especially without an accepted universal protocol. Previous work has attributed this stability to the various forms in which miRNAs exist in the circulation [26]. Previously, miRNAs have been detected in the circulation within various biofluids, such as serum, plasma and urine, enveloped within small vesicles [63,64]. The importance of which in biomarker discovery has be discussed in detail in a recent Toxicology letter published by a division of the FDA [65]. More recently, miRNAs have been detected circulating in a vesicle-free form, in which miRNAs are in complex with a protein or lipoprotein complex [26,27,66].

Vesicle-based miRNAs

Exosomes

Exosomes are a class of phospholipid nanovesicle, around 30–150 nm in diameter, which are formed within endocytic compartments called multivesicular bodies and are then released into the circulation through exocytosis [67]. Exosomes were initially thought to be cellular debris and harbor no function. However, now it is understood that exosomes play a distinct role in cellular signaling, which allows them to play a role in the development of malignancies [68] and in the spread of viral infections [69]. Their full endogenous role still requires study due to their relatively recent discovery [70]. Exosomes are released from a myriad of cell types, including hepatocytes [67] and inflammatory cells [71], and have been demonstrated to contain cellular proteins, DNA, mitochondrial DNA [72], RNA, lipids as well as miRNAs (ExoCarta provides an encyclopedia of recorded exosome contents; [73]). miRNAs can associate with multivesicular bodies at the pre-miRNA stage, controlled by the presence of specific sequence motifs in the miRNAs [74] and are then packaged into exosomes before release into the circulation, which is controlled by a ceramide secretory system [75]. Exosomes can be extracted from circulating biofluids through a variety of methods including ultracentrifugation [76], immunoprecipitation [77] and through use of specific exosome isolation solutions (Exoquick, SBI, Cambridge Bioscience, Cambdrige, UK/Life Technologies, Paisley, UK). The presence of exosomes in solution can be accessed through monitoring the presence of specific exosome markers such as CD63 [78] or TSG101 [79], using molecular biology techniques such as western blotting or through visualization and measurement using electron microscopy or nanoparticle tracking analysis [76,79,80].

Microparticles

Microparticles are a class of secretary vesicles, >100 nm in diameter, which are formed through 'blebbing' of the plasma membrane and are distinctly different from exosomes in their qualitative/quantitative content [81]. This process is regulated by intracellular calcium levels, cytoskeleton protein reorganization and changes in membrane lipid asymmetry [82]. Microparticle release has been documented to take place during cellular apoptosis and is thought to be a cellular response to attempt to reverse apoptosis [83]. Changes in the levels of plasma microparticles have been associated with many disease states, including cardiovascular disease [83], metabolic syndrome [84] and diabetes (Type 1 and 2) [85]. Similar to exosomes, microparticles have been shown to be implicated in cell–cell signaling, showing function in recipient cells [86]. Witek *et al.* demonstrated that liver-derived microparticles can alter gene expression in recipient liver endothelial cells through Hedgehog signaling [87]. Microparticles, like exosomes, have been demonstrated to contain protein, DNA, RNA and lipids. Interestingly, in a study examining the content of microparticles secreted from mesenchymal stem cells, the RNA content of microparticles almost exclusively consisted of miRNAs, demonstrating that packing of these vesicles is a selective process, which does not necessarily reflect the donor cell content [88]. Interestingly, this study found that hsa-let-7b and hsa-let-7g are secreted in their immature pre-miRNA forms, which would allow them to form a mature-miRNA/RISC complex in effector cells and elicit an effect on RNA translation [88]. This role is yet to be understood

fully and much work is still required before the role of microparticle-packaged miRNA is understood. Previous studies examining microparticles have focused on the use of ultracentrifugation techniques to separate these vesicles from other vesicles such as exosomes and also from the microparticle-depleted supernatant of biofluids. The success of this extraction is usually then monitored through the presence of microparticle markers, such as phosphatidyl serine and annexin V in both the extracted microparticle solution and the supernatant [89].

Protein & lipid complexes

miRNAs have also been detected in the circulation of protein complexes. In a study examining the miRNA content of the different fractions (microvesicles, exosomes and exosome-depleted supernatant) of cell culture medium of several human cell lines, including HepG2s, it was observed that a striking amount of miRNAs were present in the vesicle-depleted solution, suggesting that some miRNAs are present in a vesicle-free form. The authors proposed that these miRNAs were bound in protein complexes and demonstrated that a nucleophosmin 1 (NPM1), a protein which has previously been shown to be involved in ribosomal export from the cell, was able to protect synthetic miR-122 from degradation by RNAses. This provides some evidence that NPM1 may provide the remarkable stability of vesicle-free miRNA in the circulation [90]. Turchinovich *et al.* built on this work in both cell lines and also in human blood plasma, demonstrating that the majority of circulating miRNAs are present in a vesicle-free form. However, through immunoprecipitation studies they suggested that miRNAs existed in a complex in the circulation with Ago2, a member of the RISC complex, as opposed to NPM1. One viewpoint is that perhaps circulating miRNAs on the most part are a by-product of dead cells that are released into extracellular space bound to intracellular proteins upon the breakdown of the cell membrane and afforded protection from RNAses from the protein complex [27]. Recent work examining the serum of healthy human donors supported this initial paper suggesting that miRNAs form complexes in the circulation with Ago2. However, they were also able to demonstrate that the association of miRNAs with either a protein complex or a vesicle does not seem to be a random occurrence and that some miRNAs associate exclusively either with protein complexes or with extracellular vesicles, under normal conditions. In this study, it was demonstrated through differential-centrifugation and size-exclusion chromatography that different miRNAs exist within vesicles or are associated with protein-bound complexes [26]. In the serum of healthy volunteers, miR-122 was found predominantly in a protein-bound form, whereas let-7a, another miRNA, was found almost exclusively within exosomes/microparticles. However, the mechanism through which these protein complexes are released remains poorly understood [26,27].

High-density lipoproteins have also been demonstrated to transport miRNAs through a neutral sphingomyelinase-dependent mechanism [66]. miRNA/high-density lipoprotein complexes travel to recipient cells and undergo endocytosis through a scavenger receptor type class 1-dependent mechanism. Notably in this study, the delivered complexes were able to modify RNA translation in hepatocyte model of atherosclerosis, suggesting that these complexes are a form of cell–cell signaling pathway [66]. However, studies will have to be undertaken to assess whether these complexes play a role in DILI or in the release of biomarkers, which will allow a deeper understanding of the overall pathology.

miRNA packaging & function

A recent mouse study, examining drug-induced, alcoholic and inflammatory liver injury, demonstrated that miR-122 was detected in different fractions of blood during the APAP toxicity study. Early in the injury (3 h), miR-122 was elevated in the 'exosome-fraction' of the serum over the exosome-depleted supernatant. As the injury progressed to 6 h, the miR-122 levels of the exosome-depleted supernatant became elevated over the exosome-fraction [91]. This might suggest that miR-122 release in APAP injury is biphasic. For example, early in APAP injury miR-122 may be released through active mechanisms within the cell, which could possibly arise from the hepatocytes response to the toxic insult, with an aim of promoting hepatocyte proliferation and liver regeneration. But as APAP injury progresses and injury switches from an early stressed state to hepatocellular necrosis, miR-122 may be released in a similar mechanism to that of ALT, that is, when cell membrane integrity is lost. Indeed, this hypothesis of early active 'shedding' is supported by studies demonstrating that loss of cellular miR-122 is associated with hepatogenesis and cell proliferation [55,56]. This may explain why miR-122 is elevated in APAP-induced DILI before that of ALT and other markers. However, this hypothesis needs to be urgently tested and further work is required to understand both why and how miRNAs are released throughout the course of liver injury.

Analytical techniques & clinical potential

Appropriate biofluids for miRNA use as biomarker

miRNAs are detectable in various biofluids, including blood, urine, feces and breast milk, fulfilling the criteria of accessibility of a biomarker, which raises the question, which is an appropriate fluid for biomarker measurement in both the clinic and in pre-clinical testing. Clinically, measurement in a biofluid that requires no processing would be favorable, such as whole blood. Recently, in a study examining miRNA deregulation in pancreatic cancer patients, the authors were able to measure miR-122 in whole blood, which suggests that this would be a suitable biofluid for detection [92]. Previously however, much of the work examining miR-122 as a marker of DILI has focused on blood serum as the source. One advantage of using serum or plasma over whole blood is the removal of whole blood cells, which if frozen would hemolyze and release their contents, including blood cell-rich miRNAs [93]. In a study aiming

Table 2. Normalizing methods for current techniques to detect and quantify miRNAs.

Type	Function	Name	Type	Biofluid	Ref.
Exogenous	Used to remove bioanalytical bias during sample processing	Cel-miR-39	miRNA	Serum Plasma	[26,47,105]
		Cel-miR-54	miRNA	Plasma	[47]
		Cel-miR-238	miRNA	Plasma	[47]
Endogenous	Used to remove biological and sample variance	U6 (RNU-6B)	snRNA	Plasma whole blood	[8,106]
		Let-7d	miRNA	Serum	[96,107]
		miR-16	miRNA	Serum	[108]
		miR-24	miRNA	CSF	[98]
		RNU-48	snRNA	Urine	[109]
		miR-193	miRNA	Urine	[94]
		miR-323	miRNA	Urine	
		miR-675	miRNA	Urine	
None	N/A	N/A	N/A	Serum	[61]

N/A: Not applicable.

to test serum and plasma appropriate biofluids for miRNA measurement, given that much of the clinical specimens are serum, Mitchell *et al.* demonstrated that the levels of four miRNAs (miR-15b, -16, -19b and -24) correlated consistently between serum and plasma [47]. However, recent work has suggested that plasma is a favorable biofluid over serum due to the inhibition of coagulation in plasma collection tubes. Wang *et al.* compared the miRNA content of serum and plasma samples taken at identical times from healthy human donors, demonstrating more miRNA content in the serum samples compared with the plasma samples. Interestingly, the concentrations of blood cell-rich and platelet-rich miRNAs, such as miR-16 and miR-126, respectively, were identical between serum and plasma samples, suggesting the difference in miRNA content is not due to blood cell hemolysis. A suggested cause of the increased miRNA content in serum was that the coagulation process triggered miRNA release from cells contained within the sample, through a trafficking system [93]. This suggests that plasma would be a favorable biofluid over serum due to reduced changes in miRNA content in the sample preparation process. However, one counterargument to this suggestion is highlighted by work conducted by Arroyo *et al.*, in which it was demonstrated that miRNAs are in fact not resistant to plasma RNases as previously thought. This suggests that miRNAs in plasma samples are likely to degrade faster than in serum, which would support the use of serum samples for sample longevity [26].

In addition to circulating sources of biomarkers, a recent study has explored the possibility of the use of urinary miRNAs as possible biomarkers of DILI in rats administered with APAP [94]. This study examined the levels of 44 miRNAs in the urine, miR-291a-5p was found to correlate strongly with the histopathology of the liver. Furthermore, miR-291a-5p was able to distinguish between a non-toxic and toxic dose of APAP, suggesting it may also be a marker of the severity of liver injury [94]. This together suggests that urine may also be a possible source of biomarkers of DILI; however, rigorous testing in larger subject groups and different population demographics will have to be carried out before these markers can have a use within the clinic. It will also be important to understand whether these urine biomarkers offer a similar level of liver-specificity to similar blood-based biomarkers.

Inter-individual variation

Inter-individual variation will also have to be considered, if miRNAs are to be served as clinical biomarkers. This was first documented in a study using significance analysis of miRNAs, in which four miRNAs were identified that were 63–95% higher in females, compared with males [95]. In another study, Wang *et al.* demonstrated differences in miRNA content of male serum samples, specifically miR-130b and miR-18b were slightly higher in males compared with females [93]. The significance of this in DILI is still unknown and will require further study. However, this highlights the need for studies that assess baseline levels across different population groups and patient groups for individual miRNAs. This information would then allow clinicians to set an ULN for each of these biomarkers across a population.

Data normalization for reverse transcription-quantitative PCR

The current techniques used to quantify circulating miRNA levels, in particular, reverse transcription-quantitative PCR (RT-qPCR), are liable to systematic bias in the data they produce because variation exists within the assay (e.g., variation in RNA isolation). In addition to bioanalytical variation, samples

may also be biologically different, due to inter-individual variation and conditions during sample collection can also influence sample quality (e.g., storage temperature, storage time). To reduce sample variance, normalization techniques have to be utilized to account for these differences (Table 2).

Normalization to total RNA level

Previously, a commonly used method of practice for assessing miRNA level in a biofluid was to normalize RNA content in samples, through spectrophotometric analysis. However, this is not an appropriate method to reduce biological variation. Wang *et al.* was able to demonstrate that total RNA content of samples has no correlation with the miRNA content and therefore this cannot be used as a normalizer for miRNA levels [93]. Measuring a purified miRNA fraction is also not recommended as the total RNA content is typically toward the lower limit of detection of the spectrophotometer.

Relative quantification using 'spike-in' exogenous miRNA

Another common normalizing practice is to 'spike-in' a known amount of exogenous miRNA, such as non-mammalian cel-miR-39 and cel-lin-4, during the miRNA extraction process. This method serves to correct for losses in miRNA extraction and purification. However, this method is not useful in eliminating biological variation and sample variation, this procedure is analogous to using an internal standard.

Relative quantification using endogenous normalizers

For clinical samples, use of an endogenous miRNA normalizer to reduce biological sample variation is recommended, similar to the almost universal use of GAPDH in gene expression studies. Use of an endogenous normalizer aims to correct for variance in RNA content in PCR assays, reducing both biological variation and also technical variation. The use of a biological normalizer in the development of a clinical assay for miRNAs will be important due to the variable conditions, which inevitably occur in a clinic during sample collection, processing, storage and transport. Each of these stages can potentially impact the biological quality of the sample. However, currently no universal normalizer has been set for use throughout different studies and labs. Studies have chosen a wide range of endogenous normalizers such as U6 snRNA [58], let-7d [96], RNU48, miR-16 [8,97] and miR-24 [98]; however, there have been several issues regarding the use of these normalizers. Serum U6 snRNA expression has been demonstrated to have a slight, but significant change in patients undergoing severe APAP-induced ALI, when compared with healthy individuals [58]. Additionally, Qi *et al.* demonstrated that U6 snRNA levels varied significantly between young and aged subjects. In this study, it was suggested that let-7d was a superior normalizer showing less variation between patient groups (including young and aging patients, autoimmune disease and malignant melanoma) [96]. However, similar to this, work in our lab was able to demonstrate that even let-7d expression in serum was changed in APAP-induced ALI patients, suggesting that the severity of injury may affect global miRNA levels [96]. However, to further reduce sample discrepancies, both an exogenous and endogenous normalizer should be utilized together. Interestingly however, one study examining miR-122 as a serum marker of necro-inflammation in patients with chronic hepatitis C infection chose to use no normalizing strategy. Bihrer *et al.* demonstrated that even without normalization, miR-122 content was still elevated in patients undergoing necroinflammtion when compared with healthy controls. This may be a possible strategy in certain cases (e.g., APAP-induced ALI) for miR-122 quantification because of its high liver specificity [61]. This approach would be attractive in a clinical setting due to the requirement to only measure one target.

For absolute quantification of miRNA levels, a standard-curve can be utilized; this technique utilizes a synthetic form of the miRNA of interest of a known concentration, from which a standard curve is created, which can be assayed alongside clinical samples. This will then provide a value for the number of miRNA of interest in each sample, in a copies/l format, similar to ALT, which is measured in units/l [99]. To further develop the potential of these markers within the clinic, a robust, simple and relatively cheap assay will be required to streamline the process of quantifying these markers.

Assays to detect & quantify miRNA

Currently, the development of miRNAs as clinical biomarkers has been hindered by the assays used to quantify them in the circulation. The most common techniques for miRNA quantification are PCR-based, such as RT-qPCR, northern blotting, microarray or next-generation sequencing. Despite RT-qPCR having a high level of bioanalytical sensitivity, it is inappropriate for clinical use as it can take up to 8 h to perform the assay. In the case of APAP-induced ALI, the onset of toxicity may be rapid and therefore this test would be too slow to provide prognostic value. Additionally, RT-qPCR is liable to bioanalytical bias through different methods of miRNA extraction and user error due to the highly technical nature of the assay. To facilitate the transition of miRNAs from a proof-of concept biomarker to a true clinical bedside test, a fast, robust, simple and sensitive new clinical assay must be developed for the rapid quantification of miRNAs in accessible biofluids.

Several novel assays are currently in development for the detection of miRNAs, which would be more suitable in a clinical setting; however, none has yet undergone the rigorous testing required for use. The scientists at the National University of Singapore have developed a label-free method to quantify miRNAs through the use of gold nanoparticle networks and a duplex-specific nuclease, which allow miRNAs detection at subfemtomolar levels, with almost no sample preparation required [100]. Additionally, Cissell *et al.* have developed a microtiter plate assay to quantify miRNAs, using *Renilla-luciferase* labeled miRNA as a competitor to free miRNA for binding to

Table 3. Current and emerging assays to detect and quantify miRNAs in biofluids.

Assay	Detail	Available or under development?
RT-qPCR	Assay converts miRNA present within the fluid of interest into cDNA, then RNA is amplified from cDNA through the PCR. miRNA is quantified through the use of a user set copy cycle threshold. The more abundant the miRNA the quicker it will be amplified and cross the threshold, therefore having a lower Ct value	Available (not in clinical practice)
Microarray	Assay allows quantification of a large number of miRNAs in a single reaction. miRNAs are hybridized with fluorescent probes and the level of fluorescence measured relates to the miRNA level	Available (not in clinical practice)
Northern blotting	miRNAs are separated through electrophoresis and then quantified through hybridization with a fluorescent probe	Available (not in clinical practice)
Bioluminescent microtiter assay [101]	Competitive oligonucleotide hybridization assay using bioluminescent *Renilla luciferase* probes to quantify miRNAs	Under development
Gold nanoparticle network and duplex-specific nuclease assay [100]	Assay utilizes homogenous hybridization, the amplification power of a duplex-specific nuclease and gold nanoparticle networks for signal amplification. This allows quantification of miRNAs down to subfemtomolar levels without the need for labeling	Under development
Silicon nanowire biosensors [102]	Assay allows ultra-sensitive detection of miRNAs through use of SiNWs. miRNAs attach directly to peptide nucleic acids immobilized on the surface of the SiNWs. Resistance changes before and after hybridization allow quantification of miRNA	Under development

SiNWs: Silicon nanowire structures.

a complementary miRNA probe. This bioluminescence assay takes a total of 1.5 h, requires no PCR amplification step and is sensitive to a femtomolar level [101]. Apart from these examples, many other novel methods for miRNA detection and quantification have emerged in the literature, such as label-free detection of miRNAs with silicon nanowire biosensors [102], use of universal tagged probes and time-resolved fluorescence technology [103] and solution-phase detection of miRNAs [104]. However, before these methods become applicable in the clinic, robust testing must be done to assess the repeatability of these assays (Table 3).

Expert commentary & five-year view

DILI is a major concern both within the clinic and in the development of safer drugs. To aid in the diagnosis of DILI in the clinic and also within the development of new drugs, sensitive and specific biomarkers, which are detectable in accessible biofluids are required. The current gold-standard biomarkers are held back, either by non-specific tissue expression or that they are not detectible early enough in the course of a disease to be prognostic.

Recently, miRNAs have emerged as promising class of biomarkers of various diseases and tissue injury. Specifically miR-122, a liver-enriched miRNA has demonstrated its use both in animal and human studies as a sensitive and specific biomarker of DILI. Much of this initial work has focused on APAP as an experimental model to examine DILI and so it will be important in the future to identify additional DILI scenarios to further test the wider applicability of these biomarkers. Additionally, before miR-122 can find use within the clinic, a more robust, less technical and importantly, a quicker assay, will have to be developed for its quantification. Several potential new assays have been developed, but none of these has undergone the rigorous testing required for use within the clinic. In the coming years, work will have to be done to establish the new gold-standard assay to detect miRNAs and studies will have to be done to assess baseline values of these biomarkers across varying population groups. However, these biomarkers show qualities over and above the current markers, so it is likely in the next 5 years a marker, such as miR-122 should progress into clinical use. Additionally, it will also be important to further our understanding of the release mechanisms of miRNAs into the circulation. This knowledge may aid us in understanding the current physiology of the cell and how they react to injury, which could aid in the direction of treatment and also in the development of safer medicines in the future.

Financial & competing interests disclosure

The authors' research is supported by the BBSRC, MIP-DILI and the MRC. The authors have no other relevant affiliations or financial involvement with any organization or entity with a financial interest in or financial conflict with the subject matter or materials discussed in the manuscript apart from those disclosed.

No writing assistance was utilized in the production of this manuscript.

Key issues

- Drug-induced liver injury (DILI) is a leading adverse drug reaction experienced in the clinic.
- Sensitive biomarkers of DILI are required in clinical diagnosis and in drug development.
- The current gold-standard biomarkers for DILI have well-recognized limitations. New specific, sensitive and robust markers of DILI must be found to aid in clinical diagnosis and pre-clinical drug development.
- miRNAs, a class of small non-coding RNAs hold many of the properties required for potential biomarkers; certain miRNAs are tissue specific, non-invasive, sensitive and easily quantifiable.
- miRNAs are released into the circulation in several forms, including vesicle-bound and protein-bound forms; however, the physiological function of these mechanisms is still not understood in DILI.
- Current PCR-based assays are liable to bioanalytical, biological and sample variance. Therefore, both endogenous and exogenous miRNA normalizers must be used to reduce variation in the current assays.
- The current assays for miRNA quantification are time-consuming and vary between laboratories; therefore, new robust assays must be developed before these markers could be used in the clinic.
- Techniques using bioluminescence and label-free miRNA quantification are under development; however, robust testing will first be required before they have application in the clinic.

References

1. Park BK, Boobis A, Clarke S, et al. Managing the challenge of chemically reactive metabolites in drug development. Nat Rev Drug Discov 2011;1(4):292-306
2. Hussaini SH, Farrington EA. Idiosyncratic drug-induced liver injury: an overview. Expert Opin Drug Saf 2007;1(6):673-84
3. LiverTox. Available from: www.livertox.nih.gov/
4. Murphy SL, Xu J, Kochanek KD. Deaths: final data for 2010. Natl Vital Stat Rep 2013;61:4
5. McShane L. Statistical challenges in the development and evaluation of marker-based clinical tests. BMC Med 2012;1(1):1-5
6. Ozer J, Ratner M, Shaw M, et al. The current state of serum biomarkers of hepatotoxicity. Toxicology 2008;1(3):194-205
7. Lindblom P, Rafter I, Copley C, et al. Isoforms of alanine aminotransferases in human tissues and serum—Differential tissue expression using novel antibodies. Arch Biochem Biophys 2007;1(1):66-77
8. Zhang Y, Jia Y, Zheng R, et al. Plasma microRNA-122 as a biomarker for viral-, alcohol-, and chemical-related hepatic diseases. Clin Chem 2010;1(12):1830-8
9. Koutedakis Y, Raafat A, Sharp NC, et al. Serum enzyme activities in individuals with different levels of physical fitness. J Sports Med Phys Fitness 1993;33(3):252
10. Kubo M, Yonemoto K, Ninomiya T, et al. Liver enzymes as a predictor for incident diabetes in a Japanese population: the Hisayama study. Obesity 2007;1(7):1841-50
11. Lee K-L, Kenney FT. Induction of alanine transaminase by adrenal steroids in cultured hepatoma cells. Biochem Biophys Res Commun 1970;1(2):469-75
12. Danan G, Benichou C. Causality assessment of adverse reactions to drugs – I. A novel method based on the conclusions of international consensus meetings: application to drug-induced liver injuries. J Clin Epidemiol 1993;1(11):1323-30
13. Tajiri K, Shimizu Y. Practical guidelines for diagnosis and early management of drug-induced liver injury. World J Gastroenterol 2008;14(44):6774
14. Rochon J, Protiva P, Seeff LB, et al. Reliability of the Roussel Uclaf Causality Assessment Method for assessing causality in drug-induced liver injury. Hepatology 2008;1(4):1175-83
15. Lewis JH, Larrey D, Olsson R, et al. Utility of the Roussel Uclaf Causality Assessment Method (RUCAM) to analyze the hepatic findings in a clinical trial program: evaluation of the direct thrombin inhibitor ximelagatran. Int J Clin Pharmacol Ther 2008;1(7):327-39
16. O'Grady JG, Alexander GJ, Hayllar KM, Williams R. Early indicators of prognosis in fulminant hepatic failure. Gastroenterology 1989;1(2):439-45
17. Anand AC, Nightingale P, Neuberger JM. Early indicators of prognosis in fulmitant hepatic failure: an assessment of the King's criteria. J Hepatol 1997;1(1):62-8
18. Shi Q, Hong H, Senior J, Tong W. Biomarkers for drug-induced liver injury. Exp Rev Gastroenterol Hepatol 2010;1(2):225-34
19. Ohmori S, Shiraki K, Inoue H, et al. Clinical characteristics and prognostic indicators of drug-induced fulminant hepatic failure. Hepatogastroenterology 2003;1(53):1531-4
20. Fabris L, Cadamuro M, Okolicsanyi L. The patient presenting with isolated hyperbilirubinemia. Dig Liver Dis 2009;1(6):375-81
21. Reust CE. What is the differential diagnosis of an elevated alkaline phosphatase (AP) level in an otherwise asymptomatic patient? Dowden Publishing Corp; 110 Summit Ave, Montvale, NJ 07645-1712, USA: 2001. p. 496-7
22. Chen K, Rajewsky N. The evolution of gene regulation by transcription factors and microRNAs. Nat Rev Genet 2007;1(2):93-103
23. Wightman B, Bürglin TR, Gatto J, et al. Negative regulatory sequences in the lin-14 3'-untranslated region are necessary to generate a temporal switch during Caenorhabditis elegans development. Genes Dev 1991;1(10):1813-24
24. Arasu P, Wightman B, Ruvkun G. Temporal regulation of lin-14 by the antagonistic action of two other heterochronic genes, lin-4 and lin-28. Genes Dev 1991;1(10):1825-33
25. Lee RC, Feinbaum RL, Ambros V. The C. elegans heterochronic gene lin-4 encodes small RNAs with antisense complementarity to lin-14. Cell 1993;1(5):843-54
26. Arroyo JD, Chevillet JR, Kroh EM, et al. Argonaute2 complexes carry a population of circulating microRNAs independent of vesicles in human plasma. Proc Natl Acad Sci USA 2011;1(12):5003-8

27. Turchinovich A, Weiz L, Langheinz A, Burwinkel B. Characterization of extracellular circulating microRNA. Nucleic Acids Res 2011;1(16):7223-33
28. Sempere LF, Freemantle S, Pitha-Rowe I, et al. Expression profiling of mammalian microRNAs uncovers a subset of brain-expressed microRNAs with possible roles in murine and human neuronal differentiation. Genome Biol 2004;5(3):R13
29. Ai J, Zhang R, Li Y, et al. Circulating microRNA-1 as a potential novel biomarker for acute myocardial infarction. Biochem Biophys Res Commun 2010;1(1):73-7
30. Lagos-Quintana M, Rauhut R, Yalcin A, et al. Identification of tissue-specific microRNAs from mouse. Curr Biol 2002; 1(9):735-9
31. Lee Y, Ahn C, Han J, et al. The nuclear RNase III Drosha initiates microRNA processing. Nature 2003; 1(6956):415-19
32. Bohnsack MT, Czaplinski K, GÖRlich D. Exportin 5 is a RanGTP-dependent dsRNA-binding protein that mediates nuclear export of pre-miRNAs. RNA 2004; 1(2):185-91
33. Chendrimada TP, Gregory RI, Kumaraswamy E, et al. TRBP recruits the Dicer complex to Ago2 for microRNA processing and gene silencing. Nature 2005;1(7051):740-4
34. Cullen BR. Transcription and processing of human microRNA precursors. Mol cell 2004;1(6):861-5
35. Ørom UA, Nielsen FC, Lund AH. MicroRNA-10a binds the 5′UTR of ribosomal protein mRNAs and enhances their translation. Mol Cell 2008;1(4):460-71
36. Xu H, He JH, Xiao ZD, et al. Liver-enriched transcription factors regulate microRNA-122 that targets CUTL1 during liver development. Hepatology 2010;1(4): 1431-42
37. Pauli A, Rinn JL, Schier AF. Non-coding RNAs as regulators of embryogenesis. Nat Rev Genet 2011;1(2):136-49
38. Tay Y, Zhang J, Thomson AM, et al. MicroRNAs to Nanog, Oct4 and Sox2 coding regions modulate embryonic stem cell differentiation. Nature 2008; 1(7216):1124-8
39. Miyaki S, Sato T, Inoue A, et al. MicroRNA-140 plays dual roles in both cartilage development and homeostasis. Genes Dev 2010;1(11):1173-85
40. Datta J, Kutay H, Nasser MW, et al. Methylation mediated silencing of MicroRNA-1 gene and its role in hepatocellular carcinogenesis. Cancer Res 2008;1(13):5049-58
41. Horie T, Ono K, Nishi H, et al. Acute doxorubicin cardiotoxicity is associated with miR-146a-induced inhibition of the neuregulin-ErbB pathway. Cardiovasc Res 2010;1(4):656-64
42. Stern-Ginossar N, Elefant N, Zimmermann A, et al. Host immune system gene targeting by a viral miRNA. Science 2007;1(5836):376-81
43. Pasquinelli AE, Reinhart BJ, Slack F, et al. Conservation of the sequence and temporal expression of let-7 heterochronic regulatory RNA. Nature 2000;1(6808):86-9
44. Lee WM. Acetaminophen and the US Acute Liver Failure Study Group: lowering the risks of hepatic failure. Hepatology 2004;1(1):6-9
45. Rumack BH, Matthew H. Acetaminophen poisoning and toxicity. Pediatrics 1975;1(6): 871-6
46. Dear JW, Antoine DJ, Starkey-Lewis P, et al. Letter to the Editor: Early detection of paracetamol toxicity using circulating liver microRNA and markers of cell necrosis. Br J Clin Pharmacol 2013. [Epub ahead of print]
47. Mitchell PS, Parkin RK, Kroh EM, et al. Circulating microRNAs as stable blood-based markers for cancer detection. Proc Natl Acad Sci USA 2008;1(30): 10513-18
48. miRTarBase: the experimentally validated microRNA-target interactions database. Available from: http://mirtarbase.mbc.nctu.edu.tw/
49. Esau C, Davis S, Murray SF, et al. miR-122 regulation of lipid metabolism revealed by in vivo antisense targeting. Cell Metab 2006;1(2):87-98
50. Jopling CL, Yi M, Lancaster AM, et al. Modulation of Hepatitis C virus RNA abundance by a liver-specific MicroRNA. Science 2005;1(5740):1577-81
51. Girard M, Jacquemin E, Munnich A, et al. miR-122, a paradigm for the role of microRNAs in the liver. J Hepatol 2008; 1(4):648-56
52. Janssen HLA, Reesink HW, Lawitz EJ, et al. Treatment of HCV infection by targeting microRNA. N Engl J Med 2013; 1(18):1685-94
53. Kutay H, Bai S, Datta J, et al. Downregulation of miR-122 in the rodent and human hepatocellular carcinomas. J Cell Biochem 2006;1(3):671-8
54. Gramantieri L, Ferracin M, Fornari F, et al. Cyclin G1 is a target of miR-122a, a microRNA frequently down-regulated in human hepatocellular carcinoma. Cancer Res 2007;1(13):6092-9
55. Tsai W-C, Hsu S-D, Hsu C-S, et al. MicroRNA-122 plays a critical role in liver homeostasis and hepatocarcinogenesis. J Clin Invest 2012;122(8):2884
56. Hsu S-h, Wang B, Kota J, et al. Essential metabolic, anti-inflammatory, and anti-tumorigenic functions of miR-122 in liver. J Clin Invest 2012;122(8):2871
57. Wang K, Zhang S, Marzolf B, et al. Circulating microRNAs, potential biomarkers for drug-induced liver injury. Proc Natl Acad Sci USA 2009;1(11):4402-7
58. Starkey-Lewis PJ, Dear J, Platt V, et al. Circulating microRNAs as potential markers of human drug-induced liver injury. Hepatology 2011;1(5):1767-76
59. Antoine DJ, Dear JW, Lewis PS, et al. Mechanistic biomarkers provide early and sensitive detection of acetaminophen-induced acute liver injury at first presentation to hospital. Hepatology 2013;1(2):777-87
60. Harrill AH, Roach J, Fier I, et al. The effects of heparins on the liver: application of mechanistic serum biomarkers in a randomized study in healthy volunteers. Clin Pharmacol Ther 2012;1(2):214-20
61. Bihrer V, Friedrich-Rust M, Kronenberger B, et al. Serum miR-122 as a biomarker of necroinflammation in patients with chronic hepatitis C virus infection. Am J Gastroenterol 2011;1(9):1663-9
62. Xu Y, Xia F, Ma L, et al. MicroRNA-122 sensitizes HCC cancer cells to adriamycin and vincristine through modulating expression of MDR and inducing cell cycle arrest. Cancer Lett 2011; 1(2):160-9
63. Cortez MA, Calin GA. MicroRNA identification in plasma and serum: a new tool to diagnose and monitor diseases. Expert Opin Biol Ther 2009;9(6): 703-11
64. Nilsson J, Skog J, Nordstrand A, et al. Prostate cancer-derived urine exosomes: a novel approach to biomarkers for prostate cancer. Br J Cancer 2009;1(10):1603-7
65. Yang X, Weng Z, Mendrick DL, Shi Q. Circulating extracellular vesicles as a potential source of new biomarkers of drug induced liver injury. Toxicol Lett 2014; 225(3):401-6
66. Vickers KC, Palmisano BT, Shoucri BM, et al. MicroRNAs are transported in plasma

and delivered to recipient cells by high-density lipoproteins. Nat Cell Biol 2011;1(4):423-33

67. Conde-Vancells J, Rodriguez-Suarez E, Gonzalez E, et al. Candidate biomarkers in exosome-like vesicles purified from rat and mouse urine samples. Proteomics Clin Appl 2010;1(4):416-25
68. Taylor DD, Gercel-Taylor C. Tumour-derived exosomes and their role in cancer-associated T-cell signalling defects. Br J Cancer 2005;1(2):305-11
69. Ramakrishnaiah V, Thumann C, Fofana I, et al. Exosome-mediated transmission of hepatitis C virus between human hepatoma Huh7. 5 cells. Proc Natl Acad Sci USA 2013;1(32):13109-13
70. Pan B-T, Johnstone RM. Fate of the transferrin receptor during maturation of sheep reticulocytes in vitro: selective externalization of the receptor. Cell 1983; 1(3):967-78
71. Brooks KB. IgE enhances B cell-derived exosomal induced T cell proliferation. Virginia Commonwealth University Richmond; VA, USA: 1986
72. Sharma K, Karl B, Mathew AV, et al. Metabolomics reveals signature of mitochondrial dysfunction in diabetic kidney disease. J Am Soc Nephrol 2013; 1(11):1901-12
73. Exosome protein, RNA and lipid database. Available from: www.exocarta.org
74. Villarroya-Beltri C, Gutiérrez-Vázquez C, Sánchez-Cabo F, et al. Sumoylated hnRNPA2B1 controls the sorting of miRNAs into exosomes through binding to specific motifs. Nat Commun 2013;4:2980
75. Cocucci E, Racchetti G, Meldolesi J. Shedding microvesicles: artefacts no more. Trends Cell Biol 2009;1(2):43-51
76. Pisitkun T, Shen R-F, Knepper MA. Identification and proteomic profiling of exosomes in human urine. Proc Natl Acad Sci USA 2004;1(36):13368-73
77. Taylor DD, Zacharias W, Gercel-Taylor C. Exosome isolation for proteomic analyses and RNA profiling. In: Serum/plasma proteomics. Methods Mol Biol; 2011. p. 235-46
78. Valadi H, Ekström K, Bossios A, et al. Exosome-mediated transfer of mRNAs and microRNAs is a novel mechanism of genetic exchange between cells. Nat Cell Biol 2007; 1(6):654-9
79. Conde-Vancells J, Rodriguez-Suarez E, Embade N, et al. Characterization and comprehensive proteome profiling of exosomes secreted by hepatocytes. J Proteome Res 2008;1(12):5157-66
80. Oosthuyzen W, Sime NEL, Ivy JR, et al. Quantification of human urinary exosomes by nanoparticle tracking analysis. J Physiol 2013;1(23):5833-42
81. Jy W, Horstman LL, Jimenez JJ, Ahn YS. Measuring circulating cell-derived microparticles. J Thromb Haemost 2004; 1(10):1842-3
82. Yano Y, Kambayashi J, Shiba E, et al. The role of protein phosphorylation and cytoskeletal reorganization in microparticle formation from the platelet plasma membrane. Biochem J 1994;299:303-8
83. Boulanger CM, Amabile N, Tedgui A. Circulating microparticles: a potential prognostic marker for atherosclerotic vascular disease. Hypertension 2006;1(2): 180-6
84. Agouni A, Lagrue-Lak-Hal AH, Ducluzeau PH, et al. Endothelial dysfunction caused by circulating microparticles from patients with metabolic syndrome. Am J Pathol 2008;1(4):1210-19
85. Sabatier F, Darmon P, Hugel B, et al. Type 1 and type 2 diabetic patients display different patterns of cellular microparticles. Diabetes 2002;1(9):2840-5
86. Mesri M, Altieri DC. Leukocyte microparticles stimulate endothelial cell cytokine release and tissue factor induction in a JNK1 signaling pathway. J Biol Chem 1999;1(33):23111-18
87. Witek RP, Yang L, Liu R, et al. Liver Cell–Derived Microparticles Activate Hedgehog Signaling and Alter Gene Expression in Hepatic Endothelial Cells. Gastroenterology 2009;136(1):320-30.e322
88. Chen TS, Lai RC, Lee MM, et al. Mesenchymal stem cell secretes microparticles enriched in pre-microRNAs. Nucleic Acids Res 2010;1(1):215-24
89. Théry C, Boussac M, Véron P, et al. Proteomic analysis of dendritic cell-derived exosomes: a secreted subcellular compartment distinct from apoptotic vesicles. J Immunol 2001;1(12):7309-18
90. Wang K, Zhang S, Weber J, et al. Export of microRNAs and microRNA-protective protein by mammalian cells. Nucleic Acids Res 2010;1(20):7248-59
91. Bala S, Petrasek J, Mundkur S, et al. Circulating microRNAs in exosomes indicate hepatocyte injury and inflammation in alcoholic, drug-induced, and inflammatory liver diseases. Hepatology 2012;1(5):1946-57
92. Schultz NA, Dehlendorff C, Jensen BV, et al. MicroRNA biomarkers in whole blood for detection of pancreatic cancer. JAMA 2014;1(4):392-404
93. Wang K, Yuan Y, Cho J-H, et al. Comparing the MicroRNA spectrum between serum and plasma. PLoS One 2012;7(7):e41561
94. Yang X, Li Z, Su Z, et al. Urinary microRNAs as noninvasive biomarkers for acetaminophen-induced liver injury. J Postgenom Drug Biomark Develop 2011; 1(101):2153-0769.1000101
95. Duttagupta R, Jiang R, Gollub J, et al. Impact of cellular miRNAs on circulating miRNA biomarker signatures. PLoS One 2011;6(6):e20769
96. Qi R, Weiland M, Gao X-H, et al. Identification of endogenous normalizers for serum MicroRNAs by microarray profiling: U6 small nuclear RNA is not a reliable normalizer. Hepatology 2012;1(5):1640-2
97. Wang G-K, Zhu J-Q, Zhang J-T, et al. Circulating microRNA: a novel potential biomarker for early diagnosis of acute myocardial infarction in humans. Eur Heart J 2010;1(6):659-66
98. Baraniskin A, Kuhnhenn J, Schlegel U, et al. Identification of microRNAs in the cerebrospinal fluid as marker for primary diffuse large B-cell lymphoma of the central nervous system. Blood 2011;1(11):3140-6
99. Kroh EM, Parkin RK, Mitchell PS, Tewari M. Analysis of circulating microRNA biomarkers in plasma and serum using quantitative reverse transcription-PCR (qRT-PCR). Methods 2010;1(4):298-301
100. Shen W, Deng H, Ren Y, Gao Z. A real-time colorimetric assay for label-free detection of microRNAs down to sub-femtomolar levels. Chem Commun 2013;49(43):4959-61
101. Cissell KA, Rahimi Y, Shrestha S, et al. Bioluminescence-based detection of microRNA, miR21 in breast cancer cells. Anal Chem 2008;1(7):2319-25
102. Zhang G-J, Chua JH, Chee R-E, et al. Label-free direct detection of MiRNAs with silicon nanowire biosensors. Biosens Bioelectron 2009;1(8):2504-8
103. Jiang L, Duan D, Shen Y, Li J. Direct microRNA detection with universal tagged probe and time-resolved fluorescence technology. Biosens Bioelectron 2012;1(1): 291-5
104. Broyles D, Cissell K, Kumar M, Deo S. Solution-phase detection of dual microRNA biomarkers in serum. Anal Bioanal Chem 2012;1(1):543-50

105. Mahn R, Heukamp LC, Rogenhofer S, et al. Circulating microRNAs (miRNA) in serum of patients with prostate cancer. Urology 2011;77(5):1265. e9-16

106. Meder B, Keller A, Vogel B, et al. MicroRNA signatures in total peripheral blood as novel biomarkers for acute myocardial infarction. Basic Res Cardiol 2011;1(1):13-23

107. Chen S, Xuan J, Guo L. microRNAs in drug-induced liver toxicity. In: Sahu SC, editor. microRNAs in Toxicology and Medicine. John Wiley & Sons Inc; NY, USA: 2013. p. 33

108. Wang F, Zheng Z, Guo J, Ding X. Correlation and quantitation of microRNA aberrant expression in tissues and sera from patients with breast tumor. Gynecol Oncol 2010;1(3):586-93

109. Wang G, Chan ES-Y, Kwan BC-H, et al. Expression of microRNAs in the urine of patients with bladder cancer. Clin Genitourin Cancer 2012;1(2):106-13